Hydrazine and carbazate complexes of chromium and manganese: their role in the catalytic decomposition of hydrazine

Thompsett, David

Award date:
1987

Awarding institution:
University of Bath

HYDRAZINE AND CARBAZATE COMPLEXES OF CHROMIUM AND MANGANESE. THEIR ROLE IN THE CATALYTIC DECOMPOSITION OF HYDRAZINE

submitted by

David Thompsett

for the Degree of Doctor of Philosophy

of the University of Bath

1987

ProQuest LLC
789 East Eisenhower Parkway
P.O. Box 1346
Ann Arbor, MI 48106-1346

ACKNOWLEDGEMENTS

I wish to thank my academic supervisor, Dennis Edwards, for his help and patience over the last three years and in the preparation of this thesis. Also wish to thank my industrial supervisor, John Bellerby, for this help within the project, especially during the period of industrial placement at RMCS Shrivenham.

I would like to thank the staff of the Inorganic Chemistry Department at Bath and my colleagues in Laboratory 2.10 for making the three years a most enjoyable period.

I would also like to thank Derek Sutton and Roy Bennett of RO Westcott for their help and provision of the original decomposition rate computer programs. Also I would thank Shelaine Green for the use of the Me_2NNH_2 vibrational data.

Finally I wish to acknowledge the Science & Engineering Research Council for provision of funds.

SUMMARY

Chromium and manganese have been implicated as catalysts for the homogeneous decomposition of hydrazine. With the aim of extending our knowledge of the factors involved in this decomposition, an investigation of chromium- and manganese-hydrazine chemistry has been undertaken. This study has been concerned with the carbazate chemistry of these metals because carbazic acid, $^{-}O_2CNHN^{+}H_3$, is formed by contact of atmospheric carbon dioxide with hydrazine. Since no significant previous work on chromium-substituted hydrazine chemistry has been reported, the analogous chemistry using methyl-, 1,1-dimethyl- and phenylhydrazine has also been developed.

The manganese(II)-hydrazine complexes $[Mn(N_2H_4)_2X_2]_n$ (X=Cl, Br, I, NCO, NCS, NCSe, N_3, O_2CMe and two forms with NO_2) have been prepared and characterised using spectroscopic (uv/visible, infrared, Raman and ESR) methods and bulk magnetic measurements. Vibrational spectroscopic assignments have been assisted by comparison with results on the N_2H_4-d_4 complexes $[M(N_2D_4)_2Cl_2]_n$ (M=Mn, Zn). Suspensions of $[Mn(N_2H_4)_2X_2]_n$ (X=O_2CMe and one form with NO_2) in methanol were found to be readily oxidised by atmospheric oxygen and the relevance of this observation to the proposed catalytic activity of manganese ions in hydrazine is discussed.

The known chromium(II) complexes $[Cr(N_2H_4)_2X_2]_n$ (X=Cl, Br) have been prepared by previously reported and by new routes and the novel polymeric complex $[Cr_2(O_2CMe)_4(\mu\text{-}N_2H_4)]_n$ containing metal-metal quadruple bonds also prepared and fully characterised. The analogues $[CrX_2(PhNHNH_2)_2]_n$ (X=Cl, Br), $[Cr_2(O_2CMe)_4(PhNHNH_2)_2]$,

$[CrCl_2(\mu\text{-}NH_2NHMe)_2]_n$, $[Cr_2(O_2CMe)_4(\mu\text{-}NH_2NHMe)]_n$, $[CrCl_2(NH_2NMe_2)_2]_n$ and $[Cr_2(O_2CMe)_4(\mu\text{-}NH_2NMe_2)]_n$ have also been prepared and characterised.

Magnetic susceptibility, conductiometric and electronic spectral evidence is presented to support the proposal that dissolution of anhydrous $CrCl_2$ or $CrCl_3$ in anhydrous N_2H_4 under nitrogen generated solutions containing chromium(III). Thus, it is suggested that hydrazine is capable of acting as an oxidising agent with respect to chromium(II). Attempted isolation of discrete solid products from these solutions was not sucessful.

A method for the production of high yields of pure carbazic acid, $\overset{-}{O}_2CNH\overset{+}{N}H_3$, and its d_4-isotopmer, $\overset{-}{O}_2CND\overset{+}{N}D_3$, has been developed and the vibrational spectra of these zwitterionic species assigned, with attempted comparison with the isoelectronic glycine, $O_2CCH_2NH_3$. Reactions of chromium species with carbazic acid and hydrazinium carbazate have subsequently been studied. Thus, aqueous reactions of chromium(II) species (e.g. $[Cr(OH_2)_6]^{2+}$ and $[Cr_2(O_2CMe)_4(OH_2)_2]$) with $[N_2H_5][O_2CNHNH_2]$ under nitrogen and carbon dioxide result in the formation of the novel, air-stable carbazate complex $[Cr(O_2CNHNH_2)_2.H_2O]$ which has been fully characterised. The known chromium(III) carbazate $[Cr(O_2CNHNH_2)_3].2H_2O$, obtained from $[Cr(OH_2)_4Cl_2]Cl.2H_2O$ and $[N_2H_5][O_2CNHNH_2]$, has also been extensively studied.

A study of phenylcarbazic acid has also been carried out. The product of the reaction of $PhNHNH_2$ and CO_2 in methanol is best regarded as the adduct $PhNHNHCO_2H.PhNHNH_2$ rather than as the salt $[PhNHNH_3][O_2CNHNHPh]$. Similar reactions carried out in the presence of alkali metal alkoxides, MOR (M=Li,Na,K; R=Me,Et), have led to the isolation of the metal phenylcarbazates $MO_2CNHNHPh$. These

compounds have been characterised using fast atom bombardment mass spectrometry.

Some reactions of $PhNHNHCO_2H.PhNHNH_2$ with first-row transition metal ions have been studied and a variety of products e.g. $[CuX(PhNHNH_2)]_n$ (X=Cl,Br), $[Co(O_2CNHNHPh)_2(MeOH)_2]$ and $[Ni(O_2CNHNHPh)_2(PhNHNH_2)_2]$ isolated and characterised. The nature of the reaction product with $[Cr(OH_2)_6]^{2+}$ was unexpected, being the very air-sensitive, dinuclear carboxylate-type complex $[Cr_2(\mu\text{-}O_2CNHNHPh)_4(MeOH)_2]$ ($Cr{\equiv}Cr$).

Thermally unstable $[MeNH_2NH_2][O_2CMeNNH_2]$ results from the reaction of $MeNHNH_2$ with CO_2 and this salt reacts with $[Cr(OH_2)_4Cl_2]Cl.2H_2O$ in ethanol to give the chromium(III) methylcarbazate $Cr(O_2CMeNNH_2)_3.H_2O$. Oxidation of chromium(II) in this system prevents the isolation of a chromium(II) methylcarbazate.

Finally, a preliminary investigation of the effect of chromium ions, (added as $Cr(O_2CNHNH_2)_3.2H_2O$ in N_2H_4), and acid, (added as $[N_2H_5][O_2CNHNH_2]$ in N_2H_4), on the homogeneous decomposition of hydrazine has been undertaken. The decomposition rates have been monitored by measuring pressure increases in closed titanium vessels resulting from nitrogen gas evolution. Sucessive additions of chromium ions generally reduced the decomposition rate, but no specific correlations between increasing chromium concentration and rate of decomposition were noted. The subsequent addition of acid to chromium-doped hydrazine was found to have little influence on the decomposition rate of hydrazine. The complete data sets obtained are given in Appendices to the thesis, together with listings of the programs used to calculate decomposition rates and activation energies.

TABLE OF CONTENTS

ABBREVIATIONS

Cp	- Cyclopentadienyl, C_5H_5
Me_2pz	- 2,3-Dimethylpyrazol-1-yl, $\overline{NNC(Me)CHC(Me)}$
triphos	- Bis(diphenylphosphinoethyl)phenylphosphine $PhP(CH_2CH_2PPh_2)_2$
dttd	- 2,3,8,9-Dibenzo-1,4,7,10-tetrathiadecane
cod	- Cycloocta-1,5-diene
THF	- Tetrahydrofuran
dppe	- 1,2-Bis(diphenylphosphino)ethane, $Ph_2PCH_2CH_2PPh_2$
acac	- Acetylacetonate Anion
UDMH	- Unsymmetrical dimethylhydrazine, Me_2NNH_2
MMH	- Monomethylhydrazine, $MeNHNH_2$
py	- Pyridine
en	- Ethylenediamine
dipyram	- 2,2'-Dipyridylamine
γ-pic	- γ-Picoline, 4-Methylpyridine
3-Clpy	- 3-Chloropyridine
cbz	- Carbazate, $NH_2NHCO_2^-$
Mecbz	- 2-Methylcarbazate, $H_2NN(Me)CO_2^-$
Me_2cbz	- 3,3-Dimethylcarbazate, $Me_2NNHCO_2^-$
Phcbz	- 3-Phenylcarbazate, $PhNHNHCO_2^-$
bipy	- Bipyridyl
DMSO	- Dimethylsulphoxide
DMF	- *N,N*-Dimethylformamide
Me	- Methyl
Et	- Ethyl
Ph	- Phenyl
PERME	- Propellant, Explosives and Rocket Motor Establishment, Westcott, Aylesbury
RO	- Royal Ordnance

Vibrational notation

ν	- stretch
δ	- deformation
b	- bend
π	- out-of-plane bend
ω	- wag
r	- rock
t	- twist

CHAPTER No 1

INTRODUCTION

INTRODUCTION

The Year 1987 marks the centenary of the discovery of hydrazine by Theodor Curtius [1]. During these one hundred years hydrazine has to quote Eckart Schmidt '... grown from a laboratory curiosity to a major industrial commodity' . Indeed it has taken nearly one hundred years for the first comprehensive reference work to be compiled; 'Hydrazine and its Derivatives, Preparation, Properties, Applications' by Schmidt [2].

Despite its extensive usage within the chemical industry, many features of hydrazine chemistry still remain worthy of investigation. This is especially true of its coordination behaviour towards transition metals, despite the occasional appearance of new work reported as a byproduct of nitrogen fixation research. This thesis presents some new results on transition metal-hydrazine and substituted hydrazine compounds arising out of an interest in propellants rather than nitrogen fixation.

1.1 HYDRAZINE CHEMISTRY

Anhydrous hydrazine is a colourless, fuming molecular liquid at room temperature (liquid range 2.0 - 114.2°C). As a solvent it readily promotes ionic reactions and strongly solvates metal ions.

Many of its physical properties are remarkably similar to those of water. Comparisons with ammonia and the isoelectronic hydrogen peroxide are also instructive, (see TABLE No 1.1).

In the gas phase four conformational isomers are conceivable (see FIG No 1.1). However the presence of a large dipole moment clearly eliminates the staggered trans-conformer and indicates that

the NH_2 groups do not freely rotate about the N-N bond. A rotational energy barrier of 25 - 41 kJ has been calculated [3].

TABLE No 1.1 Comparison of N_2H_4 with other solvents

Solvent	N_2H_4	N_2H_5OH	H_2O	NH_3	H_2O_2
M.Pt/°C	2.01	-51.6	0.00	-77.73	-0.43
B.Pt/°C	114.2	116.4	100.0	-33.41	150.20
Density at 298K/g cm^{-3}	1.0004	1.032	1.000	0.663 (239K)	1.443
η/centipoise	0.913	-	0.890	0.254 (239K)	1.249
Dielectric Cons't, ε	51.7	61.2	78.4	22.0 (239K)	70.7
Dipole Moment, μ/Debye	1.84	-	1.84	1.46	-
Conductivity at 298K, $/\Omega^{-1}cm^{-1}$	-2.5×10^{-6}	1.3×10^{-5}	5.7×10^{-8}	2.0×10^{-7} (234K)	5.1×10^{-8}

NOTE centipoise = 10^{-3}kg m^{-1} s^{-1}
Debye = 3.336×10^{-30} C m

FIGURE No 1.1 Possible Conformations of N_2H_4

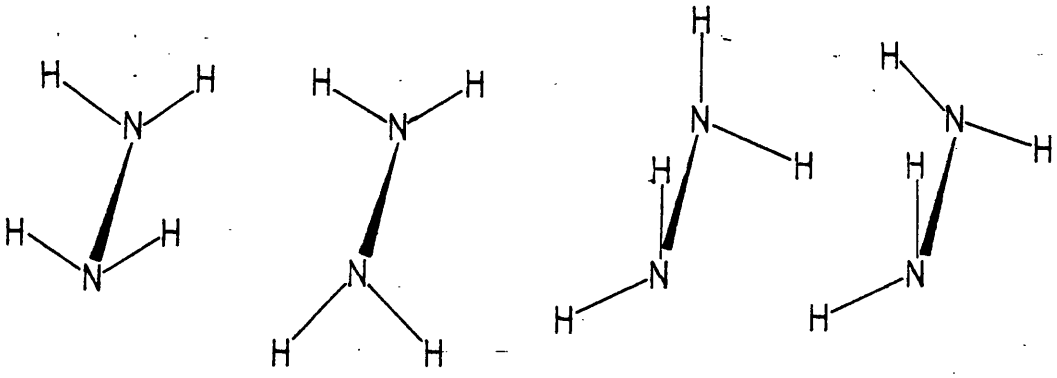

Eclipsed *cis*-C_{2v} | Staggered *trans*-C_{2h} | Semi-eclipsed C_2 | Gauche C_2

Electron diffraction data, in conjunction with infrared studies, [4,5] indicate that the gauche-conformation with an angle 90 - 95°

from the eclipsed position is favoured. As FIG No 1.2 shows, the angle between lone pairs is ~95°, the lone pairs effectively positioned *syn* to each other. This configuration has important consequences when considering hydrazine coordination geometry.

FIGURE No 1.2 *Syn* configuration of Lone Pairs of N_2H_4

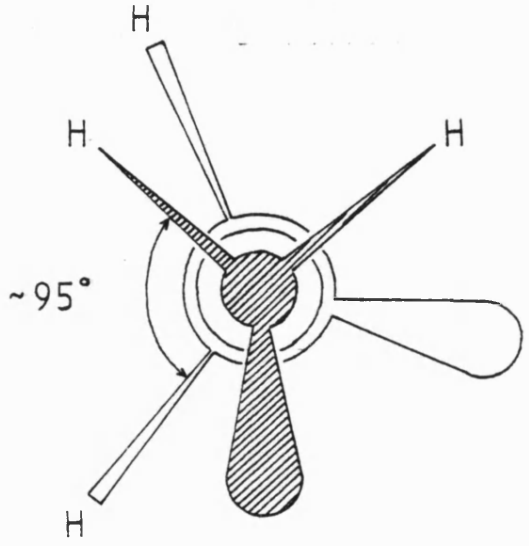

Like many other protic solvents, pure hydrazine, (even in the absence of acidic or basic additives), undergoes self-ionization (1.1).

$$2N_2H_4 \rightleftharpoons N_2H_5^+ + N_2H_3^- \qquad K = 2\times10^{-25} \qquad (1.1)$$

The equilibrium constant is nine orders of magnitude smaller than that of H_2O, but eight orders of magnitude larger than that of NH_3. Consequently, N_2H_4 is a weaker acid than H_2O.

At room temperature, pure N_2H_4 and its aqueous solutions are kinetically stable with respect to decomposition despite the endothermic nature of the compound and its positive free energy of formation (1.2).

$$N_{2(g)} + 2H_{2(g)} \longrightarrow N_2H_{4(l)} \quad \Delta H_f^{\ominus} = 50.6 \text{ kJmol}^{-1}, \ \Delta G_f^{\ominus} = 149.2 \text{ kJmol}^{-1} \qquad (1.2)$$

When ignited, N_2H_4 burns rapidly and completely in air with considerable evolution of heat (1.3).

$$N_2H_{4(l)} + O_{2(g)} \longrightarrow N_{2(g)} + 2H_2O_{(l)} \ ; \ \Delta H = -621.5 \text{ kJmol}^{-1} \qquad (1.3)$$

This reaction with O_2 occurs even in aqueous solution which makes N_2H_4 attractive as a deoxygenating agent in high pressure boiler installations.

The singularly most important feature of hydrazine is the presence of a N-N bond. This feature dominates much of hydrazine chemistry, in particular influencing the extensive range of redox reactions which hydrazine undergoes.

Hydrazine is a strong reducing agent and as such reduces many metal ions to lower oxidation states or even to base metal. The standard redox potentials of hydrazine and the hydrazinium(1+) ion (1.4 and 1.5) indicate that hydrazine is a better reducing agent in basic than in acidic solution.

$$N_2H_4 + 4OH^- \longrightarrow N_2 + 4H_2O + 4e^- \quad E^\circ = +1.16V \qquad (1.4)$$

$$N_2H_5^+ \longrightarrow N_2 + 5H^+ + 4e^- \quad E^\circ = +0.23V \qquad (1.5)$$

In common with hydrogen peroxide, hydrazine can also act as an oxidising agent, a process thermodynamically favourable particularly under acidic conditions (1.6 and 1.7).

$$N_2H_4 + 2H_2O + 2e^- \longrightarrow 2OH^- + 2NH_3 \quad E^\circ = +0.1V \qquad (1.6)$$

$$N_2H_5^+ + 3H^+ + 2e^- \longrightarrow 2NH_4^+ \quad E^\circ = +1.275V \qquad (1.7)$$

Although thermodynamically feasible, few examples of oxidation are known because of the high activation energy required to break the N-N bond. Also such reactions are usually kinetically controlled.

Hydrazine forms two series of protonated salts, depending on the number of nitrogen atoms protonated. The monoprotonated ion $N_2H_5^+$ can still act as an electron donor and form complexes, e.g. $[M^{II}(N_2H_5)_2(SO_4)_2]_n$ (M=Cr,Co,Ni,Cu,Zn) [198,199].

However the second nitrogen atom is more difficult to protonate once the first has been, as shown by the pK_a values (1.8 and 1.9).

$$N_2H_4 + H_2O \longrightarrow N_2H_5^+ + OH^- \quad pK_1 = 6.07 \qquad (1.8)$$

$$N_2H_5^+ + H_2O \longrightarrow N_2H_6^{2+} + OH^- \quad pK_2 = 15.05 \qquad (1.9)$$

Only very strong acids such as perchloric form dibasic salts. If such salts form, they are not stable in aqueous solution as hydrolysis occurs with water acting as a base (1.10).

$$N_2H_6^{2+} + H_2O \longrightarrow N_2H_5^+ + H_3O^+ \qquad (1.10)$$

The hydrazine-water system shows two eutectic compositions, one at 69% (219K) corresponding to $N_2H_4.H_2O$, and one at approximately 41% (190K), roughly corresponding to $N_2H_4.2H_2O$.

The reaction of hydrazine with carbon dioxide, the anhydride of carbonic acid, does not lead to hydrazinium carbonate as expected by comparison with the corresponding ammonia system (1.11 and 1.12).

$$2NH_3 + CO_2 + H_2O \longrightarrow (NH_4)_2CO_3 \qquad (1.11)$$

$$2N_2H_4 + CO_2 + H_2O \longrightarrow (N_2H_5)_2CO_3 \qquad (1.12)$$

Instead the reaction of hydrazine with carbon dioxide leads to the formation of hydrazinium carbazate, a viscous hygroscopic liquid that crystallizes only reluctantly after storage over concentrated H_2SO_4 *in vacuo*. If an excess of carbon dioxide is passed into an aqueous solution of hydrazine hydrate, the insoluble hygroscopic carbazic (also known as hydrazinecarboxylic) acid is obtained (1.13).

$$2N_2H_4 + CO_2 \longrightarrow [N_2H_5][O_2CNHNH_2] \xrightarrow{CO_2} 2H_2NNHCO_2H \qquad (1.13)$$

In common with its amino acid analogue glycine, $\overset{-}{O}_2CCH_2\overset{+}{N}H_3$, it is thought to exist as the zwitterion, $\overset{-}{O}_2CNH\overset{+}{N}H_3$, in the solid state with extensive intermolecular hydrogen-bonding accounting for its insolubility.

Carbazic acid dissolves in hydrazine and water to give solutions of hydrazinium carbazate, which is also formed when carbazic acid is thermally decomposed at 360K [6].

The salts of carbazic acid with transition metals are of particular interest because these compounds are invariably found as corrosion products when hydrazine stored in stainless steel is allowed to absorb carbon dioxide from the air (see SECTION 1.2).

1.2 HYDRAZINE DECOMPOSITION

Probably the most dramatic application of hydrazine (and its methyl derivatives) is its use as a rocket propellant. Hydrazine has been considered as a rocket fuel from as long ago as 1932 [7] but it was only in 1964 that hydrazine was first used as a launch vehicle propellant [8]. Since then, although less used in primary launch systems having been largely replaced by cryogenic fuels, hydrazine has been extensively employed in secondary and tertiary applications.

Hydrazines as hypergolic fuels undergo spontaneous combustion when added to an external oxidiser in bipropellant systems. The most widely employed oxidisers used in conjunction with hydrazine have been dinitrogen tetroxide, fuming nitric acid and fluorine. Hydrazine is also used extensively as a monopropellant for lower thrust applications e.g. attitute control and orbital correction. In these systems hydrazine is spontaneously decomposed on contact with a catalytic surface without the need for an external oxidiser. The most successful catalytic system is 'Shell 405', an alumina-supported iridium catalyst bed.

Hydrazine decomposition is governed by the general equation (1.14).

$$3N_2H_4 \longrightarrow 4(1-x)NH_3 + (1+2x)N_2 + 6x\ H_2 \qquad (1.14)$$

This equation is the combination of two separate decomposition pathways (1.15 and 1.16) and the products can therefore be specified for a particular set of conditions depending only on the value of x.

$$3N_2H_4 \longrightarrow 4NH_3 + N_2 \qquad (1.15)$$

$$N_2H_4 \longrightarrow N_2 + 2H_2 \qquad (1.16)$$

One requirement for long-term missions is a low hydrazine decomposition rate on storage. Titanium alloys are the preferred container materials as a result of good strength : weight ratios and extremely good compatibility with hydrazine (i.e. low decomposition rates). However for the construction of large storage vessels, titanium becomes expensive and difficult to work into extensive structures. In these cases, stainless steel is the preferred alternative.

Studies have shown that over long periods of time hydrazine stored in stainless steel containers undergoes slow decomposition mainly according to equation (1.15) (i.e. x~0 in 1.14). The decomposition reaction is subject both to heterogeneous catalysis at containment vessel surfaces and to homogeneous catalysis within the bulk liquid. This decomposition has important consequences for hydrazine propulsion systems for although ammonia is reasonably soluble in anhydrous hydrazine (0.0785 mol NH_3/mol N_2H_4 at 298K, mol NH_3/mol N_2H_4 = exp((2615.08/T)-11.32)), nitrogen is not (7.4×10^{-6} mol N_2/mol N_2H_4 at 298K, mol N_2/mol N_2H_4 = exp((-1185.93/T)-7.84)). Over extended periods nitrogen builds up in the

ullage space of the vessel, leading to limited system lifetimes before potentially hazardous pressure build-up occurs.

This decomposition process has been studied by a number of groups. Axworthy *et al.* at Rocketdyne showed in the late 1960's that of the known impurities in propellant grade hydrazine, water, carbon dioxide and acidity all led to significant increases in hydrazine decomposition rates when in contact with stainless steel [9].

In particular, the presence of relatively small amounts (~100 ppm) of carbon dioxide impurity in contact with stainless steel leads to metal corrosion and an increase in the concentration of dissolved metal ions. The process is accompanied by a corresponding increase in the rate of homogeneous decomposition of hydrazine (measured in glassware to eliminate heterogeneous decomposition due to stainless steel).

In view of the increasing recognition of the role of impurities on the decomposition rate of hydrazine, it is interesting to look at the historical evolution of hydrazine propellant specifications.

The first hydrazine propellant specification, MPD-139C, was set on 3 Feb 1955 and required only 95% N_2H_4 and allowed up to 1.5% aniline and *n*-heptane [10]. The purity requirements for N_2H_4 have become more severe as the effect of typical contaminants on monopropellant catalysts and the decomposition of N_2H_4 itself have become better understood. In particular, the role of CO_2 in N_2H_4 decomposition has only recently been recognized resulting in the reduction of the MIL-P-26536C specification from 0.02 to 0.003% by weight [11] (see TABLE No 1.2).

TABLE No 1.2 Historical Evolution of Hydrazine Specification

Spec	MPD-139C (Feb 1955)	MIL-P-2653613 (Mar 64)	MIL-P-26536C (Admend 1) (July 74)	(Admend 2) (Feb 82)
Constituent/% by wt				
N_2H_4	95,0 min	97,5 min	98,5 min	98,5 min
H_2O	-	2,5 max	1,0 max	1,0 max
Particulate (mg/l)	-	10,0 max	1,0 max	1,0 max
Cl	-	-	0,0005 max	0,0005 max
$PhNH_2$	1,5 max	-	0,5 max	0,5 max
Fe	-	-	0,002 max	0,002 max
Nonvolatile Residue	-	-	0,005 max	0,005 max
CO_2	-	-	0,02 max	0,003 max
Volatile Carbonaceous Material	1,5 max	-	0,02 max	0,02 max

The involvement of carbon dioxide in promoting stainless steel corrosion by hydrazine and the consequent increase in decomposition rate, has prompted the proposal that certain transition metal ions arising from the elements present in the steel may function as homogeneous catalysts towards the decomposition of hydrazine. A possible reaction scheme is shown in 1.17 and 1.18.

$$4M^{x+} + N_2H_4 \xrightarrow{\text{FAST}} 4M^{(x-1)+} + N_2 + 4H^+ \qquad (1.17)$$

$$4M^{(x-1)+} + N_2H_4 + 4H^+ \xrightarrow{\text{SLOW}} 4M^{x+} + 2NH_3 + 2H^+ \qquad (1.18)$$

This scheme demands that the metal displays variable oxidation state chemistry in anhydrous hydrazine. The rate-determining step requires hydrazine to act in an oxidising capacity which although thermodynamically feasible is kinetically unfavourable, (see below). In this cycle both nitrogen and ammonia are produced.

While Axworthy's study remains the most comprehensive investigation into the effects of impurities on the decomposition rate of liquid hydrazine, the kinetic experiments were conducted at comparatively high temperatures (128°C-171°C), so the results may

not be applicable to normal storage temperatures. More recent work in the USA, most notably at Boeing [12] and JPL [13], revealed that even at moderate temperatures (40°C) very low levels of CO_2 impurity (<250ppm) can cause significant stainless steel corrosion and lead to an increase in the concentration of trace metals in hydrazine. This process corresponds with an increase in the rate of homogeneous decomposition of hydrazine.

Decomposition studies performed at PERME, Westcott recently have concentrated on investigating the effect of individual steel constituents on the decomposition rate of hydrazine in the presence of carbon dioxide [14].

A typical stainless steel composition shows the major metallic constituents to be iron, chromium, nickel and manganese (TABLE No 1.3).

The PERME approach consists of isolating metal carbazato complexes of the major stainless steel constituents, and determining their effect on the rate of hydrazine decomposition by kinetic methods. The metals were added as carbazato complexes (where possible) to mimic the species present in hydrazine stored in stainless steel after exposure to carbon dioxide.

TABLE No 1.3 A Typical Stainless Steel Composition (BS Spec 526)

Constituent	%
Fe	66.1
Cr	19.0
Ni	11.0
Mn	2.0
Si	1.0
Ti	0.7
C	0.08
P	0.035
S	0.025

The addition of iron as $[Fe(O_2CNHNH_2)_2(N_2H_4)_2]$ in increasing amounts to hydrazine in glass vessels at 43°C produced no increase in decomposition rates [15]. The addition of chromium as $Cr(O_2CNHNH_2)_3.2H_2O$ to hydrazine under similar conditions resulted in a slight decrease in N_2H_4 decomposition rate, but the addition of an acid as well produced a three-fold increase in N_2H_4 decomposition rate. Manganese was added as $MnCl_2.4H_2O$ because $[Mn(O_2CNHNH_2)_2(N_2H_4)_2]$ is insoluble in N_2H_4 and this metal ion showed a similar effect as chromium on N_2H_4 decompsition rate [16]. Nickel as $[Ni(O_2CNHNH_2)_2(N_2H_4)]$ was found to be insoluble in N_2H_4 and thought not to affect N_2H_4 decomposition rates [15]. Most interestingly, the addition of acid to hydrazine containing manganese(II) and chromium(III) in titanium vessels brought about the greatest increase in decomposition rate, well above that found by the addition of acid alone or chromium and acid [16].

It is suggested that homogeneous decomposition of anhydrous hydrazine may be catalysed by trace chromium and manganese acting in conjunction with the hydrazinium ion (the acid of the hydrazine solvent system). The work reported in this thesis therefore mainly focuses upon increasing our knowledge of chromium and manganese species capable of existence in hydrazine or substituted hydrazines.

1.3 HYDRAZINE COORDINATION CHEMISTRY

Two reviews have appeared on hydrazine coordination chemistry. Bottomley reviewed hydrazine and carbazate coordination compounds that had been reported up to 1970 [17], while Dilworth complemented this by extending the coverage to the coordination behaviour of substituted hydrazines [18]. This latter review appeared in 1976

and much of the recent work on deprotonated hydrazine derivatives is therefore not included. Bottomley stated in 1970 that hydrazine coordination chemistry '...is still in its (somewhat prolonged) infancy'. Sixteen years later this can still be said to be true.

Reactions of hydrazine with transition metals were first reported soon after the discovery of hydrazine itself. Curtius, consolidating his discovery, showed in 1894 that the product of the reaction between hydrazine and zinc chloride was the complex $[Zn(N_2H_4)_2Cl_2]$ [19].

This first account of hydrazine coordination chemistry was swiftly followed by the report of several mercury-hydrazine complexes by Hofmann and Marburg in 1897 [20]. An early maturity was reached when between 1908-11 Franzen, von Meyer and Lucking undertook an extensive investigation of the reactions between metal salts and hydrazine characterising over forty metal-hydrazine complexes, thereby providing the basis for modern hydrazine coordination chemistry [21].

The next major period of interest came during the early 1960's, when two groups of Italian workers, led by A.Ferrari and L.Sacconi, respectively, considered the application of vibrational spectroscopy as a diagnostic tool for determining hydrazine coordination geometry [22,23]. Sacconi and Sabatini reported extensive infra-red spectral data for hydrazine complexes [22], while Ferrari, Braibanti *et al.* reported the first X-ray crystal structures of metal-hydrazine complexes [24] and established the predictive use of the ν(N-N) stretching frequency as a means of distinguishing coordination mode [23].

Working in parallel to these groups Nicholls *et al.* investigated the solution behaviour of some first-row transition

metal ions in anhydrous hydrazine and concluded that they exist as hexakis(hydrazine) cationic species. However, unlike the corresponding hexakis(ammine) species, the products $[M(N_2H_4)_6]^{2+}2Cl^-$ (M = Co,Ni) were found to be unstable on isolation decomposing by loss of N_2H_4 to lower hydrazinates [25,26]. This group also undertook the first systematic investigation of the coordinative abilities of alkyl substituted hydrazines.

In addition, it has only been recognized in the last twenty years that the redox potential of hydrazine allows the generation of numerous species apart from neutral hydrazine complexes on reaction with transition metals [18].

It is now known that diazene, hydrazido- and hydrazine complexes , amongst others, can be obtained for first-row transition metals depending on the metal and reaction conditions. The ability of certain second- and third-row transition metals to form multiple bonds to nitrogen increases the potential redox character of hydrazine. Reactions of hydrazine compounds with these metals can give rise to imido-, diazenido- and nitrido- complexes as well as the species formed by first-row transition metal ions.

Since the work described in this thesis is particularly concerned with neutral hydrazine or substituted hydrazine complexes, the other species listed in TABLE No 1.4 will not be considered further in detail.

Hydrazine acting as a simple Lewis base, without oxidation or deprotonation, is a potential unidentate, bridging, or bidentate ligand [17] (see FIG 1.3)

FIGURE No 1.3 Potential Coordination Modes of Hydrazine

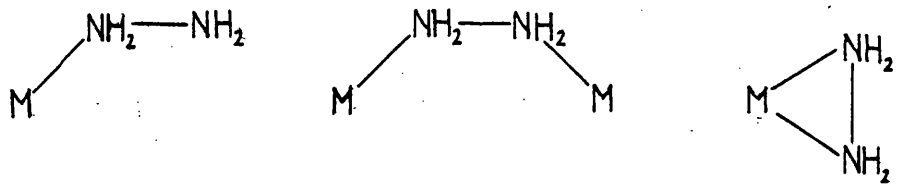

Unidentate Bridging Bidentate

TABLE No 1.4
Types of Species formed by Reaction of N_2H_4 with Transition Metals

M-NH_2NH_2 HYDRAZINE

[$Zn(O_2CNHNH_2)_2(\eta'$-$NH_2NH_2)_2$]	[27]
[$Zn(\mu$-$NH_2NH_2)_2Cl_2$]$_n$	[24]

M-$NHNH_2$ HYDRAZIDO(1-)

[$CpTiCl_2(\eta^2$-$NHNMe_2)$], [$CpTiCl_2(\eta^2$-$NH_2NPh)$]	[28]
[$Mo\{HB(Me_2pz)_3\}(NO)I(\eta'$-$NHNMe_2)$]	[29]

M-NNH_2 HYDRAZIDO(2-)

[$Mo(\eta'$-$NNH_2)$(triphos)(PPh_3)]Cl	[30]
[$\{CpTiCl_2\}_2(\mu$-η'-$NNPh_2)(\mu$-η^2,η'-$NNPh_2)$]	[31]

M-NHNH-M DIAZENE

[$\{Ru(PPh_3)(dttd)\}_2(\mu$-$\eta',\eta'$-NHNH)]	[32]
[$\{W(C_5Me_4(t$-Bu))($CCMe_3$)Cl$\}_2(\mu$-η',η'-$NH_2NH_2)(\mu$-η^2,η^2-NHNH)]	[33]

M-N=NH DIAZENIDO

[ReBr(η'-NNPh)(η'-NNHPh)(PPh_3)$_2$],	[34]
[$HNEt_3$]$_2$[$Mo_2(\eta'$-NNPh)(η'-NNHPh)(SCH_2CH_2S)$_3$(SCH_2CH_2SH)]	[35]
[$CpTiCl_2(\eta^2$-NNPh)]	[36]

M=NH IMIDO

[$ReCl_3(\eta'$-NMe)]	[37]

M≡N NITRIDO

[$Re(\eta'$-N)$Cl_2(PPh_3)_2$]	[38]

Note; All examples crystallographically characterised
Cp - C_5H_5
Me_2pz - 2,3-dimethylpyrazol-1-yl, $\overline{NNC(Me)CHC(Me)}$
dttd - 2,3,8,9-dibenzo-1,4,7,10-tetrathiadecane
triphos - $PhP(CH_2CH_2PPh_2)_2$

Generally, hydrazine prefers to bridge where possible, although unidentate coordination occurs particularly in solution where metal centres are coordinatively saturated. First-row transition metal ions probably exist as the solvated species $[M(N_2H_4)_6]^{n+}$ in anhydrous hydrazine but when isolated as solid salts these species readily lose hydrazine to form bridging hydrazine species. Of the first-row metal ions only $[Co(N_2H_4)_6]Cl_2$ has been shown to be moderately stable [25,25A]. The majority of X-ray structural studies on hydrazine-containing complexes reveal bridging coordination, however crystal structures of

TABLE No 1.5
X-ray Crystal Structure Determinations of Metal-Hydrazine and Substituted Hydrazine Complexes.

Complex	Coordination mode	Ref
$[Zn(N_2H_4)_2Cl_2]_n$	bridge	[24]
$[Zn(N_2H_4)_2(NCS)_2]_n$	bridge	[43]
$[Zn(N_2H_4)_2(O_2CMe)_2]_n$	bridge	[44]
$[Mn(N_2H_4)_2Cl_2]_n$	bridge	[45]
$[Co(O_2CNHNH_2)_2(N_2H_4)_2]$	unidentate	[39]
$[Zn(O_2CNHNH_2)_2(N_2H_4)_2]$	unidentate	[27]
$[CuCN(N_2H_4)]_n$	bridge	[46]
$[\{W(NPh)Me_3\}_2(\mu\text{-}NH_2NH_2)(\mu\text{-}NHNH)]$	bridge	[33]
$[N(C_4H_9)]_2[\mu\text{-}N_2H_4\{Fe(S_2C_6H_4)_2\}_2]$	bridge	[47]
$[RuH(\eta^4\text{-}cod)(NH_2NMe_2)_3][PF_6]$	unidentate	[48]
$[\{RuCl(H)(\eta^4\text{-}cod)\}_2(\mu\text{-}NH_2NMe_2)]$	bridge	[49]
$[Pt(PEt_3)_2(NH_2NHC_6H_4F)Cl][BF_4]$	unidentate	[50]
$[(\eta^5\text{-}C_5H_5)Mo(NO)I(NH_2NHPh)][BF_4]$	bidentate	[51]

$[M(O_2CNHNH_2)_2(N_2H_4)_2]$ (M = Co and Zn), show hydrazine acting in an unidentate mode [27,39]. Other complexes possibly containing unidentate hydrazine, but not confirmed by structure determinations, are listed in the reviews by Bottomley and Dilworth [17,18].

The remainder of the crystal structure studies that have been reported show hydrazine acting as a bridging ligand. All known crystal structures of hydrazine complexes are listed in TABLE No 1.5. Despite the large number of such complexes known, the bridging hydrazine coordination mode naturally leads to insoluble polymeric complexes which are difficult to crystallise. This feature explains the paucity of X-ray structural information.

Bridging coordination of hydrazine occurs in an extensive series of polymeric complexes, $[M(N_2H_4)_2X_2]_n$ (M = divalvent first-row transition metal, X = halide, pseudohalide or carboxylate) [17]. A limited group of related tris(hydrazine) complexes exist but are generally confined to cobalt and nickel; $[M(N_2H_4)_3]X_2$ (M = Co or Ni, X = Cl,Br,I,½SO_4,BF_4) [26,40,41,41A]. The weakly coordinating nitrate ion forms a futher group of tris(hydrazine) complexes, $[M(N_2H_4)_3](NO_3)_2$ (M = Mn,Fe,Co,Ni,Zn, or Cd) [25A,42]. All these complexes are insoluble, (except in solvents such as hydrazine itself where futher reaction occurs), and are usually air- and moisture- stable.

X-Ray crystal structures of the series $[Zn(N_2H_4)_2X_2]_n$ (X = Cl,NCS,O_2CMe) [24,43,44] show the complexes to consist of pseudo-one-dimensional chains of *syn*-bridging hydrazines between metal ions, with coordinated anions occupying the axial positions, (see FIGURE No 1.5), of an octahedral array.

FIGURE No 1.5 Crystal Structure of $[Zn(N_2H_4)_2(O_2CMe)_2]_n$ [44]

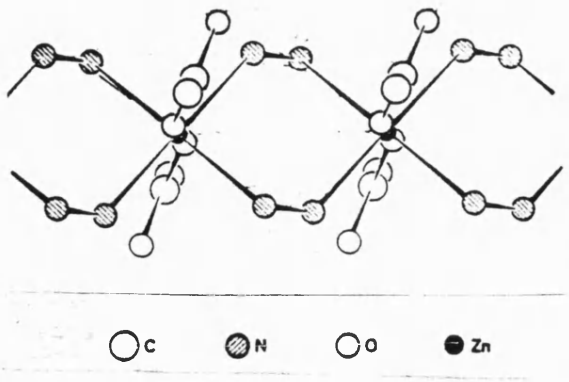

Sequential structural changes observed when hydrazine coordination changes from unidentate to bridging can be illustrated by the thermal decomposition pathway of the unstable hexakis(hydrazine) species $[Ni(N_2H_4)_6]Cl_2$ (see FIGURE No 1.6) [52].

FIGURE No 1.6 Thermal Decompsition Pathway of $[Ni(N_2H_4)_6]Cl_2$

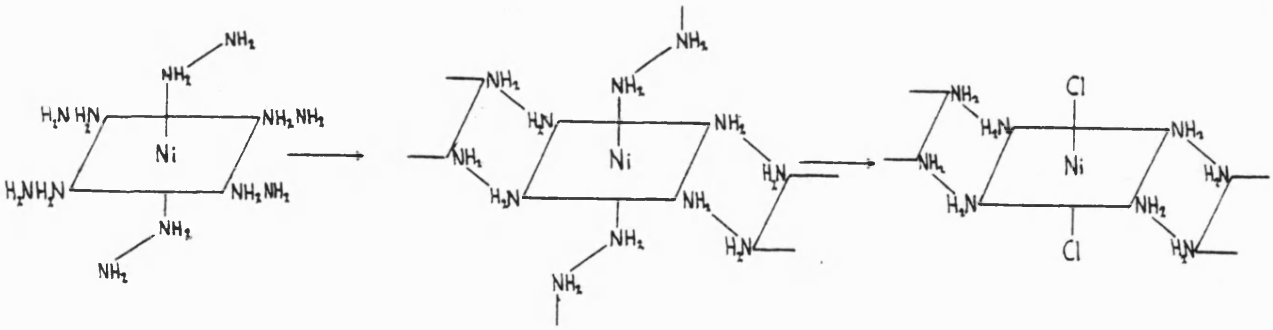

The loss of hydrazine from the hexakis-species releases additional coordination sites around the metal, inducing the change from unidentate to bridging coordination of the ligands.

The thermal decomposition of metal-hydrazine complexes has been studied by several groups [52,53,54]. In particular a group lead by N.Ray Chaudhuri has been active in studying the thermal decomposition of Mn(II) [55], Co(II) [56], Ni(II) [53], Zn(II) [57]

FIGURE No 1.7 Thermal Decomposition Pathways of $[Mn(N_2H_4)_2X_2]$ [55]

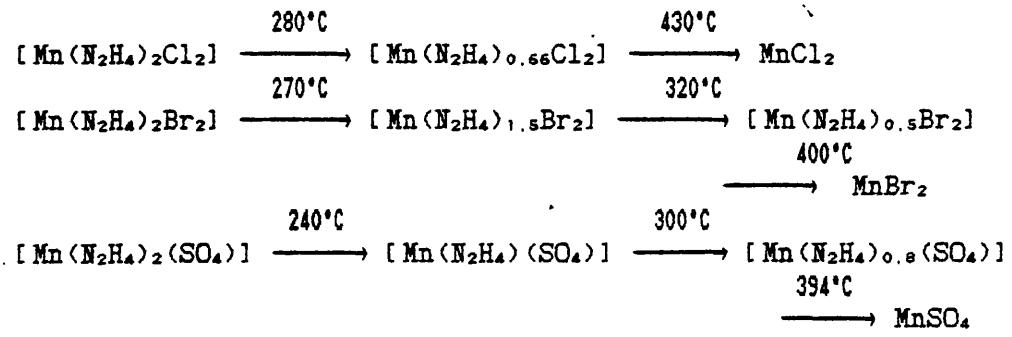

and Cd(II) [58] hydrazine complexes by DTA/TG methods. Each metal-hydrazine system was found to have its own thermal decomposition characteristics. Within each metal system a variation in anion coordination produced changes in decomposition pathway (see FIGURE No 1.7). In general, the complexes lose hydrazine step-wise to give a series of species with decreasing hydrazine:metal ratios. The final products are invariably the anhydrous metal salts.

The loss of N_2H_4 from such complexes is exothermic in contrast to endothermic loss of NH_3 from metal-ammine complexes. This is reasonable since the N_2H_4 lost is subject to futher decomposition to N_2 and NH_3, a known exothermic process.

The thermal decomposition of metal oxalate-hydrazine complexes $[M(C_2O_4)(N_2H_4)_2]$ (M = Fe,Co,Ni) proceeds in a similar fashion with loss of hydrazine to give metal oxides as final products [59,60,61]. Thermal decomposition of mixed metal oxalate complexes $MFe_2(C_2O_4)_3(N_2H_4)_6$ (M = Mn,Co,Ni,Zn) and $MCo(C_2O_4)_3(N_2H_4)_x$ (M = Mg, x=5; M=Ni, x=6) has been used as a method for low temperature formation of spinel ferrites (MFe_2O_4) and cobaltites (MCo_2O_4) respectively [62,63].

The *syn*-bridging geometry of hydrazine is taken up because of the restricted rotation about the N-N bond resulting in a rigid

arrangement of lone pairs. This geometry is futher illustrated by the structural characterisation of $[(W(NPh)Me_3)_2(\mu\text{-}NH_2NH_2)(\mu\text{-}NHNH)]$ (see FIGURE No 1.8) [33]. The hydrazine bridges the tungsten atoms in a *syn*-configuration giving rise to a zig-zag W-N-N-W arrangement.

FIGURE No 1.8 Structure of $[(W(NPh)Me_3)_2(\mu\text{-}NH_2NH_2)(\mu\text{-}NHNH)]$

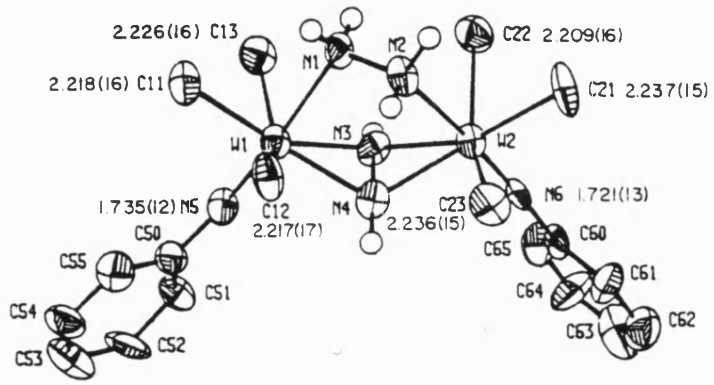

Bidentate chelating coordination of hydrazine although feasible, has yet to be unequivocally authenticated. The opportunity for hydrazine to act as a chelating ligand will undoubtedly be restricted due to the short N-N distance and the acute 'bite' angle required. However, a single phenylhydrazine complex, $[(\eta^5\text{-}C_5H_5)Mo(NO)I(NH_2NHPh)][BF_4]$, is known to contain a η^2-phenylhydrazine [51] (see FIGURE No 1.11), so this mode of coordination should not be dismissed without consideration.

Simple Lewis base behaviour of hydrazine seems to occur most readily with divalent first-row transition metal ions, although a few non-deprotonated second- and third-row transition metal complexes containing neutral hydrazine have been characterised. The metals ions in these complexes are in conventional oxidation states, such as $[Ru^{II}(\eta^4\text{-cod})(N_2H_4)_4][BPh_4]_2$ [64], $[Os^{II}(\eta^4\text{-cod})$-

$(N_2H_4)_3][BPh_4]_2$ [65], and $[Ru^{II}(\eta^5-C_5Me_5)(N_2H_4)_3]Cl_2.H_2O$ [66]. Other examples can be found in the review by Bottomley [17]. It is interesting that such complexes are stable, in view of the fact that noble metals and their salts are known to catalyse hydrazine decomposition [67]. For example, the reaction of the ruthenium(II)-nitrosyl complex, $[Ru(NH_3)_5NO]Cl_3$ with $N_2H_4.H_2O$ at room temprature results in the formation of the dinitrogen complex, $[Ru(NH_3)_5N_2]Cl_2$ [68]. Similarly the formation of $[IrBr_3(N_2H_4)_3].0.5H_2O$ from reaction of the $[IrBr_5NO]^-$ anion with $N_2H_4.H_2O$ also results in the formation of N_2 [69].

Hydrazine complexes of f-block elements have also been reported. Lanthanide metals give complexes of general stoichiometry $[Ln(N_2H_4)_x]X_3$ (Ln=Pr,Nd,Sm etc; X=Cl,Br,O_2CMe etc; x=6 or 3) [70,71,72]. Hydrazine complexes are also known for 5f metals. Uranium and thorium have been reported to form the complexes $[M(SO_4)_2(N_2H_4)_2]$ ($M=UO_2$,Th) [73].

Hydrazine also acts as a reasonably good σ-donor ligand in its reactions with low valence π-acceptor metal complexes. Thus reations with Group 6 and 7 metal carbonyl complexes can result in both unidentate and bridging hydrazine complexes (1.19) [74-78].

$$(OC)_5M(THF) + N_2H_4 \longrightarrow (OC)_5M(N_2H_4) + (OC)_5M(THF) \longrightarrow [\{(OC)_5M\}_2(\mu-N_2H_4)] \quad (M=Cr,Mo,W) \qquad (1.19)$$

This reaction sequence further illustrates the efficiency of the bidentate bridging mode of hydrazine.

These complexes are easily oxidised to the corresponding diazene complexes and under certain conditions to the analogous dinitrogen complexes (see 1.20). Of the Group 6 metals, molybdenum

exhibits the highest reactivity in this respect, which has added weight to the speculation that a molybdenum-based catalytic cycle

$$[\{(OC)_5Mo\}_2(\mu\text{-}N_2H_4)] \xrightarrow[THF/-30°C]{Cu^{2+}/H_2O_2} [\{(OC)_5Mo\}_2(\mu\text{-}NHNH)] \xrightarrow[20°C]{H_2O/THF} [\{(OC)_5Mo\}_2(\mu\text{-}N_2)] \quad (1.20)$$

in the enzyme nitrogenase is reponsible for nitrogen fixation [75]. Hydrazine can also act as a nucleophile towards coordinated ligands in low valent complexes (1.21) [79].

$$[M(CO)_3Br(PPhMe_2)_2] + N_2H_4 \longrightarrow [M(CO)_2(NCO)(N_2H_4)(PPhMe_2)_2] \quad (M = Mn \text{ and } Re) \quad (1.21)$$

In these examples hydrazine attacks a carbonyl ligand to form an isocyanate in preference to attack on the metal.

In other reactions with transition metal ions, hydrazine displays its redox character.

Oxidation of hydrazine is in itself difficult to study due to the instabilty of intermediates, but substitution of the protons of hydrazine by alkyl or aryl functions allows the isolation of oxidised intermediates or their transition metal complexes [18].

For example, the oxidation of arylhydrazines to diazonium salts by first-row transition metals in acid solution, proceeds via formation of diazene intermediates. Such intermediates can be isolated from the reaction of $Cu^{II}X_2$ with $PhNHNH_2$ (1.22) [80].

$$CuX_2 + PhNHNH_2 \longrightarrow [Cu_4X_4(PhN{=}NH)] \quad (X=Cl, Br) \quad (1.22)$$

A crystal structure determination of the similarly prepared complex $[Cu_2Cl_2(MeN{=}NMe)]$ shows dimethyldiazene molecules bridging between infinite chains of copper(I) chloride [81].

The reactions of hydrazine ligands with oxo-containing complexes lead to a different range of oxidised species. For example, reactions of the dithiocarbamato-complexes $[MoO_2(S_2CNR_2)_2]$ (R=Me,Et,Ph) with $R'R'NNH_2$ (R'=Me,Et) give the hydrazido(2-) complexes $[MoO(NNR'_2)(S_2CNR_2)_2]$ [82]. These species can also be prepared by the alkylation of coordinated dinitrogen in the complexes $[M(N_2)_2(dppe)_2]$, (M=Mo,W; dppe=$Ph_2PCH_2CH_2PPh_2$) (1.23) [83].

$$[M(N_2)_2(dppe)_2] + RBr \xrightarrow[C_6H_6]{h\nu} [MBr(N_2R)(dppe)_2] \underset{K_2CO_3}{\overset{HBr}{\rightleftharpoons}} [MBr_2(N_2HR)(dppe)_2] \quad (1.23)$$

Also the reaction of the acetylacetonate complex $[MoO_2(acac)_2]$ with $PhNHNH_2$ in methanol gives the diazenido complex $[Mo(N_2Ph)_2(acac)(\mu\text{-}OMe)]_2$ [84].

1.4 ALKYL- AND ARYL-HYDRAZINE COORDINATION CHEMISTRY

Alkyl or aryl substitution of hydrazine reduces its ability to behave as a bidentate bridging ligand, and most alkyl- and aryl-substituted hydrazines function as simple unidentate ligands towards non-oxidising transition metal ions. With substituted hydrazines e.g. $MeNHNH_2$, Me_2NNH_2 and $PhNHNH_2$, acting as unidentate ligands, linkage isomers are clearly possible although none appear to have been isolated.

1.4.1 METHYLHYDRAZINE

Methylhydrazine gives complexes with the non-oxidising transition metal ions Fe(II),Co(II) and Ni(II) of stoichiometry $[MX_2(MeNHNH_2)_2]_n$ (X=halide) [25,26,40,85]. The complexes are polymeric, but there is no direct evidence of the coordination mode of the methylhydrazine ligands due to the lack of structural studies. It is probable that methylhydrazine is capable of bridging coordination as the methyl group is unlikely to present a serious steric crowding factor. Also the inductive effect of the methyl group relative to a hydrogen of hydrazine would enhance the basic character of that nitrogen. Thus in $[Co(MeNHNH_2)_6]Cl_2$ the unidentate methylhydrazine ligands are held to be coordinated via the methyl nitrogen atoms [25].

1.4.2 1,1-DIMETHYLHYDRAZINE

Even fewer transition-metal complexes containing 1,1-dimethylhydrazine have been reported. However, two X-ray crystal structures of complexes containing 1,1-dimethylhydrazine have been reported. The structure of $[RuH(\eta^4\text{-cod})(NH_2NMe_2)_3][PF_6]$ (cod=cyclo-octa-1,5-diene) shows that the unidentate Me_2NNH_2 ligands are coordinated to the ruthenium by the unsubstituted nitrogen (FIGURE No 1.9) [48]. The three Me_2NNH_2 ligands are futher stabilised by strong hydrogen bonds (mean = 2.90 Å) which minimize the non-bonded contacts between the bulkly NMe_2 groups. Electronically, the more basic nitrogen donor atom would be the dimethyl nitrogen, but evidently steric factors outweigh electronic effects.

Remarkably, an alternative coordination mode is exhibited by Me_2NNH_2 in the closely related $[(RuCl(H)(\eta^4\text{-cod}))_2(\mu\text{-}NH_2NMe_2)]$ [49].

FIGURE No 1.9 Structure of the $[RuH(\eta^4\text{-cod})(NH_2NMe_2)_3]^+$ Cation

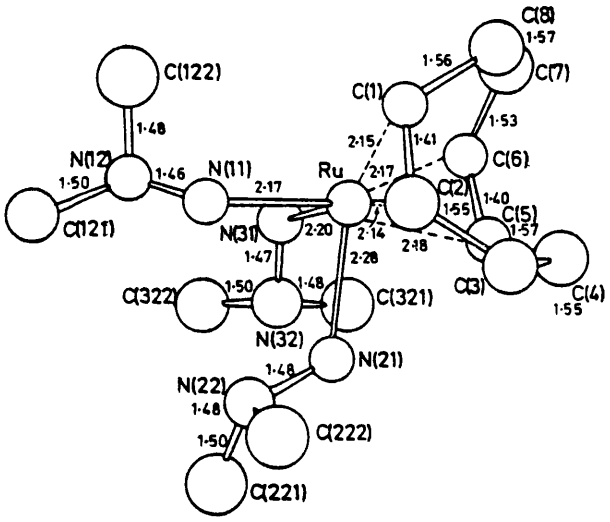

In this complex X-ray diffraction shows the Me_2NNH_2 to act as bidentate bridging ligand between two ruthenium atoms (FIGURE No 1.10).

There is significant distortion from a symmetrical arrangement which can be ascribed to the steric hindrance of the two methyl groups ($Ru\text{-}NH_2$ = 2.12Å, $Ru\text{-}NMe_2$ = 2.24Å). This structure shows that even Me_2NNH_2 is capable of bridging coordination under favourable circumstances.

FIGURE No 1.10 Structure of $[\{RuCl(H)(\eta^4\text{-cod})\}_2(\mu\text{-}NH_2NMe_2)]$

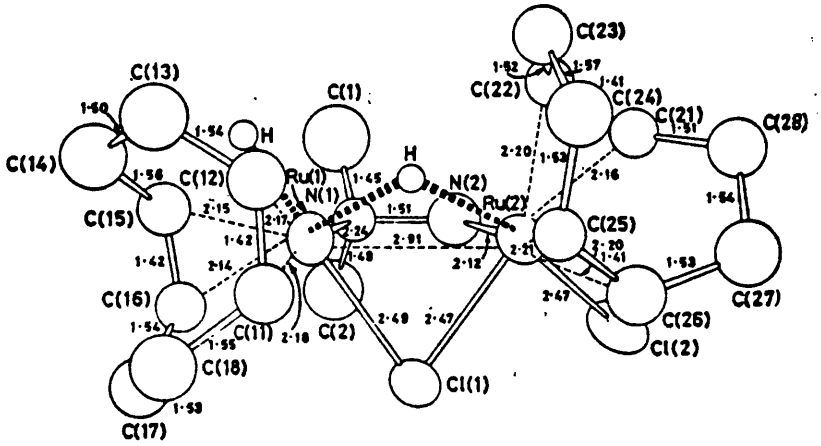

One further series of complexes have been reported where the coordination mode of dimethylhydrazine is unequivocally known. The species $[Co(Me_2NNH_2)_2X_2]$ (X=Cl,Br,I,NCS) [25,85] are known to be tetrahedral from electronic and magnetic measurements and therefore can only contain unidentate dimethylhydrazine.

1.4.3 PHENYLHYDRAZINE

The presence of the aryl substituent of phenylhydrazine results in mesomeric electron drainage from the -NHPh nitrogen of this ligand. The terminal $-NH_2$ therefore electronically becomes the most basic donating site. Additionally the -NHPh lone pair will be conjugated to some degree with the phenyl delocalized system, thus making it less available for donation.

Phenylhydrazine reacts with the non-oxidising transition metal ions Mn(II),Fe(II),Co(II),Ni(II) and Pd(II) as well the Group 10 metals Zn(II) and Cd(II) giving complexes with the stoichiometry $[MX_2(NH_2NHPh)_2]_n$ (X=Cl,Br or I) [86,87].

A Soviet group led by M.S.Novakovskii has published an extensive series of papers on the coordination behaviour of phenylhydrazine and mono-substituted phenylhydrazines towards first-row transition and Group 10 metals. Complexes of the types $[MX_2(R\text{-}C_6H_4NHNH_2)_2]$ (M=Fe,Co,Ni,Zn,Cd: R=H, *o*-Cl, *o*-Br, *p*-Br, *o*-OMe, *m*-OMe, *p*-OMe, *p*-NO_2 etc : X=Cl,Br,I etc) have been isolated [88].

The majority of these complexes are insoluble polymeric species with the nature of the bridging ligands being uncertain, although bridging halide seems likely. In certain complexes where the phenyl substitutent is a group capable of coordination (e.g. NO_2), bridging substituted hydrazine has been proposed [89].

Phenylhydrazine complexes have not been restricted to d block elements. Reactions of the lanthanide salts $MCl_3.xH_2O$ with $PhNHNH_2$ have been reported to give $[MCl_3(PhNHNH_2)_2].H_2O$ complexes (M=Y, La, Ce, Pr, Nd and Sm) [90].

In addition, phenylhydrazine was reported to react with $TiCl_4$ to give a product analysing to $TiCl_4(PhNHNH_2)_2$, which was thought to be the solvolysis mixture $TiCl_3(PhNHNH)$ and $PhNHNH_3Cl$, and so involves a phenylhydrazido(1-) moiety [91].

No crystal structures have been reported for $[MX_2(PhNHNH_2)_2]$ complexes. However two distinct modes of coordination have been established through X-ray crystal structure determinations. *p*-Fluorophenylhydrazine bonds in a unidentate manner in $[PtCl(NH_2NHC_6H_4-p-F)(PEt_3)_2][BF_4]$, as expected from the above arguments [50]. Unexpectedly, in $[(\eta^5-C_5H_5)Mo(NO)I(NH_2NHPh)][BF_4]$, phenylhydrazine acts as a bidentate chelating ligand, the only known example of a simple hydrazine exhibiting this type of coordination mode (see FIGURE No 1.11) [51]. One explanation for this coordination is that the complex was prepared by protonation of $[(\eta^5-C_5H_5)Mo(NO)I(NHNHPh)]$ in which the hydrazido(1-) function may also be dihapto-bonded. Protonation of this ligand may then result in the generation of the phenylhydrazine without change in coordination mode. It seems reasonable to suspect that the majority of known phenylhydrazine complexes contain unidentate phenylhydrazine as found in $[PtCl(NH_2NHC_6H_4F)(PEt_3)_2][BF_4]$.

FIGURE No 1.11 Structure of the [(η^5-C_5H_5)Mo(NO)I(η^2-NH_2NHPh)]

Cation

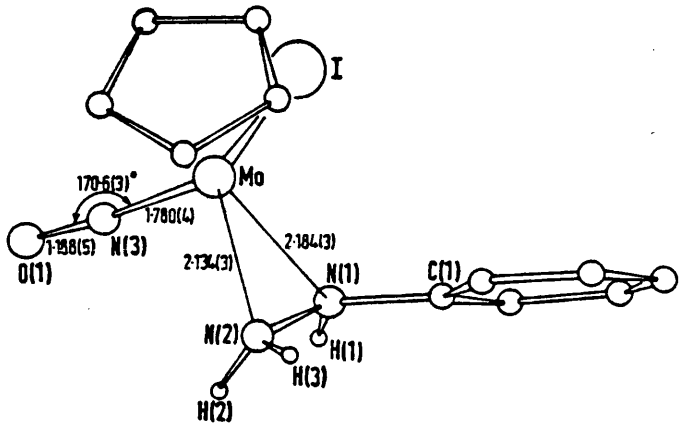

1.5 CARBAZATE COORDINATION CHEMISTRY

The reaction of N_2H_4 with CO_2 does not give hydrazinium carbonate, but initially results in a syrupy liquid, hydrazinium carbazate, $[N_2H_5][O_2CNHNH_2]$, which with an excess of CO_2 reacts futher to give carbazic acid, $\overset{-}{O}_2CNH\overset{+}{N}H_3$.

1.5.1 HISTORY

The reactions of carbazic acid (and hydrazinium carbazate) with metal salts have been only spasmodically investigated since Stollé and Hoffmann discovered the acid and described the sodium and barium salts (the latter was subsequently formulated as a hydrazine dicarboxylate salt) in 1904 [6]. The unstable ammonium salt was prepared by Fichter and Becker in 1911 [92], and the first transition metal chelates, $M(O_2CNHNH_2)_2$ (M=Ni,Cu) appear to have been reported by Callegari in 1906 [93]. Ebler and Schott found the product of the reaction between metallic zinc and $N_2H_4.H_2O$ exposed to the air to be the complex $[Zn(O_2CNHNH_2)_2(N_2H_4)_2]$ [94]. These workers believed the carbazate groups to be unidentate coordinated to the zinc through an oxygen of the carboxylate.

A Georgian group of workers led by P.V.Gogorishvili investigated the formation of cobalt and nickel carbazates from a large range of starting materials during the late 1950's. For example the reaction of either $[Co(NH_3)_5Cl]Cl_2$ or $[Co(N_2H_4)_2Cl_2]_n$ with $N_2H_3CO_2H$ in H_2O was reported to form the cobalt(II) complex, $Co(O_2CNHNH_2)_2(N_2H_4)$ which was thought to contain both 5-membered carbazate and 3-membered hydrazine chelate rings [95,96]. The action of $N_2H_4.H_2O$ with CO_2 on these and other cobalt salts gave what was formulated as $[(NH_2NHCO_2)_2Co(N_2H_5)_2CO_3]$ [97]. Identical

product stoichiometries were found for similar reactions using nickel salts [98,99].

It was not until the 1960's that systematic studies of metal-carbazate reactions were undertaken. In 1965 Funk, Eichoff and Giesder described a variety of preparative routes for metal carbazates. This proved to be the first extensive report of transition and non-transition metal carbazate chemistry [100].

At that time, a group of Italian workers led by A.Ferrari and A.Braibanti started to publish a series of reports on hydrazine and carbazate coordination behaviour [101]. The importance of these reports is that they include the majority of carbazate X-ray crystal structure determinations that have been carried out to date. These workers were also concerned with the vibrational spectroscopic features of the complexes and this work has provided the baseline for all later comparative studies [22]. However this group seem to have terminated their activity in carbazate chemistry, no publications dated later than 1971 having appeared.

More recent studies reported by Indian and Yugoslav workers have kept carbazate chemisty alive. Of particular interest to the Indian group has been the thermal decomposition of metal carbazates as precursors of metal/metal oxide dispersions [102].

1.5.2 PREPARATIONS

FIG No 1.12 shows the elements which are known to form carbazate compounds. A notable feature is the absence of heavy transition metal carbazate complexes (with the exception of zirconium which is reported to form $ZrO(O_2CNHNH_2)_2.H_2O$ [103]).

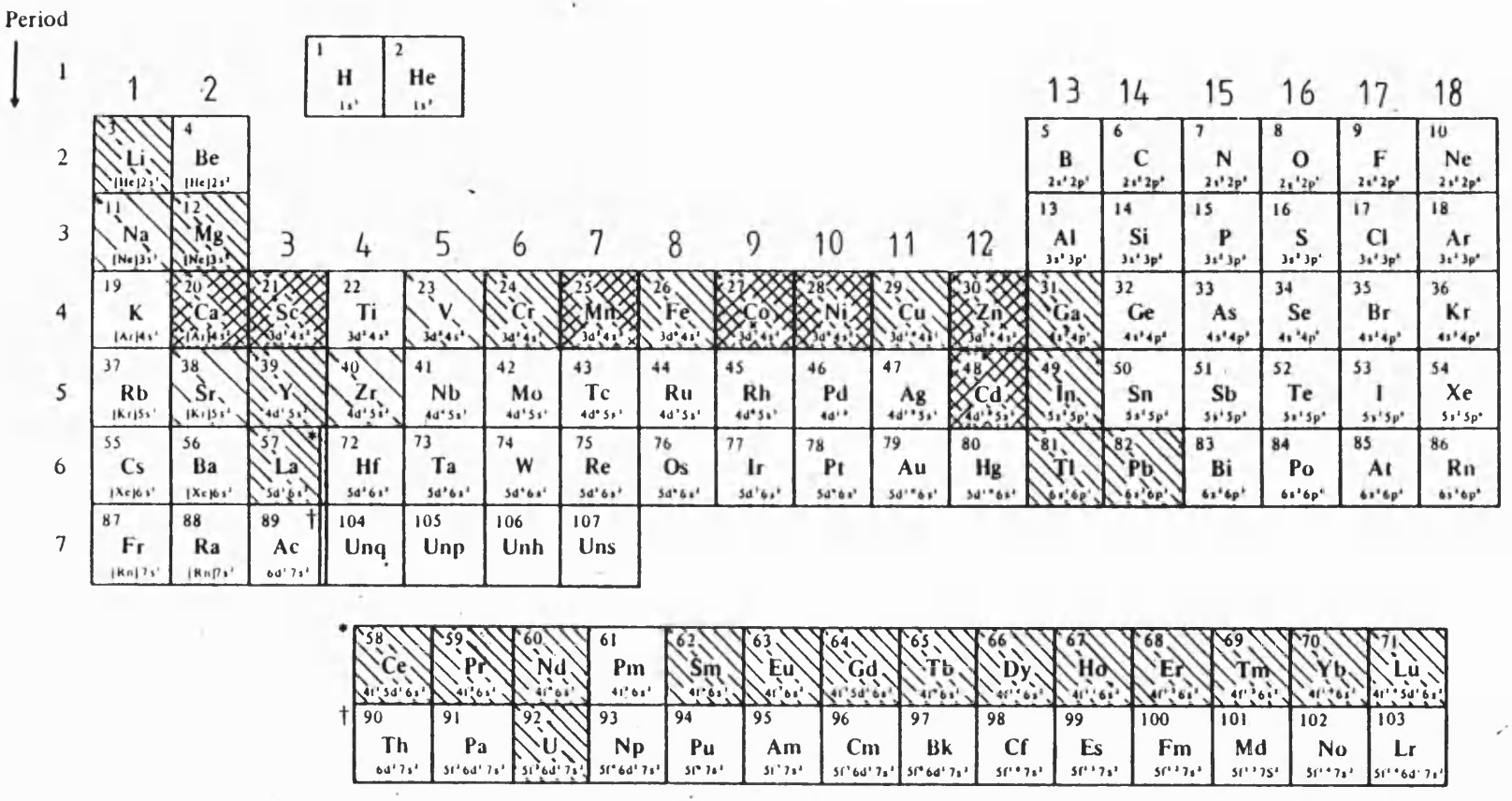

FIGURE No 1.12 Periodic Table listing Elements that are known to form Carbazate Compounds.

Comparison with the reactions betweeen N_2H_4 and these metal ions may indicate that unprotonated carbazate complexes of the second and third row transition metals will prove difficult to prepare, but this remains to be tested.

Other gaps in the Table illustrate the fragmentary knowledge of carbazate chemistry. For example, in Group 2 both magnesium and calcium carbazates are well known, whilst the beryllium salt has not been reported. Other metals in this Group should equally be able to form carbazates but presumably the reactions have never been attempted (a strontium carbazate has been reported but it has not been isolated in a pure form [104]).

In other areas of the Table it is probable that elements will form carbazates, but remain to be investigated (germanium and tin are promising candidates). The lack of a mercury carbazate is also surprising. Although susceptible to reduction in the presence of hydrazine species, mercury(II) hydrazine complexes are well known [105], and therefore there appears no additional barrier to mercury(II) carbazate formation.

TABLE No 1.6 Product Stoichiometries formed by Divalent Metal Carbazates

Complex Stoichiometry	Metal Ions
$[N_2H_5][M(O_2CNHNH_2)_3].H_2O$	Mg, Fe, Co, Ni, Zn
$[M(O_2CNHNH_2)_2(N_2H_4)_x]$ x=1 or 2	x=1 Ni, Co x=2 Mn, Fe, Co, Ni, Zn
$[M(O_2CNHNH_2)_2]_n$	Ca, Mn, Fe, Cu, Zn, Cd
$[M(O_2CNHNH_2)_2.xH_2O]$	x=1 Ca, Cd x=2 Mg, Mn, Fe, Co, Ni, Zn, Cd

The best characterised metal carbazates are those formed by the divalent ions of the first-row transition metals and those of Groups 2 and 12.

The preparation of these metal carbazates generally involve the interaction of a metal salt (e.g. halide, acetate, hydroxide, sulphate etc) with hydrazinium carbazate in aqueous solution. Dependent upon reaction conditions a number of product stoichiometries can be formed (see TABLE No 1.6).

In early reports of carbazate work, products of formulae $M(O_2CNHNH_2)_2(N_2H_5)_2CO_3$ were proposed [97,99,106]. However, an X-ray structural determination of the nickel example showed the correct formulation to be $[N_2H_5][M(O_2CNHNH_2)_3].H_2O$ [107].

Dilute solutions of $[N_2H_5][O_2CNHNH_2]$ with divalent metal salts generally give hydrates or hydrazinates of bis(carbazato)metal(II) complexes, while concentrated solutions (> 15%) give hydrazinium tris(carbazato)metallates . For example, when carbon dioxide is passed through an aqueous hydrazine solution of metal salt, $[N_2H_5][M(O_2CNHNH_2)_3].H_2O$ (M=Fe,Co,Ni,Zn) is formed, but if similar solutions are allowed to absorb carbon dioxide from the atmosphere, $[M(O_2CNHNH_2)_2(N_2H_4)_2]$ is preferentially formed [108]. Also mono-(hydrazinates) of the bis(carbazates) form in preference to bis(hydrazinates) when the carbazate:metal salt ratio is high.

Apart from the use of metal salts in the formation of tris(carbazato) complexes, the metals themselves can be employed under certain circumstances. The reaction of magnesium powder with aqueous solutions of $[N_2H_5][O_2CNHNH_2]$ leads to the formation $[N_2H_5][Mg(O_2CNHNH_2)_3].H_2O$ [108].

The formation of $[N_2H_5][M(O_2CNHNH_2)_3].H_2O$ (M=Fe,Co,Ni) has also been achieved by reaction of ammonium metal double sulphates with $N_2H_4.H_2O$ in the presence of air (1.24) [109].

$$(NH_4)_2M(SO_4)_2.6H_2O + 6N_2H_4.H_2O \longrightarrow [N_2H_5][M(O_2CNHNH_2)_3].H_2O \quad (1.24)$$

The hydrazinium tris(carbazato)metallates also undergo a limited series of reactions, usually resulting in the formation of bis-(carbazate) species.

Reaction of $[N_2H_5][M(O_2CNHNH_2)_3].H_2O$ (M=Fe,Co,Ni,Zn) with KOH yields the complexes, $K[M(O_2CNHNH_2)_3]$. The isolation of these complexes demonstrates the existence of the $[M(O_2CNHNH_2)_3]^-$ anions in solution during these reactions [110,110A].

Hydrolytic transformation of $[N_2H_5][M(O_2CNHNH_2)_3].H_2O$, by suspension in H_2O, results in the formation of bis(carbazate) species e.g. $M(O_2CNHNH_2)_2(H_2O)_2$ (M=Co,Ni) and $M(O_2CNHNH_2)_2$ (M=Zn) [111,112].

A series of carbazate interchange reactions involving the tris-(carbazato)iron(II) anion has been reported (FIG No 1.13) [113].

FIGURE No 1.13 Reactions of Iron(II) Carbazate Species.

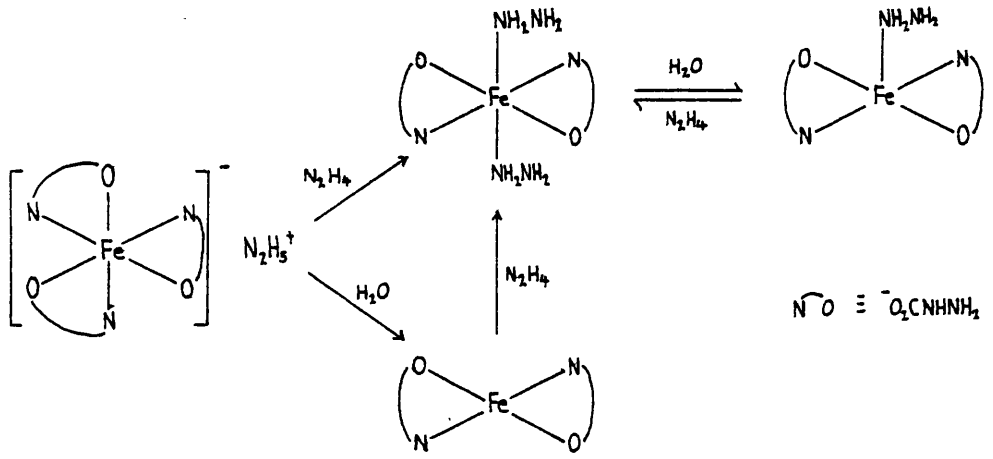

The bis(carbazato)bis(hydrazine) metal(II) complexes (M=Mn,Co,Ni,Zn) can also prepared by the evaporation of ammoniacal aqueous solutions of metal halide salts in the presence of $N_2H_4.H_2O$, the CO_2 necessary for carbazate formation being absorbed from the atmosphere [114].

Divalent non-transition metal salts generally form bis(carbazato) complexes, anionic tris(carbazato)magnesate being the sole exception known at present [108]. Evaporation of aqueous solutions of $Ca(OH)_2$ and $[N_2H_5][O_2CNHNH_2]$ initially yields $Ca(O_2CNHNH_2)_2.H_2O$ which on standing transforms to $Ca(O_2CNHNH_2)_2$ [115]. Cadmium carbazates are formed in a similar manner. Evaporation of aqueous solutions of $CdCl_2$ or $Cd(O_2CMe)_2$ and $[N_2H_5][O_2CNHNH_2]$ produces both anhydrous and monohydrated $Cd(O_2CNHNH_2)_2$ [116].

Adduct formation by preformed bis(carbazato)metal complexes appears rare. However, Srivastava claimed the reaction of copper(II) carbazate with pyridine or diethylamine yielded the adducts $Cu(O_2CNHNH_2)_2L_2$ (L=py,Et_2NH) [117]. This work is open to question as other workers have failed to repeat the reactions [118].

Trivalent metal ions generally form only tris(carbazato) complexes. For example the reaction of chromium(III) chloride with $[N_2H_5][O_2CNHNH_2]$ under aqueous conditions yields $Cr(O_2CNHNH_2)_3.2H_2O$ (1.25) [100].

$$[Cr(OH_2)_4Cl_2]Cl.2H_2O + 3[N_2H_5][O_2CNHNH_2] \xrightarrow{H_2O} Cr(O_2CNHNH_2)_3.2H_2O \qquad (1.25)$$

Lanthanide trichlorides react with $[N_2H_5][O_2CNHNH_2]$ in H_2O to form $Ln(O_2CNHNH_2)_3.3H_2O$ (Ln=Ce, Pr, Nd, Sm, Eu, Gd, Tb, Dy, Ho, Er, Tm, Yb and Lu) [119]. Lanthanum itself under similar conditions forms the complex, $La(O_2CNHNH_2)_3.2H_2O$. X-ray diffraction measurements show $Ln(O_2CNHNH_2)_3.3H_2O$ are isostructural with $Y(O_2CNHNH_2)_3.3H_2O$ but not with the lanthanum complex [120]. The remaining Group 3 congener, scandium, forms an unusual tetra(carbazato) complex on reaction with $[N_2H_5][O_2CNHNH_2]$. The complex has been shown by X-ray single crystal analysis to be $[N_2H_5][Sc(O_2CNHNH_2)_4].3H_2O$ [121].

Group 13 trivalent metal salts also form tris(carbazato) species. The reaction of $Ga(NO_3)_3$ with $[N_2H_5][O_2CNHNH_2]$ in H_2O gives $Ga(O_2CNHNH_2)_3.H_2O$, while under similar conditions $InCl_3$ reacts to give $In(O_2CNHNH_2)_3$. Reactions of trivalent aluminium salts with $[N_2H_5][O_2CNHNH_2]$ under aqueous conditions did not yield a pure aluminium carbazate [122]. The remaining member of Group 13, thallium is also known to form a carbazate under similar conditions, but this is the univalent $Tl(O_2CNHNH_2)$ [100].

Although the majority of trivalent metal carbazates contain tris(carbazato) species, Gogorishvili and Karkarashvili reported the reaction of the cobalt(III) species, $[CoCl_2(en)_2]Cl$ with $\overset{-}{O_2}CNH\overset{+}{N}H_3$ in H_2O gave $[Co(O_2CNHNH_2)(en)_2]Cl.H_2O$. Reaction with excess $\overset{-}{O_2}CNH\overset{+}{N}H_3$ resulted in reduction and formation of $[N_2H_5][Co(O_2CNHNH_2)_3]H_2O$ (1.26) [123].

$$[Co^{III}Cl_2(en)_2]Cl + \overset{-}{O_2}CNH\overset{+}{N}H_3 \xrightarrow{H_2O} [Co^{III}(O_2CNHNH_2)(en)_2]Cl.H_2O \quad (1.26)$$

$$\downarrow + 4\ \overset{-}{O_2}CNH\overset{+}{N}H_3/H_2O$$

$$[N_2H_5][Co^{II}(O_2CNHNH_2)_3].H_2O$$

A number of oxocation carbazate species have been reported. The reactions of vanadyl, zirconyl and uranyl salts in ethanol with aqueous solutions of $[N_2H_5][O_2CNHNH_2]$ yield $VO(O_2CNHNH_2)_2.H_2O$, $ZrO(O_2CNHNH_2)_2.H_2O$ and $UO_2(O_2CNHNH_2)_2.H_2O$, respectively [103]. A futher uranyl species has been reported. The dissolution of $(NH_4)_2U_2O_7$, $UO_2(NO_3)_2.6H_2O$ or UO_3 in aqueous $[N_2H_5][O_2CNHNH_2]$ gives $UO_2(O_2CNHNH_2)_2.N_2H_4.H_2O$ [124]. This formulation indicates the presence of both N_2H_4 and H_2O, which is not found in other carbazates and must be thought of as unlikely due to the acid/base reactions which these species undergo together.

1.5.3 STRUCTURES

The coordination potential of the carbazate anion is expected to be similar in scope to that displayed by the isoelectronic glycinate anion. This has been confirmed unambiguously by X-ray structural studies which show carbazate acting as a *N,O*-bidentate ligand (see FIG No 1.14).

FIGURE No 1.14 Comparison of Coordination of Glycinate and Carbazate Anions.

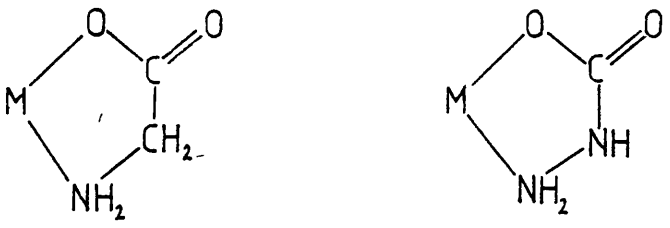

An additional mode of coordination shown by carbazate is as a tridentate ligand. In addition to the usual *N,O*-chelation, the

second carboxylate oxygen bridges to a further metal atom (see FIG No 1.15).

FIGURE No 1.15 Tridentate Coordination of the Carbazate Anion.

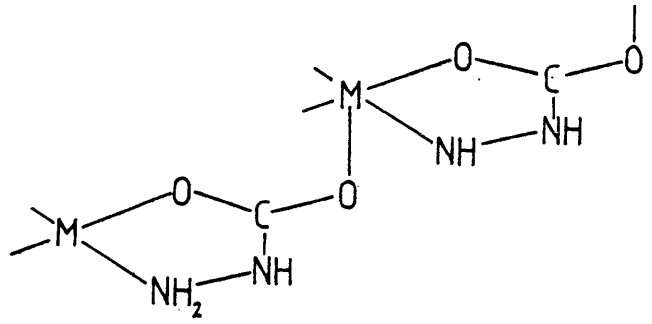

TABLE No 1.7 lists the transition and main-group metal complexes that have been adequately characterised by spectroscopic and X-ray structural techniques. The X-ray structural studies reveal a variety of stereochemistries and molecular structures. Carbazate complexes chararacterised by X-ray single crystal analysis are listed in TABLE No 1.8.

TABLE No 1.7 Adequately Characterised Carbazate Complexes

Metal Carbazate	Preparation	Characterisation
GROUP 1		
Lithium		
$Li(O_2CNHNH_2).H_2O$	[100]	
GROUP 2		
Magnesium		
$[N_2H_5][Mg(O_2CNHNH_2)_3].H_2O$	[108]	[108]
$Mg(O_2CNHNH_2)_2.2H_2O$	[104,127]	[22,125,127]

Calcium

$Ca(O_2CNHNH_2)_2,H_2O$	[104,115,127]	[22,125,128]
$Ca(O_2CNHNH_2)_2$	[115,127]	[115,127]

GROUP 3

Scandium

$[N_2Hs][Sc(O_2CNHNH_2)_4],3H_2O$	[120]	[121,125]

Yttrium

$Y(O_2CNHNH_2)_3,3H_2O$	[120]	[119]

Lanthanum

$La(O_2CNHNH_2)_3,2H_2O$	[100]	[119]

GROUP 4

Zirconium

$ZrO(O_2CNHNH_2)_2,H_2O$	[103]	[103]

GROUP 5

Vanadium

$VO(O_2CNHNH_2)_2,H_2O$	[103]	[103]

GROUP 6

Chromium

$Cr(O_2CNHNH_2)_3,2H_2O$	[15,100]	[125]

GROUP 7

Manganese

$Mn(O_2CNHNH_2)_2(N_2H_4)_2$	[108,114]	[108,114]
$Mn(O_2CNHNH_2)_2.2H_2O$	[108,111,133,139]	[108,125,132,133]
$Mn(O_2CNHNH_2)_2$	[100]	[134]

GROUP 8

Iron

$[N_2Hs][Fe(O_2CNHNH_2)_3],H_2O$	[15,100,106,108,133]	[22,106,108,125,133,137,138]
$K[Fe(O_2CNHNH_2)_3]$	[110]	[22,110A,137]
$Fe(O_2CNHNH_2)_2(N_2H_4)_2$	[15,108]	[108]
$Fe(O_2CNHNH_2)_2,2H_2O$	[113,135]	
$Fe(O_2CNHNH_2)_2$	[100]	

GROUP 9

Cobalt

$[N_2H_5][Co(O_2CNHNH_2)_3].H_2O$	[96,97,100,106,108,133]	[22,106,125,133]
$K[Co(O_2CNHNH_2)_3]$	[110]	[22,110A,125]
$Co(O_2CNHNH_2)_2(N_2H_4)_2$	[95,96,108,114]	[22,108,114,125,131]
$Co(O_2CNHNH_2)_2(N_2H_4)$	[125]	[125]
$Co(O_2CNHNH_2)_2.2H_2O$	[97,100,111]	[22,125]
$Co(O_2CNHNH_2)_2$	[95,97,125]	[125,134]

GROUP 10

Nickel

$[N_2H_5][Ni(O_2CNHNH_2)_3].H_2O$	[99,100,106,107,108,133]	[22,106,107,108,125,133,140]
$K[Ni(O_2CNHNH_2)_3]$	[110]	[22,110A]
$Ni(O_2CNHNH_2)_2(N_2H_4)_2$	[114,136]	[22]
$Ni(O_2CNHNH_2)_2(N_2H_4)$	[15,98,114]	[114]
$Ni(O_2CNHNH_2)_2.2H_2O$	[99,100,111]	[22,130]
$Ni(O_2CNHNH_2)_2$	[93]	[134]

GROUP 11

Copper

$Cu(O_2CNHNH_2)_2$	[93,100,133]	[118,125,133,134]

GROUP 12

Zinc

$[N_2H_5][Zn(O_2CNHNH_2)_3].H_2O$	[106,108,133]	[22,106,108,133]
$K[Zn(O_2CNHNH_2)_3]$	[110]	[22,110A]
$Zn(O_2CNHNH_2)_2(N_2H_4)_2$	[22,94,114,129]	[22,114,129]
$Zn(O_2CNHNH_2)_2$	[100,112]	[112,134]

Cadmium

$Cd(O_2CNHNH_2)_2.2H_2O$	[111,116]	[22,116]
$Cd(O_2CNHNH_2)_2$	[116,126]	[126]

GROUP 13

Gallium

$Ga(O_2CNHNH_2)_3.H_2O$	[122]	[122]

Indium

$In(O_2CNHNH_2)_3$	[122]	[122]

Thallium

$Tl(O_2CNHNH_2)$	[100]

GROUP 14

Lead

$Pb(O_2CNHNH_2)_2$	[100]	

4f (Lanthanide) Metals; Ln = Ce,Pr,Nd,Sm,Eu,Gd,Tb,Dy,Ho,Er,Tm,Yb,Lu

$Ln(O_2CNHNH_2)_3.3H_2O$	[119]	[119]

5f (Actinide) Metals

Uranium

$UO_2(O_2CNHNH_2)_2.H_2O$	[103]	[103]
$UO_2(O_2CNHNH_2)_2.N_2H_4.H_2O$	[124]	[124]

NOTE; Characterisation of metal carbazates has mainly been achieved by X-ray single crystal/powder diffraction, infra-red and thermal decomposition analysis. In the case of transition metal carbazates very little electronic spectral and magnetic susceptibility data has been published. The tris(carbazato)iron(II) species have been characterised by Mössbauer spectra [137,138].

TABLE No 1.8 X-ray Crystal Structure Characterisation of Metal Complexes

Complex	Reference
$Ca(O_2CNHNH_2)_2.H_2O$	[128]
$Ca(O_2CNHNH_2)_2$	[115]
$[N_2H_5][Sc(O_2CNHNH_2)_4].3H_2O$	[121]
$Mn(O_2CNHNH_2)_2.2H_2O$	[132]
$Co(O_2CNHNH_2)_2(N_2H_4)_2$	[131]
$[N_2H_5][Ni(O_2CNHNH_2)_3].H_2O$	[107,140]
$Ni(O_2CNHNH_2)_2.2H_2O$	[130]
$Zn(O_2CNHNH_2)_2(N_2H_4)_2$	[129]
$Zn(O_2CNHNH_2)_2$	[112]
$Cd(O_2CNHNH_2)_2.H_2O$	[116]
$Cd(O_2CNHNH_2)_2$	[126]

In general, transition metal complexes complexes fall into three structural types (see FIG No 1.16)

FIG No 1.16 Metal-Carbazate Structural Types

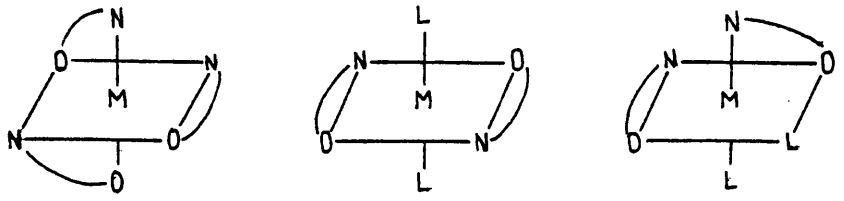

$\overset{N}{\frown}\overset{O}{} = O_2CNHNH_2$ L = N_2H_4, H_2O L = H_2O, O-CONHNH$_2$

The tris(carbazato)metallate(II) anions, as shown by the X-ray crystal structure of $[N_2H_5][Ni(O_2CNHNH_2)_3].H_2O$, contain carbazate ligands *N,O*-chelated with the oxygen and nitrogen atoms both in a *fac*-configuration around the pseudo-octahedrally bound metal ion [107]. The complex is racemic with both enantiomers co-existing within the crystal. The hydrazinium and water molecules are bound to the anion by hydrogen bonding.

The bis(carbazato)metal complexes, however, show a variety of geometries. The bis(carbazato)bis(hydrazine)metal complexes $[M(O_2CNHNH_2)_2(N_2H_4)_2]$ (M=Mn,Fe,Co,Ni,Zn), as shown by X-ray crystal structures of the Co(II) and Zn(II) species [131,129], have the bidentate carbazate ligands *N,O*-bound in a trans-configuration. The unidentate hydrazines occupy the remaining axial positions (see FIG No 1.17).

A similar coordination geometry is exhibited by $Ni(O_2CNHNH_2)_2$-$2H_2O$, the two water molecules occupying similar positions to the hydrazine molecules in $[M(O_2CNHNH_2)_2(N_2H_4)_2]$. [130]

FIGURE No 1.17 X-ray Crystal Structure of $[Co(O_2CNHNH_2)_2(N_2H_4)_2]$

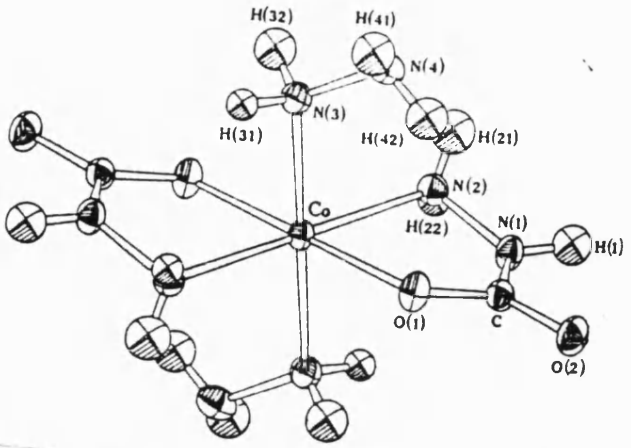

However, $Ni(O_2CNHNH_2)_2.2H_2O$ is not isostructural with other $M(O_2CNHNH_2)_2.2H_2O$ complexes. X-Ray diffraction data show the complexes with M=Mg and Co to be similar to $Mn(O_2CNHNH_2)_2.2H_2O$ for which a single crystal X-ray structural study has been reported [132]. This complex contains chains formed by two types of octahedral chelates, bridged by tridentate carbazate ligands. The first type of octahedron is constructed by two *N,O*-coordinated carbazate chelate groups, occupying four sites, with the two remaining coordination sites taken up by oxygens atoms of bridging carbazate groups. The second structural unit has the same geometric arrangement of donor atoms except that two coordinated water molecules replace the bridging groups (see FIG No 1.18). The chains are cross-linked by hydrogen bonding, either direct chain-to-chain or via waters of crystallisation.

FIGURE No 1.18 Molecular Structure of '$Mn(O_2CNHNH_2)_2.2H_2O$'

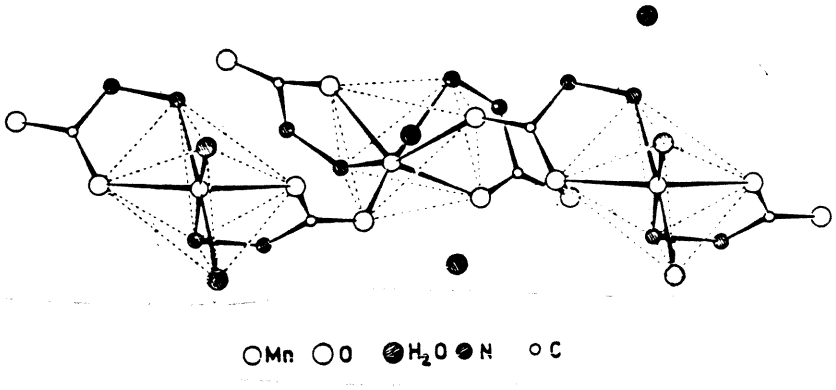

Polymeric, anhydrous $[Zn(O_2CNHNH_2)_2]_n$ displays a futher geometric variation. Again a tridentate carbazate group is used as a bridging ligand to form an infinite chain, but the geometry around the zinc differs from first-row transition metal carbazates in being square pyramidal [112]. Two carbazate anions *N,O*-chelate trans to each other with the fifth coordination site occupied by an oxygen from a bridging carbazate (see FIG No 1.19). The sixth coordination site trans to this bond is empty.

FIGURE No 1.19 X-ray Crystal Structure of $[Zn(O_2CNHNH_2)_2]_n$

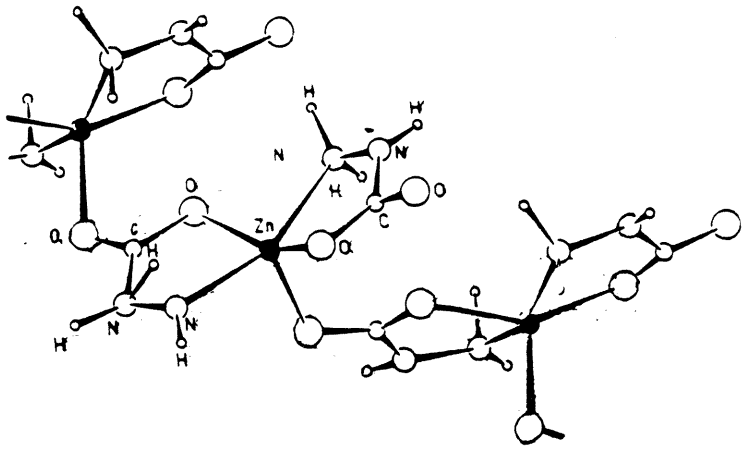

One futher structural characterisation of a metal carbazate of interest is that of $[N_2H_5][Sc(O_2CNHNH_2)_4].3H_2O$ which has four

chelating carbazate ligands around the scandium in a distorted quadratic antiprism arrangement [121].

In addition to metal chelates, essentially ionic carbazates are also known for some Group 1 and 2 metals. Thus $Li(O_2CNHNH_2).H_2O$, $Mg(O_2CNHNH_2)_2.2H_2O$ and $Ca(O_2CNHNH_2)_2.xH_2O$ (x=0 and 1) have been reported with single crystal structural studies performed on the calcium salts [115,128]. These show the calcium to possess a coordination number of seven, being surrounded by pseudo-chelating carbazate groups. For both the anhydrous and monohydrate species the coordination geometry around the calcium ions is pentagonal bipyramidal.

1.5.4 PROPERTIES

As the majority of metal carbazate complexes are insoluble, solid state characterisation techniques have been extensively employed to provide structural infomation.

In considering the vibrational spectroscopic features of carbazates, workers have tended to treat the coordinated ligand as a simple substituted hydrazine. Consequently only the assignments of immediately apparent vibrations such as ν(NH) and $\nu(CO_2)$ have been made. However, some structural infomation can be obtained using these assigned vibrations, although attempts have not been made to correlate vibrational spectroscopic data with known structural arrangements.

Braibanti *et al.* recorded the infra-red spectra of various metal carbazates and correlated bands appearing in the 1000 - 980 cm^{-1} region with similar bands in coordinated hydrazine spectra which they assigned to ν(N-N) [22]. This band is of slightly higher frequency in carbazates than in hydrazine complexes, a feature

ascribed to the H_2N-NH- radical being adjacent to a conjugated system. A distinction between non-coordinated and coordinated carbazates was proposed based on the broadening of the ν(NN) band on chelation.

Patil *et al.* recorded the infra-red spectra of $[N_2H_5][M(O_2CNHNH_2)_3].H_2O$ (M=Ni,Zn), $M(O_2CNHNH_2)_2(N_2H_4)_2$ (M=Fe,Co) and $M(O_2CNHNH_2)_2.2H_2O$ (M=Mg,Mn) and attempted a more complete assignment than had Braibanti *et al.* [102]. Bands present in the 1015 - 980 cm^{-1} region remained assigned to ν(NN) despite Sathyanarayana and Nicholls previously reassigning ν(NN) in coordinated hydrazine complexes to the 1170 - 1150 cm^{-1} region [141] (see SECTION 2.3). The carboxylate derived absorptions were assigned with the $\nu(CO_2)$ bands appearing in 1655 - 1620 cm^{-1} and 1510 - 1480 cm^{-1} regions. The metal-nitrogen stretching vibrations were assigned to the 430 - 415 cm^{-1} region.

As stated earlier, thermal decomposition analysis has been used to investigate the stability of metal carbazates. Results from TG/DTG/DTA experiments show that in general metal carbazates appear to thermally decompose, initially to metal oxalates and finally to metal oxides or metal powders.

Ravindranathan and Patil have performed an extensive study of the thermal characteristics of metal carbazates [108]. The *hydrazinium tris(carbazato)metallate(II) monohydrate* species decompose initially to a metal oxalate hydrazine adduct and finally to the metal oxide (1.27)

$$[N_2H_5][M(O_2CNHNH_2)_3].H_2O \longrightarrow MC_2O_4.N_2H_4 \longrightarrow MC_2O_4 \longrightarrow MO \quad (M=Fe,Co,Ni \text{ and } Zn) \quad (1.27)$$

The *bis(carbazato)bis(hydrazine)metal(II)* species decompose to the metal oxide via the anhydrous metal carbazate (1.28).

$$M(O_2CNHNH_2)_2(N_2H_4)_2 \longrightarrow M(O_2CNHNH_2)_2 \longrightarrow MO \quad (M=Mn, Fe, Co, Ni \text{ and } Zn) \quad (1.28)$$

The *bis(carbazato)metal(II) dihydrates* decompose thermally in a similar manner to the bis(hydrazinates) but with initial dehydration and an intermediate metal oxalate stage (1.29).

$$M(O_2CNHNH_2)_2.nH_2O \longrightarrow M(O_2CNHNH_2)_2 \longrightarrow MC_2O_4 \longrightarrow MO \quad (n=1, M=Ca;\ n=2, M=Mg, Mn) \quad (1.29)$$

1.6 N-SUBSTITUTED CARBAZATO COMPLEXES

Compared to metal carbazate complexes, *N*-substituted metal carbazates have received very little attention. Although, for example, a reaction between phenylhydrazine and carbon dioxide has been known for almost 100 years [142], apart from the formation of a potassium phenylcarbazate, $PhNHNHCO_2K$ [143], there has been little attempt to utilise the resulting phenylcarbazate as a ligand towards metals.

The reaction of 1,2-dimethylhydrazine with sodium hydroxide under a CO_2 atmosphere has been reported to form $MeNHNMeCO_2Na$. This salt was subsequently reacted with vanadyl, zirconyl and uranyl salts in aqueous/alcoholic media to form the complexes, $MO(O_2CMeNNHMe)_2.H_2O$ (M=V, Zr, UO) [103].

P.Bartz and H.P.Fritz reported the preparation of $[Zn(O_2CMeNNHMe)_2L_2]$ ($L=H_2O$, ½(MeNHNHMe)) in 1972, and this appears to be the first report of *N*-substituted carbazate metal complexes [144].

TABLE No 1.9 *N*-Substituted Metal Carbazates claimed by A.K.Srivastava.

Complex	Reference
Nickel(II)	
$[H_3NNHMe][Ni(O_2CMeNNH_2)_3].2H_2O$	[145]
$[PhNHNH_3][Ni(O_2CNHNHPh)_3].H_2O$	
$[Ni(O_2CNHNMe_2)_2(OH_2)_2].H_2O$	
$Ni(O_2CNHNMePh)_2.2H_2O$	
$Ni(O_2CNHNMePh)_2.2py$	
$Ni(O_2CMeNNHMe)_2.2H_2O$	
Copper(II)	
$Cu(O_2CMeNNH_2)_2.2H_2O$	[117]
$Cu(O_2CNHNHPh)_2.2H_2O$	
$Cu(O_2CNHNMe_2)_2$	
$Cu(O_2CNHNMePh)_2$	
$Cu(O_2CMeNNHMe)_2$	
Chromium(III)	
$Cr(O_2CMeNNH_2)_3$	[146]
$Cr(O_2CNHNHPh)_3$	
$Cr(O_2CNHNMePh)_3$	
$Cr(O_2CNHNHMe)_3$	
Cobalt(II)	
$Co(O_2CNHNHPh)_2.2H_2O$	[147]
$Co(O_2CNHNMe_2)_2$	
$Co(O_2CNHNMePh)_2$	
$Co(O_2CNHNPh_2)_2$	
$Co(O_2CMeNNHMe)_2$	

The only extensive investigation of the coordination potential of *N*-substituted carbazates has been undertaken by A.K.Srivastava from 1977 onwards. Complexes of nickel(II), copper(II), chromium(III) and cobalt(II) have been claimed. These are shown in TABLE No 1.9.

A number of dubious conclusions have been made concerning the nature of the compounds in TABLE No 1.9 especially with respect to the mode of coordination of substituted carbazates to the metals. For example, the CO_2 group in methylcarbazate was thought to be

positioned on the non-methylated nitrogen (3) even though the 2 position is the more basic site for nucleophilic attack. Consequently methylcarbazate was formulated as $O_2CNHNHMe^-$ whereas $O_2CMeNNH_2^-$ appears more probable on electronic grounds. Other discrepancies will be discussed in the RESULTS AND DISCUSSION sections of later chapters of this thesis.

CHAPTER No 2

MANGANESE(II) HYDRAZINE CHEMISTRY

MANGANESE(II) HYDRAZINE CHEMISTRY

In the view of the proposed role of manganese in homogeneous hydrazine decomposition [16], an investigation of the manganese(II)-hydrazine system was undertaken.

The dissolution of $MnCl_2$ in anhydrous hydrazine results in the formation of the hexakis(hydrazine) species $[Mn(N_2H_4)_6]^{2+}.2Cl^-$. This complex can be isolated as a pale blue crystalline solid by cooling a saturated $MnCl_2$-hydrazine solution. This solid rapidly loses hydrazine on drying at room temperature to give the well known bis(hydrazine) complex $[Mn(N_2H_4)_2Cl_2]_n$ (2.1) whose crystal structure has been determined [45].

Passage of carbon dioxide through a hydrazine solution of $MnCl_2$ yields the pale blue, air stable complex, $[Mn(O_2CNHNH_2)_2(N_2H_4)_2]$, a typical example of a divalent first-row transition metal carbazate (2.1a) [101]

$$MnCl_2 \xrightarrow{xs\ N_2H_4} [Mn(N_2H_4)_6]Cl_2 \xrightarrow[r.t.]{-N_2H_4} [Mn(N_2H_4)_2Cl_2]_n \quad (2.1)$$

$$[Mn(N_2H_4)_6]Cl_2 \xrightarrow{CO_2} [Mn(O_2CNHNH_2)_2(N_2H_4)_2] \quad (2.1a)$$

$[Mn(N_2H_4)_2Cl_2]_n$ can also be formed by reaction of anhydrous hydrazine with methanol solutions of $MnCl_2$. This complex is just one of an extensive series of general formula $[M(N_2H_4)_2X_2]_n$ (M = divalent first-row transition metal ion; X = halide, pseudohalide or carboxylate). The first examples of these complexes were reported in 1894 by Curtius and Schrader [19], with Franzen *et al.* completing an extensive study of 40 such complexes including the first manganese examples, $[Mn(N_2H_4)_2X_2]_n$ ($X=Cl, \frac{1}{2}(SO_4), NO_3$), in 1908-11 [21]. The manganese-hydrazine complex, $[Mn(N_2H_4)_2(NCS)_2]_n$ was

reported in 1921 by Ray and Sarkar, who noted the sensitivity of the complex to hydrolysis, quite unlike the analogous complexes $[M(N_2H_4)_2(NCS)_2]_n$ (M=Ni,Co,Zn) [148].

As the usual preparative method for these complexes consists of mixing ammonia, hydrazine hydrate and metal salt in aqueous solution, this hydrolysis may explain why manganese complexes were not reported as frequently as other metal-hydrazine complexes in early work. Few other reports appeared between this date and the start of the 1960's, but during this period of renaissance for hydrazine coordination chemistry, manganese-hydrazine complexes became as commonly reported as other transition metal-hydrazine complexes. Complexes reported include $[Mn(N_2H_4)_2X_2]_n$ with X = F [149], Cl, Br, I [22], ½(SO_4), O_2CH [150], O_2CMe and ½(C_2O_4) [151,152]. The tris(hydrazine) complex $[Mn(N_2H_4)_3(NO_3)_2]_n$ has been reported [22,153], to date the only known manganese example of this type. The crystal structure of $[Mn(N_2H_4)_2Cl_2]_n$ shows it to be isostructural with $[Zn(N_2H_4)_2Cl_2]_n$, having *syn*-bridging hydrazine ligands forming pseudo-one dimensional chains and axially coordinating chloride anions [45].

As stated above, the manganese complexes were found to decompose in the presence of water, therefore an alternative preparative method using an alcoholic medium was developed.

The complexes $[Mn(N_2H_4)_2X_2]_n$ (X=Cl, Br, I, NCO, NCS, NCSe, N_3, CH_3CO_2 and two isomers of NO_2) were prepared as microcrystalline solids. Only the complexes with X=Cl, Br, I, NCS and CH_3CO_2 have been reported previously and therefore as far as is known the complexes X=NCO, NCSe, N_3 and NO_2(I) and (II) are reported for the first time.

The complexes were prepared using two general methods. These consisted of the interaction of anhydrous hydrazine with either (a)

the manganese(II) salt (2.2) or (b) a manganese(II) salt plus a large excess of the desired anion as its sodium, potassium or ammonium salt in alcoholic media (2.3).

$$MnX_2 + 2\ N_2H_4 \xrightarrow{ROH} [Mn(N_2H_4)_2X_2]_n \quad X=Cl, Br, I, O_2CMe \qquad (2.2)$$

$$MnBr_2 + 10\ X^- + 2\ N_2H_4 \xrightarrow{ROH} [Mn(N_2H_4)_2X_2]_n \quad X=NCO, NCS, NCSe, N_3, NO_2(I) \text{ and } NO_2(II) \qquad (2.3)$$

The two separate isomers of $[Mn(N_2H_4)_2(NO_2)_2]_n$ were prepared by metathesis of $NaNO_2$ and MnX_2 (X=Br or O_2CMe) to give isomer(I), and $MnCl_2$ to give isomer(II). An aqueous/alcoholic reaction medium was used in some of the metathesis reactions to achieve sufficient dissolution of starting anion salts. The use of very large excesses of anion salt in non-aqueous solvents can result in the formation of insoluble complex anions which in turn are inert towards reaction with hydrazine (e.g. 2.4). Their formation is undesirable in procedures designed to produce $[Mn(N_2H_4)_2X_2]_n$.

$$MnX_2 + 10\ KNCO \xrightarrow{H_2O/MeOH} K_4[Mn(NCO)_6]\downarrow + 2KX \xrightarrow{N_2H_4} \qquad (2.4)$$

The complexes generally appear colourless, although some display a very pale blue colour. The complexes are susceptible to hydrolysis on contact with water, resulting in gas evolution and sample decomposition. The brown insoluble solid product is either a hydrate of manganese(III) hydroxide or manganese dioxide.

$[Mn(N_2H_4)_2(NCSe)_2]_n$ is subject to thermal decomposition at temperatures much above room temperature (~60°C), resulting in decomposition of the selenocyanate ligand and release of elemental selenium. The majority of the complexes dissolve in anhydrous

hydrazine forming $[Mn(N_2H_4)_6]^{2+}.2X^-$ species, but $[Mn(N_2H_4)_2(O_2CMe)_2]_n$ is not readily soluble, presumably as a result of additional interchain hydrogen-bonding as observed in the crystal structure of the zinc acetate analogue [44].

The complexes were characterised by solid state methods, in particular by vibrational and electron spin resonance spectroscopy.

2.1 MAGNETIC SUSCEPTIBILITY MEASUREMENTS

The room temperature magnetic moments of $[Mn(N_2H_4)_2X_2]_n$ (X = Cl, Br, I, NCO, NCS, NCSe, N_3, O_2CMe and NO_2) were measured using the Gouy method (see TABLE No 2.1). The values shown by the complexes are all close to the spin-only magnetic moment of 5.92 BM. Therefore no spin-orbit coupling is observed, confirming the presence of a high spin $3d^5$ configuration with a $^6A_{1g}$ ground state.

TABLE No 2.1 Magnetic Moments of $[Mn(N_2H_4)_2X_2]_n$ Complexes

X	μ/BM	T/K
Cl	5.80	295
Br	5.68	297
I	5.75	294
NCO	5.72	295
NCS	5.67	295
NCSe	5.75	293
N_3	5.75	294
O_2CMe	5.74	294
NO_2 (I)	5.74	296
NO_2 (II)	5.92	296

2.2 ELECTRONIC SPECTRA

The electronic transitions of d^5 high-spin systems in octahedral fields are spin-forbidden as well as parity-forbidden, resulting in the extremely pale colour of such compounds. The most noticeable features of high-spin d^5 electronic spectra are; i) the weakness of bands, ii) the large number of bands and iii) the variation in band width.

The observed d-d transitions of $[Mn(N_2H_4)_6]Cl_2$ in anhydrous hydrazine are well resolved in comparison with the diffuse reflectance electronic spectral bands of $[Mn(N_2H_4)_2X_2]_n$ (X=Cl, NCS, $MeCO_2$) (see TABLE No 2.2).

TABLE No 2.2 Comparison of $[Mn(N_2H_4)_6]^{2+}$ and $[Mn(OH_2)_6]^{2+}$ Solution Electronic Spectra/nm.

Peak Maxima/nm		Assignment
$[Mn(N_2H_4)_6]^{2+}$	$[Mn(OH_2)_6]^{2+}$	
624	529	$^4T_{1g}(G) \leftarrow {}^6A_{1g}$
484 463	433	$^4T_{2g}(G) \leftarrow {}^6A_{1g}$
418	401 395	$^4A_{1g}(G), {}^4E_g(G) \leftarrow {}^6A_{1g}$
376	357	$^4T_{2g}(D) \leftarrow {}^6A_{1g}$
352	337	$^4E_g(D) \leftarrow {}^6A_{1g}$

The observed d-d transitions of solid $[Mn(N_2H_4)_2X_2]_n$ (X=Cl, NCS, O_2CMe) are considerably weaker in intensity and difficult to resolve from the background (see TABLE No 2.3). Overall the peak maxima are accurate to ~±5nm, though with broader absorptions the error may be larger. Indeed it was found to be difficult to obtain consistent results for these solids on different occasions.

The most prominent band in high-spin d^5 spectra is due to the $^6A_{1g} \rightarrow {}^4A_{1g}(G), {}^4E_g(G)$ transition, which in hydrazine complexes was found to occur at ~420nm (24000 cm^{-1}). The $^6A_{1g} \rightarrow {}^4T_{2g}(G)$ transition splits into two components, presumably as a result of a symmetry lower than O_h. This feature has been noted for other complexes e.g. $Mn(dipyam)_2Cl_2$ (dipyam = 2,2'-dipyridylamine) which is axially distorted and shows two components for the $^6A_{1g} \rightarrow {}^4T_{2g}(G)$ transition at 475 and 495 nm [154].

The d-d transitions of the two isomers of $[Mn(N_2H_4)_2(NO_2)_2]_n$ could not be detected due to the presence of intense NO_2 charge-transfer absorptions which tail into the visible region. Diffuse reflectance electronic spectra of the remaining complexes were not investigated.

TABLE No 2.3 Diffuse Reflectance Electronic Spectra of $[Mn(N_2H_4)_2X_2]_n$ /nm.

$[Mn(N_2H_4)_2Cl_2]$	$[Mn(N_2H_4)_2(NCS)_2]$	$[Mn(N_2H_4)_2(O_2CMe)_2]$	
615 (br)	650 (br)	625 (br)	$^4T_{1g}(G) \leftarrow {}^6A_{1g}$
490 (br)	515 (br)	515 (br)	$^4T_{2g}(G) \leftarrow {}^6A_{1g}$
463 (sp)	474 (sp)	474 (sp)	
421 (sp)	421 (sp)	419 (sp)	$E_{1g}(G), {}^4A_{1g}(G) \leftarrow {}^6A_{1g}$
375 (sp)	-	371 (sp)	$^4T_{2g}(D) \leftarrow {}^6A_{1g}$

(br) = broad, (sp) = sharp

2.3 VIBRATIONAL SPECTRA

The infra-red and Raman spectra of solid $[Mn(N_2H_4)_2X_2]_n$ (X = Cl, Br, I, NCO, NCS and O_2CMe) were recorded, together with the infra-red spectra of $[Mn(N_2H_4)_2X_2]_n$ (X = NO_2 (I) and (II), NCSe and N_3).

Raman spectra of the nitrite species could not be measured due to explosive decomposition of the samples on exposure to the laser beam.

In addition, the infra-red spectra of $[M(N_2D_4)_2Cl_2]_n$ (M = Mn and Zn) were measured.

The vibrational spectral data of $[Mn(N_2H_4)_2X_2]_n$ can be conveniently sub-divided into two separate sections, one concerned with the vibrations of the coordinated hydrazine ligands and the other with the vibrations of the axially coordinated anions.

2.3.1 COORDINATED HYDRAZINE VIBRATIONS

The vibrational spectra of $[M(N_2H_4)_2X_2]_n$ (M=Cr,Mn,Fe,Co,Ni,Cu, Zn,Cd,Hg ; X=Cl,Br,I) have been reported previously by several workers. Sacconi and Sabatini [23] measured the infra-red spectra of $[M(N_2H_4)_2Cl_2]_n$ (M=Mn,Fe,Co,Ni,Cu,Zn,Cd) between 4000-300 cm^{-1}. Assignment of the spectra was achieved by comparison with the analogous ammine complexes and deuteration studies of $[Cd(N_2H_4)_2Cl_2]_n$. Complexes containing unidentate coordinated hydrazine ligands were proposed to exhibit the ν(NN) mode at 931-936 cm^{-1} whereas this mode was suggested to lie between 948-985 cm^{-1} for complexes containing bridging coordinated hydrazine. These assignments were based on a ν(NN) assignment for free hydrazine of 873 cm^{-1}, an assignment subsequently questioned. These frequency shifts were ascribed to changes in electron pair repulsions as the lone pairs become involved in bonding.

As indicated above, the assignment of ν(NN) to a band at 873 cm^{-1} in the IR spectrum of liquid hydrazine was later challenged by Durig, Bush and Mercer [155]. This group achieved a reliable vibrational assignment for hydrazine and hydrazine-d_4 using infra-

red and Raman data obtained from liquid, solid and gas phase spectra. In particular, ν(NN) was reassigned to a band at 1098 cm^{-1} on the basis of its highly polarised character in the Raman spectra and its small shift on deuteration. This reassignment was supported by the normal coordinate analysis of Sathyanarayana and Nicholls [141] employing both general valence and modified Urey-Bradley force fields. The results obtained were used to reassess the vibrational assignments for $[M(N_2H_4)_2Cl_2]_n$ (M=Co,Ni,Zn,Cd) and $[M(N_2D_4)_2Cl_2]_n$ (M=Zn,Cd). The majority of the previous assignments of Sacconi and Sabatini [23] were confirmed, but as ν(NN) had been reassigned for free hydrazine, it was essential to reassign this band in the spectra of $[M(N_2H_4)_2Cl_2]_n$. Absorptions present in the 1150-1170 cm^{-1} region were thus assigned to ν(NN) in the complexes. This band was also observed to be sensitive to the type of hydrazine coordination and to the nature of the metal ion. It thereby parallels the behaviour exhibited by the 873 cm^{-1} band of liquid hydrazine, the latter band now assigned to an anti-symmetrical NH_2 rocking vibration.

Assignments of the fundamental vibrations of coordinated hydrazine have now reached a level of maturity, but the same cannot be said of the assignments of the metal-ligand vibrations where a number of problems remain. In an attempt to resolve some of these difficulties, an infra-red study of $[M(N_2H_4)_2Cl_2]_n$ (M=Mn,Zn) and their N_2D_4 analogues was extended into the 700-200 cm^{-1} region.

In C_2 point group symmetry (*gauche* N_2H_4 structure), the 12 fundamental vibrations are classified into 7 symmetric (A) and 5 antisymmetric (B) vibrations. In addition to these vibrations, a torsional vibration belonging to an A mode is also predicted (see TABLE 2.4).

TABLE No 2.4 Vibrational Spectra of N_2H_4 and N_2D_4 /cm^{-1}

	N_2H_4	N_2D_4	Main Character of Vibration
A modes	3332	2493	νNH_2
	3189	2353	νNH_2
	1608	1194	δNH_2
	1283	936	ωNH_2
	1098	1032	νNN
	871	727	rNH_2
	625	495	tNH_2
B modes	3332	2493	νNH_2
	3189	2415	νNH_2
	1628	1194	δNH_2
	1324	987	ωNH_2
	1042	787	rNH_2

The observed vibrational spectra of $[Mn(N_2H_4)_2X_2]_n$ (X=Cl, Br, I, NCO, NCS, NCSe, N_3, O_2CMe, NO_2 (I) and (II)) (see TABLE No 2.5) all appear very similar once the vibrational modes of the coordinated anions have been subtracted. This is indicative of the expected structural feature of bridging hydrazine groups with *trans*-axial X groups giving an octahedral environment around the metal.

The coordinated hydrazine bands in the infra-red spectra of $[M(N_2R_4)_2Cl_2]_n$ (M=Mn, Zn; R=H, D) (see TABLE No's 2.5 and 2.6 and FIG No 2.1) can be assigned using the approach of Sathyanarayana and Nicholls [141] who studied the complexes $[M(N_2R_4)_2Cl_2]_n$ (M=Zn, Cd; R=H, D). The $\nu(NH_2)$, $\delta(NH_2)$ and $\omega(NH_2)$ vibrations show H/D ratiosof ~1.35 indicating high NH character. The reassigned $\nu(NN)$ shows a H/D ratios of ~1.12 (a shift of 1157 to 1046 cm^{-1} on deuteration of $[Mn(N_2H_4)_2Cl_2]_n$) indicating minor NH_2 character. The previously assigned $\nu(NN)$ found at 961 cm^{-1} in $[Mn(N_2H_4)_2Cl_2]_n$ is shifted to 832 cm^{-1} on deuteration, an isotopic shift of 1.16. It is clear that

this low isotopic shift would have caused initial confusion over the assignment of $\nu(NN)$.

TABLE No 2.5 Infra-red Spectra of $[Mn(N_2R_4)_2Cl_2]_n$ (R=H,D) /cm^{-1}

$[Mn(N_2H_4)_2Cl_2]_n$	$[Mn(N_2D_4)_2Cl_2]_n$	H/D ratio	Assignment
3284 (vs)	2472 (vs)	1.33	
	2417 (w,sh)		νNR_2
3233 (m)	2386 (m)	1.36	
3147 (vw)	2326 (vw)	1.35	
1606 (s)	1183 (s)	1.36	δNR_2
1574 (s)	1166 (ms)	1.35	
1340 (mw)	1021 (m)	1.31	ωNR_2
1298 (mw)	954 (m)	1.36	
	926 (w)		
1157 (vs)	1046 (w)	1.11	νNN
	855 (s)	1.35	rNR_2
961 (m)	832 (ms)	1.16	
596 (m)	456 (m)	1.31	tNR_2
527 (m)	410 (m)	1.29	
344 (m)	335 (mw)	1.10	νMN
	314 (mw)		

Furthermore, this assignment problem is compounded because the reassigned $\nu(NN)$ bands often occur as shoulders on or hidden under the $r_a(NH_2)$ absorption. The 961 cm^{-1} band of $[Mn(N_2H_4)_2Cl_2]_n$ is now assigned to essentially $r_s(NH_2)$ even though the NH_2 character appears small, as assessed by deuteration studies. Even in hydrazine, the $r_s(NH_2)$ band at 871 cm^{-1}, has an isotopic shift of 1.20 on deuteration, indicating a reasonable degree of skeletal (i.e. $\nu(NN)$) character in the nature of this vibration. i.e. the 1157 and 961 cm^{-1} bands show a greater and lesser proportion of $\nu(NN)$ character in their vibrational description.

FIGURE No 2.1 Infra-red Spectra of $[Mn(N_2R_4)_2Cl_2]_n$ (R=H and D)

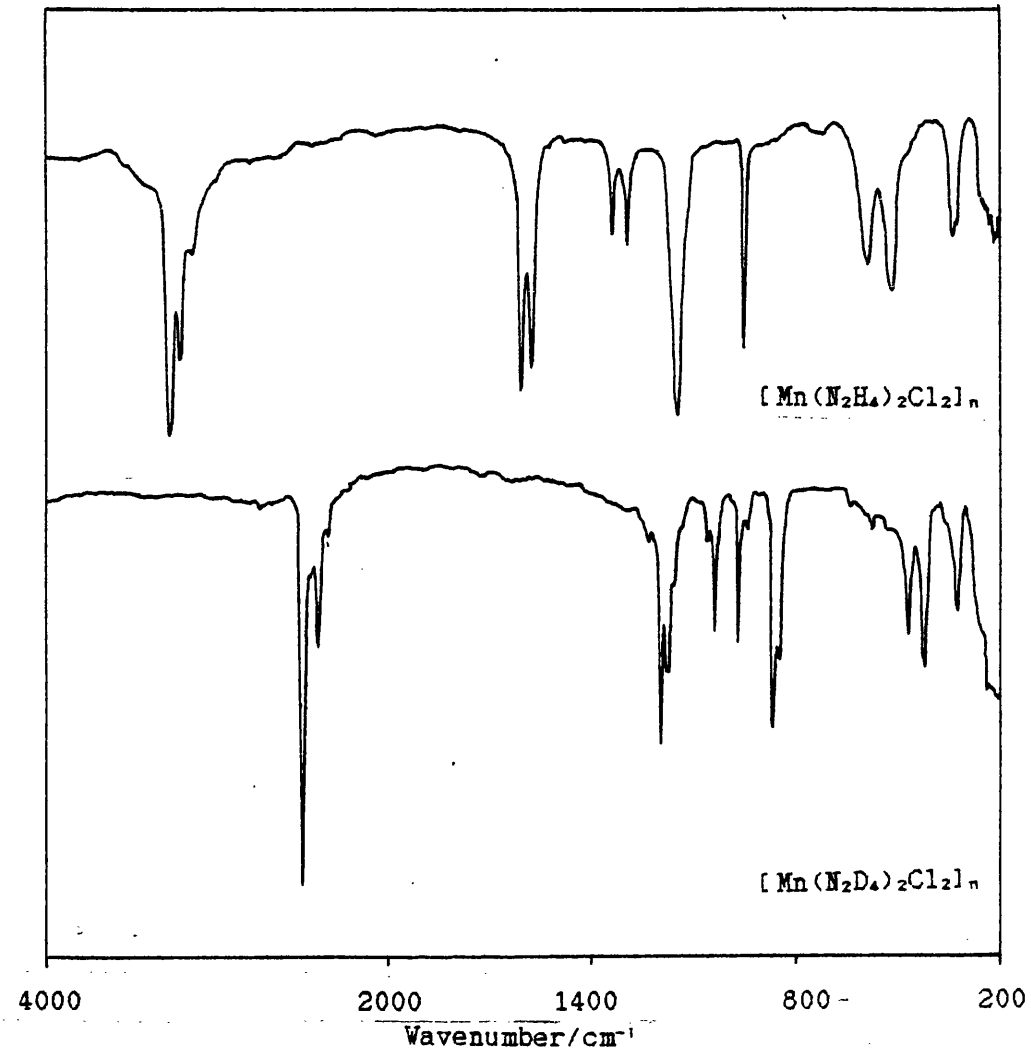

TABLE No 2.6 Infra-red Spectra of $[Zn(N_2R_4)_2Cl_2]_n$ (R=H,D) /cm^{-1}

$[Zn(N_2H_4)_2Cl_2]_n$	$[Zn(N_2D_4)_2Cl_2]_n$	H/D ratio	Assignment
3286 (vs)	2467 (vs)	1.33	
3233 (m)	2383 (w)	1.36	νNR_2
3143 (vw)	2322 (vw)	1.35	
1608 (s)	1186 (s)	1.36	δNR_2
1570 (s)	1158 (m)	1.36	
1342 (mw)	1033 (m)	1.30	ωNR_2
1308 (mw)	965 (m)	1.36	
1184 (m,sh)	1046 (w)	1.13	νNN
1170 (vs)	865 (s)	1.35	rNR_2
978 (m)	854 (m)	1.15	
630 (m)	487 (m)	1.29	tNR_2
586 (m)	460 (m)	1.27	
388 (mw)	348 (mw)	1.12	νMN
347 (mw)	318 (mw)	1.09	

On coordination, the NH_2 groups of hydrazine show a slight decrease in their stretching and bending frequencies, while the NH_2 rocking modes are found to be very sensitive to coordination, their frequencies increasing by ~100 cm^{-1}. This is expected as, for example, the CH_2 rocking modes of ethylenediamine increase at least 100 cm^{-1} on coordination. The large shifts in the NH_2 rocking frequencies have been ascribed to changes in the conformation of the hydrazine molecule rather than any change on coordination.

The $\nu(NN)$ frequency of free hydrazine is found at 1098 cm^{-1} and increases by ~50-70 cm^{-1} on complexation. This may be due to changes in electronic repulsion brought about by the involvement of the nitrogen lone pairs in bonding. The $r_s(NH_2)$ vibration appears to be sensitive to the nature of the axial ligand present,

FIGURE No 2.2 Infra-red Spectra of $[Mn(N_2H_4)_2X_2]_n$

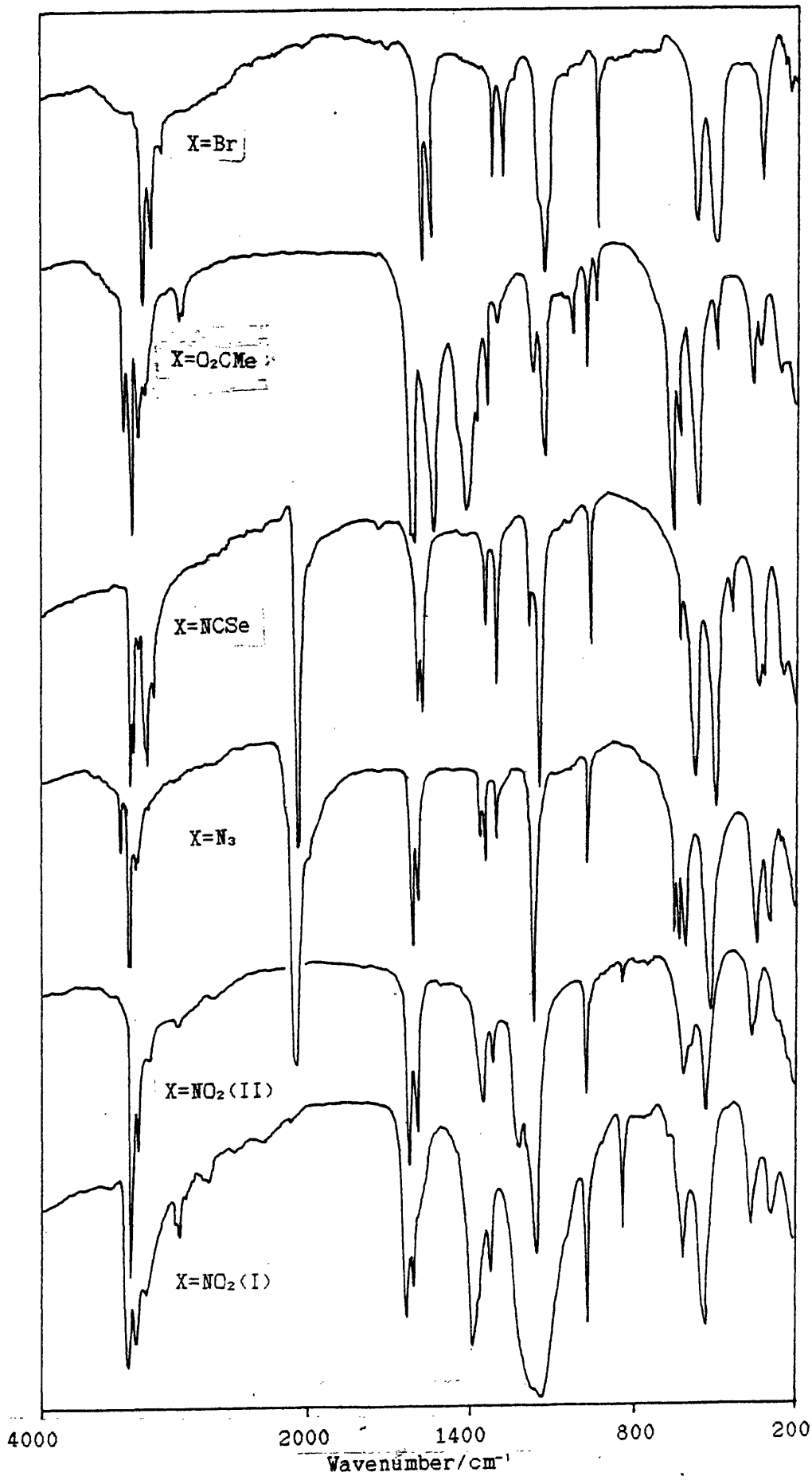

TABLE No 2.7 Vibrational Spectra of $[Mn(N_2H_4)_2X_2]_n$ /cm^{-1}
(N_2H_4 absorptions)

X	νNH_2	δNH_2	ωNH_2	νNN	rNH_2	tNH_2	νMN
Cl	3284s(3289m)	1606s(1612m)	1340w(1346w)	1157s*(1165s)	1157s*(1165s)	596m	344m
	3233m(3231vs)	1574s(1581m)	1298w(1302m)		961s (960vs)	527s	
	3147w						
Br	3275s(3271m)	1603s(1605m)	1343w(1345w)	1173m(1174m)	1150s	589m	344m
	3220m(3221s)	1575s(1580s)	1300w(1305w)		948m (951s)	503m	
	3135w						
NCO	3345s(3327w)	1618m(1601w)	1338w	1135s*	1135s*	604m	331m
	3280m(3267m)	1595m(1581w)	1295w		958m	525s	
NCS	3320s(3316w)	1596s(1592m)	1339m(1345w)	1174m(1175m)	1140vs	571s	329w
	3303s(3299mw)	1581s(1570m)	1295s(1291w)		981s (951m)		
	3211s(3218m)						
	3151w(3154w)						
NCSe	3320s	1593m	1340w	1178w	1143s	578m	334mw
	3300s	1578m	1298m		950m	490s	
	3210m						
	3200m						
	3150w						
N_3	3385w	1619s	1348m	1163s*	1163s*	599w	343m
	3325s	1591m	1299w		964m	519s	
	3293s						
	3258w						
	3240w						

TABLE No 2.7 (cont)

X	νNH_2	δNH_2	ωNH_2	νNN	rNH_2	tNH_2	νMN
O_2CMe	3353vs(3343w) 3310vs(3307m) 3258s (3255ms) 3234m (3227ms) 3190m (3186m)	1623s 1613s(1612m)	1336s(1344w) 1296m	1166s(1175w)	1121vs 959s (961vs)	558ms	350w
NO_2 (I)	3315vs 3260m 3175w	1623s 1594m	1348m 1308w	1183ms	1146vs 946m	595m 519s	346m
NO_2 (II)	3295vs 3243m 3155w	1618s 1583m	1343m 1305w	1178ms	1144vs 953m	598m 515ms	348m

Raman data in parentheses * - coincident band (ν(NN) with $r_a(NH_2)$)

TABLE No 2.8 Vibrational Spectra of $[Mn(N_2H_4)_2X_2]_n$ /cm^{-1}
(Anion absorptions)

X				
NCO	2215vs[a] (2186w)[a]	1318m[b] (1315vs)[b]	624m, sh[c] (622 w)[c]	
	2 35w[a] (2166w)[a]		620s[c]	
	(2102vs)[a]			
NCS	2068s[d] (2070vs)[d]	794w[e] (791s)[e]	491s[c]	314w[f]
	2015w[d] (2060vs)[d]		480m[c]	
			417m[c]	
NCSe	2075vs[d] (2103w)[d]	616w[e]	419w[c]	311w[f]
	2020w[d] (2061w)[d]			
N_3	2080vs[g]	1360w[h]	640s[i]	295m[f]
			620s[i]	
O_2CMe	2930w[k] (2926vs)[k]	1544vs[l] (1551w)[l]	1045w[m] (1048m)[m]	
		1419vs[l] (1405s)[l]	1014ms[m]	
	922ms[n] (922vs)[n]	648m[o] (646m)[o]	619w[p] (620w)[p]	
	480w[q] (481w)[q]	315w[r] (319w)[r]		
NO_2(I)	1384s[s]	818m[t]	283w[u]	
			271w[u]	
NO_2(II)	1211s[s]	820w[t]	264mw[u]	
			243mw[u]	

a = ν_a(NCO) b = ν_s(NCO) c = δ(NCX) d = ν(CN)
e = ν(CX) f = ν(M-NCX) g = ν_a(NNN) h = ν_s(NNN)
i = δ(NNN) j = ν(M-NNN) k = ν(CH_3) l = ν(CO_2)
m = r(CH_3) n = ν(CC) o = δ(OCO) p = π(COO)
q = r(OCO) r = ν(MO) s = ν(NO_2) t = δ(NO_2)
u = ν(MO)?

Raman data in parentheses

increasing in the order NCO>Cl>N_3>O_2CMe>Br>NCS>I>NCSe>ONO (as well as being sensitive to the hydrazine coordination mode as explained above).

The vibrational spectra of $[Mn(N_2H_4)_2X_2]_n$ (X=O_2CMe, NCO, NCS, NCSe, N_3) show further splitting in the $\nu(NH_2)$ region and a reduced frequency difference between the A and B modes of $\delta(NH_2)$ (see TABLE No 2.7). Single crystal X-ray structural studies of

$[Zn(N_2H_4)_2(O_2CMe)_2]_n$ [44] show hydrogen-bonding present between the pseudo-one dimensional chains involving the uncoordinated oxygen of an acetate and a hydrogen of a hydrazine molecule. Such an interaction would be expected to have an effect on the vibrational spectrum. However, a crystal structure determination of $[Zn(N_2H_4)_2(NCS)_2]_n$ shows no corresponding hydrogen-bonding [43]. Electron spin resonance spectra (see SECTION 2.4) indicate that all the above carboxylate and pseudohalide complexes have pseudo-octahedral geometry around the manganese atoms, the halide complexes having tetragonally distorted structures. The additional splitting observed in the vibrational spectra of the former complexes could therefore result from interactions arising from the proximity of the axial ligands to other hydrazine ligands. Such interactions would be absent in the halide complexes leading to a less complex pattern of bands for these compounds.

The far-infrared spectra of $[M(N_2H_4)_2X_2]_n$ (M=Mn,Co; X=Cl,Br) have been reported in part by Goldstein and Unsworth [156]. They confirmed that ν(MN) occurs in the 400-340 cm^{-1} region, as previously assigned [23]. However ν(MX) was assigned to bands in regions normally associated with complexes containing bridging halide. This apparent anomaly was rationalised using crystallograpic data which showed the Mn-Cl bond of $[Mn(N_2H_4)_2Cl_2]_n$ to be exceptionally long (2.570Å) for a terminal metal-chloride bond. The weak interaction thus results in a low ν(MX) frequency.

The work reported here supports these assignments. The far-infrared spectral bands of $[M(N_2H_4)_2X_2]_n$ (M=Mn,Zn; X=Cl,Br) and $[M(N_2D_4)_2Cl_2]_n$ (M=Mn,Zn) are listed in TABLE No 2.9 and assignments given.

TABLE No 2.9 . Low Frequency Vibrational Spectra of $[M(N_2H_4)_2X_2]_n$ (M=Mn,Zn; X=Cl,Br) and $[M(N_2D_4)_2Cl_2]_n$ (M=Mn,Zn) /cm^{-1}

$[Mn(N_2H_4)_2Cl_2]_n$	$[Mn(N_2D_4)_2Cl_2]_n$	$[Mn(N_2H_4)_2Br_2]_n$	$[Zn(N_2H_4)_2Cl_2]_n$	$[Zn(N_2D_4)_2Cl_2]_n$	$[Zn(N_2H_4)_2Br_2]_n$	Assignment
596ms (650vw)	456ms	589m (629m)	630ms	487ms	620ms	tNH_2
527s	410ms	518ms	586s	460s	573s	
344m (357vw)	335w,sh	344m	388m	348w,sh	381m	ν MN
	314m		347w	318m	342w	
253mw (276m)		250mw (270mw)				δNMN
213mw (234m)		206mw (229m)				
(140m,sh)		(122m,sh)				δXMX

Raman data in parentheses All data in cm^{-1}

The bands assigned to t(NH_2) are derived from the torsional vibration of hydrazine, found at 627 cm^{-1} in the solid phase of the free ligand (495 cm^{-1} on deuteration). In the infrared spectra of $[M(N_2H_4)_2Cl_2]_n$ (M=Mn,Zn) this vibration is split into two components. On deuteration these bands shift some ~130 cm^{-1} with a H/D ratio of ~1.29 thus confirming the high NH_2 character involved.

Goldstein and Unsworth [156] considered the $[Mn(N_2H_4)_2X_2]_n$ polymer to have C_{2h} local symmetry. Group Theory predicts four MN stretchs for this symmetry of which only two are IR-active and only two are Raman-active with no coincidences. Bands at 344 cm^{-1} (M=Mn) and 388, 347 cm^{-1} (M=Zn) are halogen-insensitive, as shown by comparison with the bromide analogues, and show H/D shifts of ~1.10. These bands can be confidently assigned to ν(MN) modes. For the complex with M=Zn, both the A_u and B_u modes are observed, while these modes appear coincident in the complex with M=Mn. The corresponding Raman-active bands have not been detected, but are expected to be of low intensity.

Other halogen-insensitive bands are found in the 280-200 cm^{-1} region which can be attributed to δ(NMN) by analogy with halogen-bridged metal(II) ammine complexes, $[MX_2(NH_3)_2]_n$ [157].

2.3.2 COORDINATED ANION VIBRATIONS

Halide Vibrations

Goldstein and Unsworth [156] assigned ν(MX) in $[Mn(N_2H_4)_2X_2]_n$ (X=Cl,Br) to IR-active bands at 210 and 175 cm^{-1} respectively. No significant Raman bands were observed in this region in this work and so the above assignments remain unconfirmed. Halide-sensitive bands have been observed in the Raman spectra of $[Mn(N_2H_4)_2X_2]_n$ at 140 cm^{-1} (X=Cl) and 122 cm^{-1} (X=Br) and may tentatively be assigned

to δ(XMX) vibrations. Neither the ν(MI) or δ(IMI) vibrations were observed in either the infrared or Raman spectra of $[Mn(N_2H_4)_2I_2]_n$.

Psuedohalide Vibrations

Three normal vibrations are expected for a linear triatomic molecule NCX, which can be described as;

$\rightarrow\ \rightarrow\ \leftarrow$
N-C-X ν_1, pseudo-asymetric stretch (ν(CN))

$\uparrow$
N-C-X ν_2, δ(NCX)
$\downarrow\quad\downarrow$

$\leftarrow\quad\rightarrow$
N-C-X ν_3, pseudo-symmetric stretch (ν(CX))

The designation in parentheses is commonly used, and approximates the major bond deformation involved in the vibration. However in cyanate, the modes are appreciably mixed (i.e. mixing between the ν(CO) and ν(CN) modes.

Cyanate has been shown to almost exclusively coordinate through its N atom [158]. On coordination there appears an increase in ν_1 (~ν(CN)) and usually ν_3 (~ν(CO)) and a decrease in ν_2 (δ(NCO)) from the free ion values. In $[Mn(N_2H_4)_2(NCO)_2]_n$ ν_1 is found at 2215 cm^{-1}, an increase from 2165 cm^{-1}, the value found in KNCO. The ν_3 band also increases from 1254 to 1318 cm^{-1} while the deformation band ν_2 is observed to decrease slightly from 637,628 cm^{-1} to 624,620 cm^{-1}.

It is possible from the observed vibrational shifts to conclude that NCO in $[Mn(N_2H_4)_2(NCO)_2]_n$ is coordinated through its N atom.

The thiocyanate ligand is capable of three common types of coordination [158];

M-N-C-S	M-S-C-N	M-N-C-S-M
I	II	III

These modes of coordination can be distinguished by differences in the fundamental vibrations. Thus ν_1 (ν(CN)) is generally lower in N-bonded complexes (~>2050 cm^{-1}) than in S-bonded complexes (~2100 cm^{-1}). The bridging complexes exhibit ν(CN) well above 2100 cm^{-1}. The ν_3 (ν(CS)) vibration in N-bonded complexes is found between 860-780 cm^{-1}, while for S-bonded complexes the corresponding region is 720-690 cm^{-1}. Also δ(NCS) shows a sharp peak at ~480 cm^{-1} for N-bonded complexes, while for S-bonded complexes a series of low intensity peaks appear at ~420 cm^{-1}.

From these criteria, $[Mn(N_2H_4)_2(NCS)_2]_n$ can be shown to contain N-bonded iso-thiocyanate ligands (ν(CN) 2068 cm^{-1}, ν(CS) 794 cm^{-1}, δ(NCS) 491-471 cm^{-1}). This is expected as in general first-row transition metal ions tend to form N-coordinated thiocyanates in preference to S-coordinated ones. According to the concepts of Pearson [159], the nitrogen end of this ion is a hard, and the sulphur end a soft, base. Consequently, N-bonding is expected with the hard (class a) metal ions while S-bonding should take place with those of the soft category (class b).

Trends of band shifts of selenocyanate on coordination closely follow those seen for thiocyanate [158]. The ν_1 (ν(CN)) is generally found below the free ion value of 2070 cm^{-1} for N-coordination, although some examples are known with higher values typical of Se-bonding. However ν_3 (ν(CSe)) is clearly diagnostic, with N-bonded examples showing bands above 558 cm^{-1}, the free ion value, and Se-bonded examples showing bands below it. The ν_2

(δ(NCSe) band also appears to follow the NCS^- pattern. Se-bonded compounds show at least one component of this vibration below 400 cm^{-1}, while for N-bonded complexes, bands are not observed at such low frequencies.

The NCSe bands in $[Mn(N_2H_4)_2(NCSe)_2]_n$ generally follow the trends for N-coordination with both ν(CSe) at 616 cm^{-1} and δ(NCSe) at 419 cm^{-1} above the free ion values. However, ν(CN) at 2075 cm^{-1} is slightly above the free ion value of 2070 cm^{-1}. Since ν_2 and ν_3 are more diagnostic it is considered that selenocyanate is N-bonded in $[Mn(N_2H_4)_2(NCSe)_2]_n$.

There appears no clearly defined vibrational correlation for azide coordination unlike the other pseudohalides [160]. It appears the majority of examples known are unidentate, although N_3 can act as a bridging ligand in a number of different geometries. Three fundamentals are observed as with NCX and are described as ν_1 (ν_a(NNN)) a pseudo-antisymmetric stretch, ν_2 (δ(NNN)) and ν_3 (ν_s(NNN)) a pseudo-symmetric stretch. The free ion frequencies are 2041, 645 and 1344 cm^{-1} respectively. On coordination these bands are often split due to the non-linearity of the M-NNN group. In general, ν_a(NNN) increases while both ν_s(NNN) and δ(NNN) decrease on coordination.

In $[Mn(N_2H_4)_2(N_3)_2]_n$, both ν_a(NNN), at 2080 cm^{-1}, and δ(NNN), at 640 and 620 cm^{-1}, follow the above trends. However ν_s(NNN) appears at 1360 cm^{-1}, higher than the free ion value. As with selenocyanate, this band may not be as diagnostic as the other fundamentals. Given the stoichiometry of $[Mn(N_2H_4)_2(N_3)_2]_n$ and the vibrational data, it is probable that N_3^- acts as a unidentate ligand.

Acetate vibrations

Using the criterion of Δ [160], the frequency difference between the $\nu_a(CO_2)$ and $\nu_s(CO_2)$ vibrations, it would seem that $[Mn(N_2H_4)_2(O_2CMe)_2]_n$ contains bridging acetate ligands. However the X-ray crystal structure of $[Zn(N_2H_4)_2(O_2CMe)_2]_n$ [44], shows the acetates to be unidentate. Since the vibrational spectrum of $[Mn(N_2H_4)_2(O_2CMe)_2]_n$ indicates bridging hydrazine ligands and the e.s.r. spectrum indicates an octahedral environment for the metal, the acetate groups of this complex must be similarly unidentate. The failure of Δ to accurately indicate coordination type can be explained by additional hydrogen-bonding between the uncoordinated oxygen of the acetate and neighbouring hydrazine hydrogens. In this way acetate appears to be acting in a bridging role giving rise to an anomolous Δ value. It has been shown by Deacon *et al.* [161] that use of the Δ value as a means of assessing the mode of coordination of acetate to metals needs to be used with caution. An extensive survey of reported acetate $\nu(CO_2)$ values revealed that the use of Δ is limited to i) recognition of complexes with unidentate carboxylate coordination [$\Delta_{unidentate} > \Delta_{ionic}$] and ii) identification of some complexes with chelating or (and) bridging bidentate carboxylate groups [$\Delta_{bridging\ or\ (and)\ chelating}$ often $< \Delta_{ionic}$]. Even these criteria cannot be regarded as universally valid. For example, apart from $[Mn(N_2H_4)_2(O_2CMe)_2]_n$, $[Ni(OH_2)_4(OCOMe)_2]$ is known to be octahedral with unidentate acetate groups [162]. A large Δ value is however not observed and it has been suggested that hydrogen-bonding with the water ligands may make the C-O bonds more equivalent than expected for unidentate acetate coordination.

Nitrite vibrations

The nitrite ion has 3 fundamental vibrations; $\nu_a(NO_2)$, $\nu_s(NO_2)$ and $\delta(NO_2)$, which for the free ion occur in the infrared at 1330 (w), ~1260 (vs) and 828 (m) cm^{-1}, respectively. In the Raman spectrum a reversal in intensities is expected for the two $\nu(NO_2)$ bands [163].

When the ion is involved in *N*-bonded nitro coordination $\nu_a(NO_2)$ generally falls between 1280-1380 cm^{-1}. For *O*-bonded nitrito coordination $\nu_a(NO_2)$ falls between 1350-1380 cm^{-1}, while $\delta(NO_2)$ is not normally greatly affected by coordination. Nitro groups also characteristically exhibit an out-of-plane wagging mode at ~620cm^{-1} which is absent in nitrito complexes.

The infra-red spectra of $[Mn(N_2H_4)_2(NO_2)_2]_n$ (I and II) reveal the NO_2^- ligands to be in different environments in the two isomers. Neither complex shows wagging modes, therefore suggesting the NO_2 groups are *O*-coordinated. Nitrite (I) exhibits a $\nu_a(NO_2)$ at 1384 cm^{-1} which can be related to unidentate *O*-coordination. Nitrite (II) exhibits $\nu_a(NO_2)$ at 1211 cm^{-1}, a frequency outside of the ranges established for either *O*- or *N*-bonded nitrito/nitro coordination. The $\nu_s(NO_2)$ modes are thought to be weak and hidden by coordinated hydrazine bands in the 1130-1190 cm^{-1} region.

It is concluded from the IR spectra that isomer (I) has the molecular formula of $[Mn(N_2H_4)_2(NO_2)_2]_n$ with O-bonded unidentate nitrito groups, while the isomer (II) may contain bridging nitrito groups which give rise to an uncharacteristic $\nu_a(NO_2)$ band position.

2.4 ELECTRON SPIN RESONANCE SPECTRA

The application of e.s.r. is particularly useful in the investigation of manganese(II) compounds. Manganese(II) complexes are almost invariably high spin and hence possess five unpaired electrons. The half-filled shell, $3d^5$, implies that the ground state for the ion will be an orbital singlet, ^6S. There are no other sextet states, and the nearest excited state is a triplet, $^4T_1$.

The spectra of manganese(II) species can only be discussed adequately by a consideration of *zero-field splitting* and *Kramer's degeneracy*.

When a metal ion is placed in a crystalline field, the degeneracy of the *d* orbitals will be resolved by the electrostatic interactions. When the species contains more than one unpaired electron, the spin degeneracy can also be resolved by the crystal field. Therefore the *spin levels* may be split even in the absence of a magnetic field. This phenomenon is called *zero-field splitting* (see FIG No 2.3). In transition metal systems, the zero-field effect is employed to describe any effect that removes the spin degeneracy including dipole interactions and spin-orbital splitting.

When a system contains an odd number of unpaired electrons (such as Mn^{2+}) the spin degeneracy of every level remains doubly degenerate. This is known as *Kramer's degeneracy*.

In FIG No 2.3 the model system has two unpaired electrons i.e. $S=1$ and $M_s=-1,0,+1$. In the absence of zero-field splitting, the two possible transitions, $0\rightarrow+1$; $-1\rightarrow0$ ($\Delta M_s=\pm1$), are degenerate and only

one absorption is observed. Zero-field splitting removes this degeneracy and as a result two absorptions are observed.

FIGURE No 2.3 The Energy Level Diagram for a System with S=1, (a) in the Absence of and (b) in the Presence of Zero-field Splitting.

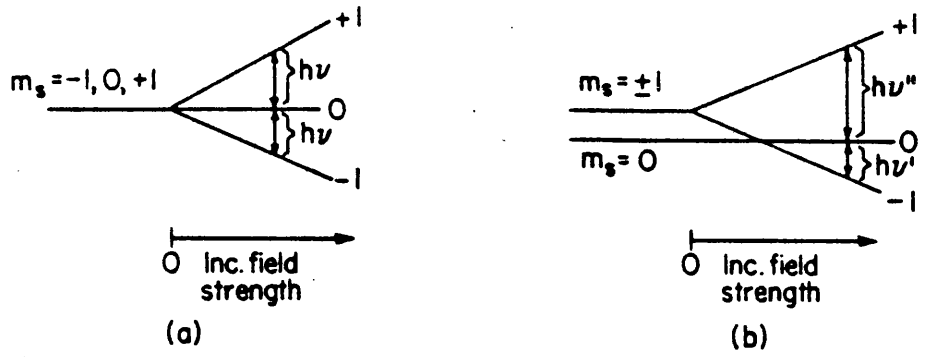

Manganese(II) has an odd number of electrons, so Kramer's degeneracy must exist. Zero-field splitting produces three doubly degenerate spin states (M_s=±5/2, ±3/2, ±1/2) (see FIG No 2.4) Each of these is split into two singlets by the applied field, producing six levels. As a result of this splitting five transitions (-5/2 → -3/2, -3/2 → -1/2, -1/2 → +1/2, +1/2 → +3/2, +3/2 → +5/2) are expected. The spectrum is further complicated by the hyperfine splitting due to the manganese nucleus (I=5/2). Therefore the five peaks are each split into six *hyperfine* components (see FIG No 2.4).

The magnitude of the zero-field splitting in transition metal ions can generally be described as arising from the crystal field. However manganese(II) has a spherically symmetric electron distribution, so that the ^6S ground state is not split by the crystal field, but does show a zero-field splitting. This is explained by spin-orbit coupling which mixes into the ground state excited triplet states (such as $^4T_1$), which are split by the crystal field, and allows weak zero-field splitting. In this case

the spectra observed exhibit g values very close to the free electron value (g=2.0023).

FIGURE No 2.4 Splitting of the Energy Levels in Octahedral Manganese(II).

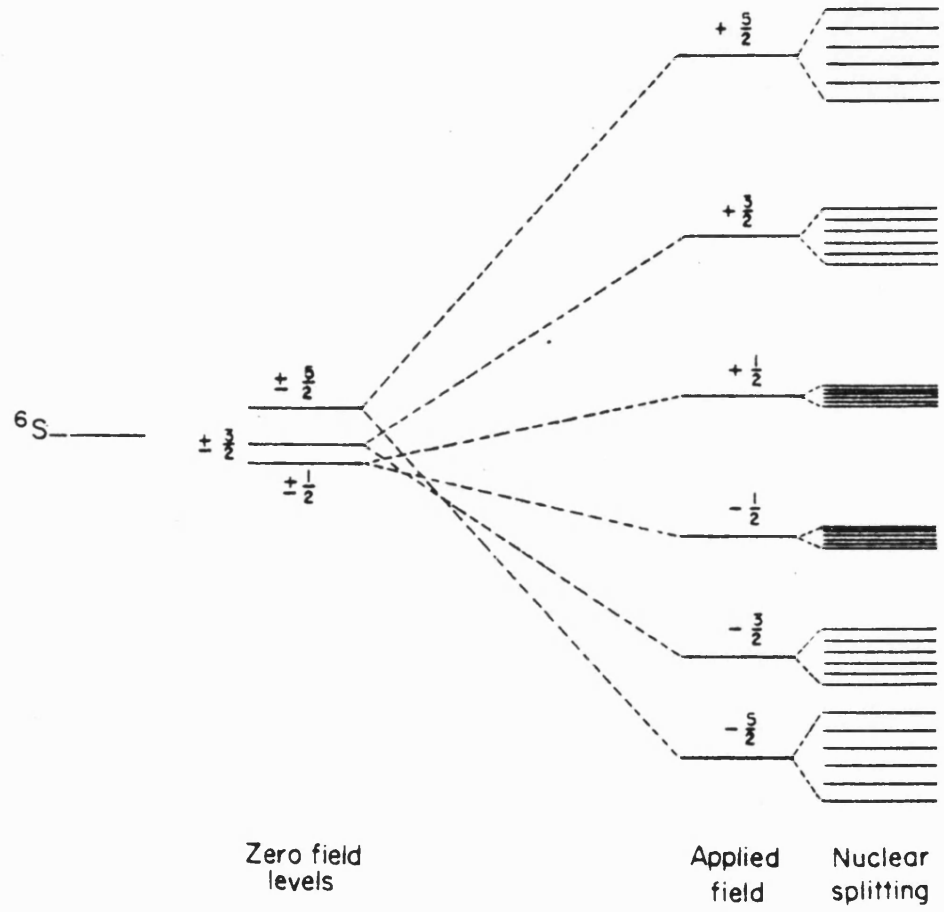

It was observed that certain iron(III) $3d^5$ systems gave e.s.r. spectra displaying g_{eff} values greatly removed from the free electron value [163A]. Subsequently Dowsing *et al.* [164] found that certain manganese(II)-substituted pyridine complexes also displayed such anomolous e.s.r. behaviour.

The *spin Hamiltonian* is a mathematical expression which describes the different interactions that exist in transition metal ions or radicals. The e.s.r. spin Hamiltonian for an ion in an axially symmetric field, i.e., tetragonal or trigonal is;

$$H = D[S_z^2 - {}^1/_3 S(S+1)] + g_z H_z S_z + g_x (H_x S_x + H_y S_y) +$$
$$A_z (S_z I_z) + A_x (S_x I_x + S_y I_y) + Q'[I_z^2 - {}^1/_3 I(I+1)] - g_N \beta_N H_0 I \quad (2.5)$$

The first term describes the zero-field splitting. The remaining terms describe the effect of the magnetic field on the spin multiplicity remaining after zero-field splitting, the hyperfine splitting, the quadrupole interaction and interaction of the nuclear magnetic moment with the external field.

In species that display a distortion to lower symmetry, the g values become g_x, g_y, and g_z and an additional zero-field term is required, i.e. $E(S_x^2 - S_y^2)$. The spin Hamiltonian can be written in a simplified form as the hyperfine splitting and quadrupole interaction terms can be neglected (2.6).

It was shown that certain features of manganese(II) e.s.r. spectra could be related to the zero-field splitting parameters D and E of the simplified spin Hamiltonian [165];

$$H = g\beta H.S + D[S_z^2 - {}^1/_3 . S(S+1)] + E(S_x^2 - S_y^2) \quad (2.6)$$
$$= g\beta H + H_0$$

In (2.6) S is the spin operator, D is a measure of axial distortion and E is a measure of rhombic distortion. For ease of manipulation the parameter $\lambda = E/D$ can be used, so H_0 can be defined solely in terms of D (see (2.7)).

$$H_0 = S_z^2 - {}^1/_3 . S(S+1) + \lambda(S_x^2 - S_y^2) \quad (2.7)$$

Symmetry considerations show that the only significant values for λ must lie between zero when the compound will show axial symmetry and 0.33 when it will display rhombic symmetry.

Before the studies of Dowsing *et al.* [166], it was generally thought that D was always small for manganese(II). This will be true for manganese(II) compounds of high symmetry i.e. regular octahedral or tetrahedral where $D \sim 10^{-3}-10^{-1}$ cm^{-1} and $\lambda \approx 0$. Compounds of such symmetry only show resonance signals near the free electron value ($g \approx 2$), further split by hyperfine interactions.

However, if the symmetry of the compound is reduced either by geometric distortion or by the introduction of differing ligand types, so D and λ increase. The e.s.r. spectra become more complex, the transition at $g_{eff}=2$ being split and further components are observed at higher and lower fields. Compounds with $D > 0.05$ cm^{-1} are found to show resonances well away from $g_{eff}=2$. For example, a complex with axial symmetry, with $D > 0.15$ cm^{-1} should have its strongest line at $g_{eff}=6$ with other transitions also detectable. A complex much distorted from axial symmetry with $D > 0.15$ cm^{-1} *and* λ close to 0.33 should show a very strong signal near $g_{eff}=4.27$ [166]. Using these calculations it should be possible to deduce the stereochemical environment of a manganese(II) ion from its e.s.r. spectrum (see TABLE No 2.10).

Unfortunately, some compounds only give a single resonance near $g_{eff}=2$ even though their structures must be distorted. This is likely to be the result of magnetic interactions between neighbouring Mn^{2+} ions in polymeric structures. These 'magnetically concentrated' compounds can be studied to some degree by dilution of the compound in an isomorphous but diamagnetic matrix.

TABLE No 2.10 E.s.r. Spectral-structural Correlations for Manganese(II) Complexes.

Complex type	Example	Spectral Features	Structural Type
$[MnL_6]^{n+}$	$Mn(OH_2)_6^{2+}$	$g_{eff}=2$	Regular
	$Mn(NCS)_6^{4-}$	$g_{eff}=2$ with hyperfine splitting	Near Regular
$[MnL_4X_2]$	$Mn(\gamma\text{-pic})_4Br_2$	$g_{eff}=6$	Axial distortion
$[MnL_2X_2]$	$Mn(\gamma\text{-pic})_2Cl_2$	$g_{eff}=2$, broad	Polymeric
	$Mn(Ph_3AsO)_2Br_2$	$g_{eff}=4,27$	Tetrahedral

The solid state e.s.r. spectra of the complexes $[Mn(N_2H_4)_2X_2]_n$ (X=Cl,Br,I) have been studied in detail, particularly when diluted in the diamagnetic, isomorphous matrices of the Group 12 metal complexes $[M(N_2H_4)_2X_2]_n$ (M=Zn,Cd, X=Cl,Br or I; M=Hg, X=Br) [167]. The objective of this work was to use the spectral results as a probe of the stereochemistry of the Group 12 metals. The spectra were interpreted in terms of D and λ. D was found to increase with ligand field distortion in the series Cl<Br<I as expected from the above arguments.

In this work X-band e.s.r. spectra of $[Zn(Mn)(N_2H_4)_2X_2]_n$ have been re-measured when X=Cl,Br,I and measured for the first time for X=NCO,NCS,NCSe,N_3,O_2CMe,NO_2(I) and (II). The spectra were interpreted by comparison with complexes of known structural type using the approach described above.

The e.s.r. spectra of the undiluted complexes were merely very broad signals centred at $g_{eff}=2$. Resolution of the spectra could be achieved by nominal doping (1-5%) of manganese(II) in the analogous zinc(II) matrix.

The spectra of the diluted complexes were found to be dependent on the nature of the axial ligand present. In general

four types of spectra were observed for the $[Mn(N_2H_4)_2X_2]_n$ complexes, the types being; a) X=Cl,Br,I b) X=NCO,NCS,NCSe,O_2CMe, or NO_2(I) c) $X=N_3$ and d) $X=NO_2$.

The complexes $[Mn(N_2H_4)_2X_2]_n$ (X=Cl,Br,I) show e.s.r. profiles similar to those reported previously [167]. The main features of the spectra consist of a strong transition near $g_{eff}=6$ (~1300 G using an operating frequency of ~9.5 GHz) another strong line near $g_{eff}=2$ (~3400 G) and a weak resonance at 5000 G. The bands at $g_{eff}=6$ and 2 were hyperfine split into six components (see TABLE No 2.11 and FIG No 2.5). The overall appearance of each spectrum indicated a tetragonally distorted octahedral environment surrounding the manganese ion for each complex.

The e.s.r. spectra of the complexes $[Mn(N_2H_4)_2X_2]_n$ (X=NCO,NCS, NCSe,O_2CMe and NO_2(I)) have not been reported before. The only feature of each spectrum is a strong absorption near $g_{eff}=2$ (3400 G) which is hyperfine split (see TABLE No 2.11 and FIG No 2.5). Correlation with the data presented in TABLE No 2.10 indicates a more regular environment around the manganese when compared with $[Mn(N_2H_4)_2X_2]_n$ (X=Cl,Br,I).

This conclusion is supported by X-ray crystallographic studies on analogous zinc complexes. The structural characterisations of $[Zn(N_2H_4)_2X_2]_n$ (Cl,NCS and O_2CMe) [43,44,168] reveal the chloride to have a marked tetragonal distortion as result of elongated axial bonds when compared with the acetate and isothiocyanate (Zn-Cl = 2.578Å, Zn-NCS = 2.190Å, Zn-OC(O)Me = 2.147Å). Assuming the manganese complexes show similar bond length variations (crystallographic data for $[M(N_2H_4)_2Cl_2]_n$ (M=Mn,Zn) show little change in metal-chloride distances; Mn-Cl = 2.570Å, Zn-Cl = 2.578Å [45,168]), the nature of the e.s.r. spectra probably indicate that

the acetate and isothiocyanate complexes have more regular octahedral structures than the chloride. This would also imply that the other complexes in this group with X=NCO, NCSe and NO_2(I) also have reasonably regular octahedral structures.

The other complexes $[Mn(N_2H_4)_2X_2]_n$ (X=N_3 and NO_2(II)) show more complicated e.s.r. spectra (see TABLE No 2.11 and FIG No 2.5). The nitrite(II) displays a major absorption at g_{eff}=4.27 together with other signals, this type of spectrum being characteristic of rhombically distorted octahedral symmetry. The azido-complex displays a rather complex spectrum, which although suggesting a regular structure, contains several unexplained absorptions not consistent with either an octahedral or a tetrahedral structure. It is possible that these two complexes may not be isomorphous with

TABLE No 2.11 X-Band E.s.r. Spectra of $[Zn(Mn)(N_2H_4)_2X_2]_n$ / Gauss

X	Centre of Major Resonances /gauss	Operating Frequencies/GHz
Cl	1275 vs, 3556 m, 5019 w	9.550
Br	1155 s, 3411 s, 5785 w	9.536
I	1152 s, 3403 w, 5761 w, 6680 w	9.536
NCO	3403 vs	9.537
NCS	3399 vs, 3441 vs	9.550
NCSe	3365 vs, 3403 vs	9.530
N_3	~1580 m, ~2700 vs 3411 vs	9.538
O_2CMe	3370 vs, 3424 vs	9.550
NO_2(I)	3411 vs	9.550
NO_2(II)	1825 vs, 2858 w 3429 s, 5088 m	9.545

FIGURE No 2.5 E.s.r Spectra of $[Zn(Mn)(N_2H_4)_2X_2]_n$

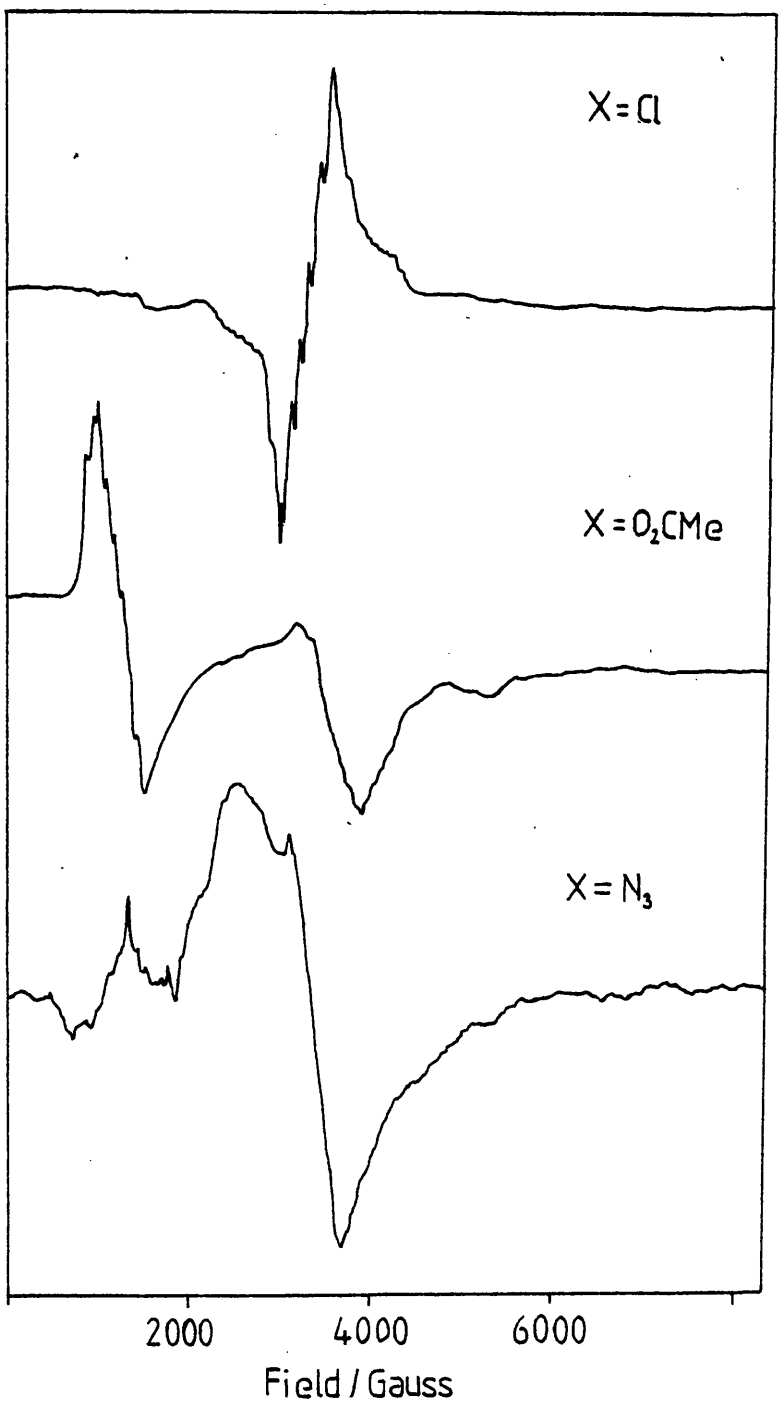

their zinc hosts thus generating more complicated spectra than expected.

2.5 X-RAY POWDER DIFFRACTION MEASUREMENTS

Spectroscopic data have shown that two isomers of '$[Mn(N_2H_4)_2(NO_2)_2]_n$' have been isolated, the particular isomer being determined by the nature of the manganese salt used in the preparation. An X-ray powder diffraction study was carried out on the two isomers to definitely confirm that they were genuinely different species. Chromium K_α-radiation was employed in the diffraction experiments. The d spacings were obtained by diffractometer analysis of the resulting powder photographs. The d spacings were subsequently indexed using a computer routine developed to provide unit cell infomation from powder data.

This routine is based on combination theory and was developed following the work of Taupin [168], the principles of which are outlined below;

The following equation can be derived for the measured values of d,

$$d^2_{hkl} = \frac{1}{(h/a)^2 + (k/b)^2 + (l/c)^2} \qquad (2.8)$$

with planes hkl and Miller indices (abc) [169]. This can be rearranged for the program to;

$$H_i^2A + K_i^2B + L_i^2C + 2H_iK_iD + 2K_iL_iE + 2L_iH_iF = Q_i \qquad (2.9)$$

such that $Q_i = 1/d_i^2$, $A=a^2$, $B=b^2$, $C=c^2$, $D=a.b$, $E=b.c$ and $F=c.a$; n = i to 1.

If N lines are measured it is possible to select the first n lines equivalent to the number of unknowns and assigned indices $H_iK_iL_i$ which satisfy the n equations produced above. The number of

unknowns are the parameters needed to define the unit cell and will be 1,2,3,4,6 for the crystal systems cubic, tetragonal and hexagonal, orthorhombic, monoclinic and triclinic respectively.

The program starts with the first n lines and assigns H_i, K_i and L_i values, computes the positions of all possibilities and compares them with the input values. If fits between the calculated and experimental can be found for all lines then a solution is obtained. A series of checks such as unit cell volume and precision are carried out and if the solution passes then it will be printed. If a fit is not found the program systematically increases the values of H_i, K_i and L_i, and if a fit is still not found the program then makes trials for a system with lower symmetry.

To reduce the number of trials and the size of the calculated tables certain symmetry conditions are applied, i.e. A=B=C and D=E=F=0 for cubic systems, and hence only a table of $h^2+k^2+l^2$ need be computed for this system. Other restrictions of the type A>B>C prevent treatment of equivalent cells related by permutation and translation. Experimental error can also be accommodated.

The data obtained includes details of trials which have failed, deviations between calculated and observed lines for solutions found, with a figure of merit. Details of the unit cell are given with the lattice type and the number of lines indexed.

TABLE No 2.12 Possible Unit Cells for $[Mn(N_2H_4)_2(ONO)_2]_n$(I)

Cell	a	b	c	α	β	γ
(i)	7.560	13.661	4.517	90.00	90.00	96.48
(ii)	7.546	13.825	4.517	90.00	90.00	96.48

a,b,c values in Å, α,β,γ values in degrees

The program produced two very similar monoclinic unit cells for $[Mn(N_2H_4)_2(ONO)_2]_n$(I) of high merit (see TABLE No 2.12). As can be seen the two calculated cells have very similar dimensions and angles. It is clear that as the cells have similiar merit ratings, the true cell must have very similar values to these.

The data can be compared with powder diffraction results obtained for $[M(N_2H_4)_2(NCS)_2]_n$ (M=Zn,Cd,Mn) as reported by Ferrari *et al.* [44] (see TABLE No 2.13). The isothiocyanate ligand is expected to possess a broadly similar volume to the nitrite ligand, even though the former is linear and the latter is non-linear.

TABLE No 2.13 X-ray Powder Data for $[M(N_2H_4)_2(NCS)_2]_n$ (M=Cd,Zn and Mn) compared to that of $[Mn(N_2H_4)_2(ONO)_2]_n$(I).

	$[Cd(N_2H_4)_2(NCS)_2]_n$	$[Zn(N_2H_4)_2(NCS)_2]_n$	$[Mn(N_2H_4)_2(NCS)_2]_n$	$[Mn(N_2H_4)_2(NO_2)_2]_n$(I)	
a(Å)	7.28	7.14	7.21	7.56	7.55
b(Å)	14.94	14.76	14.82	13.66	13.83
c(Å)	4.41	4.21	4.37	4.52	4.52
α(°)	90.00	90.00	90.00	90.00	90.00
β(°)	106.43	105.98	105.98	90.00	90.00
γ(°)	90.00	90.00	90.00	96.48	96.27
Z	2	2	2		

Z = number of formula weights in unit cell

Given the similarity of the unit cell dimensions, it can be concluded that the unit cell of $[Mn(N_2H_4)_2(ONO)_2]_n$(I) contains two monomer units, assuming a common $M(N_2H_4)_2$ backbone. The other dimensions are broadly comparable given the differences between the shapes of NCS and NO_2. The large b parameter observed in

$[Mn(N_2H_4)_2(ONO)_2]_n$(I) precludes the possibility of bridging ONO and hydrogen-bonding between chains.

The computer program produced one monoclinic cell for $[Mn(N_2H_4)_2(ONO)_2]_n$(II) of high merit (see TABLE No 2.14).

TABLE No 2.14 Unit cell Parameters for $[Mn(N_2H_4)_2(ONO)_2]_n$(II).

a	b	c	α	β	γ
8.662	12.266	6.166	90.00	90.00	104.79

The calculated values do not compare well with any reported $[M(N_2H_4)_2X_2]_n$ unit cell parameters, so it is apparent that the crystal structure is unlike those known for other $[M(N_2H_4)_2X_2]_n$ complexes.

Considering all spectroscopic and powder diffraction results it is reasonable to suggest that nitrite isomer (I) is $[Mn(N_2H_4)_2(ONO)_2]_n$ containing *O*-unidentate nitrito ligands.

It is not possible to assign a satisfactory molecular structure to isomer (II) on the basis of the characterisation data presented. The very anomalous $\nu(NO_2)$ frequency observed in the infra-red spectrum indicates the NO_2 ligand to be in an unusual coordination mode. It is possible that NO_2 is acting in a bridging role between $[Mn(N_2H_4)_2]$ chains, but given the lack of infra-red correlation data on the more uncommon bridging modes of NO_2 it is not possible to come to a definite conclusion.

2.6 OXIDATION OF $[Mn(N_2H_4)_2X_2]_n$ COMPLEXES (X = O_2CMe, NO_2)

Manganese, (along with chromium), has been implicated as a possible homogeneous catalyst for hydrazine decomposition [16]. In proposed mechanisms of this catalysis, manganese is required to display variable oxidation states in anhydrous hydrazine. As

manganese(II) is well known to survive in hydrazine (see SECTION 2.2) we were interested in investigating whether manganese(II)-hydrazine complexes could be oxidised to discrete manganese(III) complexes.

On contact with air, methanol suspensions of $[Mn(N_2H_4)_2X_2]_n$ ($X=O_2CMe$, NO_2(I)) were found to be susceptible to oxidation giving intense brown solutions. Other complexes of the group $[Mn(N_2H_4)_2X_2]_n$ were found not to oxidise under similar conditions. Further investigation of this process was limited to $[Mn(N_2H_4)_2(O_2CMe)_2]_n$.

Complete conversion of $[Mn(N_2H_4)_2(O_2CMe)_2]_n$ into its oxidation product was achieved using Soxhlet extraction of a methanol solution. No oxidation occurred when the extractions were run under nitrogen or carbon dioxide indicating the necessity of dioxygen. During the initial stages of reaction, solids could be recovered that gave analytical results in broad agreement with the stoichiometry $[Mn(N_2H_4)(O_2CMe)_2]_n$, i.e. the loss of one hydrazine but retention of the metal +2 oxidation state. Also gas evolution, presumably dinitrogen, is observed at this stage.

The subsequent brown solution product gave an electronic spectrum which could be explained on the basis of the presence of manganese(III) (see TABLE No 2.15).

TABLE No 2.15 Electronic Spectrum of $[Mn(N_2H_4)_2(O_2CMe)_2]_n$ Oxidation Product in Methanol Solution /nm.

577±1 (s,sh), 518 (w,sh), 487 (m,sh), 440 (m,sh), 403 (m,sh)

The electronic spectrum, which is typical of manganese(III) [170] showed a charge transfer band rising in the UV, with d-d transitions appearing as shoulders.

Solid products were isolated either by evaporating the solvent to dryness or by addition of inert solvents (e.g. Et_2O). The infrared spectrum of the dried product showed the presence of coordinated O_2CMe ($\nu(CO_2)$ ~1560 and 1410 cm^{-1}, $\delta(CH_3)$ 1330 cm^{-1}, $\nu(CC)$ 938 cm^{-1}, $\delta(OCO)$ 661 cm^{-1}, $\pi(COO)$ 615 cm^{-1}) with the Δ value indicating the probable presence of bridging acetate ligands. However no absorption bands were observed assignable to N_2H_4 modes.

Elemental analysis of the isolated samples did not give a firm indication of a discrete molecular formula. However a C:H ratio of 1:2 was readily apparent. It is probable, given the presence of manganese(III) and acetate, that the species formed are similar to the well known $[Mn_3(\mu_3\text{-}O)(\mu\text{-}O_2CR)_6L_3]^{x+}$ (L= O and N donors; x=0 or 1) complexes [171]. In this case the determined C:H ratio could be fitted to the molecular formula $[Mn_3(\mu_3\text{-}O)(\mu\text{-}O_2CMe)_6(MeOH)_3]$ (i.e. C:H = 15:30).

Methanol solution e.s.r. spectra of the oxidised species revealed a $I=^5/_2$ hyperfine split g_{eff}~2 (3408 G) absorption indicating the presence of manganese(II). Spectra of the known complexes $[Mn_3(\mu_3\text{-}O)(\mu\text{-}O_2CMe)_6][O_2CMe].MeCO_2H$ and $[Mn_3(\mu_3\text{-}O)(\mu\text{-}O_2CMe)_6L_3]$ (L=py and 3-Clpy) were investigated for comparative purposes.

Complexes possessing d^4 electronic configurations are generally e.s.r. silent, probably due to short spin-lattice relaxation times, together with large zero-field splittings [172].

As expected for $[Mn_3(\mu_3\text{-}O)(\mu\text{-}O_2CMe)_6][O_2CMe].MeCO_2H$ in which all the metal atoms are in the +3 oxidation state, no e.s.r. spectrum could be recorded for a methanol solution.

Conversely, $[Mn_3(\mu_3\text{-}O)(\mu\text{-}O_2CMe)_6(3\text{-}Clpy)_3]$ is a one-electron reduced species which has been shown by X-ray crystallography to

contain one discrete manganese(II) ion and two discrete manganese(III) ions in the solid state [173]. The methanol solution e.s.r. spectrum is in agreement with this formulation, an absorption with $I=^5/_2$ hyperfine splitting at $g_{eff}\sim2$ (3415±3 G) being observed. In the solid state the complex $[Mn_3(\mu_3\text{-}O)(\mu\text{-}O_2CMe)_6(py)_3]$ has been shown crystallographically to be rather different than the 3-chloropyridine analogue in that it contains 3 equivalent manganese atoms, each thereby having a formal oxidation state of $+^8/_3$ [174]. The methanol solution e.s.r. spectrum of this complex shows a $I=^5/_2$ hyperfine split absorption at $g_{eff}\sim2$ (3413±3 G). The spectra of the two pyridine adducts therefore appear essentially the same indicating similar manganese(II) environments for each complex in solution. On first inspection this would seem contrary to the solid state structures deduced from X-ray crystallographic analysis. However, it is possible that in methanol solution the manganese atoms in $[Mn_3(\mu_3\text{-}O)(\mu\text{-}O_2CMe)_6(py)_3]$ may be reorganised to the discrete +2,+3,+3 pattern observed in solid $[Mn_3(\mu_3\text{-}O)(\mu\text{-}O_2CMe)_6(3\text{-}Clpy)_3]$. Alternatively, the manganese(II) signal observed in both species may represent a rapid 'flipping' of a manganese(II) character between the three atoms within the timescale of the e.s.r. experiment (10^{-4}-10^{-8} sec), in an averaged magnetically equivalent Mn_3O moiety.

The above e.s.r. behaviour appears to be mirrored by the $[Mn(N_2H_4)_2(O_2CMe)_2]_n$ oxidation product, a further indication that a $[Mn_3(\mu_3\text{-}O)(\mu\text{-}O_2CMe)_6L_3]$ species may possibly be formed.

The fate of the hydrazine released is unknown. Analysis showed no nitrogen remained in the oxidised solid and it is clear that free hydrazine would reduce any manganese(III) centre because it is known that addition of hydrazine to solutions of $[Mn_3(\mu_3\text{-}O)(\mu\text{-}$

$O_2CMe)_6]$ species causes rapid reduction to manganese(II). The evolution of gas observed in the initial stages of reaction suggests hydrazine decomposition.

If this is so, it is interesting to speculate whether hydrazine is involved in the oxidation process. One possibility is that all hydrazine must be consumed before oxidation commences. This could be achieved by reaction with dissolved dioxygen which would result in H_2O and evolved N_2. However this would leave only $Mn(O_2CMe)_2$ in solution which is known not to be susceptible to atmospheric oxidation.

It is possible that hydrazine is acting as an oxidising agent towards manganese(II), or is activating the manganese(II) centre towards oxidation by atmospheric dioxygen. This is not impossible as hydrazine is known to act as an oxidising agent towards certain transition metals (e.g. rhenium [175], ruthenium [176] and molybdenum [177], also see SECTION 1.2). The apparent cleavage of hydrazine ligands from $[Mn(N_2H_4)_2(O_2CMe)_2]_n$ may be the rate-determining step of the reaction.

Although this reaction system remains to be fully understood, it is clear that hydrazine is playing an important role in a manganese(II) oxidation. Normally, high-spin manganese(II) complexes are highly resistant to oxidation, a feature which has been attributed to the effect of the symmetrical d^5 configuration despite zero CFSE. However the presence of hydrazine appears to overcome this stability. The ability of hydrazine to show oxidation potential towards manganese(II) is a significant step in proposed mechanisms for homogeneous catalytic decomposition of hydrazine. In these models a combined chromium/manganese system is suggested to

decompose hydrazine by succesive oxidation and reduction at $Mn^{(II)/(III)}$ and $Cr^{(II)/(III)}$ metal centres.

2.7 EXPERIMENTAL

Details of physical techniques and purification of solvents and reagents appear in appendices 1 and 2.

2.7.1 PREPARATIONS OF MANGANESE(II)-HYDRAZINE COMPLEXES

a) *catena*-Dichlorodi-μ-hydrazinemanganese(II) $[Mn(N_2H_4)_2Cl_2]_n$

Anhydrous $MnCl_2$ (1.26 g, 10 mmol) was dissolved in methanol (40 cm^3). To this stirred solution was added a methanol solution (20 cm^3) of N_2H_4 (0.95 cm^3, 30 mmol). The white product precipitated immediately and was filtered off, washed with MeOH, Et_2O and dried under vacuum.

b) *catena*-Dibromodi-μ-hydrazinemanganese(II) $[Mn(N_2H_4)_2Br_2]_n$

As for $[Mn(N_2H_4)_2Cl_2]_n$ but using $MnBr_2$ (2.15 g, 10 mmol) as the manganese salt. Yield. (1.51 g, 77%).

c) *catena*-Di-μ-hydrazinediiodomanganese(II) $[Mn(N_2H_4)_2I_2]_n$

i) As for $[Mn(N_2H_4)_2Cl_2]_n$, but using MnI_2 (3.09 g, 10 mmol) as the manganese salt.

ii) To a stirred methanol solution (150 cm^3) of NH_4I (36.35 g, 0.251 mol) was added $MnBr_2.4H_2O$ (1.47 g, 5.13 mmol), (Mn:I ratio = 1:48.9). To this solution was added dropwise a methanol solution of N_2H_4 (0.50 cm^3, 15.8 mmol). The white product precipitated immediately and was filtered off, washed with MeOH, Et_2O and dried under vacuum. Yield. (1.29 g, 68%).

d) *catena*-Diacetato-*O*-di-μ-hydrazinemanganese(II) $[Mn(N_2H_4)_2(OCOMe)_2]_n$

Reaction of $Mn(O_2CMe)_2.4H_2O$ with N_2H_4 in methanol resulted in products that gave poor elemental analysis.

Suspension of $Mn(O_2CMe)_2.4H_2O$ (1.19 g, 5 mmol) in excess liquid N_2H_4 (15 cm^3), resulted in rapid formation of the white product. This was filtered off, washed with MeOH, Et_2O and dried under vacuum.

e) ***catena*-Di-μ-hydrazinediisocyanato-*N*-manganese(II)**
$[Mn(N_2H_4)_2(NCO)_2]_n$

To an aqueous solution (25 cm^3) of KNCO (4.25 g, 52.4 mmol) was added dropwise an ethanol solution (50 cm^3) of $MnBr_2.4H_2O$ (1.45 g, 5.1 mmol). To the resulting reaction mixture was added N_2H_4 (0.50 cm^3, 15.8 mmol). The resulting white product was filtered off, washed with EtOH, Et_2O and dried under vacuum.

f) ***catena*-Di-μ-hydrazinediisothiocyanato-*N*-manganese(II)**
$[Mn(N_2H_4)_2(NCS)_2]_n$

To a stirred methanol solution (100 cm^3) of NH_4NCS (7.61 g, 100 mmol) was added a methanol solution (30 cm^3) of anhydrous $MnCl_2$ (1.26 g, 10 mmol). To the resulting reaction mixture was added a methanol solution (20 cm^3) of N_2H_4 (0.95 cm^3, 30 mmol). The resulting white product was filtered off, washed with MeOH, Et_2O and dried under vacuum. Yield. (2.20 g, 94%).

g) ***catena*-Di-μ-hydrazinediisoselenocyanato-*N*-manganese(II)**
$[Mn(N_2H_4)_2(NCSe)_2]_n$

To a methanol solution (130 cm^3) of KNCSe (7.20 g, 50 mmol) was added $MnBr_2.4H_2O$ (1.42 g, 4.95 mmol). To this stirred suspension was added a methanol solution (50 cm^3) of N_2H_4 (0.50 cm^3, 15.8 mmol). The resulting white product was filtered off, washed with MeOH, Et_2O and dried under vacuum. Yield. (1.54 g, 94%).

h) *catena*-Diazidodi-μ-hydrazinemanganese(II) $[Mn(N_2H_4)_2(N_3)_2]_n$

To a stirred aqueous/methanol solution (50/130 cm^3) of NaN_3 (9.88 g, 152 mmol) was added $MnBr_2.4H_2O$ (1.43 g, 5 mmol). To the resulting solution was added a methanolic solution (20 cm^3) of N_2H_4 (0.50 cm^3, 15.8 mmol). The white product precipitated slowly on stirring. This was filtered off, washed with MeOH, Et_2O and dried under vacuum. Yield. (0.82 g, 81%).

i) *catena*-Di-μ-hydrazinedinitritomanganese(II) $[Mn(N_2H_4)_2(ONO)_2]_n$

Isomer(I)

To a stirred methanol solution (140 cm^3) of $NaNO_2$ (6.90 g, 100 mmol) was added anhydrous $Mn(O_2CMe)_2$ (1.73 g, 10 mmol). To the resulting solution was added a methanol solution (20 cm^3) of N_2H_4 (0.95 cm^3, 30 mmol). A pale brown solid precipitated immediately, was filtered off, washed with MeOH, Et_2O and dried under vacuum. Yield. (1.80 g, 85 %)

Found: C, 0.97; H, 3.88; N, 37.8 (Calc for. $[Mn(N_2H_4)_2(NO_2)_2]_n$: H, 3.82; N, 39.82 %.)

The same product can be prepared by the substitution of $MnBr_2$ for $Mn(O_2CMe)_2$.

Isomer(II)

To a stirred methanol solution (100 cm^3) of $NaNO_2$ (6.90 g, 100 mmol) was added anhydrous $MnCl_2$ (1.26 g, 10 mmol). To the resulting solution was added a methanol solution (10 cm^3) of N_2H_4 (0.95 cm^3, 30 mmol) dropwise. A pale brown solid precipitated immediately, was filtered off, washed with MeOH, Et_2O and dried under vacuum. Yield. (1.68 g)

Found: C, 0.86, H, 3.88; N, 35.9 %.

j) Zinc diluted electron spin resonance samples

These were prepared as for the pure complexes, but using a mixture of the appropriate zinc salt (10 mmol) and manganese salt (0.1 mmol, 1% dilution).

TABLE No 2.16 Elemental Analysis of $[Mn(N_2H_4)_2X_2]_n$

Complex	% Expected (Found)					
	C		H		N	
$[Mn(N_2H_4)_2Cl_2]_n$	0.0	(0.0)	4.25	(4.42)	29.50	(29.50)
$[Mn(N_2H_4)_2Br_2]_n$	0.0	(>0.3)	2.89	(2.93)	20.09	(19.95)
$[Mn(N_2H_4)_2I_2]_n$	0.0	(0.0)	2.16	(2.29)	15.03	(15.23)
$[Mn(N_2H_4)_2(NCO)_2]_n$	11.83	(11.71)	3.97	(4.02)	41.39	(40.73)
$[Mn(N_2H_4)_2(NCS)_2]_n$	10.21	(10.21)	3.43	(3.23)	35.73	(35.13)
$[Mn(N_2H_4)_2(NCSe)_2]_n$	7.30	(7.22)	2.45	(2.60)	25.55	(25.00)
$[Mn(N_2H_4)_2(N_3)_2]_n$	0.0	(>0.5)	3.97	(3.91)	68.98	(68.95)
$[Mn(N_2H_4)_2(O_2CMe)_2]_n$	20.26	(20.10)	5.95	(6.10)	23.63	(23.87)

2.7.2 DEUTERATED HYDRAZINE COMPLEXES

a) *catena*-Dichlorodi-μ-hydrazine[^2H]manganese(II) $[Mn(N_2D_4)_2Cl_2]_n$

To a methanol-d_1 solution (5 cm^3) of anhydrous $MnCl_2$ (0.251 g, 1.99 mmol) was added $N_2H_4.H_2O$-d_6 (0.20 cm^3, 4.12 mmol) dropwise under N_2. The white product precipitated immediately, was filtered off in air, washed with MeOH-d_1, Et_2O and dried under vacuum. Yield. (0.36 g, 90%).

b) *catena*-Dichlorodi-μ-hydrazine[^2H]zinc(II) $[Zn(N_2D_4)_2Cl_2]_n$

To a methanol-d_1 solution (5 cm^3) of anhydrous $ZnCl_2$ (0.234 g, 1.72 mmol) was added $N_2H_4.H_2O$-d_6 (0.20 cm^3, 4.12 mmol) dropwise under N_2. The white product precipitated immediately, was filtered off in air, washed with MeOH-d_1, Et_2O and dried under vacuum. Yield. (0.33 g, 92%).

2.7.3 MANGANESE(III) COMPLEXES

a) 'Manganese(III) acetate dihydrate $Mn(OCOMe)_3.2H_2O$' [178]

$Mn(O_2CMe)_2.4H_2O$ (12 g) in glacial acetic acid (125 cm^3) was heated under reflux for 20 mins. The solution was cooled to just below the boiling point, then maintained at gentle reflux by the slow portionwise addition of $KMnO_4$ (2.0 g). The mixture was heated under reflux for a further 30 mins and then cooled to room temperature. After water (45 cm^3) had been added, the dark solution was left for 16 hours to crystallise. The solid was filtered off and washed several times with cold $MeCO_2H$ and dried in a desiccator over calcium oxide.

b) Hexa-μ-acetato-*O,O*-μ_3-oxotrimanganese(III,III,III) acetate ethanoic acid $[Mn_3(\mu_3\text{-}O)(\mu\text{-}O_2CMe)_6]^+[O_2CMe]^-.MeCO_2H$

The above compound '$Mn(O_2CMe)_3.2H_2O$' (5.0 g) was dissolved in glacial acetic acid acid (50 cm^3) containing 10% H_2O and heated to 100°C. The hot solution was filtered and on cooling the dark brown product precipitated. This was filtered off and dried under vacuum.

c) Hexa-μ-acetato-*O,O*-μ_3-oxotris(pyridine)trimanganese($^9/_3$,$^9/_3$,$^9/_3$) $[Mn_3(\mu_3\text{-}O)(\mu\text{-}O_2CMe)_6(py)_3]$

The product '$Mn(O_2CMe)_3.2H_2O$' (5.0 g) and pyridine (5.0 cm^3) were dissolved in ethanol (30 cm^3). The solution was heated at 75° for 30 mins. The hot solution was filtered and allowed to

cool to room temperature to yield a dark brown precipitate. This was filtered off, washed with EtOH, Et_2O and dried under vacuum.

d) Hexa-μ-acetato-*O,O*-μ_3-oxotris(3-chloropyridine)-trimanganese(III,III,II) $[Mn_3(\mu_3\text{-}O)(\mu\text{-}O_2CMe)_6(3\text{-}Clpy)_3]$

This complex was prepared as for $[Mn_3(\mu_3\text{-}O)(\mu\text{-}O_2CMe)_6(py)_3]$ except that 3-chloropyridine replaced pyridine at the initial stage.

e) $[Mn(N_2H_4)_2(OCOMe)_2]_n$ oxidation product

The complex $[Mn(N_2H_4)_2(O_2CMe)_2]_n$ (1.75 g, 7.4 mmol) was placed in a paper extraction thimble (3×10 cm) of a Soxhlet apparatus containing methanol (75 cm^3). The methanol was gently refluxed in air for 72 hours. At the end of this time, all of the $[Mn(N_2H_4)_2(O_2CMe)_2]_n$ had been consumed to give an intense brown solution in the receiver flask. The resulting solution was reduced *in vacuo* to dryness.

Elemental analysis: Found. C, 26.1; H, 4.52; N, 0.0 %. Calc. for $[Mn_3(\mu_3\text{-}O)(\mu\text{-}O_2CMe)_6(MeOH)_3]$: C, 28.5; H, 4.79 %..

If the reaction is stopped after a few hours of extraction and the methanol in the receiver flask is cooled, the precipitation of a manganese(II) solid is observed. This was filtered off, washed with MeOH, Et_2O and dried under vacuum.

Elemental analysis: Found. C, 19.94; H, 4.40; N, 10.59 %. C:H:N = 2.18:5.75:1.00. Calc. for $[Mn(N_2H_4)(O_2CMe)_2]_n$: C, 23.43; H, 4.92; N, 13.66 %. C:H:N = 2:5:1.

f) $[Mn(N_2H_4)_2(ONO)_2]_n$ oxidation product

The complex $[Mn(N_2H_4)_2(ONO)_2]_n$(I) could be oxidised under similar conditions to $[Mn(N_2H_4)_2(O_2CMe)_2]_n$ using a methanol

Soxhlet extraction. No further characterisation was performed on this system.

CHAPTER No 3

THE HYDRAZINE - CARBON DIOXIDE SYSTEM AND ITS REACTIONS WITH CHROMIUM(II) AND (III)

THE HYDRAZINE - CARBON DIOXIDE SYSTEM

The reaction of carbon dioxide with hydrazine under aqueous conditions initially leads to the formation of the molecular ion-pair hydrazinium(1+) carbazate, $[N_2H_5][O_2CNHNH_2]$. Prolonged exposure to carbon dioxide leads to the formation of carbazic acid (hydrazine carboxylic acid) which most probably exists as the insoluble zwitterion $\overset{-}{O}_2CNH\overset{+}{N}H_3$.

3.1 HYDRAZINIUM(1+) CARBAZATE

The kinetics of the interaction of carbon dioxide with hydrazine has been studied by two groups. Staal and Fourholt [179] showed that the reaction of N_2H_4 with CO_2 in the presence of OH^- led to the formation of a 'carbamate' and carbonate ions. A rate constant of $10^{6.51}$ was found for 'carbamate' formation. The 'carbamate' was thought to have the formula, $NH_2NHCO_2^-$. Caplow [180] whilst investigating the kinetics of carbamate formation from amines, showed that the reaction of N_2H_4 with CO_2 at 10° followed the Brønsted relationship log k_{amine} ($M^{-1}sec^{-1}$) = 0.48 pK - 0.20. Acid-catalysed decarboxylation was fitted to the relationship log k_{H^+} ($M^{-1}sec^{-1}$) = 0.77 pK + 3.6 at 10° between pK 1.05 to -5.

The compound $[N_2H_5][O_2CNHNH_2]$ is a viscous liquid, which crystallizes only reluctantly after extended storage over concentrated sulphuric acid under vacuum. This solid melts near 344K and is readily soluble in water. If heated in a sealed tube at 413K, it is partially converted to carbohydrazide, $OC(NHNH_2)_2$ [6].

Only a limited number of Group 1 and 2 carbazate salts have been reported. $LiO_2CNHNH_2.H_2O$ was prepared by reaction of LiCl with $[N_2H_5][O_2CNHNH_2]$ by Funk, Eichhoff and Giesder [100]. The preparation of NaO_2CNHNH_2 was reported in a patent and recommended

as a sensitizer for light-sensitive materials [181]. Group 2 salts have been characterised rather more fully. The magnesium salt, $Mg(O_2CNHNH_2)_2.2H_2O$ has been reported by several groups and characterised by IR and thermal decomposition techniques [100,108, 125]. Two forms of $Ca(O_2CNHNH_2)_2$ have been prepared and characterised by single crystal X-ray diffraction analysis [115,128]. The major structural features have been mentioned in SECTION 1.5.

The hydrazinium(1+) carbazate system has been investigated in the present work with the aim of preparing carbazate salts for use in metal-carbazate reactions where the absence of free hydrazine was essential. The strong ion-pair nature of $[N_2H_5][O_2CNHNH_2]$, which was demonstrated by the inability to exchange the $N_2H_5^+$ cation for other desired cations, proved to be a severe practical difficulty. Although a number of methods for the preparation of carbazate salts of main-group and organic cations were attempted, none were totally successful. The routes employed are summarised in TABLE No 3.1

The reaction of HO_2CNHNH_2 with $LiOH.H_2O$ (using an analogous method to the preparation of lithium glycinate [182,183]), gave a stable colourless solid product. Elemental analysis indicated the molecular formula $LiO_2CNHNH_2.H_2O$. The IR spectrum showed the probable presence of carbazate and water (see TABLE No 3.2). The spectrum was tentatively assigned by reference to the spectrum of $Cr(O_2CNHNH_2)_2.H_2O$ (see SECTION 3.7.5). The carboxylate absorptions are easily assigned ($\nu(CO_2)$ 1593 and 1504 cm^{-1}, $\delta(OCO)$ 832 cm^{-1}, $\pi(COO)$ 611 cm^{-1} and $r(COO)$ 481 cm^{-1}) with the majority of remaining bands assignable to NH vibrations.

The compound $LiO_2CNHNH_2.H_2O$ had been reported earlier by Funk, Eichhoff and Giesder [100] but no infra-red data were published so

TABLE No 3.1 Attempted Cation Exchange Reactions of $[N_2H_5][O_2CNHNH_2]$*

i) $[N_2H_5][cbz]_{(aq)} + NaOH \xrightarrow[ii)\ EtOH]{i)\ H_2O}$	insoluble viscous liquid, no evidence of Na[cbz]
ii) $[N_2H_5][cbz]_{(aq)} \xrightarrow[column]{Na^+\ ion\text{-}exchange}$	decomposition of carbazate on column
iii) $[N_2H_5][cbz]_{(aq)} + Ph_4PBr \xrightarrow[N_2,\ CO_2]{N_2H_4,\ 0^\circ}$	$Ph_3P{=}O$ formed, no evidence of $[Ph_4P][cbz]$
iv) $[N_2H_5][cbz]_{(aq)} + Ph_4AsCl \xrightarrow[N_2,\ CO_2]{N_2H_4,\ 0^\circ}$	unidentified $[Ph_4As]^+$ species formed
v) $[N_2H_5][cbz]_{(aq)} + Cs_2CO_3 \xrightarrow{H_2O}$	colourless viscous liquid, no evidence of Cs[cbz]

NOTE * - $O_2CNHNH_2^-$ = cbz^-

comparison between their compound and the product prepared here is not possible.

$$LiOH.H_2O + HO_2CNHNH_2 \xrightarrow[N_2]{MeOH,\Delta} LiO_2CNHNH_2.H_2O \qquad (3.1)$$

On exposure of a solution of $BaCl_2.2H_2O$ in anhydrous hydrazine to a CO_2 atmosphere, a white crystalline solid formed. Elemental analysis of this water-soluble solid indicated the molecular formula $Ba(O_2CNHNH_2)_2.N_2H_4$. The IR spectrum of the solid appears to indicate the presence of both carbazate and hydrazine groups (see TABLE No 3.3).

As with $LiO_2CNHNH_2.H_2O$, the carboxylate absorptions are easily assigned. Two $r(NH_2)$ appear in 1000-900 cm^{-1} region which implies

TABLE No 3.2 Infra-red Spectrum of $LiO_2CNHNH_2.H_2O$ /cm^{-1}

Absorption	Assignment	Absorption	Assignment
3382 m		1372 vs	ν(CN)
3365 m	ν(NH)	1206 vw	
3340 w,sh		1090 w	b(NH)
3295 w		1055 w	
3215 w		995 w	r(NH_2)
2974 m		832 w	δ(OCO)
2945 m	H-bonding	611 w	π(COO)
2875 m		481 mw	r(COO)
1637 m	δ(NH_2)	416 w	t(NH_2)?
1593 vs	ν_a(CO_2)	361 w	
1504 vs	ν_s(CO_2)		

TABLE No 3.3 Infra-red Spectrum of $Ba(O_2CNHNH_2)_2.N_2H_4$ /cm^{-1}

Absorption	Assignment	Absorption	Assignment
3350 s		1138 w	
3282 vs	ν(NH)	1080 m,sh	b(NH)?
3185 s		1068 s	r(NH_2)
1646 m	δ(NH_2)	955 w	r(NH_2)
1596 vs	ν_a(CO_2)	922 w	
1524 s		821 mw	δ(OCO)
1484 vs	ν_s(CO_2)	726 m	
1361 s	ν(CN)	587 s	π(COO)
1266 w	ω(NH_2)		
1203 w			

the presence of two hydrazine-derived species as would be expected if carbazate and hydrazine were both present. Other absorptions are tentatively assigned to further NH motions by comparison with other hydrazine/carbazate species. Attempts to obtain single crystals of this product for an X-ray structural determination were not successful.

$$BaCl_2.2H_2O \xrightarrow[ii)\ CO_2]{i)\ N_2H_4} [Ba(O_2CNHNH_2)_2.N_2H_4] \qquad (3.2)$$

3.2 CARBAZIC ACID, HO_2CNHNH_2

Carbazic acid was first reported as a colourless, hygroscopic, sparingly water-soluble solid in 1904 by Stollé and Hofmann [6]. When heated to 363K HO_2CNHNH_2 lost CO_2 and formed $[N_2H_5][O_2CNHNH_2]$. More recent DTA experiments [184] showed that decomposition begins at 314K and becomes rapid at 357K. The same conversion can be achieved by distillation of HO_2CNHNH_2 under CO_2 at ambient or reduced pressure [6]. Carbazic acid has also been used as source of anhydrous hydrazine. It has also been reported that heating a suspension of HO_2CNHNH_2 in MeCN at 408K produces a dilute solution of anhydrous hydrazine [184].

The thio- and selenocarbazic acids and their hydrazinium and potassium salts have been well characterised by Anthoni *et al.* [185]. The free acids are thought to exist in zwitterionic form.

Previous attempts to prepare anhydrous carbazic acid have not been entirely successful. It was difficult to eliminate the last traces of water, attempts to dry samples under vacuum at ambient and elevated temperatures resulting in thermal decomposition.

In this work anhydrous HO_2CNHNH_2 has been obtained by passage of CO_2 through a cooled aqueous solution of N_2H_4 for 12 hours. The resulting white solid was filtered off under N_2 and then left to stand over anhydrous MeOH for several days after which it was re-filtered under N_2. The resulting solid was dry enough to mull in liquid paraffin and to pack into glass capillaries for study of its IR and Raman spectra, respectively.

Additionally HO_2CNHNH_2-d_4 was prepared in a similar manner, by passage of CO_2 through a H_2O-d_2 solution of $N_2H_4.H_2O$-d_6 for 12 hours.

3.2.1 VIBRATIONAL SPECTRA

The infra-red spectra of $\overset{-}{O}_2CNH\overset{+}{N}H_3$ and $\overset{-}{O}_2CND\overset{+}{N}D_3$ were recorded as paraffin and hexachlorobutadiene mulls and the Raman spectra as powdered samples (see TABLE No 3.4 and FIG No 3.1). Solution studies were not possible because of further reactions of the acid in solvents in which it is soluble such as water and hydrazine.

Although 21 normal modes of vibration are expected for an isolated O_2CNHNH_3 molecule, the molecular geometry and hence point group is unknown for carbazic acid, so any vibrational assignments of the solid state spectra must be regarded as tentative.

The molecular symmetry will undoubtably be low and many of the absorptions observed are unlikely to be associated with isolated vibrations. Coupling with other modes giving vibrations of highly mixed character is very probable. However, assignments have been suggested by considering the predominant mode of vibration likely to be associated with a particular vibrational band.

Carbazic acid is expected to be zwitterionic in the solid state, as known for the iso-electronic amino acid glycine and assumed for its thio- and seleno-analogues. However, comparison with the vibrational spectrum of glycine [186] has been found to be of only limited value. This lack of correlation is probably a consequence of increased hydrogen bonding in carbazic acid relative to glycine. The spectra of $\overset{-}{O}_2CNH\overset{+}{N}H_3$ and $\overset{-}{O}_2CND\overset{+}{N}D_3$ are therefore complex, especially in the $\nu(NH)$ and $\delta(NH_2)$ regions.

Assignments have been made by comparison with (i) coordinated glycinate and acetate for the carboxylate derived vibrations, and (ii) hydrazinium(1+) and (2+) and coordinated carbazate anion spectra for the N-H derived and skeletal vibrations.

The carboxylate absorptions are most readily assigned by a consideration of their low deuteration shifts and their insensitivity to variation in the nature of adjacent groups.

Five carboxylate normal modes are expected, but these may be split by the extensive hydrogen-bonding present and by solid state effects. There are two (CO_2) stretching modes, an OCO deformation, a COO out-of-plane bend and a COO rocking mode.

In glycine, the two $\nu(CO_2)$ vibrations occur at 1610 and 1415 cm^{-1}. The spectrum of $^{-}O_2CNHN^{+}H_3$ contains a number of strong absorptions in this region, that at 1668 cm^{-1} being the most intense. On deuteration only one broad band appears at 1627 cm^{-1}, an isotopic shift ratio of 1.03. The $\nu_a(CO_2)$ mode is assigned to these absorptions.

The corresponding $\nu_s(CO_2)$ vibration can be expected to be lower in frequency than $\nu_a(CO_2)$, e.g. a reduction of between ~160 cm^{-1} ($Na^{+}O_2CMe^{-}$) to ~326 cm^{-1} ($Na^{+}O_2CCBr_3^{-}$) [187] . Suitable bands for assignment as $\nu_s(CO_2)$ appear at 1476 and 1351 cm^{-1}. On deuteration only one band appears in this region, a particularly intense band at 1373 cm^{-1}. This may indicate coincidence between $\nu_s(CO_2)$ and a skeletal vibration expected to lie in this region. A similar effect is seen the IR spectrum of $Cr(O_2CNDND_2)_2.D_2O$. No corresponding $\nu_s(CO_2)$ Raman bands are seen in this region, but the skeletal vibration shifts on deuteration from 1465 cm^{-1} to the coincident band at 1367 cm^{-1}. Therefore $\nu_s(CO_2)$ is assigned to the band at 1351 cm^{-1} in $^{-}O_2CNHN^{+}H_3$ shifting to 1373 cm^{-1} on deuteration.

The remaining carboxylate bands can be assigned by reference to bands present in acetate and glycine spectra.

The $\delta(OCO)$ band is found at 646 cm^{-1} in NaO_2CMe [188] and 694 cm^{-1} in $^{-}O_2CCH_2N^{+}H_3$ [186] (NOTE: this band is assigned in the

orginal work as ω(COO), with δ(OCO) appearing at lower frequencies. As shown for the acetate anion, only three carboxylate modes are expected below 700 cm^{-1}; δ(OCO), π(COO) and r(COO), so this may indicate a confusion in the description of the vibration). In the IR spectrum of $\overset{-}{O}_2CNH\overset{+}{N}H_3$, a strong absorption appears at 656 cm^{-1}. However no corresponding band appears in the spectrum of $\overset{-}{O}_2CND\overset{+}{N}D_3$, indicating significant NH character associated with the vibration. A deuteration-insensitive absorption does, however, appear at higher frequency (838 cm^{-1} in $\overset{-}{O}_2CNH\overset{+}{N}H_3$, 817 cm^{-1} in $\overset{-}{O}_2CND\overset{+}{N}D_3$). As no NH-derived absorptions are expected in this region, these absorptions have been assigned to δ(OCO). A high frequency δ(OCO) was also found in the IR spectrum of $Cr(O_2CNHNH_2)_2.H_2O$ at 802 cm^{-1}.

The π(COO) band in NaO_2CMe appears at 615 cm^{-1} [188], and at 607 cm^{-1} in $\overset{-}{O}_2CCH_2\overset{+}{N}H_3$ [186]. An intense absorption in $\overset{-}{O}_2CNH\overset{+}{N}H_3$ at 586 cm^{-1} in the IR with a Raman counterpart at 579 cm^{-1}, appears to shift on deuteration to 581 cm^{-1}. This isotopic shift ratio of 1.01 confirms an assignment of these bands to π(COO).

The final carboxylate band, r(COO), occurs at 460 cm^{-1} in NaO_2CMe [188] and 504 cm^{-1} in $\overset{-}{O}_2CCH_2\overset{+}{N}H_3$ [186]. A strong absorption appears at 514 cm^{-1} in the IR spectrum of $\overset{-}{O}_2CNH\overset{+}{N}H_3$, but no band is found near this frequency in deuterated carbazic acid, so the band is assigned to t(NH_2). However, a further deuteration-insensitive absorption occurs at 380 cm^{-1} in $\overset{-}{O}_2CNH\overset{+}{N}H_3$, which may be assignable to the true r(COO) vibration.

Assignment of NH-derived bands is hampered by the lack of firm, well-founded assignments of these bands in closely related molecules. Thus, assignments of ν(NH) bands in hydrazinium salts are uncertain. For example, the vibrational spectrum of N_2H_5Cl was completely assigned by Schettino and Salomen [189] using

deuteration studies, but comparison with the assignments proposed by Milicéur and Márek [190] for the vibrational spectra of N_2H_5F and $N_2H_6Cl_2$ is confused by their differing descriptions of the NH_2/NH_3^+ modes. Despite these difficulties it is possible to make some general comments concerning $-NHNH_3^+$ absorptions.

The $-NH_3^+$ moiety can simply be assumed to vibrate in a similar manner to $-CH_3$. Therefore nine normal vibrations can be associated with it. These can be described as three NH stretches, three deformations, a wagging, a rocking and a torsional mode. In addition, there will be three vibrations from the -NH- bond; a NH stretch and two bending motions. It is expected that some of these vibrations will be mixed and it is unlikely that 12 pure NH/NH_3^+ vibrations will be observed.

In $\overset{-}{O}_2CNH\overset{+}{N}H_3$ the NH stretching region is complex, with six major broad bands extending from 3226 to 2524 cm^{-1}, and an additional band at 2102 cm^{-1}. Undoubtedly some of these absorptions arise from hydrogen-bonding within the solid state lattice. Raman spectra reveal only three bands in this region. On deuteration nine bands are found in the corresponding ND stretching region, both in the infra-red and Raman spectra. Therefore it is not possible to distinguish between fundamentals and hydrogen-bond-derived absorptions in these regions.

Three $\delta(NH_2)$ vibrations are expected and can be assigned to the group of absorptions found at 1579, 1553 and 1539 cm^{-1}. On deuteration, these absorptions appear to shift to a multiple absorption centred at 1163 cm^{-1}, an isotopic shift ratio of ~1.35.

The $\omega(NH_2)$ bands of N_2H_4 are found at 1324 and 1283 cm^{-1}. A vibration of comparable frequency is found at 1331 cm^{-1} in N_2H_5F although it was not assigned to a wagging mode by the authors

[190]. The IR spectrum of $^{-}O_2CNH\overset{+}{N}H_3$ contains a band at 1264 cm^{-1}, the Raman spectrum only showing a band at 1329 cm^{-1}. On deuteration, a very weak IR band at 1042 cm^{-1} with a Raman counterpart of medium intensity at 1045 cm^{-1} can be assigned to $\omega(NH_2)$, the isotopic shift ratio being 1.32.

The $r(NH_2)$ absorptions of N_2H_4 and coordinated N_2H_4 appear ~100-200 cm^{-1} below the wagging motions and can be assigned in $^{-}O_2CNH\overset{+}{N}H_3$ to the strong band at 1224 cm^{-1}. On deuteration the band is found at 948 cm^{-1}, an isotopic shift ratio of 1.29.

A weak absorption at 1116 cm^{-1} is likely to be a NH derived vibration, possibly b(NH) as absorptions present in this region for coordinated carbazate spectra have been assigned to this mode. A second b(NH) is expected from the above simple treatment of the -NH-NH_3 system and may contribute to the mainly skeletal absorption observed at 1003 cm^{-1} in the IR spectrum of $^{-}O_2CNH\overset{+}{N}H_3$.

The $t(NH_2)$ vibration in glycine occurs at 519 cm^{-1} [186], while in the spectrum of N_2H_5Cl it has been assigned to a band at 435 cm^{-1} [189]. A deuteration-sensitive absorption in $^{-}O_2CNH\overset{+}{N}H_3$ appears at 514 cm^{-1} in the IR, its deuterated analogue being found at 343 cm^{-1}.

Two pure skeletal vibrations are expected. These can simply be described as ν(CN) and ν(NN).

The antisymmetric vibration (ν(CN)) is readily assigned to a band at 1476 cm^{-1} in the IR spectrum of $^{-}O_2CNH\overset{+}{N}H_3$ with a medium-intensity Raman counterpart at 1465 cm^{-1}. This band shifts on deuteration to 1375 cm^{-1} to become coincident with $\nu_s(CO_2)$. A skeletal description for this band is suggested by the intense Raman counterpart at 1365 cm^{-1}.

The symmetric vibration (ν(NN)) is difficult to assign to a particular absorption. As indicated before, the absorption present at 1003 cm^{-1} in the IR spectrum of $\overset{-}{O}_2CNH\overset{+}{N}H_3$ appears to be shifted on deuteration to 992 cm^{-1}, an isotopic shift ratio of 1.01. A further skeletal vibration of $\overset{-}{O}_2CNH\overset{+}{N}H_3$ appears at 1264 cm^{-1} and shifts on deuteration to 1202 cm^{-1}, an isotopic shift ratio of 1.05. This situation is similar to that found in the vibrational spectrum of N_2H_4. So-called ν(NN) in N_2H_4 is found at 1098 cm^{-1}, but is known not to be a pure vibrational mode, the $r_s(NH_2)$ vibration also containing a high proportion of skeletal character.

Several unassigned absorptions remain in the spectra of $\overset{-}{O}_2CNH\overset{+}{N}H_3$ and $\overset{-}{O}_2CND\overset{+}{N}D_3$. They all appear to be deuteration-sensitive to some degree, but are found in regions (i.e. below 800 cm^{-1}) where pure NH vibrations are not expected, if comparisons are made with spectral data for N_2H_4 and $N_2H_5^+$.

In summary, a provisional vibrational assignment for $\overset{-}{O}_2CNH\overset{+}{N}H_3$ has been attempted using deuteration methods. However, many assignments are uncertain as a consequence of confusion over the vibrational assignments of hydrazine derivatives in general. More assured assignments will only be possible when the configuration and point group of the molecule in the solid state is known and the nature of the hydrogen-bonding present is clarified.

TABLE No 3.4 Vibrational Spectra of $\bar{O}_2CNH\dot{N}H_3$ and $\bar{O}_2CND\dot{N}D_3$ /cm^{-1}

$\bar{O}_2CNH\dot{N}H_3$		$\bar{O}_2CND\dot{N}D_3$		H/D ratio	Assignment
IR	RAMAN	IR	RAMAN		
3226 vs	3320 m,br	2431 s	2423 m	1,33	
	3119 w	2383 s,br	2369 mw,br		
	3072 mw,br	2335	2345		
2959 m		2253 s,br	2244 w,br	1,31	ν(NH) + ν(NH$_3$)
2859 m		2223	2212		+
2729		2148	2165 mw	1,27	hydrogen-bonding
2628 vs,br		2117 s,br	2133 mw,br		
			2102 mw,br		
2524		2079	2070 w		
		2030 ms	2020 w,br		
1668 vs		1627 vs,br	1625 w	1,03	ν_a(CO$_2$)
1631 s					
	1615 mw				
1603 s					
1579 s					δ(NH$_3$)
1553 s	1552 w	1163 s	1155 m	1,34	
1539 s,sh	1535 w	1152 m,sh		1,34	
1476 s	1465 mw	1373* vs	1367* s	1,08	skeletal stretch
1351 s,br		1373* vs	1367* s		ν_s(CO$_2$)
	1329 vs	1042 vw	1045 m	1,28	ω(NH$_3$)
1264 s	1262 w	1202 m	1202 mw	1,05	skeletal stretch
1224 vs	1225 m	948 mw	947 mw	1,29	τ(NH$_2$)
1116 w					b(NH)
1003 ms	996 s	992 m	990 w	1,01	skeletal stretch + b(NH) ?
		885 s	877 m		?
838 s,br		817 s	812 vw,br	1,03	δ(OCO)
780 s	774 w	698 vs	-691 vw,br	1,12	
728 w					
656 vs	643 w	543 s	536 w,br	1,21	
586 vs	579 m	581 s	570 vw,br	1,01	π(COO)
514 s		343 s,br		1,50	t(NH$_3$)
380 vs		372 ms,sh		1,02	r(COO)

TABLE No 3.4 (cont) Vibrational Spectra of $\bar{O}_2CNHN\dot{H}_3$ and $\bar{O}_2CNDN\dot{D}_3$ /cm^{-1}

$\bar{O}_2CNHN\dot{H}_3$		$\bar{O}_2CNDN\dot{D}_3$		H/D ratio	Assignment
IR	RAMAN	IR	RAMAN		
359 s	350 mw				
304 vs					
	288 mw		303 w,sh		lattice modes
269 m		271 s	258 w,sh		
225 s			236 w,sh		

FIGURE 3.1 Infra-red Spectra of $\bar{O}_2CNHN\dot{H}_3$ and $\bar{O}_2CNDN\dot{D}_3$

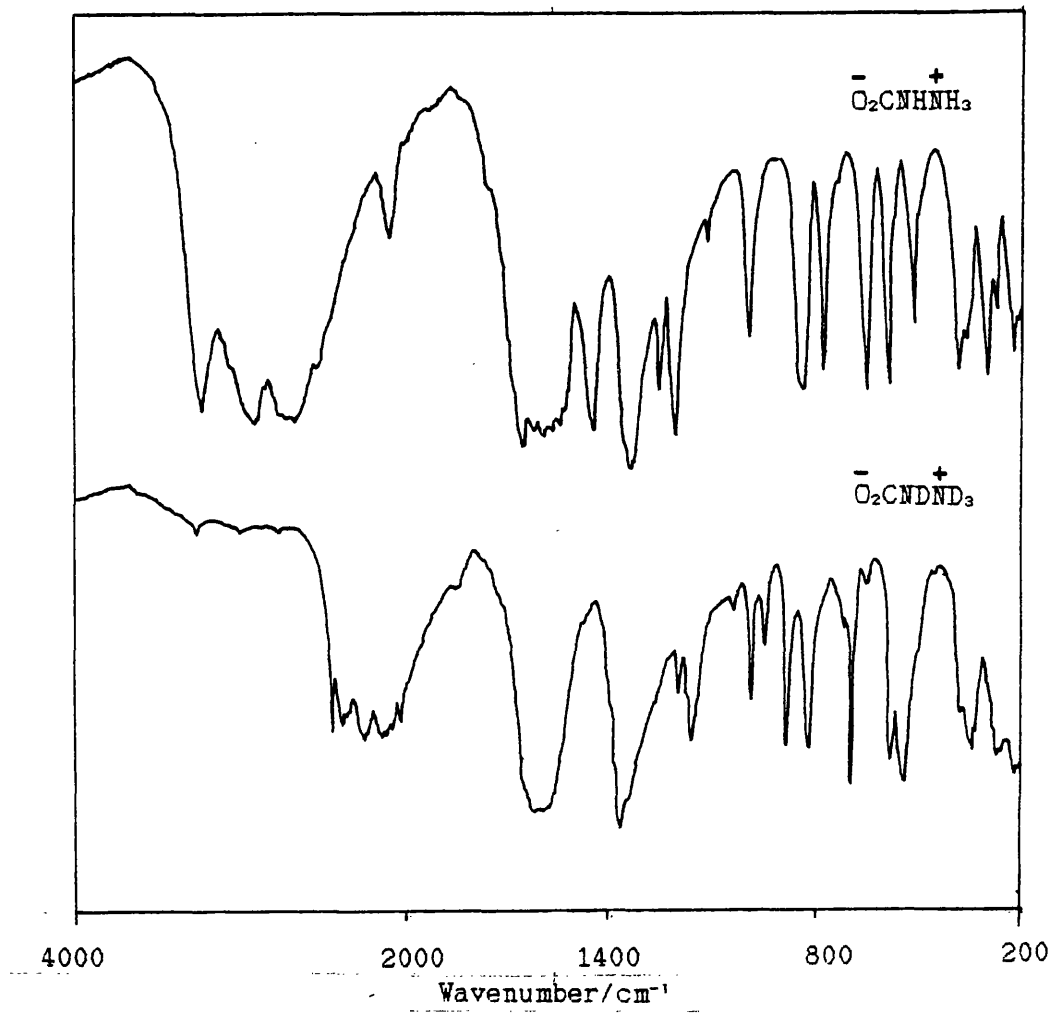

3.3 CHROMIUM(II)-HYDRAZINE CHEMISTRY

3.3.1 BACKGROUND

The reactions of hydrazine with chromium(II) species has received less attention than comparable reactions employing other first-row transition metal ions.

In 1913 Traube and Passarge [191] reported the preparation of the surprisingly air-stable pale lilac compounds $[Cr(N_2H_4)_2X_2]_n$ (X=Cl,Br,I). Hein and Bähr claimed that the reaction between CrI_2 and N_2H_4 gave a red solution. Evaporation of this solution under various conditions gave $CrI_2(N_2H_4)_x$ (x=6,4,3). The reaction of the latter compound with water apparently gave $Cr_4(OH)_4I_4(N_2H_4)_5(H_2O)_6$, an unlikely formulation [192]. Reaction of the compound with ethanol gave a similarly unlikely $Cr_2(OEt)_2I_2(N_2H_4)_5$. These workers also found that the reaction of $CrCl_3$ with N_2H_4 produced a red solution similar to that formed by CrI_2. This observation was rationalised as a reduction of Cr(III) to Cr(II) by hydrazine. Fazlur-Rehman and Malik reported [193] the formation of the tris(hydrazine) complex $[CrCl_2(N_2H_4)_3].3H_2O$, for which an anomalous room temperature magnetic moment of 3.4 BM was reported.

The most reliable work is that reported by Earnshaw, Larkworthy and Patel [194] who confirmed the stoichiometry of $[Cr(N_2H_4)_2X_2]_n$ and found these compounds to be isostructural with other divalent first-row transition metal-bis(hydrazine) complexes. These complexes have also been reported by Kauffman and Saugisaka [195], who prepared $[Cr(N_2H_4)_2Cl_2]_n$ by reduction of $[Cr(OH_2)_4Cl_2]Cl.2H_2O$ with Na/Hg amalgam and subsequent reaction with N_2H_4, and by Aliev [196] who reported the preparation of $[Cr(N_2H_4)_2X_2]_n$ (X=Cl,Br,I,½(SO_4)).

Recently, CrF_2 has been shown [197] to react with N_2H_4 to give impure $[Cr(N_2H_4)_2F_2]_n$, a complex unstable at room temperature.

In addition, the chromium(II) hydrazinium sulphate, $(N_2H_5)_2Cr(SO_4)_2$ has long been known to be stable towards atmospheric oxidation, X-ray powder diffraction studies [198] revealing it to be isostructural with $(N_2H_5)_2Zn(SO_4)_2$ in having coordinated unidentate hydrazinium and bridging sulphate ions [199].

3.3.2 THE BIS(HYDRAZINE) COMPLEXES $[Cr(N_2H_4)_2X_2]_n$ (X=Cl,Br)

The complexes $[Cr(N_2H_4)_2X_2]_n$ (X=Cl,Br) have been prepared in this work by the addition of hydrazine to aqueous-ethanolic solutions of chromium(II) chloride or bromide. These solutions have been prepared by the reaction of aqueous hydrogen halide with chromium metal in ethanol under nitrogen (3.3), a method first employed by Lux *et al.* [200] and subsequently used by Fackler and Holah [201]. The hydrazine complexes precipitate immediately, and once dry are stable towards prolonged atmospheric exposure.

$$Cr + 2\ HX_{(aq)} \xrightarrow[N_2]{EtOH,\Delta} [Cr(OH_2)_6]X_2 + 2N_2H_4 \xrightarrow[N_2]{EtOH} [Cr(N_2H_4)_2X_2]_n \qquad (3.3)$$

It was observed that some reaction products contained hydroxide impurities. This was thought to arise from a competing reaction in which N_2H_4 attacks a coordinated H_2O molecule forming a Cr^{II}-OH species which is then subject to atmospheric oxidation producing chromium(III) hydroxides.

The reflectance electronic spectra of the complexes as reported by Earnshaw *et al.* [194] indicate that the octahedral geometry is extensively distorted in a tetragonal manner, the d-d transition energies being independent of halide. This result

implies that the mutually *trans* chromium-halide interactions are very weak, the geometry being almost pseudo-square planar. Crystallographic data for $[M(N_2H_4)_2Cl_2]_n$ (M=Mn,Zn) [24,45] show that even in typical complexes of this type the metal environment is approximately D_{4h} with long M-Cl bonds. The additional Jahn-Teller distortion present in the chromium(II) species would magnify this structural distortion to the point where the MX bonds could be regarded as semi-ionic in nature.

The vibrational spectra of $[Cr(N_2H_4)_2X_2]_n$ are similar to those of other $[M(N_2H_4)_2X_2]_n$ species. Earnshaw *et al.* [194] assigned the spectra following the arguments of Sacconi and Sabatini [23]. The revised assignments listed in TABLE No 3.5 are based on the approach of Sathyanarayana and Nicholls [141]. The spectral range has been extended to 200 cm^{-1}, previous spectra only being recorded to 400 cm^{-1}.

Assuming C_{2h} local symmetry (see SECTION 2.3), Group Theory predicts two IR active ν(MN) bands and for $[Cr(N_2H_4)_2X_2]_n$ (X=Cl,Br) two such bands can be assigned. The ν(MX) bands are expected to appear below 200 cm^{-1} as a result of the weakness of the M-X bonds as discussed above.

3.3.3 ATTEMPTS TO PREPARE $[Cr(N_2H_4)_2(NCS)_2]_n$

To complement the known complexes $[Cr(N_2H_4)_2X_2]_n$ (X=Cl,Br,I), attempts were made to increase the range of anions coordinated to the $[Cr(N_2H_4)_2]$ backbone, as had been achieved with the analogous manganese complexes (see CHAPTER No 2).

The preparation of $[Cr(N_2H_4)_2(NCS)_2]_n$ was attempted following a successful procedure developed for $[Mn(N_2H_4)_2(NCS)_2]_n$. This involved

an anion exchange in solution, with additional precautions being essential in view of the ease of oxidation of chromium(II).

TABLE No 3.5 Infra-red Spectra of $[Cr(N_2H_4)_2X_2]_n$ /cm^{-1}

X	Cl	Br	I*	Assignment
	3237	3226	3192	
	3209	3192	3175	$\nu(NH_2)$
	3125	3125	3093	
	1613	1608	1592	$\delta(NH_2)$
	1572	1570	1555	
	1357	1350	1344	$\omega(NH_2)$
	1326	1326	1325	
	1218	1221	1221	$\nu(NN)$
	1199	1192	1186	$r(NH_2)$
	968	961	948	
	656	644	624	$t(NH_2)$
	612	601	594	
	427	420	~400	$\nu(MN)$
	346	338		

NOTE * - from ref. 194

Addition of an ethanolic solution of potassium thiocyanate to $[Cr(OH_2)_6]Cl_2$ resulted in the formation of soluble $K_3[Cr(NCS)_5]$, (following Larkworthy *et al.* [202]). However, subsequent addition of hydrazine induced oxidation and precipitation of a pink chromium(III) species, as shown by reflectance electronic spectroscopy (spectrum of oxidised product /nm ; 545 (s,br), 410 (s,br), assignable to $^4A_{2g} \rightarrow {}^4T_{2g}$ and $\rightarrow {}^4T_{1g}$ transitions respectively) (3.4).

$$Cr + 2\,HCl_{(aq)} \xrightarrow[N_2]{EtOH} [Cr(OH_2)_6]Cl_2 + 5KNCS \longrightarrow K_3[Cr(NCS)_5] \xrightarrow{N_2H_4} \text{solid chromium(III) compound} \quad (3.4)$$

Hydrazine is apparently acting as an oxidising agent towards chromium(II) in this reaction. The nature of the chromium(III) product was not explored.

3.3.4 ATTEMPTS TO PREPARE $[Cr(N_2H_4)_2(BF_4)_2]_n$

The reaction of aqueous tetrafluoroboric acid in ethanol with HCl-activated chromium metal under nitrogen resulted in the formation of royal blue '$[Cr(OH_2)_6][BF_4]_2$' (solution electronic spectrum showed one broad peak at 694 nm assignable to the $^5E_g \rightarrow {}^5T_{2g}$ transition). Activation of the metal by treatment with $HCl_{(aq)}$ allows the tetrafluoroboric acid to react by providing an oxide free surface. This compound and the hexafluorophosphate analogue could provide useful chromium(II) starting materials in reactions where non-coordinating anions are required (3.5).

$$Cr + 2\ HBF_{4(aq)} \xrightarrow[N_2]{EtOH} '[Cr(OH_2)_6][BF_4]_2'_{(EtOH)} \qquad (3.5)$$

It was hoped that the addition of hydrazine to this solution would allow the formation of hydrazine complexes with a higher N_2H_4:Cr stoichiometry than 2:1 as shown by $[Cr(N_2H_4)_2X_2]_n$ (X=halide). There is precedence with other divalent first-row transition metals forming $[M(N_2H_4)_x]^{2+}$ (x=3 or 6) [25,26]. However, the addition of N_2H_4 to $[Cr(OH_2)_6][BF_4]_2$ under N_2 resulted in the rapid precipitation of a dark lilac solid, which was shown by reflectance electronic spectra to be a chromium(III) species (see TABLE No 3.6)

As further evidence that oxidation had occured, it was found that the addition of N_2H_4 to deliberately air-oxidised $[Cr(OH_2)_6][BF_4]_2$ caused the preciptation of a solid with similar

electronic spectral and magnetic susceptibility properties confirming the presence of chromium(III) in the product (see TABLE No 3.6 and SCHEME 3.6)

TABLE No 3.6 Comparison of Electronic Spectral and Magnetic Susceptibility Properties of the Products of Chromium Tetrafluoroborate-Hydrazine Reactions

Reaction product	Electronic Spectrum /nm	Magnetic Susceptibility /$\times 10^{-6}$ cm^3 g^{-1}
$Cr(BF_4)_2 + N_2H_4$	571(s,br),409(s,br)	23.11
oxidised $Cr(BF_4)_2$ + N_2H_4	574(s,br),412(m.br)	24.12

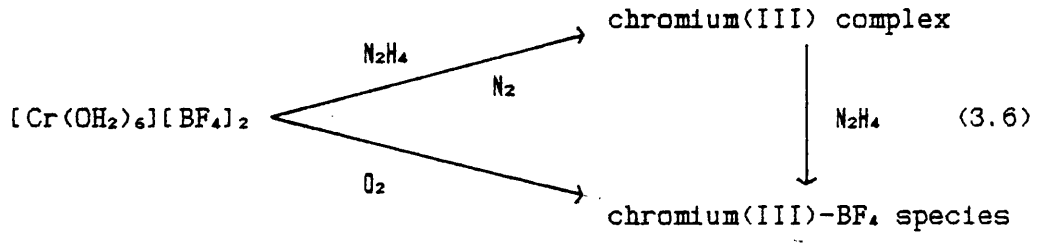

(3.6)

Infra-red spectra of the products show several absorptions assignable to hydroxy- and tetrafluoroborate vibrations (e.g. ν(OH) 3280, $\delta(OH_2)$ 1605, ν(BF) 1040, δ(FBF) 520 cm^{-1}), but no bands which could be assigned to coordinated hydrazine. The product is likely to be a hydroxy-bridged chromium(III) complex.

The lack of hydrazine coordination towards chromium(II) tetrafluoroborate suggests that oxidation is a more thermodynamically favoured process than the formation of a $[Cr(N_2H_4)_6]^{2+}$ cation.

3.3.5 THE CHROMIUM(II) ACETATE-HYDRAZINE REACTION PRODUCT, $[Cr_2(\mu\text{-}O_2CMe)_4(\mu\text{-}N_2H_4)]_n$

The reaction of $Cr_2(O_2CMe)_4(OH_2)_2$ with hydrazine in deoxygenated ethanol under nitrogen gives the orange-red air-sensitive solid $[Cr_2(\mu\text{-}O_2CMe)_4(\mu\text{-}N_2H_4)]_n$.

The essential diamagnetism (χ_{cgs} = 1.09×10^{-6} cm^3 g^{-1}, μ_{eff} = 0.57 BM per Cr at 296K), reflectance electronic spectrum (see TABLE No 3.7) and infrared spectrum (see TABLE No 3.8 and FIG No 3.3) support a structure in which the quadruple metal-metal bond of the hydrate is retained but axial bridging hydrazine replaces the water ligands generating a chain of alternating dichromium(II) and hydrazine units as in $[Cr_2(\mu\text{-}O_2CMe)_4(\mu\text{-pyrazine})]_n$ [203].

The complex can be compared with the known $Cr_2(\mu\text{-}O_2CMe)_4(NH_3)_2$ [204] where the two ammonia molecules replace the water ligands in $Cr_2(O_2CMe)_4(OH_2)_2$. This compound is very weakly paramagnetic (μ_{eff} = 0.6 BM at 295 K) and displays a diffuse reflectance electronic spectrum typical of a quadruply bonded dichromium(II) species (513 (s,br), ~345 (s,vbr), 270 (s,br) /nm).

The diffuse reflectance electronic spectrum of $[Cr_2(\mu\text{-}O_2CMe)_4(\mu\text{-}N_2H_4)]_n$ is compared with that of $Cr_2(\mu\text{-}O_2CMe)_4(OH_2)_2$

FIGURE No 3.2 Proposed Structure of $[Cr_2(\mu\text{-}O_2CMe)_4(\mu\text{-}N_2H_4)]_n$

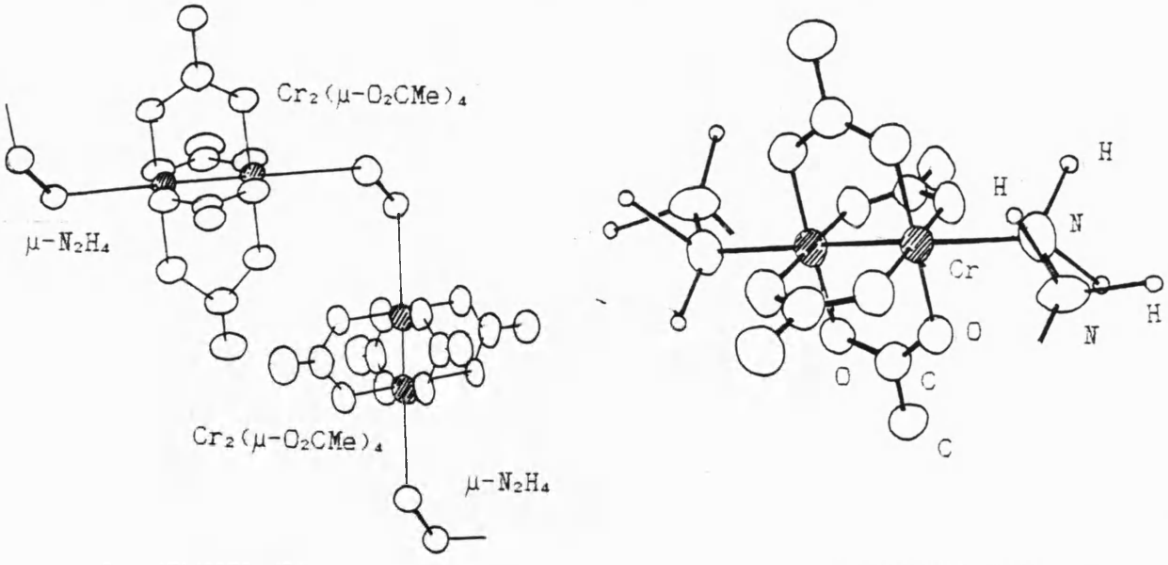

in TABLE No 3.7. Solomen *et al.* [205] have concluded that both major bands I and II are derived from orbitally degenerate (E) electronic states assuming an approximate D_{4h} symmetry for the molecule. It was concluded that I and II were associated with $\delta \rightarrow \pi^*$ and $np_x \rightarrow \pi^*$ transitions respectively.

TABLE No 3.7 Diffuse Reflectance Electronic Spectra

L =	OH_2	½(N_2H_4)	Assignment[a]
	486 s,br	478 s,br	I
	469 w,br	462 w,sh	
		445 w,sh	
		390 w,sh	
	347 s,sh	360 s,sh	
	326 vs	333 vs	II
		294 vs	

[a]-see text for assignment description

The infra-red spectrum of $[Cr_2(\mu\text{-}O_2CMe)_4(\mu\text{-}N_2H_4)]_n$ displays absorptions assignable to both coordinated O_2CMe and N_2H_4 (see TABLE No 3.8 and FIG No 3.3). The infra-red spectra of $[Cr_2(\mu\text{-}O_2CMe)_4(OH_2)_2]$ and a typical bridging hydrazine species $[M(N_2H_4)_2X_2]_n$ have been used to provide reference data.

Both ν(NN) and $r_s(NH_2)$ have lower frequencies than normally found in bridging hydrazine complexes (e.g. ν(NN) $[Cr_2(\mu\text{-}O_2CMe)_4(\mu\text{-}N_2H_4)]_n$ = 1162, $[Cr(\mu\text{-}N_2H_4)_2Cl_2]_n$ = 1218 cm^{-1}). This could be a consequence of coordination to the Cr_2^{4+} moiety. There is some uncertainty over the specific assignments of ν(CC) and $r_s(NH_2)$ which occur in the same region. In $[Cr_2(\mu\text{-}O_2CMe)_4(OH_2)_2]$, ν(CC) is assigned to a weak absorption at 966 cm^{-1}. In $[Cr_2(\mu\text{-}O_2CMe)_4(\mu\text{-}N_2H_4)]_n$ the same vibration appears at 961 cm^{-1}. This leaves $r_s(NH_2)$ to be assigned to a weak sharp absorption at 926 cm^{-1}. Such a

frequency would normally be characteristic of unidentate hydrazine coordination, but the band position may again be influenced by the Cr_2^{4+} centre. This also implies that use of the frequency of $r_s(NH_2)$ vibration as a indicator of hydrazine coordination mode may not be valid in all cases.

FIGURE No 3.3 Infra-red Spectrum of $[Cr_2(\mu\text{-}O_2CMe)_4(\mu\text{-}N_2H_4)]_n$

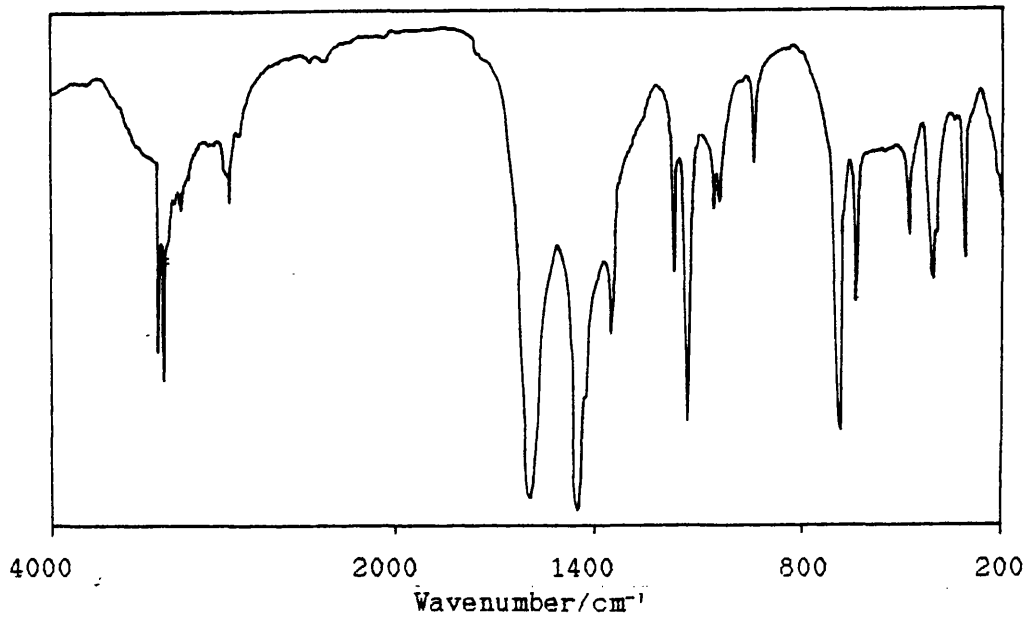

A band at 469 cm^{-1} has been assigned to ν(CrN) as no absorption is present at this frequency in the spectrum of the hydrate. The same vibration has been reported at 475 cm^{-1} for $[Cr_2(\mu\text{-}O_2CMe)_4(NH_3)_2]$ [204].

TABLE No 2.8 Infra-red Spectra of $[Cr_2(\mu\text{-}O_2CMe)_4L_2]$ ($L=OH_2, \frac{1}{2}(N_2H_4)$)

L =	OH_2	$\frac{1}{2}(N_2H_4)$	Major bands /cm^{-1} Assignment
	3493 m		
	3373 m		ν(OH)
	3275 m		
	3175 sh		
		3444 mw	$\nu(NH_2)$
		3316 mw	
	1576 s	1595 vs	$\nu_a(CO_2)$ + $\delta(OH_2)$ or $\delta(NH_2)$
	1476 s	1453 vs	$\nu_s(CO_2)$
	1420 ms	1433 sh	$\delta(CH_3)$
		1413 sh	
		1349 m	$\omega(NH_2)$
		1162 m	ν(NN)
		1125 s	$r_a(NH_2)$
	1047 m	1049 s	$r(CH_3)$
	1029 m	1032 vw	
	966 w	961 vw, br	ν(CC)
		926 w	$r_s(NH_2)$
	680 m	679 s	δ(OCO)
	624 mw	621 m	π(COO)
		469 m	ν(MN)
	407 m	402 s	ν(MO)
	384 m	384 m, sh	

3.4 CHROMIUM(III)-HYDRAZINE CHEMISTRY

3.4.1 BACKGROUND

Very few chromium(III)-hydrazine complexes have been reported. The interaction of $Cr_2(C_2O_4)_3.6H_2O$ with hydrazine has been reported by several Soviet workers [206-9]. The hydrated chromium(III) oxalate was reported to react with hydrazine in ethanol to give the

complex $Cr_2(C_2O_4)_3.4N_2H_4.4H_2O$. Reaction of the oxalate with N_2H_4 vapour additionally gave $Cr_2(C_2O_4)_3.7N_2H_4.H_2O$ as well as $Cr_2(C_2O_4)_3.4N_2H_4.4H_2O$ [206]. Thermal decomposition of these compounds was claimed to give the further chromium(III) oxalate-hydrazine species; $Cr_2(C_2O_4)_3.6N_2H_4$ and $Cr_2(C_2O_4)_3.2N_2H_4$ [209]. These formulations indicating the presence of both hydrazine and water are suspect as it is probable that internal proton transfers would occur, forming hyrazinium(1+) and hydroxide species.

The complex $[Cr(N_2H_4)_2(ClO_4)_2]ClO_4$ has been reported to be produced from the reaction of $[Cr(OH_2)_6](ClO_4)_3$ with N_2H_4 [210]. The complex is said to be reasonably stable with low friction and dropweight sensitivities to explosive decomposition.

The chromium(III) fluoride-anhydrous hydrazine system has been investigated by Glavic, Slivnik and Bole [197]. Anhydrous CrF_3 was found to be inert towards anhydrous hydrazine, but reaction with $CrF_3.2H_2O$ or M_3CrF_6 (M=NH_4 or N_2H_5) resulted in the formation of air-sensitive $Cr(N_2H_4)_3F_3$. It was also reported that in $N_2H_4.H_2O$, CrF_2, $CrF_3.2H_2O$ and M_3CrF_6 gave non-stoichiometric addition compounds containing CrF_2, N_2H_4 and H_2O. Again it is likely that these compounds contain hydroxide species given the presence of hydrazine and water.

In addition, the complexes $Cr(O_2CMe)_3(N_2H_4)_3.H_2O$ and $CrCl_3(N_2H_4)_3.2H_2O$ have been reported [196] by Aliev but little if any characterisation was carried out and the actual existence of complexes of these stoichiometries must be said to be doubtful.

Hein and Bähr in their work on the reactions of chromium(II) iodide with hydrazine [192], also reported that addition of hydrazine to $CrCl_3$ caused an explosive reaction with gas evolution,

but if $CrCl_3$ was added slowly to excess hydrazine, a less violent reaction occurred to give a red solution.

3.4.2 REACTION OF $[Cr(OH_2)_4Cl_2]Cl.2H_2O$ WITH HYDRAZINE

The reaction of $[Cr(OH_2)_4Cl_2]Cl.2H_2O$ with N_2H_4 was found to give hydroxide species rather than chromium(III)-hydrazine coordination compounds. This occurred whether anhydrous or aqueous/alcoholic solutions of hydrazine were used. Thus, the interaction of hydrazine with the chromium(III) metal centre appears to proceed as a simple acid-base reaction, whereby in the presence of water, hydroxide formation occurs.

3.5 CHROMIUM(II) AND (III)-HYDRAZINE SOLUTION CHEMISTRY

As chromium has been implicated as a possible catalyst for the homogeneous decomposition of hydrazine, an investigation of the behaviour of chromium(II) and -(III) in anhydrous hydrazine was undertaken.

As indicated in the background sections earlier in this Chapter, previous work reported on chromium-hydrazine chemistry has not been particularly definitive, apart from the preparation of the chromium(II) complexes $[Cr(N_2H_4)_2X_2]_n$ (X=Cl,Br,I). In particular no information is available on the relative stabilities of oxidation states of chromium in hydrazine solution. As part of a PERME investigation [211], Ratcliffe assumed that when anhydrous $CrCl_2$ dissolved in anhydrous hydrazine, the metal +2 oxidation state was retained, but little direct evidence was presented to support this assumption. Following this, it was proposed that dissolution of $CrCl_3$ in anhydrous hydrazine effected a rapid reduction to chromium(II).

In view of the suggestion that chromium and manganese ions are involved in an internal redox couple when leached from stainless steel by anhydrous hydrazine and, further, that this couple is implicated in the catalytic homogeneous decomposition of the solvent, it was thought necessary to investigate which oxidation state(s) of chromium survive in anhydrous hydrazine.

Anhydrous $CrCl_2$ and $CrCl_3$ were employed as the sources of the +2 and +3 oxidation states of the metal and solution electronic spectra, conductiometric and magnetic susceptibility measurements were used to determine the resultant oxidation state(s) of the solution products.

Both anhydrous chromium(II) and -(III) chlorides dissolved in anhydrous hydrazine to give deep red solutions on standing. This mirrors the observations of Hein and Bähr [192] who reported that dissolution of both chromium(II) iodide and chromium(III) chloride in anhydrous hydrazine gave red solutions. Both reactions are exothermic with considerable gas evolution. Initially $CrCl_2$ dissolved to give a pale violet solution which rapidly converted into the final red solution product.

3.5.1 ELECTRONIC SPECTRA

The solution electronic spectra of $CrCl_2$, $CrCl_3$ and $Cr(O_2CNHNH_2)_3.2H_2O$ in deoxygenated hydrazine were recorded under nitrogen. The very closely related spectral profiles of the solution products obtained from both $CrCl_2$ and $CrCl_3$ starting materials suggest that identical or at least very similar species exist in both solutions (see TABLE 3.9 and FIG No 3.4). However, these solution spectra although similar to each other are not typical of octahedral chromium(III) as displayed by $Cr(O_2CNHNH_2)_3.2H_2O$ in N_2H_4 solution. This observation led to the original suggestion that reduction of chromium(III) chloride had taken place [211].

TABLE No 3.9 Solution Electronic Spectra of Chromium Species in Anhydrous Hydrazine /nm

$CrCl_2$	$CrCl_3$	$Cr(O_2CNHNH_2)_3.2H_2O$
694 w,br,sh	698 w,br,sh	700 vw,sh
525 s,br	532 s,br	522 s,br
387 s,sh	390 s,sh	402 s,br
364 s,sh	356 s,sh	

3.5.2 CONDUCTIOMETRIC MEASUREMENTS

Conductiometric measurements were performed on 10^{-3} M solutions of $CrCl_2$ and $CrCl_3$ in hydrazine under nitrogen. The hydrazine used was purified by distillation from CaH_2 to ensure the absence of water. It was found that conductivity measurements of salts in 'propellant grade' hydrazine (~1-5 % H_2O present) gave values inconsistent with the presence of 1:1, 1:2 or 1:3 electrolytes. Hydrazine purity was assessed by specific conductivity measurements. Values less than 5×10^{-6} $\Omega^{-1}cm^{-1}$ were considered to be acceptable for further work. Typical reference values for 1:1, 1:2 and 1:3 electrolytes were obtained by measuring the conductivities of a number of salts as 10^{-3} M solutions in the same batch of pure hydrazine. The conductivities of solutions of $CoCl_2$ and $NiCl_2$ in anhydrous hydrazine were also measured for comparison with the values reported by Nicholls *et al.* [25,26]. From the results presented in TABLE No 3.10, acceptable ranges for 1:1, 1:2 and 1:3 electrolytes can be suggested (see TABLE No 3.11).

The Λ_M values determined for $CrCl_3$ in N_2H_4 suggest that reduction is unlikely to have occurred, the chromium remaining in the +3 state in solution. The molar conductance values are somewhat higher than those of the 1:3 reference electrolyte, probably due to impurities produced when $CrCl_3$ is added to N_2H_4, this being a highly exothermic process. However, the Λ_M values suggest that a species such as $[Cr(N_2H_4)_6]^{3+}.3Cl^-$ is the major solution product. It is possible that the exothermicity and gas evolution occurs because of some catalytic decomposition of hydrazine, although no decomposition products could be detected.

The Λ_M values determined for $CrCl_2$ and $[Cr(N_2H_4)_2Cl_2]_n$ in N_2H_4 are considerably lower, being only slightly above the values of typical 1:2 electrolytes. Therefore although electronic spectral

TABLE No 3.10 Conductivity Measurements of Dissolved Salts in Anhydrous Hydrazine.

Compound	Concentration / 10^{-3} mol l^{-1}	Conductivity / $10^{-4}\Omega^{-1}cm^{-1}$	Molar Conductance, Λ_M / $\Omega^{-1}m^{-2}Kmol^{-1}$
Me_4NI	1.000	1.210	11.96
KI	0.994	1.283	12.83
$Sr(NO_3)_2$	1.011	1.401	21.46
$CoCl_2$	1.017	1.711	23.73
	1.017	1.496	22.56
$NiCl_2$	1.049	1.320	19.78
	1.049	1.255	19.72
$[Co(NH_3)_6]Cl_3$	1.043	2.318	32.70
$CrCl_2$	1.123	1.910	25.70
	1.212	1.867	25.47
$[Cr(N_2H_4)_2Cl_2]_n$	0.978	1.488	24.76
$CrCl_3$	0.998	2.372	36.60
	1.029	2.482	37.53

TABLE No 3.11 Λ_M Values for Reference Electrolytes in Anhydrous Hydrazine.

Electrolyte type	Λ_M / $\Omega^{-1}m^{-2}Kmol^{-1}$
1:1	12 ± 1
1:2	21.5 ± 2
1:3	33

evidence suggests that identical oxidation states are present in these solutions irrespective of whether chromium(II) or -(III) is employed, the nature of ions generated seems to differ. This is not

unreasonable since dissolution of $CrCl_2$ can at most only generate two chloride anions. A solution species such as $[Cr(N_2H_4)_5(NHNH_2)]^{2+}.2Cl^-$ is a possible solvolysis product.

The Λ_M values determined for 10^{-3}M $CoCl_2$ and $NiCl_2$ solutions although numerically different to those reported by Nicholls *et al.* [25,26], do indicate 2:1 electrolytes when compared to the other 2:1 reference electrolytes measured in this work. It is therefore suggested that $[M(N_2H_4)_6]^{2+}.2Cl^-$ (M=Co,Ni) are likely to be present in these solutions and, indeed, $[Co(N_2H_4)_6]Cl_2$ has been isolated as a solid from hydrazine solution [25].

3.5.3 MAGNETIC SUSCEPTIBILTY MEASUREMENTS

Magnetic measurements were carried out using the Gouy method and Evans nmr method [211A] on solutions of $CrCl_2$ and $CrCl_3$ in hydrazine to complement the conductiometric study. As a reference, the magnetic susceptibility of a solution of $CoCl_2$ in hydrazine was also determined.

There have been no previous reports of the magnetic susceptibilities of transition metal ions in hydrazine solutions, although Nicholls *et al.* [25] reported a solid state magnetic susceptibility of $[Co(N_2H_4)_6]Cl_2$, the species almost certainly present in solutions of $CoCl_2$ in hydrazine.

It was assumed that the susceptibility of the solid complex and its solution in hydrazine would be identical. Therefore comparisons could be made of the susceptibilities of the cobalt and the chromium solutions.

The magnetic moment of $[Co(N_2H_4)_6]Cl_2$ was reported to be 4.92 BM at 290 K which corresponds to a mass susceptibility of 31.86×10^{-6} cm^3g^{-1}. Using this value, magnetic susceptibilities of

$CrCl_2$ and $CrCl_3$ in N_2H_4 can be calculated as 14.82 and 11.93 $\times 10^{-6}$ cm^3g^{-1} respectively (see TABLE No 3.12).

In order to avoid any assumptions concerning the nature of the species present in the solutions, only a comparison of susceptibilities was attempted.

TABLE No 3.12 Magnetic Susceptibility Measurements of Salts in Anhydrous Hydrazine at 296K.

Compound	Concentration / mol l^{-1}	χ / 10^{-6} cm^3g^{-1}
$CoCl_2$	0.7814	31.86*
$CrCl_2$	0.8349	14.71
	0.7340	14.93
$CrCl_3$	0.8949	11.64
	1.0855	12.22

*-assumed value from solid state compound (see text)

High spin octahedral cobalt(II) complexes (d^7 ; 3 unpaired electrons) have magnetic moments in the range 4.8-5.2 BM at room temperature, rather than 3.8 BM expected from spin-only considerations. The increase is due to a temperature-dependent orbital contribution. Therefore given similar molecular weight species in solution, cobalt(II) could be expected to have susceptibility values of similar magnitude to high-spin octahedral chromium(II) species which also have magnetic moments close to 4.9 BM.

The results obtained show that the susceptibility values are not similar to those of $CoCl_2$ and so it is unlikely that the chromium solutions contain four unpaired electrons per metal ion as expected for high-spin octahedral chromium(II).

The values determined for the $CrCl_2$-N_2H_4 solutions were consistently slightly greater than those found for the $CrCl_3$-N_2H_4 system. This is presumably a consequence of generating a species of smaller molecular mass in the $CrCl_2$ reaction. However, the susceptibility values are sufficently in agreement to suggest that at least most of the chromium ions are present in the +3 oxidation state irrespective of the chromium chloride used.

The Evans nmr method for determining magnetic susceptibility has the advantage that only dilute solutions are required and no reference value is required for the calculation of a susceptibility value. Therefore it is possible to test the assumption that the solid state susceptibility value of $[Co(N_2H_4)_6]Cl_2$ is unchanged when in hydrazine solution.

Solutions (10^{-3}M) of $CoCl_2$, $CrCl_2$ and $CrCl_3$ in anhydrous hydrazine were prepared and their magnetic susceptibilities measured by the Evans method (see TABLE 3.13).

TABLE 3.13 Magnetic Susceptibility Measurements of Salts in Anhydrous Hydrazine as determined by the Evans nmr Method at 296K.

Compound	Concentration /10^{-3}×g cm^3	Frequency Separation/Hz	χ / 10^{-6} cm^{3}g^{-1}
$CoCl_2$	4.144	30.0	57.0
	5.356	43.7	62.8
$CrCl_2$	5.148	15.7	23.7
	1.852	5.9	24.7
$CrCl_3$	3.664	7.6	15.8
	3.700	7.2	14.9

The usual frequency shift indicator, tetramethylsilane (TMS), was found to be insoluble in hydrazine. As an alternative indicator the methyl resonance of methyl cyanide was used. Only a small

volume (~0.01 ml) of MeCN was added to each solution, as larger additions caused partial precipitation of the dissolved species.

The susceptibilities show the same general trends as those determined by the Gouy method, the chromium solutions having much lower susceptibilities than those of the $CoCl_2$-N_2H_4 solution. Also the $CrCl_2$-N_2H_4 solutions have slightly greater susceptibilities than the $CrCl_3$-N_2H_4 solutions.

The susceptibilities of the $CoCl_2$-N_2H_4 solutions are greater than those obtained by the Gouy method. Assuming that cobalt(II) is an octahedral environment (and thus has an effective magnetic moment of 4.8-5.2 BM), a species of lower molecular weight than $[Co(N_2H_4)_6]Cl_2$ would need to be proposed to account for the high susceptibility value.

Assuming that $[Cr(N_2H_4)_6]Cl_3$ is the dominant species in the $CrCl_3$-N_2H_4 solutions, a magnetic moment of 3.7 BM can be calculated from the susceptibility value. This is in good agreement with the spin-only value of 3.88 BM for octahedral chromium(III) systems.

The higher susceptibility value for the $CrCl_2$-N_2H_4 solutions implies that a species of lower molecular weight than $[Cr(N_2H_4)_6]Cl_3$ is the dominant complex in solution. Given the presence of residual water in anhydrous hydrazine, it is conceivable that hydroxide ions could be generated which may replace one or more hydrazine ligands in the coordination sphere , thus producing a lower molecular weight species in solution such as $[Cr(N_2H_4)_5OH]Cl_2$.

3.5.4 CONCLUSION

The above evidence indicates that chromium(II) is oxidised to chromium(III) on dissolution in hydrazine. Therefore the stable oxidation state of chromium in anhydrous hydrazine is +3.

This conclusion implies that hydrazine must be acting as an oxidising agent towards the powerful reductant chromium(II). Presumably, the species obtained by the reduction of hydrazine will be ammonia although no evidence of its formation was found. There is a precedent for this proposal, Wells and Salam [212] reporting a kinetic study of the reduction of hydrazine in perchloric acid by chromium(II). However the conclusions drawn from that work have subsequently been questioned by two groups of workers [213,214].

As discussed in SECTION 1.1, thermodynamically, hydrazine is a good oxidising agent but due to the high activation energy involved in the breaking of the N-N bond it rarely behaves as an oxidant. Also the oxidation of chromium(II) appears to conflict with the well established stability of the complexes $[Cr(N_2H_4)_2X_2]_n$ (X=Cl, Br, I). However, it is worth noting that these complexes cannot be prepared from a chromium(III) source in hydrazine and their stability owes more to their polymeric structure than the oxidising ability of hydrazine with respect to chromium(II). It should also be pointed out that these complexes have been isolated from *aqueous* or *alcoholic* hydrazine solutions, and not from anhydrous hydrazine.

3.6 ATTEMPTED ISOLATION OF $CrCl_2$- AND $CrCl_3$-N_2H_4 SOLUTION SPECIES

3.6.1 ISOLATION

In an attempt to elucidate more positively the nature of the chromium species present in hydrazine solution, attempts were made to isolate solid products from the solutions. Unstable hexakis-(hydrazine) species can be isolated from divalent first-row transition metal ion-N_2H_4 solutions, either by reduction of solvent volume or by addition of inert solvents to aid precipitation.

Two isolation techniques were employed in this work, similar to those reported for the isolation of $[M(N_2H_4)_6]X_2$ (M=Co.Ni) [25, 26], i.e. (i) direct evacuation of the chromium-hydrazine solutions and (ii) addition of organic solvents followed by evacuation. Technique (ii) was found to be more effective. Addition of either excess ROH (R= Me or Et) or MeCN to concentrated chromium-hydrazine solutions (>1M) causes the precipitation of dark red oils. Evacuation of these oils under high vacuum left gelatinous, hygroscopic, red solids.

3.6.2 DIFFUSE RELECTANCE ELECTRONIC SPECTRA

The reflectance electronic spectra of the isolated solid $CrCl_3$-N_2H_4 species appear to be dependent on the extent of evacuation.

The spectra of the solids show more typical octahedral chromium(III) profiles than those of the solutions (see TABLE No 3.14). After isolation, the $^4A_{2g} \rightarrow {}^4T_{2g}$ transition (ν_2) of the freshly isolated solid (I) is now resolved as a peak instead of being just a shoulder on an intense charge-transfer absorption. After prolonged evacuation to give solid (II), the maximum of this peak appears to shift to 357 nm. However, if this peak is correctly

assigned as ν_2, a B value of 930 cm^{-1} can be calculated. This value is clearly impossible, being greater than the Cr^{3+} free ion value (918 cm^{-1}), so the 357 nm band is more likely to be of charge-transfer orgin.

TABLE No 3.14 Electronic Spectra of the $CrCl_3$-N_2H_4 System /nm.

$N_2H_{4(sol'n)}$	I	II	Assignment
698 (w,sh)	710 (w,sh)	691 (w,sh)	$^2E_g, {}^2T_{1g} \leftarrow {}^4A_{2g}$
532 (s,br)	520 (m)	521 (m)	$^4T_{2g} \leftarrow {}^4A_{2g}$, ν_1
390 (s,sh)	379 (s)		$^4T_{1g} \leftarrow {}^4A_{2g}$, ν_2
364 (s,sh)		357 (s)	charge-transfer?
18800	19200	19200	Δ_o / cm^{-1}
660	706		B / cm^{-1}
0.72	0.77		β
246	239		calculated ν_3 /nm ($^4T_{1g} \leftarrow {}^4A_{2g}$)

I - precipitated oil, II - oil after 72 hrs evacuation.

$\nu_1 \equiv \Delta_o$. B, β and ν_3 values were calculated using a computer program based on Transition Ratio Tables published by Lever [215] (see APPENDIX No 3).

Assuming that in solution chromium is present as $[Cr(N_2H_4)_6]^{3+}$, the Δ_o values can be compared to other related chromium(III) species. $Cr(NH_3)_6^{3+}$ shows absorption bands at 464 and 351 nm [216] of which the first is ν_1, hence Δ_o = 21550 cm^{-1}. From these B and β values of 652 and 0.71 can be calculated. Similarly $Cr(en)_3^{3+}$ shows a Δ_o of 21850 cm^{-1} and B and β values of 615 and 0.67 can be calculated. The $CrCl_3$-N_2H_4 species have lower Δ_o values suggesting the introduction of ligands of higher electronegativity e.g. H_2O or OH^- into the coordination sphere, (c.f. $Cr(NH_3)_5(H_2O)^{3+}$, Δ_o = 20800 cm^{-1}; $Cr(NH_3)_5(OH)^{2+}$, Δ_o = 19700 cm^{-1}).

Analysis of the spectral data indicates an increasing electronegative environment (increasing B and β) around the chromium(III) cation on evacuation. This may be related to the apparent loss of hydrazine from the coordination sphere of the metal with possible replacement by hydroxide species.

The $CrCl_2$-N_2H_4 system appeared to exhibit similar behaviour on evacuation, although this system was not investigated further using diffuse reflectance electronic spectroscopy.

3.6.3 VIBRATIONAL SPECTRA

The IR spectra of the two isolated species were recorded as liquid films between NaCl plates. It was not possible to mull the dried solids in liquid paraffin because of their gelatinous nature.

The IR spectra of the two solids resemble each other (see TABLE No 3.15), an indication that the same or a very similar ligand set, presumably mainly N_2H_4, is present in both species.

TABLE No 3.15 Infra-red Spectra of isolated Chromium-Hydrazine Species / cm^{-1}.

from $CrCl_2$	from $CrCl_3$	Assignment
3400-3200 (s,br)	3200 (s,br)	$\nu(NH)$, $\nu(OH)$?
2625 (m,br)	2600 (m,br)	
1610 (s)	1610 (s)	$\delta(NH_2)$, $\delta(OH_2)$?
1385 (w)	1410 (w,br)	$w(NH_2)$
1290 (w,sh)	1300 (w,br)	
1100 (s)	1105 (s,br)	$r(NH_2)$
945 (m)	945 (m)	

Assuming hydrazine to be involved in the ligand set, the type of hydrazine coordination present can be proposed using the $r_s(NH_2)$

absorption as a guide (see SECTION 2.3). The observed $r_s(NH_2)$ bands are found towards the lower end of the bridging hydrazine range. These absorptions also have shoulders on their lower frequency edges falling in the unidentate coordination range. This evidence is, perhaps, indicative that each product contains both unidentate and bridging hydrazine ligands.

3.6.4 ELEMENTAL ANALYSIS

$CrCl_3$-N_2H_4 Product

The Cr:Cl ratio was found to be 1:2.99 indicating that no chloride is lost on reaction of $CrCl_3$ with N_2H_4, followed by the removal of excess hydrazine. Considering the overall results a molecular formula of $Cr(N_2H_4)_4Cl_3.H_2O$ is indicated. A better fit to the experimental results is achieved if the Cr:N_2H_4 ratio is reduced to the non-stoichiometric 1:3.8. The suggested presence of H_2O is not unreasonable given the hygroscopic nature of the product and the consequent handling difficulties.

$CrCl_2$-N_2H_4 Product

The Cr:Cl ratio is 1:2.20 also indicative of no loss of chloride on reaction and isolation. An overall formulation is more uncertain than for the $CrCl_3$ species, as the nature of the third anion required for charge balance on oxidation from chromium(II) to (III) is unknown. As the presence of H_2O is suspected in the $CrCl_3$ reaction product, a possible additional anion could be hydroxide. A molecular formula which fits the analytical results is $Cr(N_2H_4)_5Cl_2.OH.H_2O$, but there is little other evidence to justify such a formulation.

3.6.5 REACTIONS OF THE CHROMIUM-HYDRAZINE SPECIES

In the hope of isolating more easily characterised compounds, attempts were made to react the isolated solids with 2,2'-bipyridyl. It was felt that replacement of the N_2H_4 ligands by 2,2'-bipyridyl would occur and this would have the conceivable advantage of allowing the identification of the third anion in the $CrCl_2$-N_2H_4 system (3.7).

$$Cr(N_2H_4)_xXCl_2 + 3\ bipy \longrightarrow [Cr(bipy)_3]XCl_2 + xN_2H_4 \qquad (3.7)$$
$$X = Cl \text{ or unknown anion}$$

Unfortunately, no reaction occurred when the $CrCl_3$-N_2H_4 solid species was reacted with 2,2'-bipyridyl in anhydrous MeCN, even after heating under reflux for 16 hours. It was expected that the $CrCl_2$-N_2H_4 species would similarly remain inert to substitution, so this approach was not pursued further.

As an alternative approach, the isolated $CrCl_2$- and $CrCl_3$-N_2H_4 solids were reacted with CO_2 in the presence of N_2H_4. It was anticipated that the products would be stable carbazato-complexes and once again the nature of the unknown third anion may be more easily elucidated (3.8).

$$[Cr(N_2H_4)_6]XCl_2 \xrightarrow[CO_2]{N_2H_4} Cr(O_2CNHNH_2)_x^{(3-x)+} \qquad (3.8)$$

The solids were separately dissolved in N_2H_4 and CO_2 was passed slowly through while maintaining the temperature at ~0°C. The reactions were continued until the solutions had become too viscous for further passage of gas. Electronic spectral data suggest that chromium(III) carbazates had been formed (see TABLE No 3.16), but exact stoichiometries are uncertain.

TABLE No 3.16 Diffuse Reflectance Electronic Spectra of Cr-N_2H_4-CO_2 Reaction Products / nm.

$CrCl_3$ product	$CrCl_2$ product	$Cr(O_2CNHNH_2)_3.2H_2O$
		693 (vw)
579 (s,br)	510 (m,br)	512 (s,br)
387 (m.br)	361 (s,br)	396 (m,br)

3.6.5 CONCLUSIONS

No well-defined discrete solid compounds have been isolated from either the $CrCl_2$-anhydrous N_2H_4 or $CrCl_3$-anhydrous N_2H_4 systems. As hydrazine is removed by evacuation, the Cr:N_2H_4 ratio of the products decreases. It is probable that in anhydrous hydrazine, chromium forms a soluble hexakis(hydrazine) species, $[Cr(N_2H_4)_6]^{3+}$ in common with a number of divalent first-row transition metal ions M^{2+} (M=Mn,Co,Ni). However, on isolation at least some of these ligands are lost and the hydrazine remaining successively changes from a unidentate to a bridging coordination mode. This would imply a final product of stoichiometry $[CrCl_3(N_2H_4)_{1.5}]_n$, assuming the presence of terminal chlorides. From the above evidence there is no indication that this formulation is achieved, loss of hydrazine becoming progressively more difficult to achieve.

The identity of the $CrCl_2$-N_2H_4 species isolated is open to speculation. It is probable that using the work-up conditions employed hydroxide may have provided the extra anion required for oxidation of chromium(II) to (III), i.e. $[Cr(N_2H_4)_6]Cl_2.OH$. In strictly anhydrous hydrazine systems, the possible presence of either NH_2^- or $NHNH_2^-$ exists.

The acidic nature of the chromium(III) cation (pK_a~4) may preferentially promote acid-base reactions with hydrazine rather than Lewis acid acceptor behaviour. Also water, which acts as an acid within the hydrazine solvent system, would exist almost exclusively in the form of OH^- (3.9).

$$N_2H_4 + H_2O \longrightarrow N_2H_5^+ + OH^- \qquad (3.9)$$

Chromium(III) would thus form strong bonds with hydroxide in preference to hydrazine coordination and generate a kinetically inert hydroxo-complex, which may account for the product observed. Also coordinated hydrazine may be subject to deprotonation in the manner of chromium(III) aquo complexes;

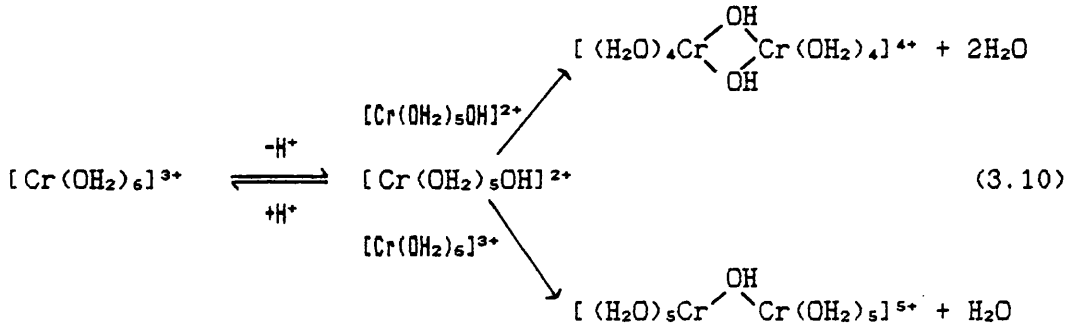

(3.10)

A combination of hydrazine and hydroxide ligands could lead to hydroxide bridged polynuclear complexes;

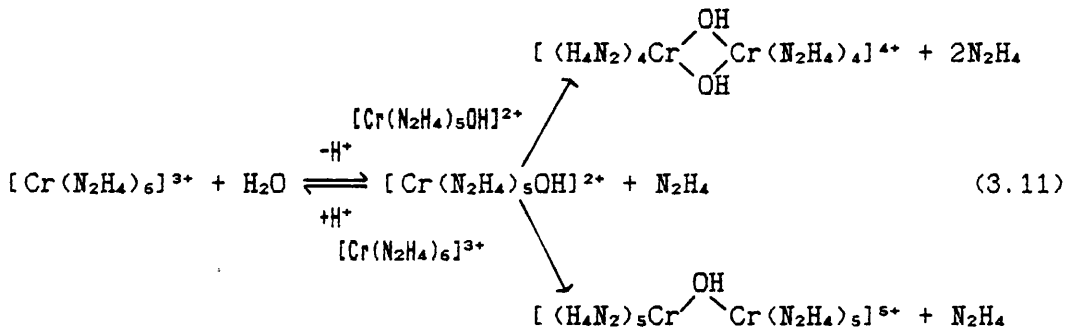

(3.11)

The possibility of bridging hydroxide groups could imply partial spin-pairing of adjacent metal d electrons as observed in other

hydroxide-bridged chromium(III) amine complexes such as in $[(NH_3)_5Cr\text{-}OH\text{-}Cr(NH_3)_5]X_5$ [217]. This may explain why the solution magnetic susceptibility values are lower than expected for octahedral chromium(III) species.

The oxidation of chromium(II) by bulk hydrazine contrasts sharply with the stabilization of this lower oxidation state by N_2H_4 and $N_2H_5^+$ in the complexes $[Cr(\mu\text{-}N_2H_4)_2Cl_2]_n$ and $[Cr(N_2H_5)_2(SO_4)_2]$. It is noted that these complexes are insoluble in all solvents which do not destroy them. However, in this work it has been shown that $[Cr(N_2H_4)_2Cl_2]_n$ undergoes oxidation in bulk hydrazine in line with the behaviour of $CrCl_2$ itself. It is probable that the rapid formation and resultant insolubility in reaction solutions assists the retention of the chromium(II) oxidation state, whereas if soluble these complexes would probably undergo rapid oxidation. This proposal is further illustrated in chromium(II) carbazate chemistry (see SECTION 3.7).

3.7 CHROMIUM(II)-CARBAZATE CHEMISTRY

3.7.1 BACKGROUND

As chromium, in conjunction with manganese, has been implicated as a possible homogeneous catalyst towards hydrazine, the investigation of the $CrCl_2$-N_2H_4 system was extended to include reactions with $[N_2H_5][O_2CNHNH_2]$ and $\overset{+}{N}H_3NHC\overset{-}{O}_2$. The carbazate anion is known to be present in hydrazine which has been exposed to CO_2 and would be a logical ligand for those variable oxidation state metal ions thought to induce homogeneous decomposition of the solvent. Chromium(III) is known to form a stable carbazate [15,100] but no reactions of carbazate anions with chromium(II) have been reported.

3.7.2 PREPARATION

The reactions of either $[Cr(OH_2)_6]X_2$ (X=Cl,Br) or $[Cr_2(O_2CMe)_4(OH_2)_2]$ in aqueous solution with $[N_2H_5][O_2CNHNH_2]$ results in the novel, air-stable mononuclear lilac chromium(II) complex, $Cr(O_2CNHNH_2)_2.H_2O$.

Analytical data cannot easily distinguish between $Cr^{II}(O_2CNHNH_2)_2.H_2O$ and the hydroxo-bridged $[Cr^{III}(O_2CNHNH_2)_2(OH)]_2$. Hence characterisation rests with other physical measurements.

The atmospheric stability of this new complex is in marked contrast to the analogous glycinate complex, $Cr(O_2CCH_2NH_2)_2.H_2O$ which in common with the majority of mononuclear chromium(II) compounds, is extremely air-sensitive [218,219].

The complex $[Cr(O_2CNHNH_2)_2.H_2O]_n$ can be prepared from several chromium(II) starting materials and aqueous $[N_2H_5][O_2CNHNH_2]$ (see (3.11).

The reaction of $[Cr_2(O_2CMe)_4(OH_2)_2]$ with aqueous $[N_2H_5]$-$[O_2CNHNH_2]$ under N_2 producing $Cr(O_2CNHNH_2)_2.H_2O$ is a particularly

interesting reaction because it involves cleavage of the quadruple metal-metal bond to yield a mononuclear species.

$[Cr_2(O_2CMe)_4(OH_2)_2]$

$[Cr_2(O_2CMe)_4(\mu\text{-}N_2H_4)]_n$

$CrCl_2.4H_2O$ $\xrightarrow[H_2O,N_2]{[N_2H_5][O_2CNHNH_2]}$ $Cr(O_2CNHNH_2)_2.H_2O$ (3.11)

$CrBr_2.6H_2O$

$[CrX_2(\mu\text{-}N_2H_4)_2]_n$ (X=Cl or Br)

The stability of $Cr(O_2CNHNH_2)_2.H_2O$ on exposure to normal laboratory atmospheres, a feature also shown by $[CrX_2(\mu\text{-}N_2H_4)_2]_n$, contrasts with the oxidative potential of hydrazine towards chromium(II). This dichotomy is observed in the formation of $Cr(O_2CNHNH_2)_2.H_2O$. The addition of chromium(II) to $[N_2H_5][O_2CNHNH_2]$ initially results in a dark blue solution from which $Cr(O_2CNHNH_2)_2.H_2O$ rapidly precipitates. Prolonged contact of insoluble $Cr(O_2CNHNH_2)_2.H_2O$ with a solution of $[N_2H_5][O_2CNHNH_2]$ results in dissolution and oxidation to form a bright red solution from which air-stable chromium(III) carbazate can subsequently be isolated (see 3.12). The rate of this oxidation appears to depend on the concentration of $[N_2H_5][O_2CNHNH_2]$.

In solution, such as when dissolved in excess $[N_2H_5][O_2CNHNH_2]_{(aq)}$, the chromium(II) centre is susceptible to oxidation by N_2H_4 or $N_2H_5^+$. The successful isolation of $Cr(O_2CNHNH_2)_2.H_2O$ therefore depends on its rapid formation in solution and resultant insolubility.

$$[Cr(OH_2)_6]^{2+} + 2[N_2H_5][O_2CNHNH_2] \xrightarrow[CO_2]{H_2O} Cr(O_2CNHNH_2)_2.H_2O$$

$$\xrightarrow[H_2O]{[N_2H_5][O_2CNHNH_2]} Cr(O_2CNHNH_2)_3.2H_2O \quad (3.12)$$

3.7.3 MAGNETIC MOMENT AND ELECTRONIC AND X-RAY PHOTOELECTRON SPECTRA

Magnetic susceptibility measurements indicate a high-spin d^4 electronic configuration (χ_{cgx} = 45.01×10^{-6} cm^{3}g^{-1}; μ_{eff} = 4.87 BM at 296K). This also indicates a mononuclear environment for the chromium(II) centre. Comparison with the magnetic properties of $Cr(O_2CNHNH_2)_3.2H_2O$ and $Cr(O_2CCH_2NH_2)_2.H_2O$ is shown in TABLE No 3.17.

TABLE No 3.17 Magnetic Susceptibility Measurements of Chromium Carbazate and Glycinate Species.

Complex	χ_{cgx}×10^{-6}/cm^{3}g^{-1}	μ_{eff} / BM	T / K
$Cr(O_2CNHNH_2)_3.2H_2O$	19.19	3.82	295
$Cr(O_2CNHNH_2)_2.H_2O$	45.01	4.87	296
$Cr(O_2CCH_2NH_2)_2.H_2O$	41.60	4.61	295*

* - taken from ref. 220.

TABLE No 3.18 Reflectance Electronic Spectra of Chromium Carbazate and Glycinate Species.

Complex	Spectrum / nm.
$Cr(O_2CNHNH_2)_3.2H_2O$	698 (vw), 523 (s), 395 (m), 261 (vs)
$Cr(O_2CNHNH_2)_2.H_2O$	551 (m,br),~400 (w,sh), 275 (vs)
O_2 exposed $Cr(O_2CNHNH_2)_2.H_2O$	561 (s,br), 404 (m,br), 367 (m.br) 277 (vs)
$Cr(O_2CCH_2NH_2)_2.H_2O$	833, 614*

* - taken from ref. 220.

Although once isolated $Cr(O_2CNHNH_2)_2.H_2O$ appears air-stable, it is subject to slow surface oxidation. Thus, the reflectance spectra of samples stored under nitrogen are distinctly different to the spectra of samples exposed to air for several weeks. The spectra of the former are identical to those of fresh samples, whereas the

latter contain peaks attributable to the presence of chromium(III) (see TABLE No 3.18 and FIG No 3.5).

FIGURE No 3.5 Reflectance Electronic Spectra of Chromium Carbazate Species.

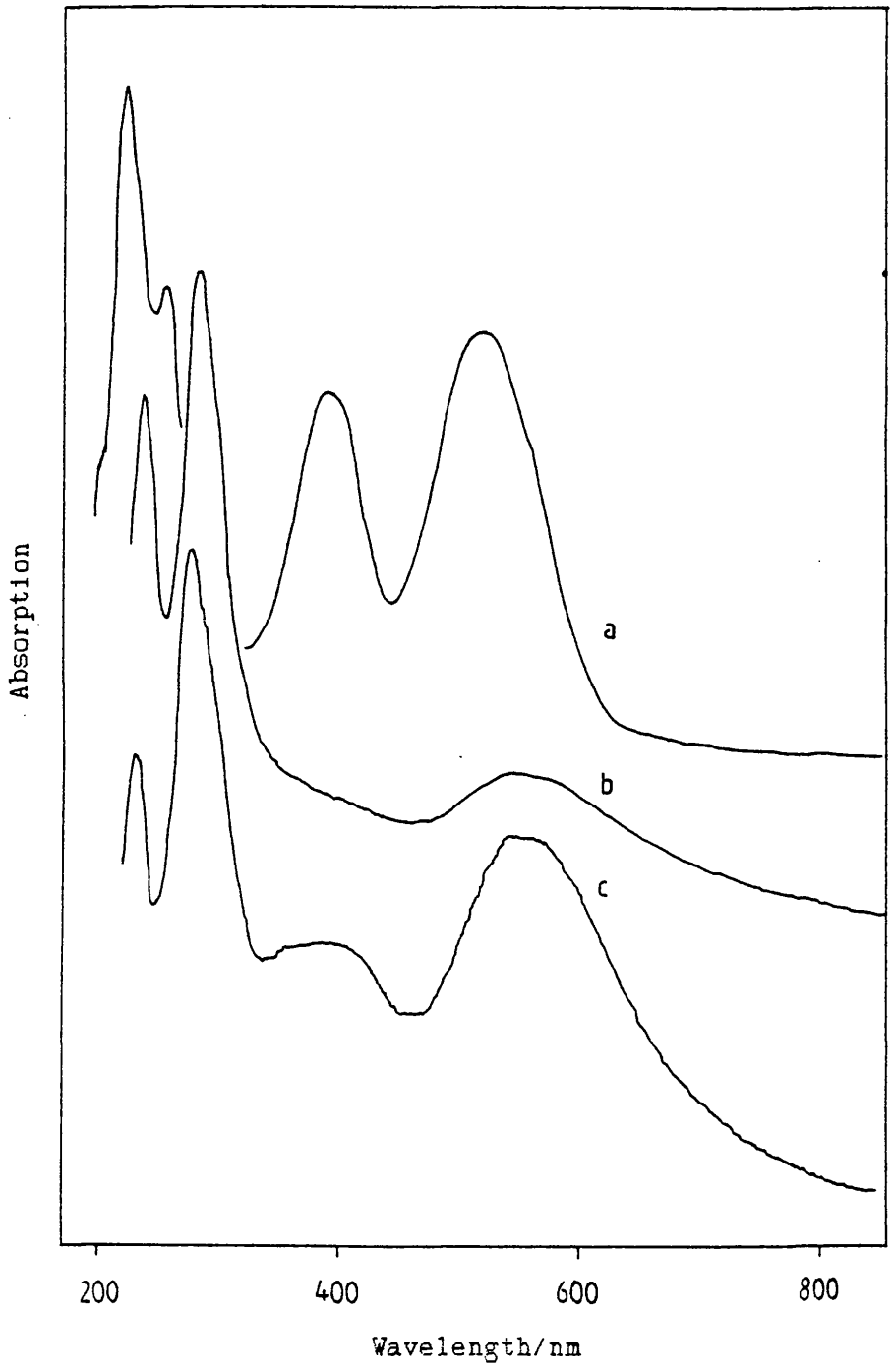

a-$Cr(O_2CNHNH_2)_3.2H_2O$ b-$Cr(O_2CNHNH_2)_2.H_2O$

c-O_2 exposed $Cr(O_2CNHNH_2)_2.H_2O$

The electronic spectrum of $Cr(O_2CNHNH_2)_2.H_2O$ shows the metal environment to be greatly distorted from tetragonally distorted octahedral chromium(II). For example $[Cr(OH_2)_6]^{2+}$ in $(NH_4)_2Cr(SO_4)_2$-$6H_2O$ shows the $^5E_g, ^5B_{2g} \leftarrow 5B_{1g}$ transition at 714 nm (14000 cm^{-1}) [221]. However in $Cr(O_2CNHNH_2)_2.H_2O$ this transition occurs at 551 nm (18200 cm^{-1}). In the analogous glycinate complex, $Cr(O_2CCH_2NH_2)_2.H_2O$, where a similar ligand set could be expected, this transition appears at 614 nm (16300 cm^{-1}), so there must be a considerable distortion from regular octahedral symmetry. Square planar chromium(II) complexes exhibit major bands at lower frequencies than octahedral complexes e.g. $Cr(O_2PPh_2)_2.H_2O$ at 495 nm (20200 cm^{-1}) [222]. It is clear that the symmetry of $Cr(O_2CNHNH_2)_2.H_2O$ is not regular octahedral or even Jahn-Teller tetragonally distorted octahedral. The spectrum is markedly similar to those of $[Cr(N_2H_4)_2X_2]_n$ (X=Cl, Br, I) complexes which show their major transition at ~570 nm (17500 cm^{-1}) [194]. As discussed earlier in this chapter (see SECTION 3.3), the structure of the latter complexes can be described as pseudo-square planar with additionally two extremely long mutually *trans*-halide ligands.

The X-ray photoelectron spectrum of $Cr(O_2CNHNH_2)_2.H_2O$ also indicates the presence of surface oxidation. The binding energies displayed by $Cr(O_2CNHNH_2)_2.H_2O$ were insignificantly shifted with respect to those of $Cr(O_2CNHNH_2)_3.2H_2O$ (see TABLE No 3.19).

Additional evidence for the presence of a chromium(II) oxidation state in the complex arises from solution electronic spectroscopy. Although $Cr(O_2CNHNH_2)_2.H_2O$ is insoluble in all solvents with which it does not react, it is possible to react it with a non-oxidising aqueous acid to give a solution without change in metal oxidation state. Thus, decomposition of $Cr(O_2CNHNH_2)_2.H_2O$

in concentrated aqueous HCl under nitrogen exclusively generates $[Cr(OH_2)_6]Cl_2$. On exposure of this solution to air, a change in the electronic spectrum occurs consistent with oxidation of chromium(II) to chromium(III) (see TABLE No 3.20).

TABLE No 3.19 X-ray Photoelectron Spectra of Chromium Carbazates / binding energies (eV).

Complex	C 1s	Cr $2p^1/_2$	Cr $2p^3/_2$	Cr 3s
$Cr(O_2CNHNH_2)_3.2H_2O$	291.1	589.1	579.4	46.6
$Cr(O_2CNHNH_2)_2.H_2O$	291.1	589.9	579.3	46.1

TABLE No 3.20 Solution Electronic Spectra of $Cr(O_2CNHNH_2)_2.H_2O$ in $HCl_{(aq)}$.

Complex	Spectrum / nm.
$Cr(O_2CNHNH_2)_2.H_2O$/ $HCl_{(aq)}$	~470 (w,br), >800 (s,br)
O_2 exposed $Cr(O_2CNHNH_2)_2.H_2O$/ $HCl_{(aq)}$	463 (s), 664 (m,br)

3.7.4 REDOX TITRIMETRY

The chromium(II) oxidation state has finally been confirmed by redox titrimetry. Decomposition of a sample under basic conditions liberates N_2H_4 and chromium(II). The released species then reduce added $[Fe(CN)_6]^{3-}$ to $[Fe(CN)_6]^{4-}$ and the generated iron(II) can be titrated with $Ce(SO_4)_2$ using *N*-phenylanthranilic acid as indicator (see 3.13)

$$4[Fe(CN)_6]^{3-} + 'N_2H_4' \longrightarrow 4[Fe(CN)_6]^{4-} + N_2 + 4H^+ \qquad (3.13)$$

A four electron change occurs when N_2H_4 is oxidised to N_2, so 4 equivalents of $[Fe(CN)_6]^{3-}$ are consumed per N_2H_4. In addition

Cr(II), if present, is oxidised to Cr(III) by a further mole of $[Fe(CN)_6]^{3-}$. All the $[Fe(CN)_6]^{4-}$ thereby generated is titrated with Ce(IV).

TABLE No 3.22 Redox Titrations on Chromium-Hydrazine and Carbazate Species.

Compound	Equivalents of $Fe(CN)_6^{3-}$ Consumed	
	theoretical	found
$N_2H_6SO_4$	4	4.2
$^{-}O_2CNHN^{+}H_3$	4	4.1
$CrCl_2$	1	1.0
$Cr(O_2CNHNH_2)_3.2H_2O$	12	12.6
$Cr(O_2CNHNH_2)_2.H_2O$	9	9.3
$[Cr(N_2H_4)_2Br_2]_n$	9	8.7
$[Cr_2(O_2CMe)_4(N_2H_4)]_n$	6	4.5

The technique was performed on various hydrazine and carbazate compounds as well as on anhydrous $CrCl_2$ to test the reliability of the oxidation, before being applied to the chromium(II) complexes, $[Cr(N_2H_4)_2Br_2]_n$, $Cr(O_2CNHNH_2)_2.H_2O$ and $[Cr_2(O_2CMe)_4(N_2H_4)]_n$. The results are listed in TABLE No 3.22.

The results appear to correspond well with the theoretical electron changes, except for $[Cr_2(O_2CMe)_4(N_2H_4)]_n$ where the complex was probably somewhat air-oxidised before treatment with $[Fe(CN)_6]^{3-}$. The value found corresponds essentially to a four-electron N_2H_4 oxidation with little oxidation of the chromium content.

Therefore the titrimetry indicates that the chromium in $Cr(O_2CNHNH_2)_2.H_2O$ is in the +2 oxidation state with the presence of

two hydrazino-groups as expected if the compound is bis(carbazato)-chromium(II) monohydrate.

3.7.5 VIBRATIONAL SPECTRA

Although selective infra-red absorptions of metal carbazates have been reported, no attempts at complete assignments based on deuteration studies have previously been undertaken.

To complement other spectroscopic data for $Cr(O_2CNHNH_2)_2.H_2O$ and to provide a baseline for the vibrational assignments of other carbazate complexes, a complete infra-red investigation of $Cr(O_2CNHNH_2)_2.H_2O$ and its deuterated analogue, $Cr(O_2CNDND_2)_2.D_2O$, has been carried out (see TABLE No 3.22 and FIG No 3.6). The deuterated complex was prepared by the addition of a solution of $CrCl_2$ in H_2O-d_2 to a solution of $N_2H_4.H_2O$-d_6 in H_2O-d_2 through which CO_2 had been passed for 120 mins. The resulting product precipitated almost immediately (see 3.14).

$$N_2D_4.D_2O \xrightarrow[CO_2]{D_2O} [N_2D_5][O_2CNDND_2] + \tfrac{1}{2}CrCl_2 \xrightarrow[CO_2]{D_2O} \tfrac{1}{2}Cr(O_2CNDND_2)_2.D_2O \qquad (3.14)$$

Previously infra-red spectra of metal carbazates have been assigned by considering the carbazate ligand as separate CO_2- and NH_2NH- moieties. This is a reasonable approach given that X-ray crystal structures of compounds containing coordinated carbazate ligands indicate planar O_2C-N units, with the NH-NH_2 unit out of this plane. This approach has therefore been followed here in assigning the infra-red spectra of $Cr(O_2CNRNR_2)_2.R_2O$ (R=H or D).

NH vibrations

The vibrations associated with the -$NHNH_2$ portion of the carbazate ligand have been assigned by comparison with those of the structurally related monomethylhydrazine [213].

As with CH_3NHNH_2, $^-O_2CNHNH_2$ is expected to have nine internal degrees of freedom which involve motions of the hydrogens bonded to the nitrogen atoms. These can be described as three stretching vibrations, a NH_2 scissoring mode, a NH_2 wagging, a NH_2 rocking, two NH bending motions and a NH_2 torsional vibration.

$Cr(O_2CNHNH_2)_2.H_2O$ shows only two definite bands which can be assigned to $\nu(NH_2)$, although the band at 3283 cm^{-1} is broad and may comprise two or more closely overlapping bands. On deuteration, three bands are found as expected with H/D ratios of ~1.36 indicating high $\nu(NH_2)$ character. The band at 2385 cm^{-1} has a prominent shoulder centred at 2415 cm^{-1}.

The $\delta(NH_2)$ vibrational band in $Cr(O_2CNHNH_2)_2.H_2O$ appears as a shoulder at 1627 cm^{-1} on the intense $\nu_s(CO_2)$ band. On deuteration this is shifted to 1219 cm^{-1}, an isotopic shift ratio of 1.34. This band may have a minor component at 1611 cm^{-1} which shifts on deuteration to a weak band appearing at 1187 cm^{-1}.

In the vibrational spectra of $[M(N_2H_4)_2X_2]_n$ complexes (M=Cr, Mn, Fe, Co, Ni, Zn etc), bands assigned to $\omega(NH_2)$ motions occur in the 1350-1290 cm^{-1} region, so the band appearing at 1319 cm^{-1} in the spectrum of $Cr(O_2CNHNH_2)_2.H_2O$ has also been assigned to $\omega(NH_2)$. This vibration usually has high NH character and on deuteration would therefore be expected to appear at ~1000 cm^{-1}. The closest absorption to this is a doublet at 997/989 cm^{-1} which is likely to also be derived from the $r(NH_2)$ motion.

As for the $[M(N_2H_4)_2X_2]_n$ species, the $r(NH_2)$ vibration is assigned to a strong band near 1200 cm^{-1}, in the present complex at 1194 cm^{-1}. As commented above, this band shifts on deuteration to 989 cm^{-1}, a H/D ratio of 1.21.

The two NH bending motions can be assigned to the two remaining non-carboxylate assigned absorptions present in the 1200-900 cm^{-1} region. These occur at 1102 and 985 cm^{-1}, and appear to shift to 896 and 879 cm^{-1} on deuteration with H/D ratios of 1.23 and 1.12, respectively. The low frequency $b(NH_2)$ shows similar behaviour to the $r_a(NH_2)$ absorption in $[M(N_2H_4)_2X_2]_n$ complexes in shifting relatively little on deuteration. This probably implies that the band has a mixed origin with a high degree of skeletal character .

The band assigned to the $t(NH_2)$ vibration appears to be split into two components at 693 and 636 cm^{-1} as found for $t(NH_2)$ in $[M(N_2H_4)_2X_2]_n$. These bands shift to 538 and 483 cm^{-1} on deuteration.

CO_2 vibrations

Carboxylate absorptions are assigned by reference to complexes containing coordinated acetate, such as $[Mn(N_2H_4)_2(O_2CMe)_2]_n$.

The band assigned to $\nu_a(CO_2)$ in $Cr(O_2CNHNH_2)_2.H_2O$ appears at 1579 cm^{-1}, and as expected, does not shift appreciably on deuteration, being found at 1572 cm^{-1}. The band assigned to the symmetric $\nu(CO_2)$ vibration occurs at 1370 cm^{-1} in $Cr(O_2CNHNH_2)_2.H_2O$, and at ~1372 cm^{-1} as a shoulder on the $\nu(CN)$ band in $Cr(O_2CNDND_2)_2.D_2O$.

The other carboxylate vibrations appear at characteristic positions when considered alongside the spectra of acetate complexes. The $\delta(OCO)$ band is split into two components at 803 and 778 cm^{-1} in $Cr(O_2CNHNH_2)_2.H_2O$, these shifting to 802 and 760 cm^{-1} on deuteration. The $\pi(COO)$ band at 604 cm^{-1} in $Cr(O_2CNHNH_2)_2.H_2O$ shifts only 6 cm^{-1} on deuteration. The $r(COO)$ band in coordinated glycinate complexes appears at ~500 cm^{-1}. However no band appears

in this region in $Cr(O_2CNHNH_2)_2.H_2O$, so no absorption has been assigned to this mode.

All the carboxylate vibrations were found to be essentially pure, shifting less than an isotopic ratio of 1.03. This observation justifies the separate consideration of the $-CO_2$ and $-NHNH_2$ vibrations of coordinated carbazate.

FIGURE No 3.6 Infra-red Spectra of $Cr(O_2CNRNR_2)_2.R_2O$ (R=H or D)

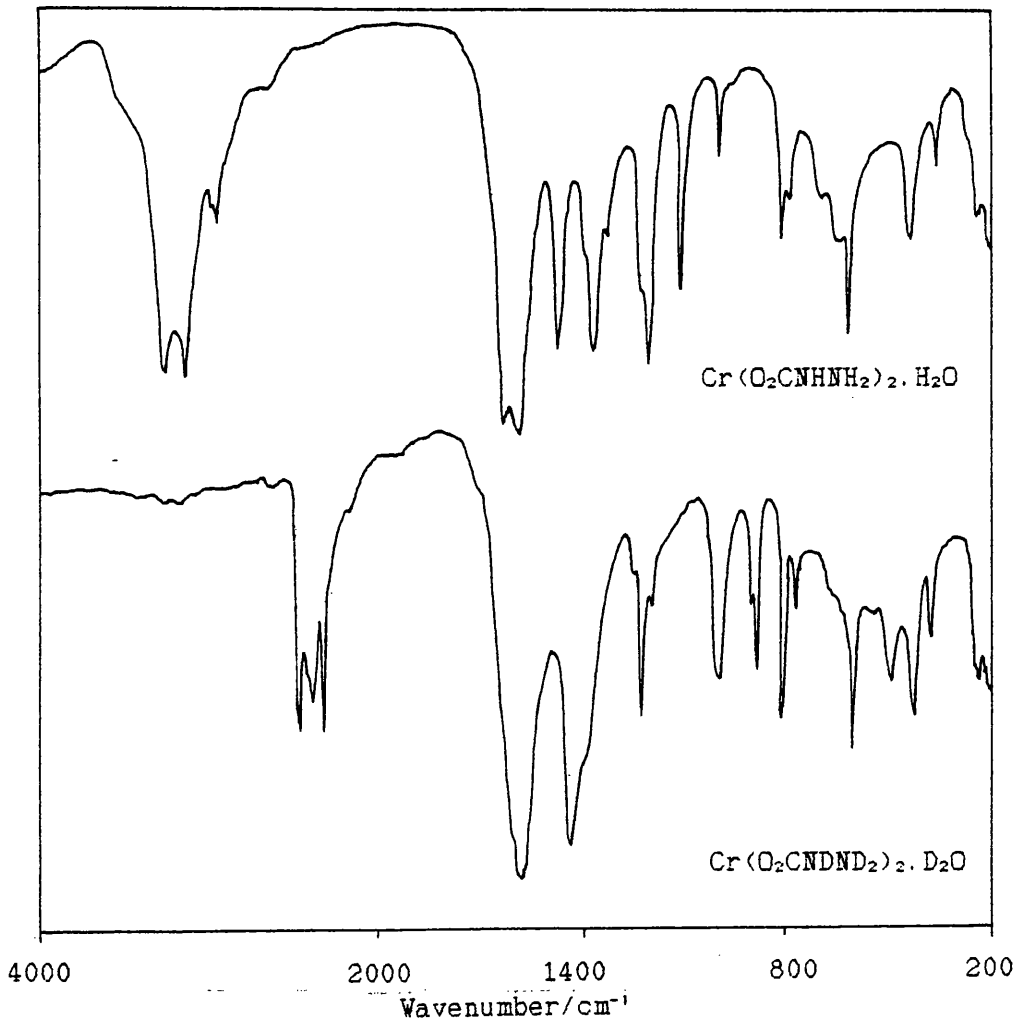

TABLE No 3.22 Infra-red Spectra of $Cr(O_2CNRNR_2)_2.R_2O$ (R=H or D) / cm^{-1}.

$Cr(O_2CNHNH_2)_2.H_2O$	$Cr(O_2CNDND_2)_2.D_2O$	H/D	Assignment
3283 (s)	2456 (s)	1.34	
	2415 (ms,sh)		$\nu(NH_2)$
	2385 (s)	1.38	
3155 (s)	2327 (s)	1.36	
1627 (s)	1219 (ms)	1.34	$\delta(NH_2)$
1611 (s)			
1579 (vs)	1572 (vs)	1.10	$\nu_a(CO_2)$
	1556 (s,sh)		
1460 (s)	1424 (vs)	1.03	antisym. skeletal stretch
1370 (s)	~1372 (vs)	~1.00	$\nu_s(CO_2)$
1319 (mw)	997 (m)	1.32	$\omega(NH_2)$
1215 (m,sh)	1187 (w)	1.02	sym. skeletal stretch
1194 (s)	989 (m)	1.21	$r(NH_2)$
1102 (m)	896 (mw)	1.23	$b(NH_2)$
985 (w)	879 (m)	1.12	
803 (m)	802 (s)	1.00	$\delta(OCO)$
778 (mw)	760 (mw)	1.02	
693 (w,br)	538 (vw,br)	1.29	$t(NH_2)$
636 (m,br)	483 (m,br)	1.32	
604 (s)	598 (ms)	1.01	$\pi(COO)$
417 (m)	415 (ms)	1.01	$\nu(MO) + \nu(MN)$
369 (w)	368 (mw)	1.00	
239 (m)	228 (m)	1.02	
226 (m)			

Skeletal vibrations

Two skeletal vibrations are expected, the antisymmetric and symmetric modes. These can also be broadly considered as $\nu(CN)$ and $\nu(NN)$ vibrations, respectively.

The antisymmetric skeletal vibration is easily assigned in $Cr(O_2CNHNH_2)_2.H_2O$ to a strong band at 1460 cm^{-1}. This shifts to 1424

cm^{-1} on deuteration, a H/D ratio of 1.03 indicating a small NH contribution as expected from a vibration involving a protonated nitrogen.

The symmetric skeletal band appears as a shoulder at 1215 cm^{-1} on the $r(NH_2)$ absorption in $Cr(O_2CNHNH_2)_2.H_2O$, a situation found in the vibrational spectra of many $[M(N_2H_4)_2X_2]_n$ complexes. On deuteration, this band appears to shift resulting in a weak absorption at 1187 cm^{-1}, which could also be assigned to a minor component of the $\delta(NH_2)$ mode.

Metal-Ligand vibrations

The two deuteration-insensitive absorptions appearing at 417 and 369 cm^{-1} in $Cr(O_2CNHNH_2)_2.H_2O$ are assigned to metal-ligand vibrations. As the symmetry of the complex is unknown, it is not possible to assign $\nu(MO)$ and $\nu(MN)$ to particular bands, even if the vibrations could be regarded as relatively pure. A further metal-ligand vibration occurs at 239/226 cm^{-1} which may be a deformation mode.

H_2O vibrations

Elemental and DTA/TG analysis both indicate the presence of a molecule of water per formula unit. Additionally, DTA indicated that the water may be directly coordinated to the chromium. However, no distinct $\nu(OH)$ or (OD) has been observed in the spectra of either complex. Such bands are likely to be obscured by the strong $\nu(NH_2)$ or $\nu(ND_2)$ vibrations. Likewise the $\delta(OH_2)$ or $\delta(OD_2)$ bands are expected to be overlaid by $\delta(NH_2)$ and $\nu_a(CO_2)$ or $\delta(ND_2)$ vibrations.

The possibility of one band in the $\nu(NH_2)$ region being assigned to $\nu(OH)$ has been rejected after comparison of the IR spectrum of $Cr(O_2CNHNH_2)_2.H_2O$ with that of anhydrous $Cu(O_2CNHNH_2)_2$ [118]. This complex similarly shows two $\nu(NH_2)$ bands at 3275 and 3150 cm^{-1} i.e. close to those found for $Cr(O_2CNHNH_2)_2.H_2O$ (3283 and 3155 cm^{-1}).

3.7.6 THERMAL DECOMPOSITION

DTA and TG determinations were performed on $Cr(O_2CNHNH_2)_2.H_2O$ both in air and argon (see TABLE No 3.23 and FIG No 3.7). Comparison of the profiles shows that the initial decomposition step is due to the loss of water. Under an argon atmosphere, two exothermic DTA peaks are found. The major peak with a maximum at 214°C appears to correspond to the loss of water, as indicated by complementary TG data. The second exothermic DTA peak with a maximium at 304°C relates to the decomposition of the carbazate groups, leaving chromium(III) oxide as the final product (see 3.15 and 3.16).

$$\text{IN AIR}\quad Cr(O_2CNHNH_2)_2.H_2O \xrightarrow{214^\circ} Cr(O_2CNHNH_2)_2 \xrightarrow{279^\circ} CrO_x^{\bullet} \xrightarrow{413^\circ} Cr_2O_3 \qquad (3.15)$$

• - unknown chromium oxide

$$\text{IN ARGON}\quad Cr(O_2CNHNH_2)_2.H_2O \xrightarrow{214^\circ} Cr(O_2CNHNH_2)_2 \xrightarrow{304^\circ} Cr_2O_3 \qquad (3.16)$$

The loss of H_2O was found to give an non-isolable anhydrous $Cr(O_2CNHNH_2)_2$ (by weight loss). It appears that the water molecule plays a crucial role in the stability of the complex. Once the water is lost, the complex decomposes spontaneously. The presence of the water may be the key in explaining the unexpected stability of the chromium(II) complex to atmospheric oxidation. On

dehydration this stability is lost and the complex oxidises forming chromium(III) oxide.

TABLE No 3.23 Differential Thermal Analysis of $Cr(O_2CNHNH_2)_2.H_2O$

Atmosphere	Peak positions (heat change) / °C
AIR	214 (+), 279 (+), 413 (+)
ARGON	214 (+), 304 (+)

The DTA/TG results give an indication of the considerable strength of the bonding of water within the complex. It is probable that the water is bound by extensive hydrogen-bonding to the carbazate groups within the lattice and such interactions would explain why attempts to either remove the water by refluxing 2,2-dimethoxypropane [224] or replacement by other donor molecules were unsuccessful.

Comparing the DTA peak for H_2O loss from $Cr(O_2CNHNH_2)_2.H_2O$ (DTA peak maximum 214°C) with similar losses from $M(O_2CNHNH_2)_2.xH_2O$ (M = Mg,Ca,Mn) [101,108] (DTA peaks with maxima in the range 130-170°C) suggests a more strongly bound water in the chromium complex.

A consideration of the bis-carbazates whose structures have been solved by X-ray crystallography, shows that only one monohydrate has been characterised, namely $Cd(O_2CNHNH_2)_2.H_2O$ [116]. The cadmium ion is in an octahedral environment being surrounded by two *N,O*-chelating carbazate groups with the remaining two coordination sites occupied by two oxygens from bridging carbazates. The water molecules are hydrogen-bonded to the carbazate groups and do not coordinate to the cadmium. The individual octahedral units are grouped into layers which are held together by bridging carbazates and hydrogen bonding involving the uncoordinated H_2O molecules.

FIGURE No 3.7 DTA/TG of Chromium Carbazate Species

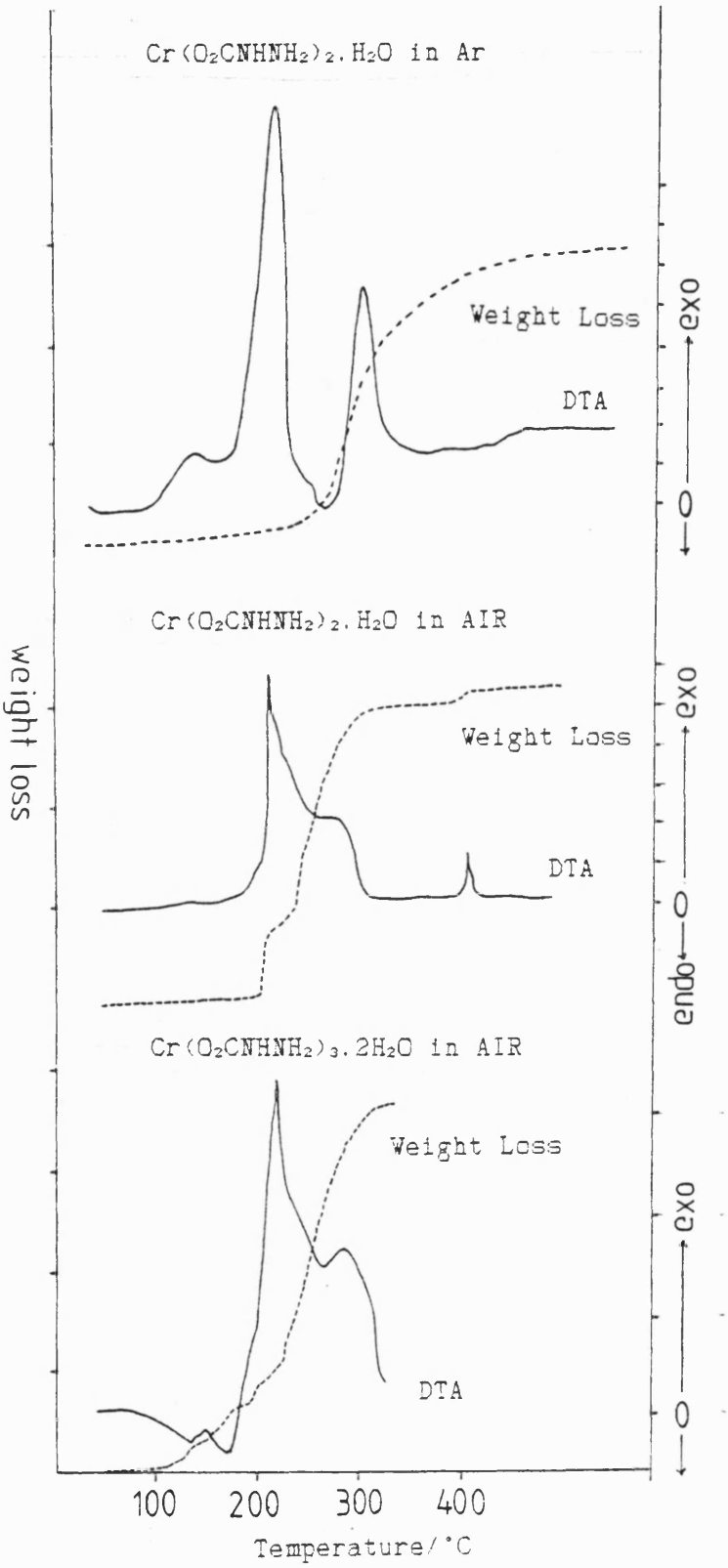

FIGURE No 3.8 Structure of $[Cd(O_2CNHNH_2)_2.H_2O]_n$.

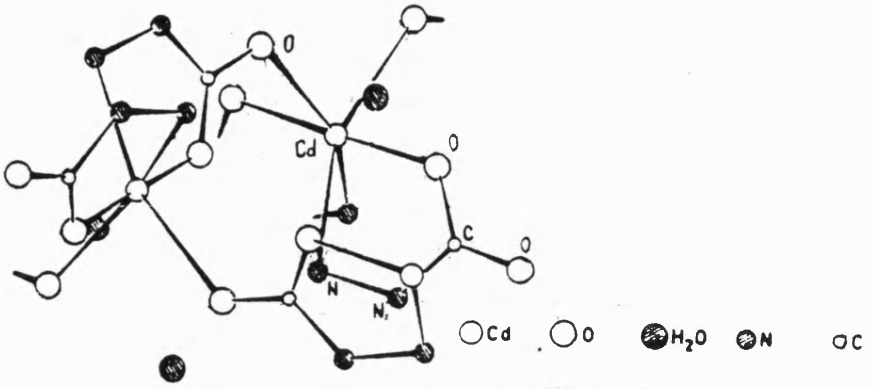

The DTA data for $Cr(O_2CNHNH_2)_2.H_2O$ suggests that the H_2O is bound strongly and probably coordinated to the chromium. The complex therefore may not be iso-structural with $Cd(O_2CNHNH_2)_2.H_2O$. However, it is not possible to assign a definitive structure using the spectroscopic data acquired in this work.

3.8 REACTIONS OF CHROMIUM(II) SPECIES WITH CARBAZIC ACID

3.8.1 BACKGROUND

In addition to reacting chromium(II) compounds with $[N_2H_5]$-$[O_2CNHNH_2]$, reactions with carbazic acid, $^{-}O_2CNH\overset{+}{N}H_3$ were also investigated. In particular, it was hoped that ligand-bridged complexes analogous to the chromium(II) glycine species, $[Cr_2(O_2CCH_2NH_3)_4X_4]xH_2O$ (X=Cl, x=3; X=Br, x=4) [219,225] could be isolated. In these complexes the glycine is in the zwitterion form, $^{-}O_2CCH_2\overset{+}{N}H_3$ and *O,O*-coordinates in a bridging manner between two chromium(II) ions. The complexes also possess quadruple metal-metal bonds.

3.8.2 REACTION OF $[Cr(OH_2)_6]Br_2$ WITH CARBAZIC ACID

The complex $[Cr(OH_2)_6]Br_2$, generated by reaction of the metal with aqueous hydrobromic acid under nitrogen, was reacted *in situ*

with O_2CNHNH_3 in the presence of CO_2 under N_2. Reactions were carried out in both ethanol and water.

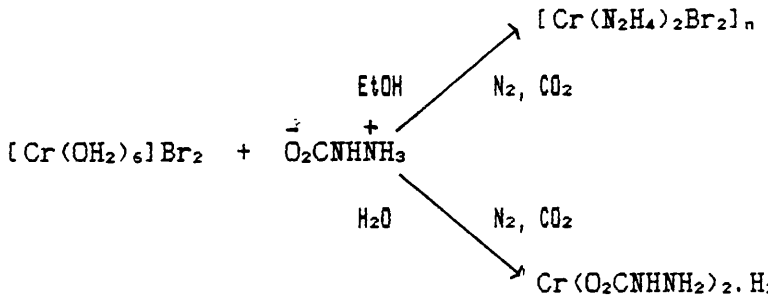

(3.17)

In ethanol, the product was shown to be $[Cr(N_2H_4)_2Br_2]_n$, while in water, $Cr(O_2CNHNH_2)_2.H_2O$ was produced. Carbazic acid is not soluble in ethanol so a suspension was used. As a consequence, the reaction proceeded slowly. Presumably, the water liberated from the chromium(II) starting material partially hydrolyses the acid releasing sufficient hydrazine to generate $[Cr(N_2H_4)_2Br_2]_n$ which is precipitated from the reaction medium.

In water, carbazic acid hydrolyses forming $[N_2H_5][O_2CNHNH_2]$. This species therefore reacts with the chromium(II) compound to form $Cr(O_2CNHNH_2)_2.H_2O$ (see 3.17).

3.8.3 REACTION OF $[Cr_2(O_2CMe)_4(OH_2)_2]$ WITH CARBAZIC ACID

The acetate, $Cr_2(O_2CMe)_4(OH_2)_2$, was reacted with carbazic acid under nitrogen in methanol using a variety of reaction temperatures.

At room temperature, little reaction was observed, the pale pink solid recovered being shown by IR spectroscopy to be mainly carbazic acid.

After 120 minutes at 55°C the reaction product was still predominately carbazic acid but mixed with a small amount of $Cr(O_2CNHNH_2)_2.H_2O$ as assessed by the IR spectrum. In refluxing

methanol (65°C) the reaction was complete after 30 minutes (see 3.18).

$$Cr_2(O_2CMe)_4(OH_2)_2 + 4\ \overset{-}{O_2}CNHN\overset{+}{H}H_3 \xrightarrow[N_2]{MeOH,\Delta} 2\ Cr(O_2CNHNH_2)_2.H_2O \quad (3.18)$$

It is apparent that carbazic acid only reacts at a significant rate at elevated temperatures where decomposition occurs readily [6,184].

3.8.4 REACTION OF $CrCl_2(MeCN)_2$ WITH CARBAZIC ACID

The reactive $CrCl_2(MeCN)_2$ was prepared by the addition of a concentrated aqueous/ethanolic solution of $[Cr(OH_2)_6]Cl_2$ to excess MeCN, and treated *in situ* with carbazic acid in methanol at room temperature. The product was shown to be $[Cr(N_2H_4)_2Cl_2]_n$ by IR spectroscopy (see 3.19).

$$CrCl_2(MeCN)_2 + 2\ \overset{-}{O_2}CNHN\overset{+}{H}H_3 \xrightarrow[N_2]{MeOH} [Cr(N_2H_4)_2Cl_2]_n + 2MeCN + 2CO_2 \quad (3.19)$$

It is clear that carbazic acid in alcoholic media usually reacts with chromium(II) species to form hydrazine complexes. No products have been isolated which contain the $\overset{-}{O_2}CNHN\overset{+}{H}H_3$ species, but only those containing $^-O_2CNHNH_2$ or N_2H_4. It is therefore, unlikely that analogues of the glycine-bridged complexes $[Cr_2(O_2CCH_2NH_3)_4]^{4+}$ will be capable of preparation. Indeed the complexes $[Cr_2(O_2CCH_2NH_3)_4]X_4.nH_2O$ (X=Cl, n=3; X=Br, n=4) [219,225] require acid solution conditions for formation otherwise the mononuclear $Cr(O_2CCH_2NH_2)_2.H_2O$ forms [219]. These conditions would destroy carbazic acid.

3.9 CHROMIUM(III) CARBAZATE CHEMISTRY

3.9.1 BACKGROUND

The chromium(III) carbazate, $Cr(O_2CNHNH_2)_3.2H_2O$, was first reported by Funk, Eichhoff and Giesder [100] in 1965. However characterisation was limited to elemental analysis. More recent work by Macek, Rahten and Slivnik [125] reported the thermal decomposition of the complex and Bellerby [16] employed the complex as a model chromium homogeneous catalyst in studies of hydrazine decomposition. Srivastava using similar preparative routes claimed [146] to have formed anhydrous $Cr(O_2CNHNH_2)_3$.

3.9.2 PREPARATION

To complement the characterisation of $Cr(O_2CNHNH_2)_2.H_2O$, a more complete characterisation of $Cr(O_2CNHNH_2)_3.2H_2O$ was undertaken.

The reaction of $[Cr(OH_2)_4Cl_2]Cl.2H_2O$ with aqueous $[N_2H_5][O_2CNHNH_2]$ resulted in the formation of pink, microcrystalline, air-stable, $Cr(O_2CNHNH_2)_3.2H_2O$ (see 3.20). Aggregated crystalline $Cr(O_2CNHNH_2)_3.2H_2O$ as red needles is formed when the $Cr:[N_2H_5][O_2CNHNH_2]$ ratio is raised above ~1:50. This complex is also formed as a by-product in reactions designed to synthesise $Cr(O_2CNHNH_2)_2.H_2O$.

$$[Cr(OH_2)_4Cl_2]Cl.2H_2O + 3[N_2H_5][O_2CNHNH_2] \xrightarrow[CO_2]{H_2O,\Delta} Cr(O_2CNHNH_2)_3.2H_2O + 3N_2H_5Cl \quad (3.20)$$

The complex is insoluble in all solvents that do not subsequently react with it, apart from some solubility in N_2H_4 and concentrated $[N_2H_5][O_2CNHNH_2]$ solutions where the $Cr(O_2CNHNH_2)_3$ moiety is suspected to survive, as based on visible spectroscopic evidence (see TABLE No 3.24).

This insolubility has frustrated attempts to grow single crystals of $Cr(O_2CNHNH_2)_3.2H_2O$ for an X-ray structure determination. As described above, crystalline material can be produced from the preparative media, but proved to be microcrystalline aggregate. It is thought that a modification of this procedure may eventually yield suitable material for structural analysis.

Following the reported deprotonation of $M(S_2CNHNH_2)_3.2H_2O$ (M=Co,Cr) [226] to form $[M(S_2CNNH_2)_3]^{3-}$ species, the action of base on $Cr(O_2CNHNH_2)_3.2H_2O$ was investigated.

It was found that although a deep red solution was initially formed on treating $Cr(O_2CNHNH_2)_3.2H_2O$ with concentrated aqueous NaOH, rapid hydrolysis followed giving green-grey solutions, presumably containing $[Cr(OH)_6]^{3-}$ anions (see 3.21).

$$Cr(O_2CNHNH_2)_3.2H_2O \longrightarrow [Cr(O_2CNNH_2)_3]^{3-} \longrightarrow [Cr(OH)_6]^{3-} \quad (3.21)$$

Attempts to stabilize the initially formed deprotonated $[Cr(O_2CNNH_2)_3]^{3-}$ species using $[Me_4N]^+$ in the form of $Me_4NOH.5H_2O$ were unsuccessful.

3.9.3 MAGNETIC SUSCEPTIBILITY AND ELECTRONIC SPECTRAL CHARACTERISATION

$Cr(O_2CNHNH_2)_3.2H_2O$ exhibits a magnetic susceptibility value (χ_{cgx} = 19.19×10^{-6} cm^3g^{-1}, μ_{eff} = 3.82 BM at 295K) which is characteristic of a octahedral chromium(III) species.

This is confirmed by the diffuse reflectance electronic spectrum (see TABLE No 3.24). Comparison with the reflectance electronic spectrum of $Cr(O_2CCH_2NH_2)_3.H_2O$ indicates a broadly similar environment around the chromium in both complexes. The calculated B values are similar as are the derived β values of both

complexes. Since the glycinate complex is known to contain three *N,O*-chelating groups around the chromium(III) [227], the similarity of the spectrum of the carbazate suggests that three *N,O*-chelating carbazate groups surround the chromium in $Cr(O_2CNHNH_2)_3.2H_2O$.

TABLE No 3.24 Electronic Spectra of $Cr(O_2CNHNH_2)_3.2H_2O$ and a Comparison with $Cr(O_2CCH_2NH_2)_3.H_2O$ / nm.

$Cr(O_2CNHNH_2)_3.2H_2O$		$Cr(O_2CCH_2NH_2)_3.H_2O$	Assignment
Reflectance	N_2H_4 sol'n	Reflectance*	
698 (vw)	700 (vw,sh)	689 (vw)	$^2E_g \leftarrow {}^4A_{2g}$
523 (s)	522 (s,br)	503 (s)	$^4T_{2g} \leftarrow {}^4A_{2g}$
395 (m)	402 (s,br)	384 (m)	$^4T_{1g} \leftarrow {}^4A_{2g}$
261 (vs)			
19100	19200	19900	Δ_o / cm^{-1}
587	533	578	B / cm^{-1}
0.64	0.58	0.63	β
245	246	237	calc ν_3 / nm

* - taken from ref. 227. B, β and ν_3 calculated from ref.215.

The calculated spectral parameters for $Cr(O_2CNHNH_2)_3.2H_2O$ in N_2H_4 are smaller than those of the solid. This implies an increase in the covalency of the metal-ligand bonds. Dissolution of the complex in hydrazine probably destroys much of the strong intermolecular hydrogen-bonding that exists in the solid, and the solution spectrum may be reflecting this.

3.9.4 VIBRATIONAL SPECTRA

The infra-red spectrum of the complex indicates the presence of *N,O*-chelating carbazate ligands, with non-coordinated hydrogen-bonded water molecules (see TABLE No 3.25 and FIG No 3.9). The band

assignments are based on those made for $Cr(O_2CNHNH_2)_2.H_2O$ (see SECTION No 3.7).

The NH vibrations are found in similar positions to those in the chromium(II) complex. There appears to be only one detectable band assignable to a b(NH) in the spectrum of $Cr(O_2CNHNH_2)_3.2H_2O$ whereas two are expected for a $-NH-NH_2$ system.

TABLE No 3.25 Infra-red Spectrum of $Cr(O_2CNHNH_2)_3.2H_2O$.

$Cr(O_2CNHNH_2)_3.2H_2O$ / cm^{-1}	Tentative Assignment
3535 (m, br)	ν(OH)
3329 (s) 3205 (s) 3106 (s) 3060 (s)	ν(NH)
1668 (vs) 1648 (s)	$\delta(NH_2) + \delta(OH_2)$
1615 (s, br)	$\nu_a(CO_2)$
1454 (vs)	antisym. skeletal stretch
1367 (m, br) 1342 (m, br)	$\nu_s(CO_2)$
1308 (w)	$\omega(NH_2)$
1246 (ms, sh)	sym. skeletal stretch
1226 (s) 1216 (s)	$r(NH_2)$
993 (m)	$b(NH_2)$
793 (m)	δ(OCO)
~742 (w, br)	$t(NH_2)$?
629 (m)	π(COO)
494 (mw)	r(COO)
413 (m) 334 (mw)	ν(MO) + ν(MN)

The ν(OH) absorption is found at ~3535 cm^{-1} and is broad indicating that the H_2O molecules are uncoordinated. The $\delta(OH_2)$ absorption is expected in the 1650-1600 cm^{-1} region, but is presumably hidden by the strong $\nu_s(CO_2)$ and $\delta(NH_2)$ absorptions also present in this region.

FIGURE No 3.9 Infra-red Spectrum of $Cr(O_2CNHNH_2)_3.2H_2O$

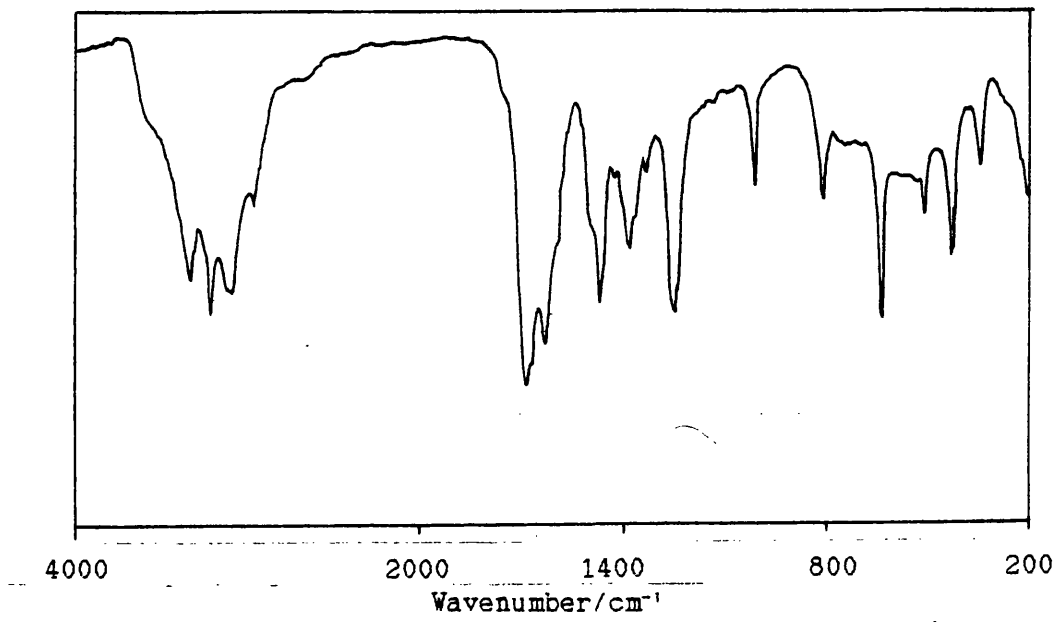

A band assignable to the r(COO) mode is present in the spectrum at 494 cm^{-1}. This band was not detected in the spectrum of $Cr(O_2CNHNH_2)_2.H_2O$, perhaps an indication that the carbazate ligands are bonding in different ways in the two complexes. Undoubtedly in the chromium(III) complex the carbazate ligands are merely acting in a bidentate chelating manner, whereas in the chromium(II) complex additional metal-carbazate oxygen interactions may be present to produce a polymeric structure, the carbazate ligands thereby being, perhaps, terdentate.

3.9.5 THERMAL DECOMPOSITION

DTA/TG experiments in air show that the two H_2O molecules are evolved at separate temperatures, endothermic peaks with maxima at 136° and 169°C being detected. The first DTA peak which can be assigned to carbazate decomposition is an exothermic change with a peak maximum at 222° (see TABLE No 3.26). However, $Cr(O_2CNHNH_2)_3.H_2O$ and $Cr(O_2CNHNH_2)_3$ are non-isolable intermediates. Attempts to dehydrate $Cr(O_2CNHNH_2)_3.2H_2O$ by heating *in vacuo* or by use of a water scavenger such as 2,2-dimethoxypropane resulted in decomposition or no reaction. Presumably the H_2O molecules occupy intermolecular positions and once removed the resulting complex is of lower stability than $Cr(O_2CNHNH_2)_3.2H_2O$ and merely decomposes further.

TABLE No 3.26 Differential Thermal Analysis of $Cr(O_2CNHNH_2)_3.2H_2O$.

	Peak positions (heat change) / °C
$Cr(O_2CNHNH_2)_3.2H_2O$	136 (-), 169 (-), 222 (+), 288 (+), 420(+)

$$Cr(O_2CNHNH_2)_3.2H_2O \xrightarrow[-2H_2O]{136/169^\circ} 'Cr(O_2CNHNH_2)_3' \xrightarrow{222/288^\circ} CrO_x^{*} \xrightarrow{420^\circ} Cr_2O_3 \qquad (3.22)$$

* - unknown oxide phase

The water molecules are lost at higher temperatures than expected for non-coordinated water (~100°) indicating that strong hydrogen-bonding exists in the complex. The structure of $Cr(O_2CNHNH_2)_3.2H_2O$ can be compared to the known crystal structure of $Cr(O_2CCH_2NH_2)_3.H_2O$ [227]. The latter complex, like the carbazate, is insoluble in water and has been shown to have an unusually high heat of

sublimation [228]. The X-ray crystal structure shows an extensive network of hydrogen bonding between the H_2O, $-NH_2$ and the -COO groups which give rise to the unusual physical properties.

It is proposed that the molecular structure of $Cr(O_2CNHNH_2)_3.2H_2O$ is similar to that of $Cr(O_2CCH_2NH_2)_3.H_2O$, in that it is enantiomorphic and displays an elaborate network of hydrogen-bonding intimately involving the two water molecules.

It is clear from the characterisation data presented in this work that the formation of an anhydrous chromium(III) carbazate is unlikely under the conditions quoted by Srivastava [146]. These consisted of the passage of CO_2 into an already prepared aqueous solution of $[Cr(OH_2)_4Cl_2]Cl.2H_2O$ and N_2H_4. This solution will undoubtedly contain chromium(III) hydroxide, which is known to be blue/grey in colour. On passage of CO_2, a red colouration develops from which $Cr(O_2CNHNH_2)_3.2H_2O$ eventually precipitates. The blue product reported by Srivastava is most likely to be mainly chromium(III) hydroxide. However, elemental analysis was claimed to correspond to a $Cr(O_2CNHNH_2)_3$ formulation. This report also contained details of other chromium(III) substituted carbazates which must now be looked upon as suspect, as must other work on carbazates reported by Srivastava.

3.10 EXPERIMENTAL

3.10.1 ATTEMPTED CATION EXCHANGE OF $[N_2H_5][O_2CNHNH_2]$

a) Reaction of NaOH with $[N_2H_5][O_2CNHNH_2]$

An aqueous solution of $[N_2H_5][O_2CNHNH_2]$ (~5.00 g, 50 mmol) was prepared by the method of Patel *et al.* [134]. To this solution, was slowly added an aqueous solution (10 cm^3) of NaOH (4.00 g, 100 mmol). The combined solution was stirred for 15 mins after which excess EtOH (50 cm^3) was added. On extended stirring two layers formed, and attempts to precipitate a solid from the lower carbazate layer failed.

b) Sodium ion-exchange of $[N_2H_5][O_2CNHNH_2]$

An aqueous solution of $[N_2H_5][O_2CNHNH_2]$ was prepared by the passage of CO_2 through an aqueous solution (45 cm^3) of N_2H_4 (5.0 cm^3, 160 mmol) for 120 mins. The carbazate solution was passed down a column of Duolite C225 (Na) cation exchange resin. Gas evolution (presumably CO_2) was observed from the column indicating carbazate decomposition.

c) Reaction of Ph_4PBr with $[N_2H_5][O_2CNHNH_2]$

To N_2H_4 (40 cm^3) at 0° was added $\overset{-}{O_2}CNH\overset{+}{N}H_3$ (5.00 g, 66mmol). This solution was stirred at 0°C while N_2 and CO_2 were passed through for 30 mins. To the resulting solution was added Ph_4PBr (0.50 g, 1.2 mmol) and the mixture stirred under N_2 at 0°C for 30 mins. The reaction mixture was allowed to warm to room temperature and opened to the atmosphere. On leaving overnight, off-white crystals had formed which were filtered off and dried under vacuum. The product was identified as $Ph_3P{=}O$, from IR, ^1H and ^{13}C nmr spectra.

d) Reaction of Ph_4AsCl with $[N_2H_5][O_2CNHNH_2]$

$Ph_4AsCl.H_2O$ was dehydrated by heating at 120°C *in vacuo* for 4 hours, the H_2O removal being checked by IR spectroscopy. To N_2H_4 (30 cm^3) at 0°C was added O_2CNHNH_3 (5.00 g, 66 mmol). This solution was stirred at 0°C while N_2 and CO_2 were passed through for 60 mins. To the resulting solution was added Ph_4AsCl (0.05 g, 1.2 mmol) and the reaction mixture stirred at 0°C for 30 mins then allowed to warm to room temperature and left overnight. During this time a white precipitate had formed, which was filtered off and dried under vacuum. IR and ^{13}C nmr spectroscopy indicated the presence of a Ph_4As^+ species.

e) Reaction of Cs_2CO_3 with $[N_2H_5][O_2CNHNH_2]$

A solution of $[N_2H_5][O_2CNHNH_2]$ was prepared by bubbling CO_2 through N_2H_4 (30 cm^3) for 90 mins at 0°C. To the resulting stirred solution, was added an aqueous solution (20 cm^3) of Cs_2CO_3 (2.00 g, 6.1 mmol) dropwise. The solution was reduced to low volume by heating and cooled to -3°C. After 48 hours, a viscous colourless liquid had resulted.

f) Preparation of $LiO_2CNHNH_2.H_2O$

$LiOH.H_2O$ (0.5 g, 12 mmol) was suspended in deoxygenated MeOH (60 cm^3). To this was added freshly prepared $\overset{-}{O_2}CNH\overset{+}{N}H_3$ (1.41 g, 18.5 mmol) and the reaction mixture heated under reflux for 90 mins. The resulting colourless product was then left to stand for 10 days before being filtered off and dried under vacuum. Calc. for $CH_5LiN_2O_3$: C, 12.01; H, 5.04; N, 28.01 %. Found: C, 11.49; H, 4.76; N, 27.67%.

g) Preparation of $Ba(O_2CNHNH_2)_2.N_2H_4$

Solid $BaCl_2$ (1.50 g, 7.2 mmol) was dissolved in N_2H_4 (40 cm^3) under N_2 and heated under reflux. Carbon dioxide was passed into the heated solution for 30 mins, after which the solution was allowed to cool overnight. The resulting white crystalline product was filtered off, washed with EtOH and dried under vacuum.

$C_2H_{10}BaN_6O_4$. Requires: C, 7.52; H, 2.98; N, 26.31 %. Found: C, 6.44; H, 2.98; N, 26.40 %.

3.10.2 CARBAZIC ACID

a) Preparation of $\overset{-}{O}_2CNHN\overset{+}{H}H_3$

Carbon dioxide was passed slowly through an aqueous solution (30 cm^3) of N_2H_4 (30 cm^3) at 0°C for 12 hours. The resulting white solid was filtered off under N_2 and suspended in anhydrous MeOH. After 3 days, the white solid was refiltered under N_2, washed with Et_2O and dried under vacuum. The resulting solid was sufficiently free-flowing to mull in nujol and to pack into glass capillaries.

Calc. for $CH_4N_2O_2$: C, 15.79; H, 5.30; N, 36.83 %. Found: C, 15.63; H, 5.42; N, 36.62 %.

b) Preparation of $\overset{-}{O}_2CNDN\overset{+}{D}D_3$

A solution of $N_2H_4.H_2O$-d_6 (1.00 cm^3, ~18.4 mmol) in D_2O (1 cm^3), was saturated with CO_2 for 10 hours until a white precipitate began to form. MeOH-d_4 (4 cm^3) was layered on this reaction solution and after 72 hours, the white product had solidified. The solid was filtered off, washed with Et_2O and dried under vacuum. Yield 1.31g (91.0% based on $N_2H_4.H_2O$-d_6 taken).

3.10.3 REACTIONS OF N_2H_4 WITH CHROMIUM(II)

a) Preparation of $[Cr(N_2H_4)_2X_2]_n$ (X = Cl, Br)

An ethanolic solution of $[Cr(OH_2)_6]Cl_2$ was prepared by reacting excess electrolytic Cr metal (1.00 g) with a solution of conc. aqueous HCl (s.g. 1.17) in deoxygenated ethanol (15 cm^3) under N_2. This was reacted with a deoxygenated solution of N_2H_4 (0.63 cm^3, 20 mmol) in EtOH (10 cm^3). The resulting grey-blue product was filtered off under N_2, washed with EtOH and Et_2O and dried under a stream of N_2.

The corresponding bromide complex was prepared by replacing HCl with aqueous HBr (s.g. 1.48) (1.06 cm^3, 9 mmol).

b) Reaction of 'Chromium(II) Thiocyanate' with N_2H_4

To a solution of $[Cr(OH_2)_6]Cl_2$ in EtOH (prepared by reaction of aqueous HCl (1.00 cm^3, 11.5 mmol) with excess Cr metal in EtOH (50 cm^3)) was added a deoxygenated solution of KNCS (4.00 g, 41 mmol) in EtOH (75 cm^3) under N_2. The resulting royal blue solution was decanted from the precipitated KCl and to this solution was added a deoxygenated solution of N_2H_4 (0.90 cm^3, 28 mmol) in EtOH (10 cm^3). A pink solid precipitated immediately and was filtered off in air, washed with EtOH and dried under vacuum. Solution electronic spectrum of the product: 545(s), 410(s) nm.

c) Reaction of 'Chromium(II) Tetrafluoroborate' with N_2H_4

The reaction of hot aqueous HBF_4 (s.g. 1.41, 2.00 cm^3, 16 mmol) with HCl-treated electrolytic Cr metal (1.00g) in EtOH (50 cm^3) under N_2 resulted in the formation of royal blue '$[Cr(OH_2)_6][BF_4]_2$' (solution electronic spectrum: 694 (s, br) nm). To this solution was added a deoxygenated solution of N_2H_4 (1.50 cm^3, 47 mmol) in EtOH (15 cm^3) under N_2. A lilac

solid precipitated immediately, was filtered off, washed with EtOH and dried under vacuum.

(Reflectance electronic spectrum: 571 (m, br) 409 (m, br) nm; χ_{cgx} = 23.11 x 10^{-6} cm^3g^{-1}).

The reaction was repeated, but the solution of '$[Cr(OH_2)_6][BF_4]_2$' was allowed to oxidise in air before the addition of N_2H_4. A lilac solid was isolated in a similar manner.

(Reflectance electronic spectrum: 687 (vw, sh), 574 (s, br), 412 (m, br) nm; χ_{cgx} = 24.12 x 10^{-6} cm^3g^{-1}).

d) Preparation of $[Cr_2(O_2CMe)_4(\mu\text{-}N_2H_4)]_n$

Preparation of $Cr_2(O_2CMe)_4(H_2O)_2$ was achieved by the reaction of $[Cr(OH_2)_6]Cl_2$ (29 mmol, prepared as in 3.10.32) with NaO_2CMe (9.00 g, 110 mmol) in H_2O (50 cm^3).

To a deoxygenated solution of $Cr_2(O_2CMe)_4.(H_2O)_2$ (2.04g, 5.42 mmol) in MeOH (30 cm^3) was added a deoxygenated solution of N_2H_4 (5.00 cm^3, 15.78 mmol) in MeOH (10 cm^3) under N_2. The reaction mixture was stirred under N_2 at room temperature for 12 hours, before the resulting orange product was filtered off, washed with MeOH and Et_2O and dried under a stream of N_2.

$C_8H_{16}CrN_2O_8$. Requires: C, 25.82; H, 4.33; N, 7.53 %

Found: C, 25.34; H, 4.26; N, 7.53 %.

3.10.4 CHROMIUM(II) AND (III) - HYDRAZINE SOLUTION CHEMISTRY

a) Conductivity Measurements of Salts in Anhydrous N_2H_4

For a description of the conductivity apparatus see Appendix 1. The conductivity of propellant grade N_2H_4 was found to be 2.321 x $10^{-3}\Omega^{-1}cm^{-1}$ which was considered too high for

conductiometric work. Therefore purification of the N_2H_4 was undertaken before use.

Anhydrous N_2H_4 was prepared by distillation from CaH_2 at ambient pressure under N_2. The N_2H_4 was heated over CaH_2 under N_2 for 60 mins to remove H_2O and CO_2 impurities before distillation. The purity of the N_2H_4 was assessed by conductivity. Values below 5 x $10^{-6}\Omega^{-1}cm^{-1}$ (literature value 1.6 x $10^{-6}\Omega^{-1}cm^{-1}$ [229]) were considered satisfactory for further use.

All conductivity measurements were performed in a dry bag under N_2, the solutions being prepared and loaded into a sealable conductivity cell under N_2. Salts employed as standards were all anhydrous. $CoCl_2.6H_2O$, $NiCl_2.6H_2O$ and $[Co(en)_3]Br_3.3H_2O$ were dehydrated by heating in air at 110°C for several days.

b) Magnetic Measurements in Anhydrous N_2H_4

For a description of the Gouy and Evans methods for determining magnetic susceptiblities see Appendix 1.

Concentrated solutions (0.75 - 1 M) of salts in propellant grade N_2H_4 were used for the Gouy method. $CoCl_2$ was dehydrated as per 3.10.4a, $CrCl_2$ and $CrCl_3$ were used as received. Solutions were prepared under N_2 and loaded into a wide bore (6mm o.d.) magnetic moment tube. The densities and hence molarities of the solutions were determined by weight difference.

10^{-3}M solutions of anhydrous $CoCl_2$, $CrCl_2$ and $CrCl_3$ in propellant grade N_2H_4 were used for the Evans nmr method. They were prepared as above. Molarities were determined by standard volume preparation.

c) Isolation of Chromium(II) and (III) Solution Products

A solution of $CrCl_2$ (1.26 g, 10.4 mmol) in N_2H_4 (10 cm^3, ~1M) was prepared under N_2. To this solution was added an excess of deoxygenated MeCN (150 cm^3). The excess MeCN was decanted after 72 hours and the red product was dried *in vacuo*. The resulting red solid was found to be hygroscopic and electostatic.

$H_{23}Cl_2CrN_{10}O_2$. Requires: Cr, 16.34; Cl, 22.29; N, 44.03; H, 7.29%. Found: Cr, 15.97; Cl, 23.98; N, 44.22; H, 7.04%.

A solution of $CrCl_3$ (1.60 g, 10.1 mmol) in N_2H_4 (10 cm^3, ~1M) was prepared under N_2. To this solution was added an excess of deoxygenated MeCN (150 cm^3). The excess MeCN was decanted and the remaining liquid was reduced in volume *in vacuo*. The resulting red solid was heated at 110°C in vacuo.

$H_{17.2}Cl_3CrN_{7.6}O$. Requires: Cr, 17.44; Cl, 35.67; N, 35.70; H, 5.82%. Found: Cr, 17.42; Cl, 35.44; N, 35.71; H, 5.71%.

d) Attempted Substitution of 2,2'-Bipyridyl into the Chromium (II) and (III) - Hydrazine Solution Products.

To a solution of 2,2'-bipyridyl (bipy) (0.12 g, 0.77 mmol) in anhydrous MeCN (50 cm^3) was added the chromium(III) - hydrazine product (prepared as in 3.10.4c) (0.073). This suspension was heated under reflux for 16 hours (82°C). After this time, the reaction was cooled to room temperature and the resulting solid filtered off, washed with Et_2O and dried under vacuum. An IR spectrum indicated the absence of bipy.

e) Reaction of Chromium(II) and (III) - Hydrazine Solutions with CO_2 in N_2H_4

Carbon dioxide was passed through a solution of the Cr(II)-N_2H_4 product in N_2H_4 (50 cm^3) at 0°C under N_2. After 90 mins the reaction was stopped, as the solution had become too

viscous for gas passage (reflectance electronic spectrum: 510 (m, br), 361 (s, br) nm).

A similar reaction was attempted for the Cr(III)-N_2H_4 product (reflectance electronic spectrum: 579 (s), 387 (m) nm).

3.10.5 CHROMIUM(II) CARBAZATE CHEMISTRY

a) Preparation of $Cr(O_2CNHNH_2)_2.H_2O$

$Cr(O_2CNHNH_2)_2.H_2O$ can be prepared by reacting a variety of chromium(II) sources (e.g. $Cr_2(O_2CMe)_4(H_2O)_2$, $[Cr_2(O_2CMe)_4(N_2H_4)]_n$, $CrCl_2.4H_2O$, $CrBr_2.6H_2O$ and $[CrX_2(N_2H_4)_2]_n$ (X = Cl or Br)) with aqueous solutions of $[N_2H_5][O_2CNHNH_2]$. A typical preparation is detailed below.

Passage of CO_2 through an aqueous solution (5.00 cm^3) of $N_2H_4.H_2O$ (0.78 cm^3, 16.0 mmol) for 125 mins gives an aqueous solution of $[N_2H_5][O_2CNHNH_2]$ (8 mmol). A deoxygenated aqueous solution (1.50 cm^3) of $CrCl_2$ (0.139 g, 1.13 mmol) was prepared under N_2 and the two solutions mixed in a N_2 atmosphere. The pale lilac product precipitated rapidly and was stirred for 15 mins before isolation. The product was filtered off under N_2, washed with H_2O, MeOH and Et_2O and dried under a stream of N_2.

Yield: 0.152g (61.0% based on $CrCl_2$ taken).

$C_2H_8CrN_4O_5$. Requires: C, 10.91; H, 3.66; N, 25.46 % Found: C, 11.21; H, 3.14; N, 25.85 %

b) Preparation of $Cr(O_2CNDND_2)_2.D_2O$

This complex was prepared in a similar manner to $Cr(O_2CNHNH_2)_2.H_2O$ using $N_2H_4.H_2O$-d_6 (0.78 cm^3, ~16mmol) and D_2O (3.50 cm^3) as solvent. The product was filtered off under N_2, washed with D_2O, MeOH-d_1 and Et_2O and dried under a stream of N_2. Yield: 0.130 g (55.2% based on $CrCl_2$ taken).

c) Oxidation Titrimetric Analysis

Direct titration of a hydrazine-containing solution by $Ce(SO_4)_2$ failed to give the expected four electron oxidation change. Use of $K_3[Fe(CN)_6]$ as an oxidant was found to be satisfactory, the resulting $[Fe(CN)_6]^{4-}$ being back titrated with $Ce(SO_4)_2$.

Typical Experimental Procedure; To a sample containing ~10^{-3}M of N_2H_4 was added 0.5M $K_3[Fe(CN)_6]$ (15 cm^3) and 2M NaOH (15 cm^3) solutions. The resulting yellow solution was diluted with an equal volume of H_2O. Once all solids had dissolved and gas evolution ceased, the solution was acidified with a small excess of H_2SO_4. The resulting $[Fe(CN)_6]^{4-}$ was titrated with a standard solution of $Ce(SO_4)_2$, (standardised by acidic $(enH_2)SO_4.FeSO_4.4H_2O$ with ferroin as indicator; colour change is sharp from red to blue), using N-phenylanthranilic acid (0.5 cm^3) as indicator. The colour change is from green to brown-red.

e.g. $Cr(O_2CNHNH_2)_2.H_2O$,

i) $Cr(O_2CNHNH_2)_2.H_2O + 8Fe(CN)_6^{3-} \longrightarrow Cr^{2+} + 2N_2 + 8Fe(CN)_6^{4-} + H_2O + 6H^+ + 2CO_2$

ii) $Cr^{2+} + Fe(CN)_6^{3-} \longrightarrow Cr^{3+} + Fe(CN)_6^{4-}$

iii) $9Fe(CN)_6^{4-} + 9Ce^{4+} \longrightarrow 9Fe(CN)_6^{3-} + 9Ce^{3+}$

3.10.6 REACTIONS OF CHROMIUM(II) WITH $\overset{-}{O_2}CNHN\overset{+}{H}H_3$

a) Reaction of $[Cr(OH_2)_6]Br_2$ with $\overset{-}{O_2}CNHN\overset{+}{H}H_3$

An ethanolic solution of $[Cr(OH_2)_6]Br_2$ (4.5 mmol) was prepared by reacting electrolytic Cr metal (1.00 g) with aqueous HBr (1.06 cm^3, 9 mmol) in EtOH (9 cm^3) under N_2. This solution was added to $\overset{-}{O_2}CNHN\overset{+}{H}H_3$ (3.04 g, 40 mmol) under N_2/CO_2 at ~-10° (ice-

salt bath). The combined reaction mixture was stirred for 60 mins, before being allowed to warm to room temperature. The pale lilac product (with unreacted $\overset{-}{O_2}CNHN\overset{+}{H}H_3$) was filtered off under N_2 and dried under a stream of N_2. The product was identified as $[Cr(N_2H_4)_2Br_2]_n$ by IR spectroscopy.

The reaction was repeated as above but using aqueous conditions. On addition of $[Cr(OH_2)_6]Br_2$ to $\overset{-}{O_2}CNHN\overset{+}{H}H_3$, a dark lilac solid formed rapidly, with all $\overset{-}{O_2}CNHN\overset{+}{H}H_3$ consumed on warming to room temperature. The solid was filtered off under N_2, washed with deoxygenated H_2O and EtOH and dried under vacuum. The product was identified as $Cr(O_2CNHNH_2)_2.H_2O$ by IR spectroscopy.

b) Reaction of $Cr_2(O_2CMe)_4(H_2O)_2$ with $\overset{-}{O_2}CNHN\overset{+}{H}H_3$

$Cr_2(O_2CMe)_4(H_2O)_2$ was prepared as in SECTION 3.10.3d. To $Cr_2(O_2CMe)_4(H_2O)_2$ (1.00 g, 2.7 mmol) and $\overset{-}{O_2}CNHN\overset{+}{H}H_3$ (1.50 g, 19.8 mmol) under N_2 was added deoxygenated MeOH (50 cm^3). The reaction was sealed under N_2 and stirred at room temperature for 14 days, after which the resulting solid was allowed to settle for a futher 14 days. This product was filtered off under N_2, washed with deoxygenated MeOH and Et_2O and dried under a stream of N_2. The product was shown to be predominately $\overset{-}{O_2}CNHN\overset{+}{H}H_3$ by IR spectroscopy.

Reaction of $Cr_2(O_2CMe)_4(H_2O)_2$ (0.50 g, 1.3 mmol) and $\overset{-}{O_2}CNHN\overset{+}{H}H_3$ (0.75 g, 9.9 mmol) in deoxygenated MeOH (50 cm^3) under N_2 at 60° (oil-bath) for 8 hours, resulted in a pink-lilac solid which was shown to be mixture of $Cr(O_2CNHNH_2)_2.H_2O$ and $\overset{-}{O_2}CNHN\overset{+}{H}H_3$ by IR spectroscopy.

A repeat of the above reaction under reflux (65°) for 120 mins resulted almost exclusively in $Cr(O_2CNHNH_2)_2.H_2O$.

c) Reaction of $CrCl_2.2MeCN$ with $^{-}O_2CNHNH_3^{+}$

The complex $CrCl_2.2MeCN$ was prepared by reaction of $[Cr(OH_2)_6]Cl_2$ (14.5 mmol) (prepared by action of aqueous HCl (2.50 cm^3, 29 mmol) on Cr metal (1.00 g) in EtOH (12 cm^3)), with hot deoxygenated MeCN (30 cm^3). The resulting solution was heated under reflux for 30 mins, during which the product precipitated and was subsequently filtered off under N_2.

To a solution of $CrCl_2.2MeCN$ (~1.50 g, 7.3 mmol) in deoxygenated MeOH (40 cm^3) was added $^{-}O_2CNHNH_3^{+}$ (1.11 g, 14.6 mmol) under N_2 and the resulting solid was filtered off in air, washed with MeOH and dried under vacuum. The product was shown to be $[Cr(N_2H_4)_2Cl_2]_n$ by IR spectroscopy.

3.10.7 CHROMIUM(III) CARBAZATE CHEMISTRY

a) Preparation of $Cr(O_2CNHNH_2)_3.2H_2O$

An aqueous solution (75 cm^3) of N_2H_4 (17 cm^3, 531 mmol), was saturated with CO_2 for 60 mins while being heated to 80°. After this time an aqueous solution (5 cm^3) of $[Cr(OH_2)_4Cl_2]Cl.2H_2O$ (1.60 g, 6.0 mmol) was added dropwise. The resulting red solution was kept at 80° for 24 hrs, then cooling produced a pink microcrystalline precipitate. This was filtered off, washed with H_2O, EtOH and Et_2O and dried under vacuum.

Calc. for $C_3H_{13}CrN_6O_8$: C, 11.51; H, 4.18; N, 26.84; Cr, 16.60%. Found: C, 11.72; H, 3.93; N, 26.76; Cr, 16.26 %.

Crystalline $Cr(O_2CNHNH_2)_3.2H_2O$ can be prepared by increasing the Cr:$[N_2H_5][O_2CNHNH_2]$ ratio to ~1:50. A typical preparation; CO_2 is passed through a heated aqueous solution (75 cm^3) of N_2H_4 (25.00 cm^3, 789 mmol) for 120 mins. To the resulting

solution was added an aqueous solution (40 cm^3) of $[Cr(OH_2)_4Cl_2]Cl.2H_2O$ (1.60 g, 6 mmol) dropwise. A layer of EtOH (50 cm^3) was carefully placed above the aqueous solution. The red crystalline product formed at the solvent interface on leaving overnight.

b) Deprotonation of $Cr(O_2CNHNH_2)_3.2H_2O$ by Base

The complex $Cr(O_2CNHNH_2)_3.2H_2O$ (0.50 g, 1.6 mmol) was added to 2M aqueous NaOH (50 cm^3) to give a deep red solution. On standing, a dark green colouration rapidly developed. Addition of an aqueous solution of Me_4NCl (0.5 g, 4.6 mmol) gave no precipitate.

A similar result is obtained if $Me_4NOH.5H_2O$ replaces Me_4NCl.

CHAPTER No 4

REACTIONS OF PHENYLHYDRAZINE WITH CARBON DIOXIDE AND FIRST-ROW TRANSITION METAL IONS

REACTIONS OF PHENYLHYDRAZINE WITH CARBON DIOXIDE AND FIRST-ROW TRANSITION METAL IONS

Since its discovery by Emil Fischer in 1875, phenylhydrazine has generally been thought of as an exclusively organic reagent [230]. Its isolation provided the impetus for a revolution in the understanding of sugar chemistry in 1880's and it is still in routine use as a spot test for carbonyl functions.

However, soon after its isolation phenylhydrazine was reported to form coordination compounds with metal ions [231,232].

4.1 REACTIONS WITH CHROMIUM(II) HALIDES

Simple Lewis base behaviour of phenylhydrazine towards non-oxidising transition metal ions give complexes of stoichiometry $[MX_2(PhNHNH_2)_2]$ (M=Mn,Fe,Co,Ni,Zn,Cd; X=Cl or Br) [86]. As there have been no reports of chromium(II) phenylhydrazine complexes, attempts have been made to prepare the analogous $[CrX_2(PhNHNH_2)_2]$ species.

The reactions of $[Cr(OH_2)_6]X_2$ (X=Cl,Br) with $PhNHNH_2$ in ethanol-diethyl ether media under nitrogen produce the very air-sensitive pale blue complexes $[CrX_2(PhNHNH_2)_2]$.

$$Cr + 2\ HX_{(aq)} \xrightarrow[N_2]{EtOH} [Cr(OH_2)_6]X_2 \quad + 2PhNHNH_2 \xrightarrow[N_2]{Et_2O} [CrX_2(PhNHNH_2)_2] \qquad (4.1)$$

4.1.1 DIFFUSE REFLECTANCE ELECTRONIC SPECTRA

The liquid paraffin mull reflectance spectrum of $[CrCl_2(PhNHNH_2)_2]_n$ shows one broad absorption with a maximium at 704 nm, assignable to the $^5B_{1g} \rightarrow {}^5B_{2g}$, ^5E_g transition assuming a pseudo-octahedral environment for the metal, as dictated by Jahn-Teller distortion. The low intensity $^5B_{1g} \rightarrow {}^5A_{1g}$ transition was not observed below 1000 nm. The spectrum (and colour) of the complex is

unlike those of $[CrCl_2(NH_2NHR)_2]_n$ (R=H or Me) (see TABLE No 5.1) which contain bridging hydrazines and pseudo-square planar chromium(II) environments with additional very long metal-chlorine interactions. This may imply a change from bridging hydrazine to bridging halide in $[CrCl_2(PhNHNH_2)_2]_n$. The reflectance spectrum of $[CrBr_2(PhNHNH_2)_2]_n$ could not be recorded due to rapid surface oxidation.

4.1.2. MAGNETIC SUSCEPTIBILITY MEASUREMENTS

The magnetic susceptibility values of $[CrX_2(PhNHNH_2)_2]_n$ indicate high-spin d^4 configurations (see TABLE No 4.1).

TABLE No 4.1 Magnetic Susceptibility Measurements

Complex	χ_{cgx} / 10^{-6} cm^3g^{-1}	μ / BM	T / K
$[CrCl_2(PhNHNH_2)_2]_n$	25.58	4.59	296
$[CrBr_2(PhNHNH_2)_2]_n$	20.61	4.61	296

The magnetic moment values are somewhat lower than those displayed by monomeric high-spin octahedral chromium(II) complexes (~4.90 BM) and this may indicate some additional electron-electron interactions through the halide bridges or in view of the air-sensitivity of the complexes, partial oxidation of the samples taken during packing into tubes.

4.1.3 INFRA-RED SPECTRA

The infra-red spectra of $[CrX_2(PhNHNH_2)_2]_n$ (X=Cl,Br) are similar, probably indicating that the phenylhydrazine ligands show

the same mode of bonding behaviour in both complexes (see FIG No 4.1).

No detailed vibrational spectral analysis seems to have been reported for $PhNHNH_2$, either as a free base or as a ligand. Glass and McBreen reported [86] the preparation of $[MCl_2(PhNHNH_2)_2]_n$ (M=Mn,Co,Ni,Zn,Cd) but although an extensive infra-red analysis of these complexes was promised in a following publication, no such report subsequently appeared. Therefore the assignments proposed in this work are based on those of N_2H_4 [141,155] and $C_6H_5NH_2$ [233]. TABLE No 4.2 lists the vibrational spectral bands of $PhNHNH_2$ as a liquid film and in CCl_4 solution, while TABLE No 4.3 lists the infra-red spectra of $[CrX_2(PhNHNH_2)_2]_n$ (X=Cl and Br).

The strong absorptions at 3338 and 3303 cm^{-1}, for X=Cl and Br, respectively, are slightly lower in frequency than analogous bands shown by $PhNHNH_2$ (CCl_4 solution) and can be assigned to ν(NH) of the NH group adjacent to the phenyl ring. Greater low frequency shifts on complexation are exhibited by two absorptions at 3235, 3202 (X=Cl) and 3255, 3237 cm^{-1} (X=Br) and these may be assigned to $\nu(NH_2)$ of the coordinated NH_2- nitrogen. The greater reduction for the complex with X=Cl may be indicative of a stronger M-N bond in the chloride than in the bromide.

Those phenyl-derived vibrations that can positively be assigned show little change from their frequencies in the free base. No NH derived absorptions (apart from the stretching modes mentioned above) can be assigned. Regions where the NH vibrations of metal-hydrazine complexes are found contain only weak absorptions for the phenylhydrazine complexes, so correlations between $[CrX_2(PhNHNH_2)_2]_n$ and $[M(N_2H_4)_2X_2]_n$ are of no value.

TABLE No 4.2 Vibrational Spectral Bands of $PhNHNH_2$ / cm^{-1}.

Infra-red liquid film	Infra-red CCl_4 sol'n	Raman liquid	Assignment
3324 (s, br)	3399 (s) 3351 (m)		$\nu(NH) + \nu(NH_2)$
3194 (m)			
3084 (w)	3099 (w)		
3049 (m)	3056 (m)		$\nu(CH)$
3021 (m)	3026 (m)		
1617 (s, sh)			$\nu(C=C) + \delta(NH_2)$
1598 (vs)	1600 (vs)		
1492 (vs)	1492 (vs)		
1428 (w)	1420 (mw)		$\nu(C=C)$
1304 (s)	1304 (s)		
1262 (s)	1262 (s)		$\nu(CN)$
1178 (s)	1178 (s)		
1154 (m)	1154 (m)		
1137 (mw)	1131 (m)		$\delta(CH)_{in\text{-}plane}$
1073 (m)	1073 (m)		
1025 (m, sh)	1024 (m)	1028 (m)	
993 (m, sh)	993 (mw)	995 (vs)	ring-breathing
884 (s)			X-sensitive, in-
824 (m, br)	obscured		plane ring def. ?
758 (vs)			
699 (vs)	695 (s) 680 (vs)		$\delta(CH)_{out\text{-}of\text{-}plane}$
563 (m, br)			t ?
515 (s)			X-sensitive in- y ? plane and out- plane ring defs
453 (w)			u ?

TABLE No 4.3 Liquid Paraffin Mull Infra-red Spectra of $[CrX_2(PhNHNH_2)_2]_n$ (X=Cl and Br) / cm^{-1}.

$[CrCl_2(PhNHNH_2)_2]_n$	$[CrBr_2(PhNHNH_2)_2]_n$	Assignment
3338 (s)	3303 (s)	ν(NH)
3235 (s)	3255 (m)	$\nu(NH_2)$
3202 (m)	3237 (m)	
3101 (m)	3079 (mw)	ν(CH)
3083 (m)		
1595 (s)	1602 (m)	
	1594 (s)	ν(C=C) + $\delta(NH_2)$
	1589 (s)	
1499 (s)	1494 (s)	ν(C=C)
1269 (vs)	1265 (s)	ν(CN)
1217 (w)	1212 (w)	
1168 (w)	1158 (vw)	
1156 (w)	1150 (vw)	$\delta(CH)_{in\text{-}plane}$
1080 (w)	1076 (w)	
1022 (w)	1015 (w)	
894 (w)	879 (mw)	X-sensitive
855 (w)	856 (w, br)	bends ?
757 (s)	754 (s)	$\delta(CH)_{out\text{-}of\text{-}plane}$
697 (vs)	687 (vs)	
603 (mw)	601 (w)	
511 (s)	505 (s)	X-sensitive in-
487 (w, sh)	478 (mw)	plane bands ?
390 (w)	393 (w)	ν(MN)
323 (s)		ν(MCl)
268 (w)	287 (w)	X-sensitive bands ?
223 (s)		δ(ClMCl) ?

FIGURE No 4.1 Infra-red Spectra of $[CrX_2(PhNHNH_2)_2]_n$ (X=Cl and Br) and $Cr_2(O_2CMe)_4(PhNHNH_2)_2$.

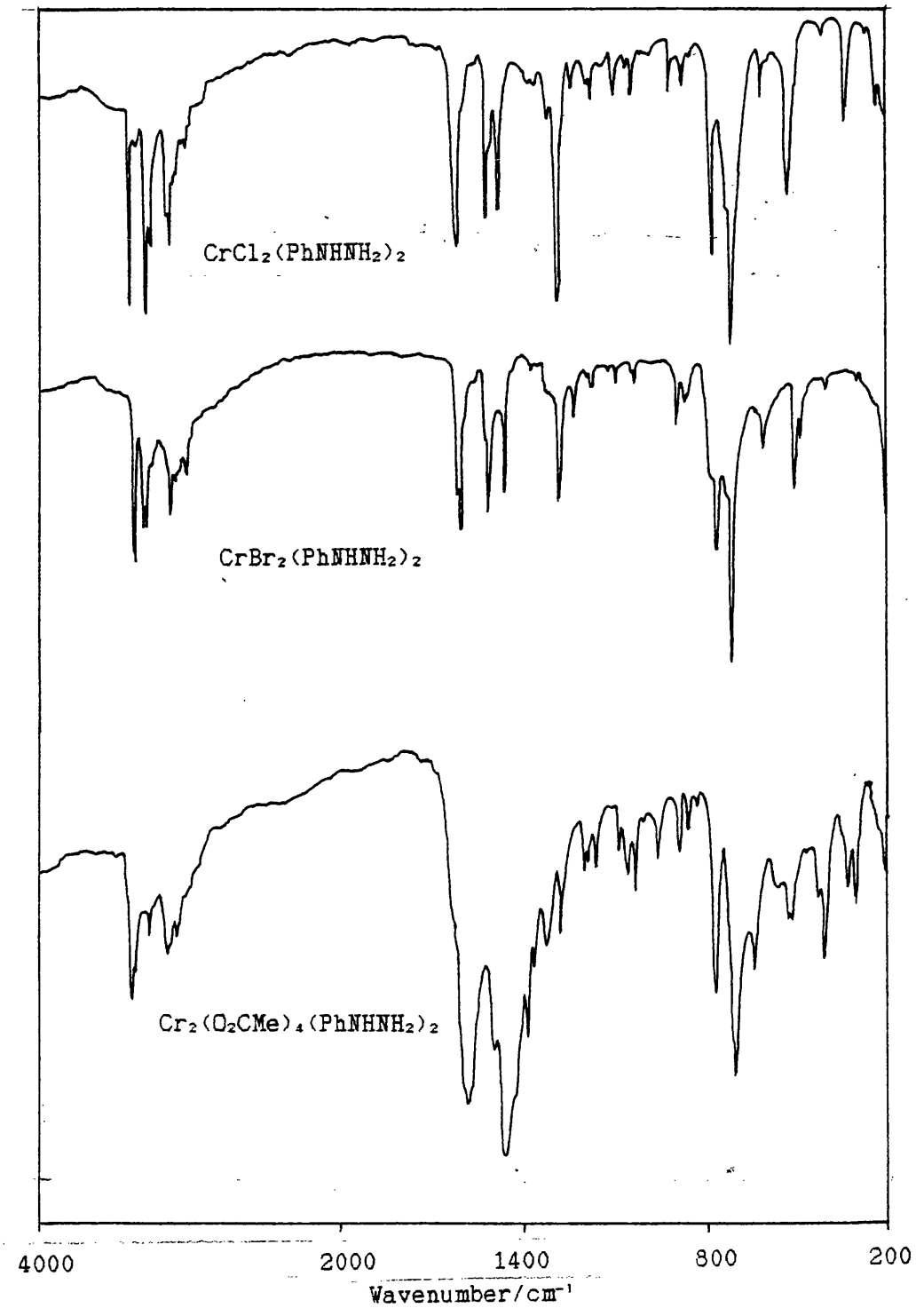

The chloride $[CrCl_2(PhNHNH_2)_2]_n$ exhibits two strong absorptions at 323 and 223 cm^{-1}, (metal-chlorine stretches in $[M(N_2H_4)_2Cl_2]_n$ appear below 250 cm^{-1} due to their weakness - see SECTION 2.3), with no counterparts in the IR spectrum of $[CrBr_2(PhNHNH_2)_2]_n$. They can therefore be assigned to ν(MCl) and δ(ClMCl) modes, respectively. Group theory predicts, one IR active ν(MX) and one IR active ν(ML) for a *trans*-MX_4L_2 octahedral system, which would appear to confirm the assignment. This implies that the Cr-Cl bonds are stronger than those found in $[M(N_2H_4)_2Cl_2]_n$ and possibly terminally bonded. However, in pseudo-octahedral $[MnCl_2(PhNH_2)_2]_n$, ν(MCl) is found at 318 cm^{-1} and bridging chlorides are thought to be present [234]. Also metal-ligand vibrations in chromium(II)-hydrazine complexes appear at higher frequencies than for other analogous first-row transition metal complexes. In $[Cr(N_2H_4)_2Cl_2]_n$ ν(MN) appears at 427 and 346 cm^{-1} compared with 344 cm^{-1} for $[Mn(N_2H_4)_2Cl_2]_n$ and 388, 347 cm^{-1} for $[Zn(N_2H_4)_2Cl_2]_n$. Therefore although the observed ν(MCl) in $[CrCl_2(PhNHNH_2)_2]_n$ is in a region where terminal metal-chloride stretches are expected, no definite structural conclusions can be made.

Weak absorptions present at 390 and 393 cm^{-1} (Cl and Br, respectively) have been tentatively assigned to ν(MN). These compare with ν(MN) displayed by $[Cr(N_2H_4)_2X_2]_n$ (X=Cl,Br) at 427, 346 and 420, 388 cm^{-1} respectively. These values can also be compared with ν(MN) of $ZnCl_2(PhNH_2)_2$ at 406 and 366 cm^{-1} [234].

From the spectral data available it is not possible to conclusively assign a molecular structure to $[CrX_2(PhNHNH_2)_2]_n$ (X=Cl,Br), but from a consideration of the coordination potential of $PhNHNH_2$, it is probable that the complexes exhibit a halide-

bridged polymeric structure with unidentate phenylhydrazine ligands (see FIG No 4.2).

FIGURE No 4.2 Possible Molecular Structure of $[CrX_2(PhNHNH_2)_2]_n$.

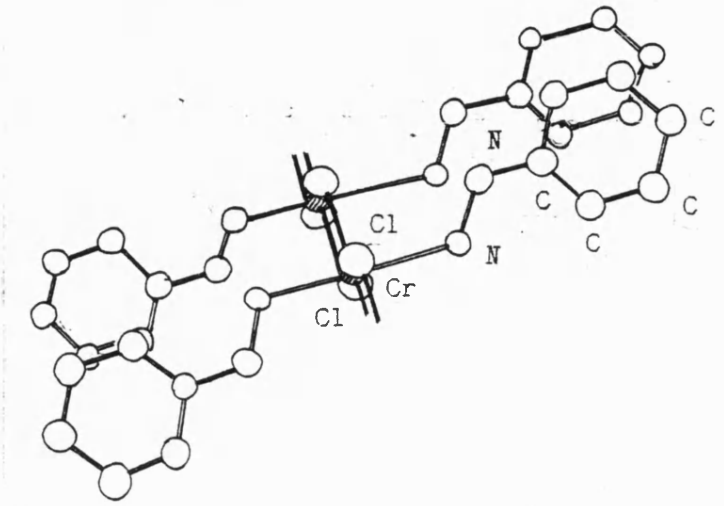

4.2 REACTION WITH CHROMIUM(II) ACETATE

The reaction of $Cr_2(\mu\text{-}O_2CMe)_4(H_2O)_2$ with $PhNHNH_2$ in ethanol under dinitrogen results in the formation of air-sensitive, pale orange, $Cr_2(\mu\text{-}O_2CMe)_4(PhNHNH_2)_2$. The complex is moderately soluble in MeOH and EtOH.

$$Cr_2(O_2CMe)_4(H_2O)_2 + 2PhNHNH_2 \xrightarrow[N_2]{EtOH} Cr_2(O_2CMe)_4(PhNHNH_2)_2 \qquad (4.2)$$

The essential diamagnetism ($\chi_{corr} = -1.42\times10^{-6}$ cm^3g^{-1}, $\mu_{eff} = 0.39$ BM per Cr at 295K) and the electronic spectrum (see TABLE No 4.4) indicates the retention of a quadruple metal-metal bond between the two chromium(II) atoms in a dinuclear arrangement.

The $np_x \rightarrow \pi^*$ band is observed only as a shoulder (in comparison with other $Cr_2(O_2CMe)_4L_2$ species in which the band is resolved), on the low-frequency side of an intense absorption band relating to a $\pi \rightarrow \pi^*$ transition of coordinated phenylhydrazine.

TABLE No 4.4 Electronic Spectrum of $Cr_2(\mu\text{-}O_2CMe)_4(PhNHNH_2)_2$ / nm.

MeOH solution	Liquid paraffin mull	Assignment
476 (m,br)	475 (m,br)	$\delta \rightarrow \pi^*$
	462 (m,br)	
346 (m,sh)	358 (m,sh)	
324 (vs,sh)	330 (m,sh)	$np_x \rightarrow \pi^*$
	312 (s,sh)	
	265 (vs,br)	$\pi \rightarrow \pi^*$ ($PhNHNH_2$)

The $\delta \rightarrow \pi^*$ transition of $Cr_2(\mu\text{-}O_2CMe)_4(PhNHNH_2)_2$ with a maximium at 475 nm is comparable to the analogous transition of $[Cr_2(\mu\text{-}O_2CMe)_4(\mu\text{-}N_2H_4)]_n$ occurring at 478 nm.

The infra-red spectrum of $Cr_2(\mu\text{-}O_2CMe)_4(PhNHNH_2)_2$ indicates the presence of both coordinated acetate and phenylhydrazine (see FIG No 4.1). The absorptions at 3358, 3330 and 3239 cm^{-1} are assignable to NH stretching vibrations, the latter being specifically assigned to $\nu(NH_2)$ of the terminally coordinated nitrogen, in view of the greatest shift from $\nu(NH_2)$ of free $PhNHNH_2$ (3324 cm^{-1}).

The phenyl and acetate derived absorptions are found in characteristic positions when considered alongside the vibrational spectra of $[CrX_2(PhNHNH_2)_2]_n$ (X=Cl,Br) and $Cr_2(\mu\text{-}O_2CMe)_4L_2$ (L=OH_2, ½(N_2H_4)) (see TABLE No's 3.5 and 4.3) and are assigned in TABLE No 4.5.

The majority of the NH derived absorptions, as for other phenylhydrazine complexes are not simple and remain, at present, unassignable. Bands assigned to $\nu(CrN)$ seem to occur at higher wavenumbers in metal-metal bonded species than in mononuclear species (i.e. $\nu(CrN)$; $Cr_2(\mu\text{-}O_2CMe)_4(NH_3)_2$ = 475 cm^{-1}; $[Cr_2(\mu\text{-}O_2CMe)_4(\mu\text{-}N_2H_4)]_n$ = 469 cm^{-1}; $[Cr(N_2H_4)_2Cl_2]_n$ = 427,346 cm^{-1}; $[CrCl_2(PhNHNH_2)_2]_n$ = 390 cm^{-1}). In $Cr_2(\mu\text{-}O_2CMe)_4(PhNHNH_2)_2$, two bands

at 427 and 401 cm^{-1} can tentatively be assigned to ν(CrN), lower than found in comparable $Cr_2(O_2CMe)_4L_2$ complexes. This may be an indication of weak metal-nitrogen bonding, possibly due to the electron-withdrawing effect of the phenyl ring of phenylhydrazine.

The complex $Cr_2(\mu\text{-}O_2CMe)_4(PhNHNH_2)_2$ is therefore likely to contain unidentate phenylhydrazine ligands, bonded axially to a $Cr_2(O_2CMe)_4$ unit (see FIGURE No 4.3).

FIGURE No 4.3 Possible Structure of $Cr_2(O_2CMe)_4(PhNHNH_2)_2$.

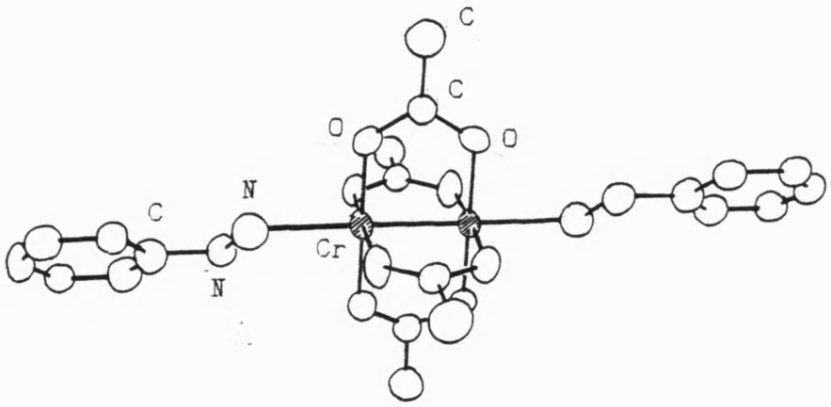

TABLE 4.5 Infra-red Spectrum of $Cr_2(\mu\text{-}O_2CMe)_4(PhNHNH_2)_2$ (major bands) / cm^{-1}.

Band maximium	Relative intensity	Tentative Assignment
3358	s	ν(NH)
3330	ms	
3239	m	$\nu(NH_2)$
1589	vs, sh	
1573	vs, br	$\nu_a(CO_2)$ +
1558	vs, sh	$\delta(NH_2)$ + ν(C=C)
1487	s	ν(C=C)
1455	vs, sh	$\nu_s(CO_2)$
1446	vs, br	
1346	m	$\delta(CH_3)$
1266	m	ν(CN)
1155	w	$\delta(CH_3)$
1150	w	
1051	w, sh	r(CH_3)
1044	mw	
945	w	ν(CC)
759	m	δ(CH)
755	m	
701	ms, sh	δ(OCO) + δ(CH)
688	s	
632	m	π(COO)
519	mw	r(COO) ?
508	mw	
427	w	ν(MN)
401	ms	
323	w	ν(MO)
299	mw	

This work shows that the $Cr_2(O_2CMe)_4$ unit can be used as an effective probe of the coordination abilities of hydrazines. Hydrazine itself bridges between two $Cr_2(O_2CMe)_4$ units as expected, while phenylhydrazine acts only as a unidentate ligand, again as expected from the arguments presented in SECTION 1.4.3.

4.3 REACTIONS OF PHENYLHYDRAZINE WITH CARBON DIOXIDE

Shortly after Fischer reported the preparation of $PhNHNH_2$ in 1875 [230], he described in 1878 the preparation of 'phenylcarbazic acid phenylhydrazine', from the reaction of $PhNHNH_2$ with CO_2 [142]. Later work by Stern [143] showed that potassium phenylcarbazate could be obtained by treatment of phenylcarbazic acid with KOH. Later workers have added little of significance to what was already known about the $PhNHNH_2$-CO_2 system.

Milla *et al.* [235] found that $PhNHNH_2$ reacted with CO_2 in the pH range 5.95-8.25, each mole of $PhNHNH_2$ taking up 0.25 moles of CO_2. Frances, within an extensive investigation of binary and tertiary systems with CO_2, found that $PhNHNH_2$ formed a salt on reaction [236]. Morrow, Keim and Gurd, as part of a study of the binding strengths of CO_2 to amino acids in D_2O solution, recorded the ^{13}C nmr signal of the carboxylate carbon of phenylcarbazate [237].

The use of phenylcarbazate as a ligand towards transition metal ions has been reported by Srivastava. A series of complexes containing Cr(III) [146], Co(II) [147], Ni(II) [145] and Cu(II) [117] have been claimed. Our interest in the ligating ability of the phenylcarbazate anion was stimulated by the failure to repeat the preparation of chromium(III) phenylcarbazate [146]. Also, it was hoped that metal phenylcarbazates could be prepared which would

retain the structural features of unsubstituted metal carbazates but advantageously display sufficient solubility for solution studies and single crystal formation after recrystallisation from an appropriate solvent.

4.3.1 PHENYLHYDRAZINIUM PHENYLCARBAZATE

The passage of CO_2 into or even over a methanolic solution of $PhNHNH_2$ causes the precipitation of colourless $[PhNHNH_3]$-$[PhNHNHCO_2]$. The yield can be improved by cooling the resultant filtrate to produce the compound as colourless platelets.

The salt is air-sensitive, decomposing in a manner similar to that of phenylhydrazine, after exposure to air for several minutes. It is moderately soluble in MeOH and DMSO, but less so in EtOH or solvents of lower polarity.

In some respects the infra-red spectrum is not of the form that might be expected assuming the presence of the ion-pair $[PhNHNH_3][PhNHNHCO_2]$ (see FIG No 4.4). Thus, absorptions present in the IR spectrum of $PhNHNH_3Cl$ (see FIG No 4.4) which are assignable to $PhNHNH_3^+$ are absent. In fact, overlaying the expected spectrum of $PhNHNHCO_2^-$, is a profile more associated with $PhNHNH_2$ than with $PhNHNH_3^+$.

Two absorptions at 3340 and 3230 cm^{-1} can be assigned to ν(NH) as expected (two absorptions for $PhNHNHCO_2^-$ and one for $PhNHNH_2$, the latter overlapping the second phenylcarbazate absorption). The hydrogen-bonded absorption appears at 2660 cm^{-1} as would be expected for $PhNHNH_3^+$ although it is very much broader than the analogous band of $PhNHNH_3Cl$. In the fingerprint region (1300-650 cm^{-1}), the $\delta(CH)_{out\text{-}of\text{-}plane}$ bands expected for $PhNHNH_3^+$ are absent, the absorptions that do appear being very intense relative to the

FIGURE No 4.4 Infra-red Spectra of $PhNHNH_2$, $PhNHNH_3Cl$, $PhNHNHCO_2Na$ and $PhNHNHCO_2H.PhNHNH_2$.

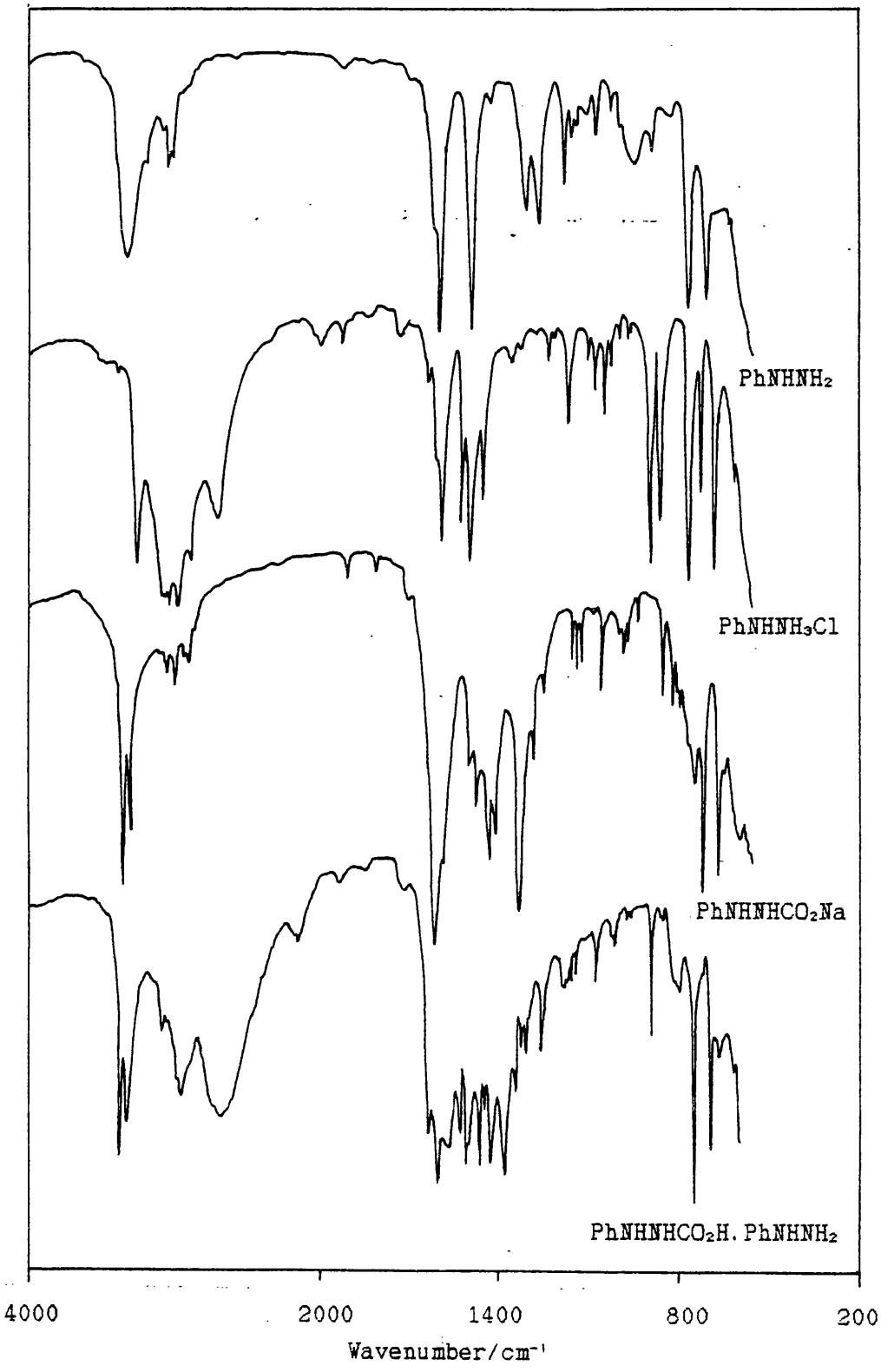

$\nu(CO_2)+\delta(NH_2)$ coincident band, indicating that the intensities of the $\delta(CH)$ bands are enhanced due to the presence of two similar species, i.e. $PhNHNHCO_2^-$ and $PhNHNH_2$ exhibiting $\delta(CH)$ at very similar frequencies.

Analysis of the IR spectrum indicates that more association is present than would be expected for an individual ion-pair. The extreme situation could be described as the removal of a proton from the phenylhydrazinium cation and its transfer to the phenylcarbazate anion, leading to the formulation as the $PhNHNH_2$ adduct of phenylcarbazic acid (see FIG No 4.5). In the solid state, considerable intermolecular hydrogen-bonding will also undoubtedly be present in the crystal lattice.

FIGURE No 4.5

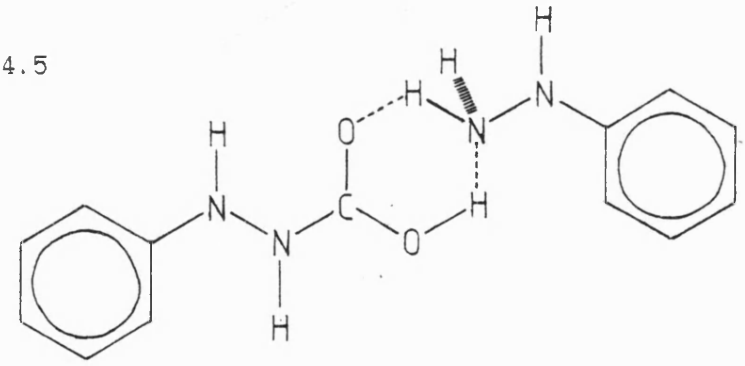

In the negative ion FAB mass spectrum of $PhNHNHCO_2H.PhNHNH_2$ (see TABLE No 4.8) the most prominent m/z peak corresponds to $PhNHNHCO_2^-$. The lack of detectable multimolecular species (unlike the alkali metal phenylcarbazates - see SECTION 4.4) is indicative of a much less strongly intermolecular bound structure. This could explain the observed differences in atmospheric stability between $PhNHNHCO_2H.PhNHNH_2$ itself and the alkali metal phenylcarbazates. The detection of several ions assignable to fragments derived from $PhNHNHCO_2H.PhNHNH_2$ rather than from $[PhNHNH_3][PhNHNHCO_2]$ is in agreement with IR and conductiometric results (see TABLE 4.9), both

of which favour an adduct rather than an ionic formulation. Further properties of $PhNHNHCO_2H.PhNHNH_2$ are discussed below alongside those of the alkali metal phenylcarbazates.

4.4 ALKALI METAL PHENYLCARBAZATES

The passage of CO_2 through an alcoholic solution of an alkali metal alkoxide and $PhNHNH_2$ results in the precipitation of $PhNHNHCO_2M$ (M=Li,Na,K) (4.3).

$$PhNHNH_2 + MOR \xrightarrow[CO_2]{ROH} PhNHNHCO_2M \quad M=Li,Na,K \quad R=Me \text{ or } Et \qquad (4.3)$$

Only the potassium salt had been reported previously [143], but no more than its preparation and analysis were described.

These colourless compounds are more resistant towards atmospheric decomposition than $PhNHNHCO_2H.PhNHNH_2$, surviving for several weeks without appreciable discoloration. The compounds are sparingly soluble in MeOH, but such solutions undergo rapid decomposition and oxidation on atmospheric exposure at room temperature. However, dissolution of the sodium salt in MeOH followed by reprecipitation by the addition of diethyl ether shows that the alkali metal carbazates display a reasonable solution stability in methanol solution if kept at low temperatures (<0°) and under an inert atmosphere (preferably CO_2).

Three different preparative procedures have been utilised to prepare $PhNHNHCO_2M$ (M=Li,Na,K).

a) A MeOH solution of the alkali metal methoxide was generated by reaction of the metal with anhydrous MeOH. To this solution was added $PhNHNH_2$ and then CO_2 introduced (4.4).

b) A MeOH solution of the alkali metal hydroxide was prepared, $PhNHNH_2$ added and then CO_2 introduced (4.5).

c) An EtOH solution of the alkali metal ethoxide was generated by reaction of the metal with anhydrous EtOH. To this solution was added freshly prepared $PhNHNHCO_2H.PhNHNH_2$ (4.6).

$$MeOH + M \xrightarrow[N_2]{MeOH} MeOM + \tfrac{1}{2}H_2 \xrightarrow[CO_2]{PhNHNH_2} PhNHNHCO_2M + MeOH \qquad (4.4)$$

$$MeOH + MOH \xrightarrow[N_2]{MeOH} MeOM + H_2O \xrightarrow[CO_2]{PhNHNH_2} PhNHNHCO_2M + MeOH \qquad (4.5)$$

$$EtOH + M \xrightarrow[N_2]{EtOH} EtOM + \tfrac{1}{2}H_2 \xrightarrow[CO_2]{PhNHNHCO_2H,PhNHNH_2} PhNHNHCO_2M + EtOH + PhNHNH_2 \qquad (4.6)$$

$PhNHNHCO_2Li$ was prepared only by route (a), while pure $PhNHNHCO_2K$ was prepared only by route (c). The potassium product obtained by method (b) was characterised as $PhNHNHCO_2K.H_2O$ by elemental analysis. $PhNHNHCO_2Na$ was prepared by all three routes.

An occasional by-product in these reactions is the formation of organic carbonate species from the reaction of the alkoxide and carbon dioxide (4.7).

$$ROM + CO_2 \longrightarrow R\text{-}CO_3M \qquad (4.7)$$

4.4.1 INFRA-RED SPECTRA

The infra-red spectra of $PhNHNHCO_2M$ are very similar with only slight differences, presumably resulting from solid state packing changes on increasing the ionic radius from Li^+ to K^+ (see FIG No 4.4 for the IR spectrum of $PhNHNHCO_2Na$).

TABLE No 4.7 Vibrational Spectra of $PhNHNHCO_2K$ (major absorptions) / cm^{-1}.

Infra-red	Raman	Assignment
	3385 (w)	
	3263 (w)	
	3344 (w)	ν(NH)
3331 (m)	3329 (w)	
3272 (m)		
3056 (w)	3955 (vs)	ν(CH)
1608 (vs)	1595 (s)	$\nu_a(CO_2)+\nu$(C=C)
1494 (m)		
1488 (m)	1487 (w)	
1456 (m, br)		ν(C=C)
1439 (ms, sh)		
1431 (ms)		
1361 (s)		
1345 (s)	1339 (w)	$\nu_s(CO_2)$?
1324 (w, sh)		
1306 (ms)		ν(CN)
1275 (w)		
1263 (w)	1248 (w, br)	
1174 (w)	1168 (mw)	
1158 (vw)		
1154 (vw)	1153 (mw, sh)	
1079 (w)	1071 (w, br)	
1023 (w)	1022 (s)	$\delta(CH)_{out\text{-}of\text{-}plane}$
1014 (w)		
994 (w)	993 (vs)	$\delta(CH)_{out\text{-}of\text{-}plane}$
759 (s)	756 (w)	$\delta(CH)_{in\text{-}plane}$
702 (s)		
	608 (w)	π(COO) ?
	567 (vw)	r(COO) ?

Two bands assignable to ν(NH) appear in the 3500-3200 cm^{-1} region for $PhNHNHCO_2M$ (M=Na and K), while these absorptions are split into four components in $PhNHNHCO_2Li$. This may reflect either stronger intermolecular bonding in $PhNHNHCO_2Li$, as indicated by its

greater atmospheric stability, or the presence of two or more distinct molecular conformations within the crystal lattice.

This additional complexity is mirrored in the $\nu_s(CO_2)$ region between 1640-1600 cm^{-1}. Thus, $PhNHNHCO_2Li$ displays a complex band pattern, while $PhNHNHCO_2M$ (M=Na or K) show a single strong band.

Band assignment within the fingerprint region (1350-650 cm^{-1}) is difficult due to the variety and generally weak intensities of the absorptions. As noted previously, no complete vibrational assignment for $PhNHNH_2$ has been made and extrapolation to $PhNHNHCO_2^-$ is therefore open to uncertainty.

TABLE No 4.7 shows the IR and Raman spectra of $PhNHNHCO_2K$ as typical of the $PhNHNHCO_2M$ group, with provisional assignments of selected absorptions based on the $PhNHNH_2$ assignments of SECTION 4.1.3. FIGURE No 4.4 shows the IR spectra of $PhNHNHCO_2M$ in comparison with those of $PhNHNHCO_2H.PhNHNH_2$ and $PhNHNH_3Cl$.

4.4.2 FAST ATOM BOMBARDMENT MASS SPECTRA

The FAB mass spectra of $PhNHNHCO_2M$ (M=Li, Na, K, $PhNHNH_3$) have been recorded using a glycerol matrix. Additionally, 70eV EI and CI techniques on $PhNHNHCO_2Na$ were found to yield no extra useful information and resulted in cleavage of the N-N bonds of the carbazate generating PhNH- type fragments.

In contrast to $PhNHNHCO_2H.PhNHNH_2$, FAB spectra of the alkali metal salts show significant proportions of negative ions of m/z greater than one molecular unit indicating the presence of polymeric ions in the vapour phase.

The positive ion FAB spectrum of $PhNHNHCO_2H.PhNHNH_2$ showed only the presence of $PhNHNH_3^+$ and species derived from it. The (+)FAB spectra of the other phenylcarbazate salts, however, show

TABLE No 4.8 Negative Ion FAB Mass Spectra of $PhNHNHCO_2M^a$

M = Li	m/z	I %	Possible species
	91	55	[glycerol-H]$^-$
	97	85	[glycerol-2H+Li]$^-$
	151	100	[Phcbz]$^-$
	157	90	[PhcbzLi-H]$^-$
	217	25	
	249	50	[PhcbzLi+glycerol-H]$^-$
	309	50	[PhcbzLi+Phcbz]$^-$
	315	45	[2×PhcbzLi-H]$^-$
	401		[PhcbzLi+Phcbz+glycerol]$^-$
	407		[2×PhcbzLi+glycerol-H]$^-$
	467		[2×PhcbzLi+Phcbz]$^-$
	473		[3×PhcbzLi-H]$^-$
	631		[4×PhcbzLi-H]$^-$

NOTE Background glycerol matrix spectrum was not subtracted as no lithium correlation data was available

M = Na	m/z	I %	Possible species
	107	35	[PhNHNH]$^-$
	113	22	[glycerol-2H+Na]$^-$
	123	21	[PhNHNHCO]$^-$
	151	50	[Phcbz]$^-$
	172	30	[PhcbzNa-2H]$^-$
	173	100	[PhcbzNa-H]$^-$
	216	20	
	277	19	[PhcbzH+PhNHNHCO]$^-$
	303	22	[2×Phcbz+H]$^-$
	325	53	[PhcbzNa+Phcbz]$^-$
	347	28	[2×PhcbzNa-H]$^-$
	369	45	[2×PhcbzNa-2H+Na]$^-$
	521	32	[3×PhcbzNa-H]$^-$
	543	20	[3×PhcbzNa-2H+Na]$^-$
	673		[4×PhcbzNa-Na]$^-$
	695		[4×PhcbzNa-H]$^-$
	717		[4×PhcbzNa-2H+Na]$^-$
	847		[5×PhcbzNa-Na]$^-$
	869		[5×PhcbzNa-H]$^-$
	891		[5×PhcbzNa-2H+Na]$^-$

M = K	m/z	I %	Possible species
	91	35	[glycerol-H]$^-$
	107	60	[PhNHNH]$^-$
	133	30	
	151	100	[Phcbz]$^-$
	189	60	[PhcbzK-H]$^-$
	341	40	[2×Phcbz+K]$^-$
	379	22	[2×PhcbzK-H]$^-$
	417	48	[2×PhcbzK-2H+K]$^-$
	460		
	498		
	569		[3×PhcbzK-H]$^-$
	607		[3×PhcbzK-3H+2K]$^-$

M = $PhNHNH_3$	m/z	I %	Possible species
	151	100	[Phcbz]$^-$
	179	23	
	243	55	[Phcbz+glycerol]$^-$
	267		
	268		
	271		
	277		
	285		
	289		
	301		[2×Phcbz-H]$^-$
	303		[2×Phcbz+H]$^-$
	325		
	333		
	334		
	335		
	339		
	351		[PhcbzH.$PhNHNH_2$+glycerol-H]$^-$

NOTE * - All peaks lacking an I % value are > 10 % in intensity

Phcbz = $PhNHNHCO_2^-$

the presence of multimolecular positive ions. Commonly observed species are of the types [nPhNHNHNHCO$_2$M + M]$^+$ and [nPhNHNHNHCO$_2$M + M + glycerol]$^+$ where n = 1,2 for M=Li and n = 1,2,3 for M= Na,K.

TABLE No 4.8 lists the ions observed in the (-)FAB spectra of $PhNHNHCO_2M$ (M=Li,Na,K,$PhNHNH_3$) with possible formulae relating to the m/z values.

For M=Li and K, the parent (-)FAB peak is 151 m/z ($PhNHNHCO_2^-$) while for M=Na, it is 173 m/z ($[PhNHNHCO_2Na-H]^-$). Other prominent species indicate the presence of multimolecular negative ions in the vapour phase, as also shown by the (+)FAB spectra. Tetra- and pentanuclear species are detected in the M=Li and Na spectra, while trinuclear species appear in the M=K spectrum (see TABLE No 4.8). This apparent decrease in intermolecular bonding is mirrored by the decrease in atmospheric stability from Li to K.

4.4.3 CONDUCTIOMETRIC STUDIES

To complement the solid state characterisation, conductivities of the phenylcarbazate salts were measured in methanol. Because only a few conductivities have been reported in this solvent [238], the conductivities of a number of standards were also measured to define a range for 1:1 electrolytes (see TABLE No 4.9) at a concentration of approximately $10^{-3}M$.

From a consideration of the conductivities of the standards a reasonable average value for a 1:1 electrolyte was 102 $\Omega^{-1}cm^2mol^{-1}$. A particularly low Λ_M value is shown by Ph_4BNa, due to the low mobility associated with the Ph_4B^- anion.

The salts $PhNHNHCO_2M$ show increasing Λ_M values from M = Li to K reflecting a variation in the strength of association and the tendency to dissociate into discrete ions in solution. Certainly lower mobilities are expected for associated species compared with monomeric ones and all three alkali metal salts show lower Λ_M values than expected for simple 1:1 electrolyte behaviour. Only $PhNHNHCO_2K$ shows a Λ_M value close to that expected for a fully dissociated monomeric species. It is probable that the lower Λ_M values of $PhNHNHCO_2M$ (M=Na,Li) reflect the expected greater

covalent character between ion pairs on decreasing the size of the cation.

$PhNHNHCO_2H.PhNHNH_2$ effectively shows non-electrolyte behaviour in methanol, indicating that only a small proportion of $[PhNHNH_3][PhNHNHCO_2]$ can be present. This confirms the conclusion drawn from vibrational spectroscopic evidence, that this compound is best considered as a molecular adduct, rather than an ionic species.

$PhNHNH_3Cl$ also shows a low Λ_M value in methanol indicating only partial dissociation into ions. The ion-pair is expected to be strongly associated, in line with solid state evidence which indicates the presence of strong -N-H---Cl hydrogen-bonding.

TABLE No 4.9 Conductiometric Measurements of $PhNHNHCO_2M$ in MeOH

Compound	Molarity / 10^{-3} M	Λ_M / $\Omega^{-1}cm^2mol^{-1}$
Me_4NI	1.050	126.7
Me_4NBr	0.857	117.0
$NaBPh_4$	1.026	79.5
KI	1.018	113.0
$PhNHNH_3Cl$	1.065	78.5
$PhNHNHCO_2Li$	0.860	76.7
	1.102	64.6
$PhNHNHCO_2Na$	0.471	84.3
	0.856	83.5
$PhNHNHCO_2K$	1.104	99.7
$PhNHNHCO_2H.PhNHNH_2$	1.137	5.4

4.4.4 ^{13}C NMR SPECTROSCOPY

To give further indications of solution stability, the ^{13}C nmr spectra of $PhNHNHCO_2M$ (M=Li,Na,K,$PhNHNH_3$) were recorded in MeOH-d_4 solution under N_2 (see TABLE No 4.10).

When the spectra of the M=Li,Na,K and M=$PhNHNH_3$ samples are compared, it is apparent that the solution behaviour is not identical for all the salts. The phenylhydrazinium salt, better regarded as the adduct $PhNHNHCO_2H.PhNHNH_2$ as discussed earlier, decomposes in methanol at room temperature. Only one set of phenyl resonances are observed whereas two would be expected. Overall the spectrum is similar to that of $PhNHNH_2$ both in chemical shift values and relative intensities. After one month in solution the ^{13}C nmr spectrum of $PhNHNHCO_2H.PhNHNH_2$ contains some additional minor signals indicating futher decomposition.

The ^{13}C nmr spectra of the alkali metal salts each display two sets of phenyl signals. A comparison of intensity ratios shows, however, that the assignment of these resonances is not consistent from one metal salt to another. For M = Li and K, the relative intensities of the $C_{3,5}$ and $C_{2,6}$ signals are reversed and furthermore the intensity ratio profile for the sodium salt is considerably different to those of the other salts.

It is possible that either partial decomposition to the species present in $PhNHNHCO_2H.PhNHNH_2$/MeOH solutions has occurred or two conformationally different phenylcarbazate species are present.

The carboxylate carbon (C_7) has only been detected for $PhNHNHCO_2K$, as a very weak signal, as expected for a quaternary carbon. The chemical shifts of 214.6 and 200.1 ppm can be compared to 222 ppm reported for C_7 when $PhNHNH_2$ was reacted with $^{13}CO_2$ in

D_2O [237]. The lack of signals assignable to C_7 in the spectra of $PhNHNHCO_2M$ (M=Li and Na) can be attributed to the higher solubility of $PhNHNHCO_2K$.

TABLE No 4.10 ^{13}C nmr MeOH-d_4 Solution Spectra of $PhNHNHCO_2M$ / ppm

$PhNHNHCO_2M$, M =	Li	Na	K	$PhNHNH_3$	$PhNHNH_2$	Assignment
			214.6			C_7
			200.1			
	153.1		153.0		152.9	C_1
		151.7	151.6	152.5		
	129.9	129.9	129.9		129.9	$C_{3,5}$
	129.7	129.7	129.8	129.6		
	120.2	120.2	120.3			C_4
	120.1		120.1	120.0	120.1	
	113.8	113.8	113.8			$C_{2,6}$
	113.7		113.7	113.5	113.6	

NOTE: Spectra referenced to TMS

Assignments refer to 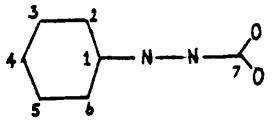

The above results imply that the solution behaviour of the alkali metal phenylcarbazate salts is clearly not straightforward. In particular when undertaking solution reactions the instability of $PhNHNHCO_2H.PhNHNH_2$ must be taken into account.

4.5 REACTIONS OF THE PHENYLCARBAZATE ANION WITH FIRST-ROW TRANSITION METAL CATIONS

Srivastava has reported the reactions of $PhNHNHCO_2H.PhNHNH_2$ with chromium(III) [146], cobalt(II) [147], nickel(II) [145] and copper(II) [117]. In each case the isolation of metal-phenylcarbazate complexes was claimed. In view of our own work on the characterisation of $PhNHNHCO_2M$ ($M=PhNHNH_3, Li, Na, K$), it was felt appropriate to confirm the coordinative ability of the anionic phenylcarbazate ligand. Any resulting phenylcarbazate complexes would provide comparisons with the better established unsubstituted carbazate complexes. There was a particular desire to characterise the phenylcarbazate analogue of $Cr(O_2CNHNH_2)_2.H_2O$. As an entry into this aspect of the work, attempts were made to repeat some of the published work of Srivastava and his co-workers.

4.5.1 THE COORDINATION POTENTIAL OF THE PHENYLCARBAZATE LIGAND

The presence of a phenyl group on the carbazate moiety potentially alters the coordination modes displayed by the ligand.

There are four possible major coordination modes of phenylcarbazate:

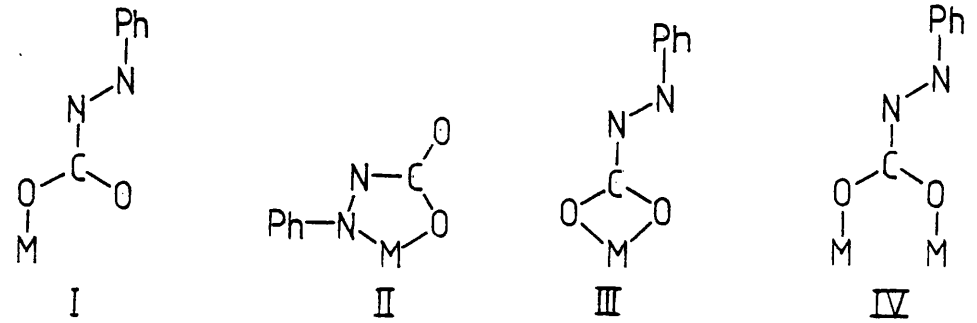

I II III IV

Mode I is unidentate *O*-bonded as shown by the majority of carboxylate anions as well as carbamate in $[Co(NH_3)_5(OCONH_2)]^{2+}$ [239,240]. Mode II is *N,O*-chelation as shown by many unsubstituted carbazates. Modes III and IV are *O,O*-chelation or bridging, similar

to those displayed by the carbamate ligand, $NH_2CO_2^-$, which can be regarded as the ammonia solvent analogue of the hydrazine solvent system derived carbazate [241-5].

Variations in carbamate coordination are illustrated by the reaction of $Cr^{IV}(NEt_2)_4$ with CO_2 which yields $Cr_2(O_2CNEt_2)_4(\mu\text{-}NEt_2)_2$ and $Cr_2(O_2CNEt_2)_4(NHEt_2)_2$, diethylcarbamate displaying Mode III type coordination in the chromium(III) product but Mode IV coordination in the dinuclear chromium(II) product in which the familiar quadruple metal-metal bond has been generated [246] (see FIG No 4.6).

FIGURE No 4.6 Structures of $Cr_2(O_2CNEt_2)_4(\mu\text{-}NEt_2)_2$ and $Cr_2(O_2CNEt_2)_4(NHEt_2)_2$.

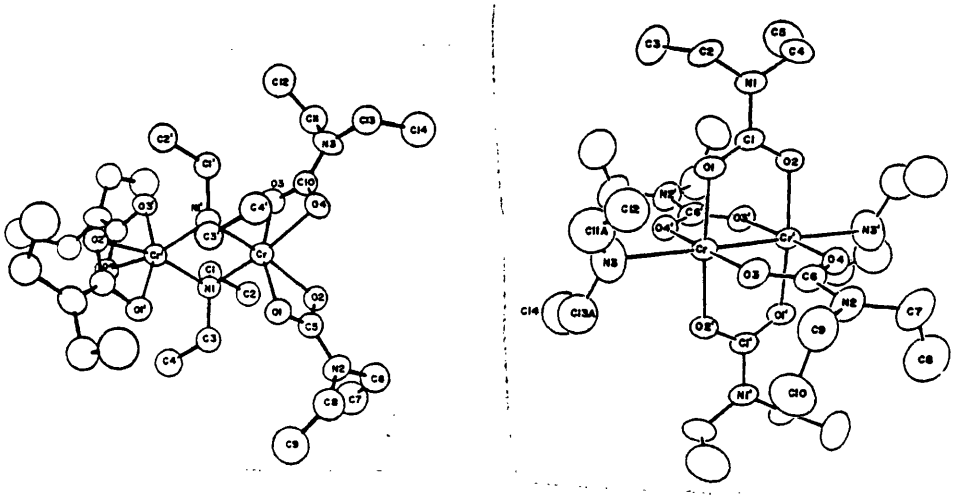

$Cr_2(O_2CNEt_2)_4(\mu\text{-}NEt_2)_2$ $Cr_2(O_2CNEt_2)_4(NHEt_2)_2$

Whether *O,O*-coordination (Modes III and IV) is favoured over *N,O*-coordination (Mode II) for phenylcarbazate is probably largely dependent on the availability of the phenyl-adjacent N lone pair for donation (and conversely its involvement in the aromatic ring conjugation). Only one example has been established where phenylhydrazine is known to act as an η^2-ligand, namely

$[(\eta^5\text{-}C_5H_5)Mo(NO)I(PhNHNH_2)]$, which has the phenyl-adjacent N active in coordination [51].

Srivastava and Tarli [145] considered N(3) of phenylcarbazate to be incapable of additional bond formation, but preferred to consider phenylcarbazate coordinated through N(2) and O.

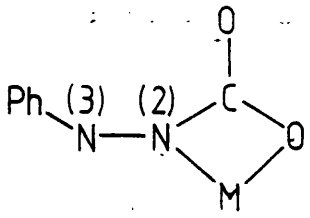

It is our contention, however, that in view of the acute bite angle required for this coordination mode and the necessary considerable rehybridisation of N(2), the other less-strained coordination modes discussed above are more likely to be favoured. In addition, although a *N(2),O*-coordination mode may be feasible the resulting chelate ring would not be planar, as would the ring of Mode III as a result of C=O multiple bonding. Indeed, it is pertinent to note that the corresponding phenyldithiocarbazate complexes $[M(S_2CNHNHPh)_2]$ (M=Ni,Pd,Pt,Zn,Cd,Hg,Sn,Pb) and $[M(S_2CNHNHPh)_3]$ (M=Cr,Co), were considered by Haines and Louch to display *S,S'*-coordination following analysis of their vibrational and electronic spectroscopic data [226]. This suggests that phenylcarbazate may favour *O,O'*-coordination i.e. Modes III and IV, where delocalisation allows planar MO_2CR or MOC(R)OM units to be present.

4.5.2 COPPER(I) AND (II) PHENYLCARBAZATE SYSTEMS

Srivastava reported [117] that reaction of copper(II) salts with phenylcarbazate in EtOH gave a copper(II) phenylcarbazate of stoichiometry $Cu(O_2CNHNHPh)_2.2H_2O$. This contrasts with the work of Petredis, Burke and Balch [247] who showed that reaction of $CuCl_2$ and $CuBr_2$ with $PhNHNH_2$ in H_2O proceeded with reduction to give the copper(I) phenyldiazene complexes $[Cu_4X_4(PhN{=}NH)]$. This has been confirmed in this present work. These results directly contradict other work reported by Srivastava in which the formation of stable copper(II) phenylhydrazine complexes has been claimed [248].

The reaction of $CuCl_2$ with $PhNHNHCO_2H.PhNHNH_2$ in MeOH at 0° under CO_2 results in the formation of off-white, diamagnetic, $[CuCl(PhNHNH_2)]_n$. The IR spectrum of this product showed the presence of coordinated $PhNHNH_2$ but no evidence of $PhNHNHCO_2^-$ (see FIG No 4.7). It is clear that reduction to copper(I) has occurred, the same complex being produced by reaction of $PhNHNH_2$ with either $CuCl_2.2H_2O$ or CuCl in alcoholic media (4.8).

The isolated complex is thermally unstable at room temperature, decomposing by loss of $PhNHNH_2$, and presumably forming a complex with a lower $PhNHNH_2$ content i.e.; $[Cu_xCl_x(PhNHNH_2)]_n$ $x>1$.

The reaction of $CuBr_2$ with $PhNHNH_2$ in EtOH gives the analogous off-white, diamagnetic, $[CuBr(PhNHNH_2)]_n$. This complex is substantially more stable than $[CuCl(PhNHNH_2)]_n$ and can be stored at room temperature in air for several days without excessive decomposition. The IR spectrum shows significant differences to that of $[CuCl(PhNHNH_2)]_n$, especially in the ν(NH) region (see FIG No 4.7), perhaps reflecting a change in molecular structure as a consequence of moving from a bridging chloride to a bridging bromide polymeric structure.

FIGURE No 4.7 Infra-red Spectra of Copper(I)-Phenylhydrazine Complexes.

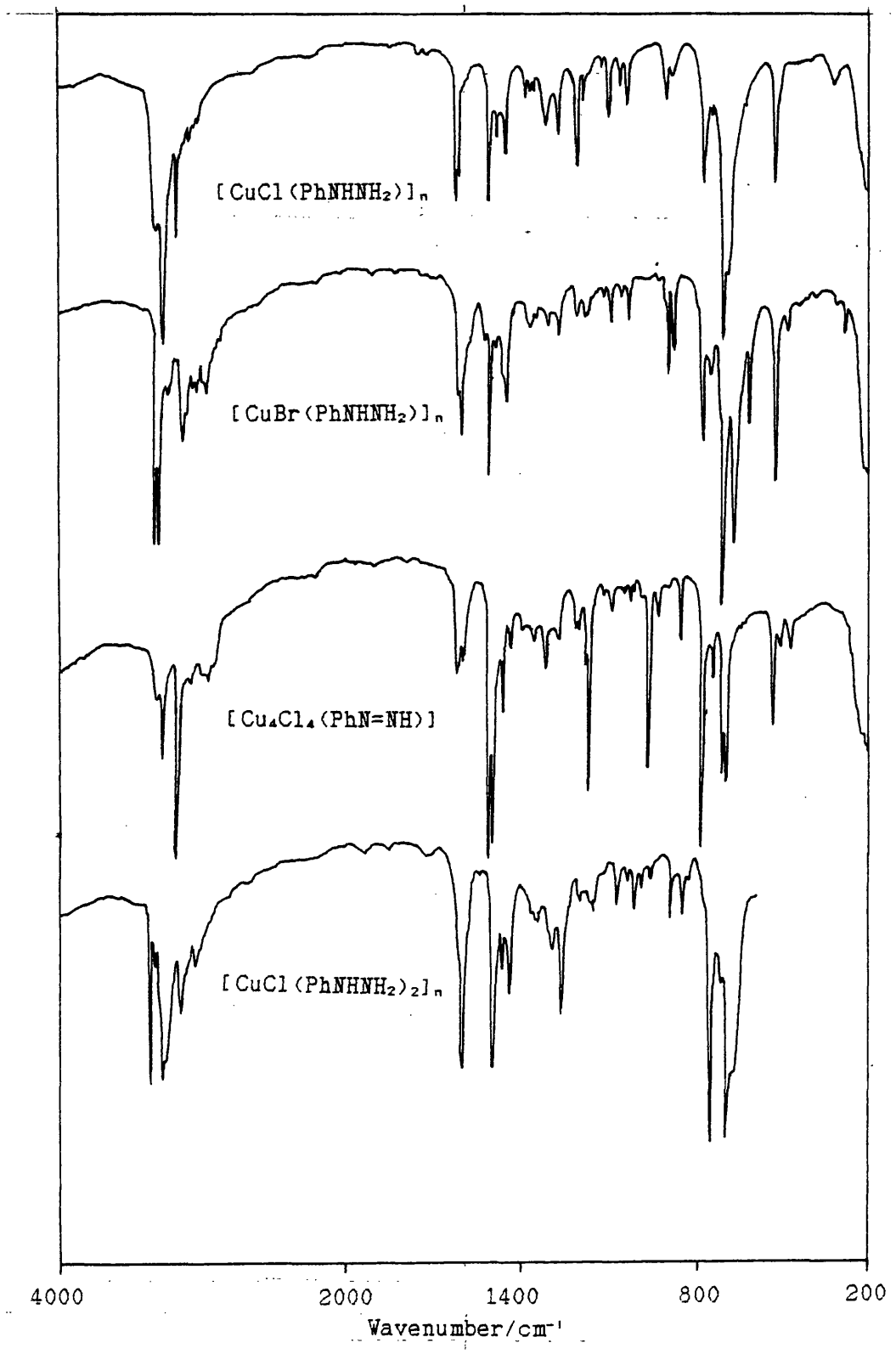

It is probable that in these complexes the copper is coordinated in a distorted tetrahedral manner with unidentate phenylhydrazine and bridging halide ligands. FIG No 4.8 shows two possible structures.

Reaction of either $CuCl_2.2H_2O$ or CuCl with excess $PhNHNH_2$ in the absence of a solvent results in an unstable, off-white, solid, whose IR spectrum and elemental analysis indicates it to be $[CuCl(PhNHNH_2)_2]$ (see FIG No 4.7). This complex was too thermally unstable for complete characterisation, but may be dimeric as are many other copper(I) halide-*bis*(nitrogen donor ligand) complexes.

FIGURE No 4.8 Two Possible Molecular Configurations of $[CuCl(PhNHNH_2)]_n$.

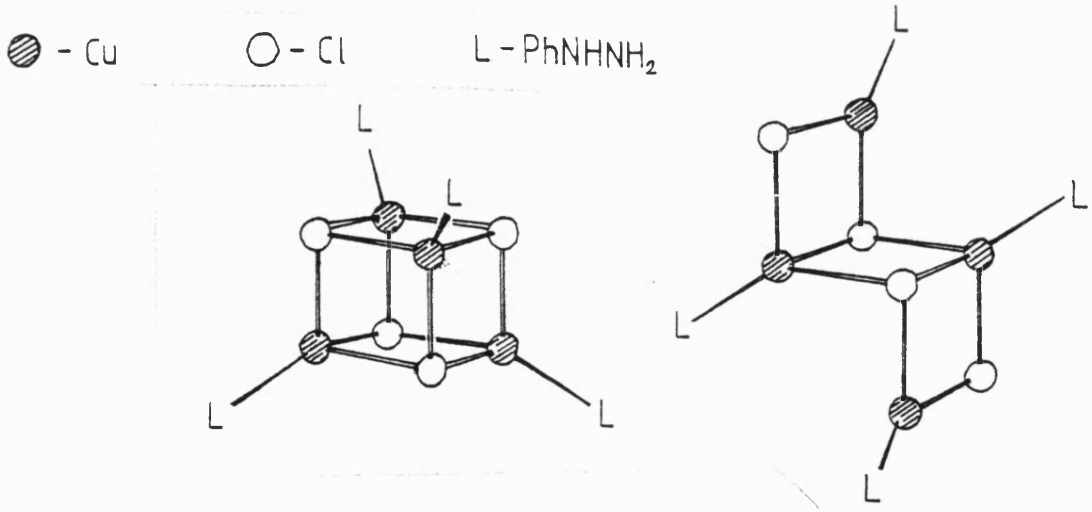

In addition to these complexes a number of other uncharacterised products were extracted from this reaction system, as indicated by IR spectra. This system may therefore resemble the Cu(I)/(II)-$N_2H_4/N_2H_5^+$ system studied by Brown *et al.* [249]. In this system, minor changes in procedure afforded a number of copper-hydrazine/hydrazinium species displaying variable oxidation states (i.e. (II), (II)/(I) and (I)). In many reactions only mixtures could be recovered.

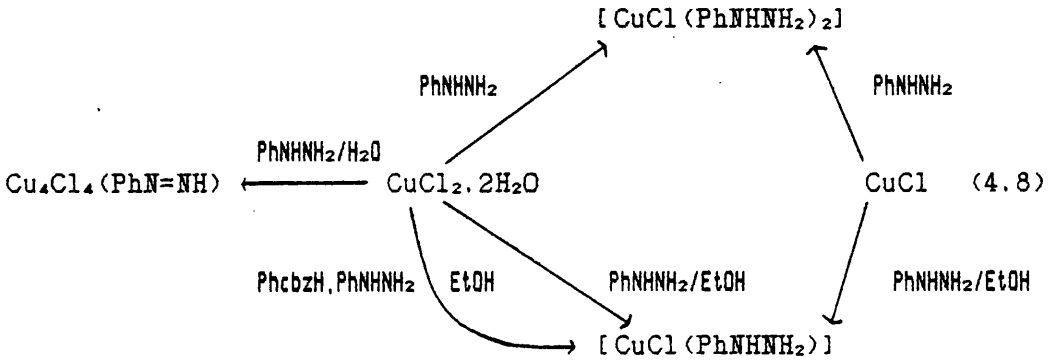

In conclusion, it is clear that phenylcarbazate or phenylhydrazine reduces copper(II) halides to copper(I) phenylhydrazine species. Given that phenylhydrazine is likely to be a more powerful reducing agent (> 0.1V) than hydrazine with respect to copper(II), a stable copper(II) phenylcarbazate/phenylhydrazine complex is probably not isolable.

4.5.3 THE NICKEL(II)-PHENYLCARBAZATE SYSTEM

Srivastava reported [145] that on reaction of $PhNHNHCO_2H.PhNHNH_2$ with $[Ni(OH_2)_6]Cl_2$ in EtOH, the complex $[PhNHNH_3][Ni(O_2CNHNHPh)_3].H_2O$ was formed. This would be analogous to the crystallographically characterised [107] carbazate $[N_2H_5][Ni(O_2CNHNH_2)_3].H_2O$ the anion of which contains *O,N*-chelating carbazate groups. However, following the precise experimental

procedure reported, the only product that could be obtained was the known phenylhydrazine complex, $[NiCl_2(PhNHNH_2)_2]_n$ [86]. However, a change in procedure did result in the formation of a phenylcarbazate complex.

The reaction of anhydrous $NiCl_2$ with $PhNHNHCO_2H.PhNHNH_2$ in MeOH at 0° under CO_2 results in the formation of the thermally unstable, pale blue, $[Ni(O_2CNHNHPh)_2(PhNHNH_2)_2]$ (4.9).

$$NiCl_2 + PhNHNHCO_2H.PhNHNH_2 \xrightarrow[CO_2]{MeOH/0^\circ} [Ni(O_2CNHNHPh)_2(PhNHNH_2)_2] + 2HCl \qquad (4.9)$$

On reaction at lower temperatures (e.g. -15°), a turquoise blue solution is initially formed from which the product precipitates on warming to 0°. The complex is thermally unstable at room temperature, but can be stored for several days without noticeable decomposition at 0° under CO_2.

The infra-red spectrum of the product indicates the presence of phenylcarbazate e.g. the intense $\nu(CO_2)$ bands at 1601 and 1494 cm^{-1} (see TABLE No 4.11). The lack of characteristic absorptions corresponding to $[PhNHNH_3]^+$ calls into question the formulation claimed [145] by Srivastava. The analytical results obtained clearly fit the suggested formula rather than that of Srivastava although the empirical formulae do not differ markedly i.e. $NiC_{26}H_{30}N_8O_4$ and $NiC_{27}H_{32}N_8O_7$, respectively. However, a molecular formula comprising two phenylcarbazate and two phenylhydrazine ligands is more consistent with the IR data (see TABLE 4.11 and FIG No 4.9). Although coordinated $PhNHNH_2$ is indicated by elemental analysis, its presence is difficult to deduce from the IR spectrum

because of overlap of phenylcarbazate and phenylhydrazine absorptions.

Magnetic susceptibility measurements (χ_{cgs} = 6.25×10^{-6} cm^3g^{-1}, μ_{eff} = 3.03 BM at 294K) are indicative of an octahedral environment around the central nickel.

TABLE No 4.11 Infra-red Spectra of $[Ni(O_2CNHNHPh)_2(PhNHNH_2)_2]$ and $[Co(O_2CNHNHPh)_2(MeOH)_2]$ (major bands) / cm^{-1}.

$Ni(Phcbz)_2(PhNHNH_2)_2$	$Co(Phcbz)_2(MeOH)_2$	Assignment
3352 (m)		
3246 (s)	3241 (m,sh)	$\nu(NH_2)$ + $\nu(NH)$
3158 (s,br)	3173 (s)	+ $\nu(OH)$
3108 (s,sh)		
1601 (vs)	1617 (vs)	$\nu_a(CO_2)$ + $\nu(CC)$
	1592 (vs)	+ $\delta(NH_2)$, $\delta(OH_2)$
1516 (s)	1522 (s,br)	$\nu(CC)$
1494 (vs)	1491 (s)	$\nu_s(CO_2)$
1486 (vs)		
1464 (m)	1462 (m)	$\nu(CC)$
1379 (vs)	1377 (s,br)	$\nu(CN)$?
	1021 (s)	$\nu(CO)$
832 (mw)	831 (m)	$\delta(OCO)$
752 (s)	756 (s)	$\delta(CH)$
693 (m)	692 (s)	
667 (m)	660 (ms)	$\pi(COO)$
509 (mw)		
454 (w)	441 (mw)	
391 (w)	383 (mw)	

FIGURE No 4.9 Infra-red Spectra of [Ni(O$_2$CNHNHPh)$_2$(PhNHNH$_2$)$_2$] and [Co(O$_2$CNHNHPh)$_2$(MeOH)$_2$] / cm^{-1}.

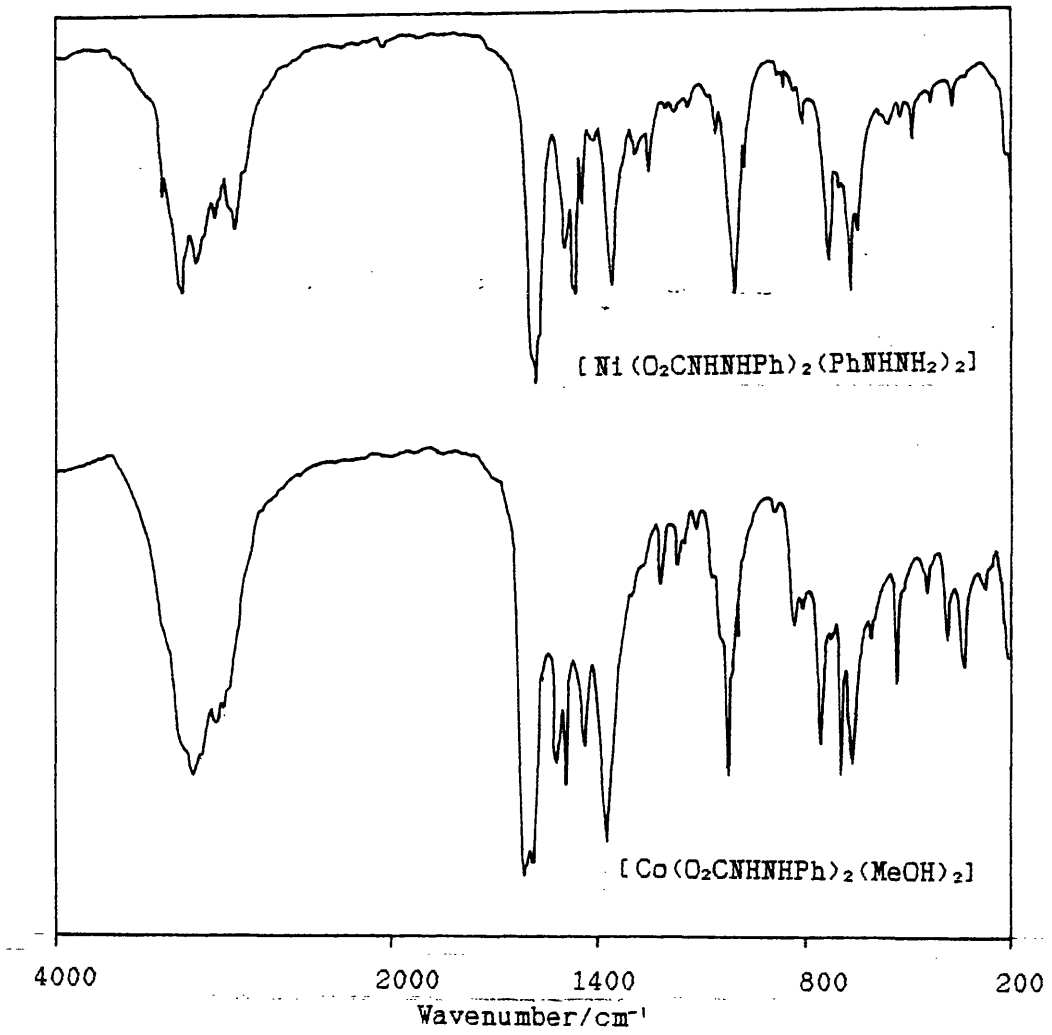

4.5.4 THE COBALT(II)-PHENYLCARBAZATE SYSTEM

Srivastava reported [147] that the product of the reaction of cobalt(II) with phenylcarbazate was $[Co(O_2CNHNHPh)_2(OH_2)_2]$. The exact procedure employed for this preparation was not available, the report, according to Chemical Abstracts, having been published in Acta.Ciencia.Indica.,[Series].Physics, but the British Lending Library has not been able to locate the article. It is possible that the bibliographical details have been incorrectly abstracted. As a result it was decided to use the method developed for the preparation of $[Ni(O_2CNHNHPh)_2(PhNHNH_2)_2]$.

The reaction of anhydrous $CoCl_2$ with $PhNHNHCO_2H.PhNHNH_2$ in MeOH at -10° under CO_2, initially results in the formation of a deep red solution from which no solid is precipitated when warmed to 0°. However, $[CoCl_2(PhNHNH_2)_2]_n$ is precipitated on warming to room temperature. On leaving the original reaction solution overnight at 0° under CO_2, the insoluble pale red product $[Co(O_2CNHNHPh)_2(MeOH)_2]$ is precipitated (4.10).

$$CoCl_2 + 2PhNHNHCO_2H.PhNHNH_2 \xrightarrow[CO_2]{MeOH} [Co(O_2CNHNHPh)_2(MeOH)_2] + 2PhNHNH_3Cl \quad (4.10)$$

The electronic spectrum of the reaction solution (489 (sh), 508 (s,br), 539 (sh) nm; MeOH solution, $^4A_{2g}(F)$ and $^4T_{2g}(P) \leftarrow {}^4T_{2g}(F)$ transitions, indicates an octahedral environment for the cobalt with a ligand set of rather similar strength to $[Co(OH_2)_6]^{2+}$ (c.f. $[Co(O_2CNHNHPh)_2(MeOH)_2]$, Δ_o = 19700 cm^{-1} and $[Co(OH_2)_6]^{2+}$, Δ_o = 19400 cm^{-1}).

The IR spectrum of the product (see TABLE No 4.11 and FIG No 4.9) resembles that of $[Ni(O_2CNHNHPh)_2(PhNHNH_2)_2]$, but has a less

complex ν(NH) region (3241, 3173 and 3123 cm^{-1}), and bands assignable to coordinated methanol (e.g. ν(CO) at 1021 cm^{-1}).

The solid complex appears to have a greater thermal stability than the nickel complex. Magnetic susceptibility measurements indicate a d^7 high-spin electronic arrangement (χ_{cgx} = 21.33×10^{-6} cm^3g^{-1}, μ_{eff} = 4.67 BM at 293K), the magnetic moment being in the range of known values for octahedral cobalt(II) species.

The nickel and cobalt phenylcarbazates must be formed by somewhat different routes. The nickel complex, $[Ni(O_2CNHNHPh)_2(PhNHNH_2)_2]$, forms on warming the initial reaction solution. Given the nature of the final cobalt species, it is possible that $[Ni(O_2CNHNHPh)_2(MeOH)_2]$ is an intermediate in the nickel system.

The formation of different adducts (i.e. $2PhNHNH_2$ in the nickel system and 2MeOH in the cobalt system), may reflect the Ni-N versus Ni-O and Co-N versus Co-O bond labilities. Thus Co(II)-N bonds are known to be more labile than Co(II)-O bonds which may explain the preferred formation of a methanol adduct in the cobalt system.

4.5.5 THE CHROMIUM(II)-PHENYLCARBAZATE SYSTEM

The reaction of chromium(II) with phenylcarbazate has not been previously studied. A chromium(II) phenylcarbazate complex would provide an interesting comparison with the unsubstituted chromium(II) carbazate, $Cr(O_2CNHNH_2)_2.H_2O$ isolated in this work (see SECTION No 3.5). However, potential differences in coordination behaviour between carbazate and phenylcarbazate have already been mentioned. In addition, the ability of chromium(II) to form both

mononuclear and binuclear metal-metal bonded complexes makes a prediction of product type somewhat hazardous.

The reaction of $[Cr(OH_2)_6]Cl_2$ with $PhNHNHCO_2H.PhNHNH_2$ in MeOH under CO_2 at 0° results in the fairly rapid formation of the extremely air-sensitive salmon-pink $[Cr_2(O_2CNHNHPh)_4(MeOH)_2]$ (4.11).

$$[Cr(OH_2)_6]Cl_2 + 2PhNHNHCO_2H.PhNHNH_2 \xrightarrow[CO_2]{MeOH,\ 0^\circ} [Cr_2(O_2CNHNHPh)_4(MeOH)_2] + PhNHNH_3Cl \quad (4.11)$$

Magnetic susceptibility measurements ($\chi_{cgs} = 0.27\times10^{-6}$ cm^3g^{-1}, $\mu_{eff} = 0.56$ BM per Cr at 296K) indicate an almost diamagnetic electronic arrangement consistent with the presence of a quadruple metal-metal bond. The formation of a mononuclear chromium(II) phenylcarbazate which would be expected to show a magnetic moment of ~4.9 BM can be ruled out. Thus, the nature of the phenylcarbazate product is remarkably different to that of chromium(II) carbazate.

The diffuse reflectance electronic spectrum confirms a binuclear structure with bands assignable to $\delta \rightarrow \pi^*$ and $np_x \rightarrow \pi^*$ transitions (see TABLE No 4.12). Oxidation products of the complex display typical octahedral chromium(III) electronic spectral profiles.

An electron impact mass spectrum (70eV ionising energy) contained a base peak at m/z 44 assignable to CO_2^+. Other prominent peaks at m/z 77 and 78 confirm the presence of Ph^+. However, there was no evidence that fragments containing the Cr_2^{4+} unit survive under the conditions employed.

TABLE No 4.12 Reflectance Electronic Spectra of Cr_2^{4+} Species / nm.

$Cr_2(O_2CNHNHPh)_4(MeOH)_2$	$Cr_2(O_2CMe)_4(OH_2)_2$	Assignment
469 (m,sh)	486	$\delta \rightarrow \pi^*$
455 (m,br)	469	
332 (s,sh)	347	$np_x \rightarrow \pi^*$
320 (vs)	326	
286 (m)		

The infra-red spectrum of the complex shows the presence of phenylcarbazate with $\nu(CO_2)$ at 1599 and 1460 cm^{-1} (see TABLE No 4.13 and FIG No 4.10). The separation of the antisymmetric and symmetric $\nu(CO_2)$ bands (Δ = 139 cm^{-1}) suggests, following acetate coordination trends, bridging *O,O'*-phenylcarbazate coordination. However. such correlations can be unreliable as shown by Deacon *et al.* [161].

TABLE No 4.13 Infra-red Spectrum of [$Cr_2(O_2CNHNHPh)_4(MeOH)_2$] (major bands only) / cm^{-1}.

Absorption	Assignment	Absorption	Assignment
3283 (s)	ν(NH) + ν(OH)	1009 (m)	$\nu(CO)_{MeOH}$
3048 (mw)	ν(CH)	792 (m)	δ(OCO)
1599 (vs)	$\nu_a(CO_2)$ + ν(CC)	754 (s)	δ(CH) + π(COO)?
1563 (s)	ν(CC)	695 (s)	
1483 (vs)	ν(CC)	503 (m)	r(COO)?
1460 (vs)	$\nu_s(CO_2)$	432 (m)	
1373 (vs)	ν(CN)	297 (mw)	ν(MO)
1302 (m)		279 (mw)	
1257 (m)			
1171 (w)	δ(CH)		
1162 (w)			

The presence of coordinated methanol is indicated by the ν(CO) vibration at 1009 cm^{-1}. Surprisingly, only one band is clearly evident in the ν(OH)/(NH) region at 3283 cm^{-1}. Attempts have not

been made to assign other bands in the spectrum in view of the uncertainties associated with assignments of phenylcarbazate modes.

FIGURE No 4.10 Infra-red Spectrum of $[Cr_2(O_2CNHNHPh)_4(MeOH)_2]$

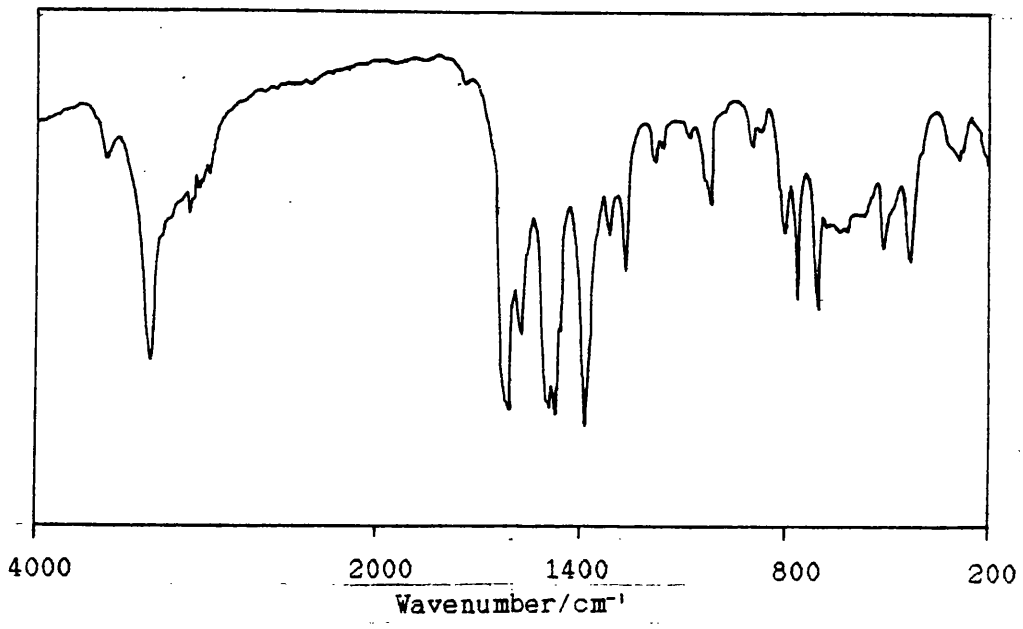

The evidence acquired therefore suggests that $[Cr_2(O_2CNHNHPh)_4(MeOH)_2]$ has a quadruple metal-metal bonded structure similar to that of $[Cr_2(O_2CNEt_2)_4(NHEt_2)_2]$ (see FIG No 4.6). The phenylcarbazate ligands will *O,O'*-bridge two chromium centres giving local Cr_2O_{10} D_{4h} symmetry. Axial methanol ligands complete the chromium coordination spheres (see FIG No 4.11).

The molecular structure of $[Cr_2(O_2CNHNHPh)_4(MeOH)_2]$ contrasts markedly with that of $Cr(O_2CNHNH_2)_2.H_2O$. The change of coordination from *N,O* to *O,O'* induced by the presence of the phenyl group on the carbazate backbone also allows the formation of a binuclear metal-metal bonded structure. With the phenyl-nitrogen lone pair not acting as a donor, the phenylcarbazate displays *O,O'*-coordination in the manner of a conventional carboxylate ligand, producing a

planar CrOC(R)OCr unit. So on reaction with chromium(II), a quadruple metal-metal bonded species is formed.

FIGURE No 4.11 Proposed Molecular Structure of $[Cr_2(O_2CNHNHPh)_4(MeOH)_2]$.

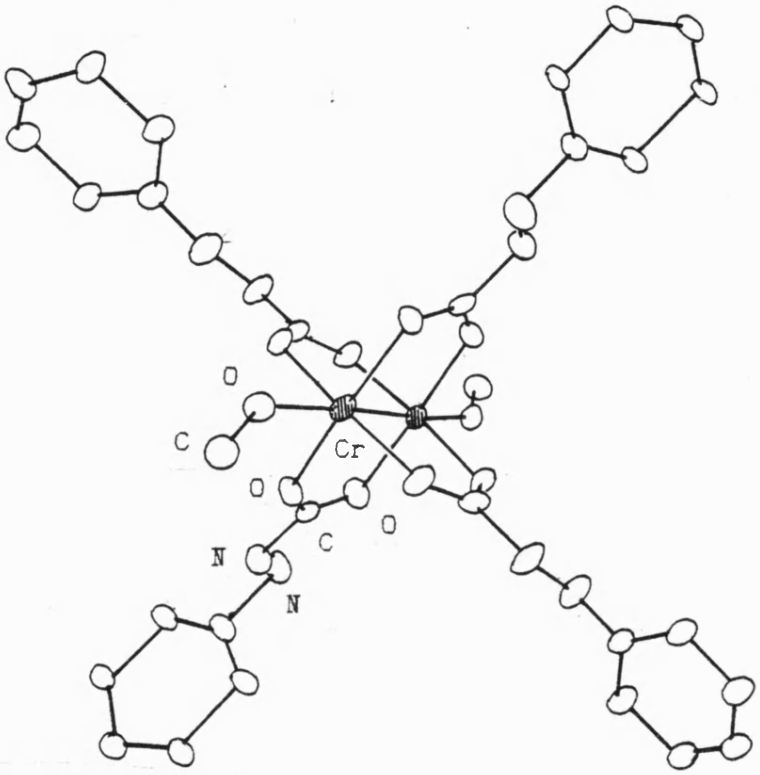

4.5.6 THE CHROMIUM(III)-PHENYLCARBAZATE SYSTEM

The reaction between $[Cr(OH_2)_4Cl_2]Cl.2H_2O$ and $PhNHNHCO_2H.PhNHNH_2$ in EtOH was reported by Srivastava [146] to give green-purple $Cr(O_2CNHNHPh)_3$. As in the other phenylcarbazate complexes reported by this group, the chelate ligands were considered to be *N(2),O*-coordinated.

As a result of not being able to confirm other aspects of the work on phenylcarbazate complexes reported by Srivastava *et al.*, a series of reactions were performed to test the authenticity of $Cr(O_2CNHNHPh)_3$ and the nature of the chromium(III)-phenylcarbazate system in general.

4.5.6a REACTION OF $[Cr(OH_2)_4Cl_2]Cl.2H_2O$ WITH $PhNHNHCO_2M$

The reaction of $PhNHNHCO_2M$ (M=Na, $PhNHNH_3$) with $[Cr(OH_2)_4Cl_2]Cl.2H_2O$ in MeOH under CO_2 results in the formation of an intensely purple solution, with no solid being produced even on lowering the reaction temperature to < -30°.

A study of the electronic spectra of such solutions over a temperature range shows that reaction between $[Cr(OH_2)_4Cl_2]Cl.2H_2O$ and $PhNHNHCO_2H.PhNHNH_2$ in MeOH occurs only above -7°, being complete between -1 and 10°C (see TABLE No 4.14).

TABLE No 4.14 Solution Electronic Spectra of Cr(III)/$PhNHNHCO_2H$ Reaction System.

Reaction Temperature / °C	Spectrum / nm
-19	584, 427
-7	577, 421
-4	576, 416
-1	574, 396
+1	574, 394
+10	574, 393
after 24 hrs, +18	576, 423

On standing at room temperature for several hours, the product in solution gradually hydrolyses, giving an absorption spectrum similar to the initial $[Cr(OH_2)_4Cl_2]Cl$/MeOH solution.

Addition of inert solvents of low polarity (e.g. Et_2O) to the solution leads to the precipitation of all product species. In the M = Na reaction, a pale violet solid has been isolated by precipitation from diethyl ether. The IR spectrum of this product contains peaks assignable to phenylhydrazido groups (e.g. δ(CH)), but elemental analysis shows the presence of large amounts of inorganic material, the Cr:PhNHNH- ratio being <1. Alternatively,

reduction of the solvent volume *in vacuo*, gave a product showing similar results.

In the M = $PhNHNH_3$ reaction, the same isolation procedures give a product whose IR spectrum contains a strong $PhNHNH_3^+$ profile. The presence of $PhNHNH_3^+$, (presumably paired with Cl^-), suggests the removal of chloride from the coordination sphere of the metal. This would account for the change in the electronic spectrum on reaction. Loss of chloride would leave an unsaturated chromium centre available for subsequent reaction with phenylcarbazate (4.12).

$$3PhNHNHCO_2H.PhNHNH_2 + [Cr(OH_2)_4Cl_2]Cl \longrightarrow 3PhNHNH_3Cl + 3PhNHNHCO_2^- + "[Cr(OH_2)_4]^{3+}" \quad (4.12)$$

The interaction of $"[Cr(OH_2)_4]^{3+}"$ and $PhNHNHCO_2^-$ could possibly follow one of two routes. Thus $PhNHNHCO_2^-$ could either a) coordinate to the metal in an *O,O'*-mode displacing H_2O ligands and generating chromium(III) phenylcarbazate (4.13)

$$3PhNHNHCO_2^- + Cr^{3+} \longrightarrow Cr(O_2CNHNHPh)_3 \quad (4.13)$$

or b) react as a base with the acidic $"[Cr(OH_2)_4]^{3+}"$ species (pK_a ~4) giving a chromium(III) hydroxo-species by deprotonation as depicted in 4.14 and 4.15.

$$3PhNHNHCO_2^- + "[Cr(OH_2)_4]^{3+}" \longrightarrow "Cr(OH)_3" + 3PhNHNHCO_2H + H_2O \longrightarrow PhNHNH_2 + CO_2 \quad (4.14)$$

$$3PhNHNHCO_2^- + "[Cr(OH_2)_4]^{3+}" \longrightarrow 3PhNHNH_2 + 3CO_2 + "[Cr(OH_2)_4]^{3+}" \longrightarrow "Cr(OH)_3" + 3PhNHNH_3^+ + H_2O \quad (4.15)$$

Although it is suggested in 4.14/15 that "$Cr(OH)_3$" is a possible product, this would be insoluble in alcoholic media, and no such precipitates are observed, suggesting that the actual reaction is more complicated than the scheme suggests.

Analysis of the changing visible spectrum profile on increasing temperature indicates a changing ligand set around the metal (see TABLE 4.15).

On reaction β increases, implying a more electronegative ligand set than in $[Cr(OH_2)_4Cl_2]^+$ with the ligand-metal bonding becoming more ionic than in $[Cr(OH_2)_4Cl_2]^+$.

Although the individual values of B and β calculated for the final purple solution product are obviously unrealistic, exceeding the most ionic chromium(III) ligand field possible (c.f. $[CrF_6]^{3-}$; β = 0.89), the increasing trend in β suggests that bonding by phenylcarbazate ligands is unlikely with a more ionic metal environment favoured.

TABLE No 4.15 Electronic Spectral Data of TABLE No 4.14 with calculated ν_3, B and β Parameters.

Band Positions / cm^{-1}						
ν_1	ν_2	ν_3	ν_2/ν_1	Dq/B	B/ cm^{-1}	β
17120	23420	37160	1.380	2.673	615	0.67
17330	23750	37600	1.371	2.760	627	0.68
17360	24040	37940	1.385	2.627	660	0.72
17420	25250	37310	1.450	2.121	820	0.89
17420	25380	39480	1.457	2.073	840	0.92
17420	25450	39570	1.463	2.033	857	0.93
17360	23640	37590	1.362	2.850	810	0.66

NOTE $\nu_1 \equiv 10Dq$. Calculated values are based on Lever's Transition Energy Ratio Tables [215]. The calculated values of B and β should only be considered to give an indication of the changing ligand field and should not be directly compared to other published data. It appears that at values of B near the free ion value (918 cm^{-1}), calculated values become unrealistic.

4.5.6b REACTION OF $CrCl_3(THF)_3$ WITH $PhNHNHCO_2H.PhNHNH_2$

The reaction of $PhNHNHCO_2H.PhNHNH_2$ with $CrCl_3(THF)_3$ in MeOH produced an intensely purple solution without precipitation of a solid. No further work was carried out on this system as it was assumed to be similar to the reaction observed in the $[Cr(OH_2)_4Cl_2]Cl/PhNHNHCO_2H.PhNHNH_2$ system.

4.5.6c CONCLUSION

The above observations on the reactions of $PhNHNHCO_2H.PhNHNH_2$ with chromium(III) show that chromium(III) phenylcarbazate has not been formed in this system. Following the procedures of Srivastava [146], no solid product could be isolated. From the arguments presented, it is thought that a soluble basic chromium(III) species not containing phenylcarbazate is produced.

This reaction system can be contrasted with that between chromium(III) and $[PhNHNH_3][PhNHNHCS_2]$ which gives $Cr(S_2CNHNHPh)_3$ [226], an easily isolable solid. The stability of this dithio-analogue can be attributed to the stability of $[PhNHNH_3][PhNHNHCS_2]$ which survives in aqueous solution without decomposition. Conversely, $[PhNHNH_3][PhNHNHCO_2]$ decomposes on contact with H_2O.

It is disconcerting to find that much of Srivastava's work on phenylcarbazate compounds could not be repeated even though detailed preparative methods were published. Indeed in view of the observations reported above, it would seem not unreasonable to suggest that, in particular, the reported isolation of copper(II) and chromium(III) phenylcarbazates is incorrect. The formulation of isolated nickel(II) and cobalt(II) phenylcarbazates was also found to be in error. It may be pertinent to note that another worker in this laboratory [118] has been unable to repeat the preparation of

copper(II) carbazate hydrate reported by Srivastava [117]. The actual product was found to be a polymeric anhydrous compound.

Thus, despite having reported the majority of transition metal substituted carbazate compounds known to date, it would appear that much of the work of Srivastava's group warrants reinvestigation.

4.6 EXPERIMENTAL

4.6.1 REACTIONS OF $PhNHNH_2$ WITH CHROMIUM(II)

a) Preparation of $[CrCl_2(PhNHNH_2)_2]_n$

A methanolic solution of $[Cr(OH_2)_6]Cl_2$ (5 mmol) was prepared by the reaction of conc. aqueous HCl (0.86 cm^3, 10 mmol) with electrolytic chromium metal (1.00 g) in MeOH (15 cm^3) under N_2. This solution was added to a deoxygenated solution of $PhNHNH_2$ (1.02 cm^3, 10.4 mmol) in Et_2O (30 cm^3). The pale blue product precipitated immediately, was filtered under N_2, washed with deoxygenated Et_2O and dried under a stream of N_2.

$C_{12}H_{16}Cl_2CrN_4$. Required: C, 42.50; H, 4.76; N, 16.52. Found: C, 42.21; H, 4.85; N, 16.37 %.

b) Preparation of $[CrBr_2(PhNHNH_2)_2]_n$

The same method as for $[CrCl_2(PhNHNH_2)_2]_n$ was employed but conc. aqueous HBr (1.20 cm^3, 10.0 mmol) replaced HCl.

c) Preparation of $Cr_2(O_2CMe)_4(PhNHNH_2)_2$

$Cr_2(O_2CMe)_4(OH_2)_2$ was prepared as in SECTION 3.10.3d. To a suspension of $Cr_2(O_2CMe)_4(OH_2)_2$ (1.20 g, 3.2 mmol) in deoxygenated EtOH (20 cm^3) was added a deoxygenated solution of $PhNHNH_2$ (0.94 cm^3, 9.6 mmol) in EtOH (10 cm^3). The resulting mixture was stirred at room temperature under N_2 for 180 mins, before the pale orange product was filtered off, washed with deoxygenated EtOH and Et_2O and dried under a stream of N_2.

$C_{20}H_{28}Cr_2N_4O_8$. Required: C, 43.17; H, 5.07; N, 10.07. Found: C, 43.10; H. 5.34; N, 10.29 %.

4.6.2 REACTIONS OF $PhNHNH_2$ WITH CO_2

a) Preparation of $PhNHNHCO_2H.PhNHNH_2$

Carbon dioxide was passed through a solution of $PhNHNH_2$ (10.0 cm^3, 102 mmol) in MeOH (150 cm^3) for 120 mins. Then the colourless product that had precipitated was filtered off, washed with Et_2O and dried *in vacuo*. Additional crystalline $PhNHNHCO_2H.PhNHNH_2$ can be obtained by cooling the above filtrate. After ~7 days, colourless platelets had formed.

$C_{13}H_{16}N_4O_2$. Required: C, 59.99; H, 6.20; N, 21.52. Found: C, 60.46; H, 6.31; N, 21.88 %.

b) Preparation of $PhNHNHCO_2M$ (M=Li, Na, K)

Three general procedures were employed, (see text for explanation).

i) M=Li, A solution of LiOMe was prepared by adding petroleum washed Li metal (0.39 g, 52 mmol) to deoxygenated anhydrous MeOH (100 cm^3) under N_2. To the resulting solution was added a deoxygenated solution of $PhNHNH_2$ (5.00 cm^3, 51 mmol) in MeOH (10 cm^3) under N_2 and the combined solutions cooled to 0°C (ice bath). Carbon dioxide was passed through the reaction mixture for 60 mins, after which time the colourless product had precipitated. The solid was filtered off under N_2, washed with Et_2O and dried *in vacuo*.

$C_7H_7LiN_2O_2$. Required: C, 53.19; H, 4.46; N, 17.72. Found: C, 53.47; H, 4.45; N, 17.74 %.

ii) M=Na, A solution of $PhNHNH_2$ (5.00 cm^3, 51 mmol) in MeOH (50 cm^3) was saturated with CO_2 for 15 mins. To this solution was added NaOH (2.04 g, 51 mmol) and CO_2 passage continued for

a further 100 mins. The resulting colourless product was filtered off, washed with EtOH and Et_2O and dried *in vacuo*. $C_7H_7N_2NaO_2$. Required: C, 48.28; H, 4.05; N, 16.09. Found C, 48.38; H, 4.09; N, 16.40 %.

iii) M=K, A solution of KOEt in EtOH was prepared by the reaction of petroleum washed K metal (~1.53 g, 39 mmol) with deoxygenated EtOH (60 cm^3) under N_2 at room temperature. To the resulting solution was added freshly prepared $PhNHNHCO_2H.PhNHNH_2$ (5.00 g, 19.2 mmol) under N_2. The resulting colourless product was filtered off, washed with Et_2O and dried *in vacuo*. Yield, 1.81 g (72 %).
$C_7H_7KN_2O_2$. Required: C, 44.19; H, 3.71; N, 14.73. Found: C, 44.19; H, 3.74; N, 14.63 %.

4.6.3 REACTIONS OF PHENYLHYDRAZINE/CARBAZATE WITH COPPER(II)/(I)

a) Preparation of $[CuCl(PhNHNH_2)]_n$

i) To a suspension of freshly prepared $PhNHNHCO_2H.PhNHNH_2$ (1.04 g, 4 mmol) in anhydrous MeOH (20 cm^3) under CO_2 at -5°C (ice-salt bath), was added dropwise a solution of anhydrous $CuCl_2$ (prepared from $CuCl_2.2H_2O$, by heating in air at 110°C for 24 hrs) (0.27 g, 2 mmol) in MeOH (20 cm^3). On initial addition, a green colour developed. However, on continued addition reduction occurred and the off-white product precipitated. This was filtered off, washed with Et_2O and dried *in vacuo*.

ii) A solution of $PhNHNH_2$ (0.40 cm^3, 4.06 mmol) in EtOH (25 cm^3) was added dropwise to a solution of $CuCl_2.2H_2O$ (0.33 g, 1.94 mmol) in EtOH (25 cm^3). The resulting off-white product

was filtered off, washed with Et_2O and dried *in vacuo*. Yield, 0.25 g (62 %).

$C_6H_8ClCuN_2$. Required: C, 34.79; H, 3.89; N, 13.52. Found C, 34.91; H, 3.90; N, 13.58 %.

iii) To an aqueous suspension of CuCl (0.43 g, 4.34 mmol) and NaCl (1.05 g, 17.97 mmol) was added $PhNHNH_2$ (2.00 cm^3, 20.32 mmol). The resulting reaction mixture was stirred at room temperature overnight. The resulting off-white product was filtered off, washed with EtOH and Et_2O and dried *in vacuo*. Yield, 0.76 g (85 %).

b) Preparation of $[CuCl(PhNHNH_2)_2]_n$

i) Excess $PhNHNH_2$ (6.50 cm^3) was added to $CuCl_2.2H_2O$ (0.34 g, 1.99 mmol) under N_2 at room temperature. The resulting reaction mixture was stirred for 30 mins, before excess deoxygenated MeOH (30 cm^3) was added. The resulting off-white product was filtered off, washed with Et_2O and dried under a stream of N_2. Yield, 0.57 g (91 %).

$C_{12}H_{16}ClCuN_4$. Required: C, 45.72; H, 5.12; N, 17.77. Found: C, 43.13; H, 4.88; N, 16.81 %.

ii) Excess $PhNHNH_2$ (10.00 cm^3) was added to CuCl (0.41 g, 4.14 mmol) under N_2 at room temperature. The reaction mixture was stirred for 30 mins, before being refrigerated overnight. After dilution with Et_2O, the off-white product was filtered off, washed with Et_2O and dried under a stream of N_2.

$C_{12}H_{16}ClCuN_4$. Required: C, 45.72; H, 5.12; N, 17.77. Found: C, 42.14; H, 4.69; N, 16.17 %.

c) Preparation of [CuBr(PhNHNH$_2$)]$_n$

To a deoxygenated solution of $CuBr_2$ (0.45 g, 2.02 mmol) in EtOH (25 cm^3) was added a deoxygenated solution of $PhNHNH_2$ (0.40 cm^3, 4.06 mmol) in EtOH (25 cm^3). The resulting off-white product was filtered off, washed with Et_2O and dried under a stream of N_2. Yield, 0.35 g (69 %).

$C_6H_8BrCuN_2$. Required: C, 28.64; H, 3.21; N, 11.13. Found: C, 28.69; H, 3.22: N, 11.20 %.

d) Preparation of [Cu$_4$Cl$_4$(PhN=NH)] [247]

To a deoxygenated aqueous solution (30 cm^3) of $CuCl_2.2H_2O$ (0.34 g, 1.99 mmol) under N_2, was added dropwise a deoxygenated aqueous solution (20 cm^3) of $PhNHNH_2$ (0.40 cm^3, 4,07 mmol). The red-brown product was filtered off, washed with MeOH and Et_2O and dried under a stream of N_2.

4.6.4 REACTION OF PHENYLCARBAZATE WITH NICKEL(II)

a) Preparation of [Ni(O$_2$CNHNHPh)$_2$(PhNHNH$_2$)$_2$]

To a suspension of freshly prepared $PhNHNHCO_2H.PhNHNH_2$ (3.25 g, 12.5 mmol) in MeOH (30 cm^3) under CO_2 at 0°C was added a solution of anhydrous $NiCl_2$ (prepared from $NiCl_2.6H_2O$ by heating at 110°C for 48 hrs) (0.65 g, 5.02 mmol) in MeOH (17 cm^3). The resulting pale blue-violet product formed rapidly. After being stirred for 30 mins at 0°C, the product was filtered off and dried *in vacuo*. The solid was stored under CO_2 at 0°C to limit decomposition.

$C_{26}H_{30}N_8NiO_4$. Required: C, 54.10; H, 5.24; N, 19.41. Found: C, 54.00; H, 5.38; N, 19.40 %.

4.6.5 REACTION OF PHENYLCARBAZATE WITH COBALT(II)

a) Preparation of $[Co(O_2CNHNHPh)_2(MeOH)_2]$

To a suspension of $PhNHNHCO_2H.PhNHNH_2$ (3.36 g, 12.9 mmol) in deoxygenated MeOH (30 cm^3) under CO_2 at 0°C, was added a solution of $CoCl_2$ (prepared from $CoCl_2.6H_2O$ by heating in air at 110°C for 24 hrs) (0.64 g, 4.93 mmol) in anhydrous MeOH (20 cm^3). A red solution formed after complete addition, from which the pale red product precipitated after 72 hrs under CO_2 at 0°C. It was filtered off, washed with MeOH and Et_2O and dried *in vacuo*.

$C_{16}H_{22}CoN_4O_6$. Required: C, 45.19; H, 5.21; N, 13.77. Found: C, 45.38; H, 5.22; N, 13.45 %.

4.6.6 REACTION OF PHENYLCARBAZATE WITH CHROMIUM(II)

a) Preparation of $[Cr_2(O_2CNHNHPh)_4(MeOH)_2]$

A solution of $[Cr(OH_2)_6]Cl_2$ (5 mmol) in MeOH was prepared by the reaction of conc. aqueous HCl (0.86 cm^3, 10.0 mmol) with electrolytic chromium metal (1.00 g) in MeOH (15 cm^3) under N_2. This solution was added to a suspension of $PhNHNHCO_2H.PhNHNH_2$ (3.00 g, 11.53 mmol) in deoxygenated MeOH (30 cm^3). The salmon-pink product precipitated rapidly and was filtered off under N_2, washed with deoxygenated MeOH and Et_2O and dried under a stream of N_2.

$C_{30}H_{36}Cr_2N_8O_{10}$. Required: C, 46.64; H, 4.70; N, 14.50. Found: C, 46.53; H, 4.72; N, 14.80 %.

4.6.7 REACTIONS OF PHENYLCARBAZATE WITH CHROMIUM(III)

a) Reaction of $PhNHNHCO_2H.PhNHNH_2$ with $[Cr(OH_2)_4Cl_2]Cl.2H_2O$

To a suspension of $PhNHNHCO_2H.PhNHNH_2$ (1.56 g, 6 mmol) in MeOH (80 cm^3) under CO_2 at -20°C (acetone-CO_2 bath) was added dropwise a deoxygenated solution of $[Cr(OH_2)_4Cl_2]Cl.2H_2O$ (0.53 g, 2 mmol) in MeOH (40 cm^3) under CO_2. The addition was completed at -20°C and then the solution allowed to warm up gradually, with UV/VIS solution spectra taken at intervals by extraction of samples using syringe/septum techniques. At 10°C, the solution was sealed under CO_2 and kept overnight at ~3°C and a final solution spectrum recorded. This procedure was repeated, but after complete reaction of $PhNHNHCO_2H.PhNHNH_2$ (violet-blue solution), the solution was cooled to -30°C and reduced to low volume *in vacuo*. The resulting purple solid was filtered off, washed with Et_2O and dried in air. The solid was soluble in MeOH (solution electronic spectrum; 564 (ms,br), 406 (s) nm) and IR spectroscopy showed the presence of $PhNHNH_3^+$.

b) Reaction of $PhNHNHCO_2Na$ with $[Cr(OH_2)_4Cl_2]Cl.2H_2O$

To a suspension of $PhNHNHCO_2Na$ (2.16 g, 12.4 mmol) in MeOH (15 cm^3) under CO_2 at 0°C, was added a solution of $[Cr(OH_2)_4Cl_2]Cl.2H_2O$ (1.04 g, 3.9 mmol) in MeOH (10 cm^3). The resulting dark blue solution was reduced in volume by futher CO_2 passage, and the solid produced filtered off, washed with Et_2O and dried *in vacuo*.

Found: C, 11.96; H, 1.26; N, 3.10 %.

c) Reaction of $PhNHNHCO_2H.PhNHNH_2$ with $CrCl_3(THF)_3$

The complex $CrCl_3(THF)_3$ was prepared as per [250]. To a deoxygenated suspension of $PhNHNHCO_2H.PhNHNH_2$ (1.63 g, 6.3 mmol) in anhydrous MeOH (75 cm^3) under CO_2 at -30°C (acetone-CO_2 bath), was added a solution of $CrCl_3(THF)_3$ (0.73 g, 2 mmol) in anhydrous MeOH (40 cm^3). After complete addition, the solution was allowed to warm to 0°C, giving a dark violet solution. Solid products were not isolated.

CHAPTER No 5

REACTIONS OF CHROMIUM(II) AND (III) WITH METHYL- AND 1,1-DIMETHYL-HYDRAZINES AND THEIR CARBAZATE DERIVATIVES

REACTIONS OF CHROMIUM(II) AND (III) WITH METHYL- AND 1,1-DIMETHYL-HYDRAZINES AND THEIR CARBAZATE DERIVATIVES

THE METHYLHYDRAZINE/METHYLCARBAZATE SYSTEM

5.1 METHYLHYDRAZINE

5.1.1 BACKGROUND

Methylhydrazine is expected to show some differences to hydrazine in its coordination behaviour, the electronic effect of the methyl substituent being to increase the basicity hence donor ability of the -NHMe nitrogen. However, the presence of the methyl substituent introduces a steric factor which opposes the possibility of the methylated nitrogen acting as a donor to a metal centre. The coordination chemistry of this ligand may well depend on a balance of these two factors.

The reactions of some first-row transition metal ions with anhydrous $MeNHNH_2$ result in the formation of sparingly soluble $[M(NH_2NHMe)_6]X_2$ species (M=Fe,Co; X=Cl,Br,I; M=Ni; X=Cl) [25,26,40]. However, thermal decomposition of these species, or reaction of metal salts in alcoholic media with $MeNHNH_2$ produce $[M(NH_2NHMe)_2X_2]_n$ species (M=Fe,Co; X=Cl,Br,I; M=Ni; X=Cl) [25,26,40,85] which appear to be structurally similar to the bridging hydrazine complexes $[M(N_2H_4)_2X_2]_n$. Methylhydrazine is a stronger reducing agent than hydrazine and some reactions with first-row transition metal ions result in reduction. Thus, the copper(I) complex $[(CuCl)_2(NH_2NHMe)]$ is the product of the reaction between copper(II) chloride and methylhydrazine in ethanol, whereas unreduced $[Cu(N_2H_4)_2Cl_2]_n$ results from use of hydrazine itself [251]. Methylhydrazine also reduces $FeCl_3$ to $[Fe(NH_2NHMe)_2Cl_2]_n$ [85].

5.1.2 REACTION OF CHROMIUM(II) CHLORIDE WITH METHYLHYDRAZINE

Reactions of $MeNHNH_2$ with either chromium(III) or (II) species have not been reported previously.

The reaction of $[Cr(OH_2)_6]X_2$ (X=Cl,Br) with $MeNHNH_2$ in methanol afforded only chromium(II) hydroxide species. As with other first-row transition metal ions, the presence of water results in hydroxide formation.

The reaction of $CrCl_2(MeCN)_2$ with $MeNHNH_2$ in acetonitrile under strictly anhydrous and inert conditions results in the formation of the pale blue-grey, air-sensitive, solid $[Cr(NH_2NHMe)_2Cl_2]_n$.

Magnetic susceptibility measurements (χ_{cor} = 44.78×10^{-6} cm^3g^{-1}, μ_{eff} = 4.82 BM at 295K) indicate a high spin d^4 electronic configuration consistent with mononuclear octahedral chromium(II).

Diffuse reflectance spectra indicate a similar electronic environment to $[Cr(N_2H_4)_2X_2]_n$ (X=Cl,Br,I) but one which is different to those in $[Cr(R^1R^2NNH_2)_2Cl_2]_n$ (R^1=R^2=Me; R^1=Ph, R^2=H) (see TABLE No 5.1).

The $^5E_g \rightarrow {}^5T_{2g}$ transition is of higher energy for both the N_2H_4 and $MeNHNH_2$ complexes than the analogous transition of $[Cr(OH_2)_6]^{2+}$ (714 nm [221]), as would be expected because of the greater ligand field of the nitrogen donors. The complex $[Cr(N_2H_4)_2Cl_2]_n$ is known to be isostructural with the manganese and zinc analogues [45,24] which have the metal ions in tetragonally distorted octahedral environments with bridging hydrazines. However, Jahn-Teller distortion effects present in the chromium(II) complex may amplify this distortion, leading to a pseudo-square planar geometry. The similar electronic spectra of $[Cr(N_2H_3R)_2Cl_2]_n$ (R=H or Me) may indicate a similar stereochemistry for both complexes.

TABLE No 5.1 Diffuse Reflectance Electronic Spectra of $[Cr(NH_2NR'R^2)_2Cl_2]_n$ species / nm.

$[Cr(N_2H_4)_2Cl_2]_n$*	$[Cr(N_2H_3Me)_2Cl_2]_n$	$[Cr(N_2H_2Me_2)_2Cl_2]$	$[Cr(N_2H_3Ph)_2Cl_2]$	Assignment
	~900 (w,br)			
~570 (m,br)	594 (m,br)	662 (m,br)	704 (m,br)	$^5T_{2g} \leftarrow {}^5E_g$
	582 (w,sh)			
	478 (w,sh)	477 (w,sh)		
	462 (w,sh)	460 (w,sh)		

* - from ref. 194.

Very little has been reported on the vibrational spectra of $MeNHNH_2$ complexes. The assignment of the IR spectrum of $[Cr(NH_2NHMe)_2Cl_2]_n$ (see TABLE No 5.2 and FIG No 5.1) has been attempted using the work of Durig *et al.* [223] on the assignment of free $MeNHNH_2$ as a basis. Comparison with the IR spectrum of $[Cr(N_2H_4)_2Cl_2]_n$ (see SECTION No 3.3) has also been helpful.

The NH stretching region shows two pairs of absorptions at 3222, 3203 and 3166, 3136 cm^{-1}, slightly decreased in frequency from the bands found for methylhydrazine. The $\nu(CH_3)$ vibrations barely shift on coordination. The NH_2 scissoring vibration occurs at 1622 cm^{-1} in the Raman spectrum of liquid $MeNHNH_2$, and is shifted to 1597 cm^{-1} in $[Cr(NH_2NHMe)_2Cl_2]_n$. Conversely, $\omega(NH_2)$ is shifted to higher frequency on coordination (1327 cm^{-1} in $[Cr(NH_2NHMe)_2Cl_2]_n$ compared with 1305 cm^{-1} in $MeNHNH_2$).

The rocking modes of N_2H_4 are very sensitive to coordination, increasing by 100 cm^{-1} or more. Likewise $r(NH_2)$ of $MeNHNH_2$ is found at 888 cm^{-1}, whereas in $[Cr(NH_2NHMe)_2Cl_2]_n$ this band is found at 1039 cm^{-1}, an increase of some 150 cm^{-1}. No other bands are found for the complex between 877 and 1039 cm^{-1}, so alternative assignments cannot be proposed.

FIGURE No 5.1 Infra-red spectra of $[Cr(NH_2NHMe)_2Cl_2]_n$ and $[Cr_2(O_2CMe)_4(NH_2NHMe)]$

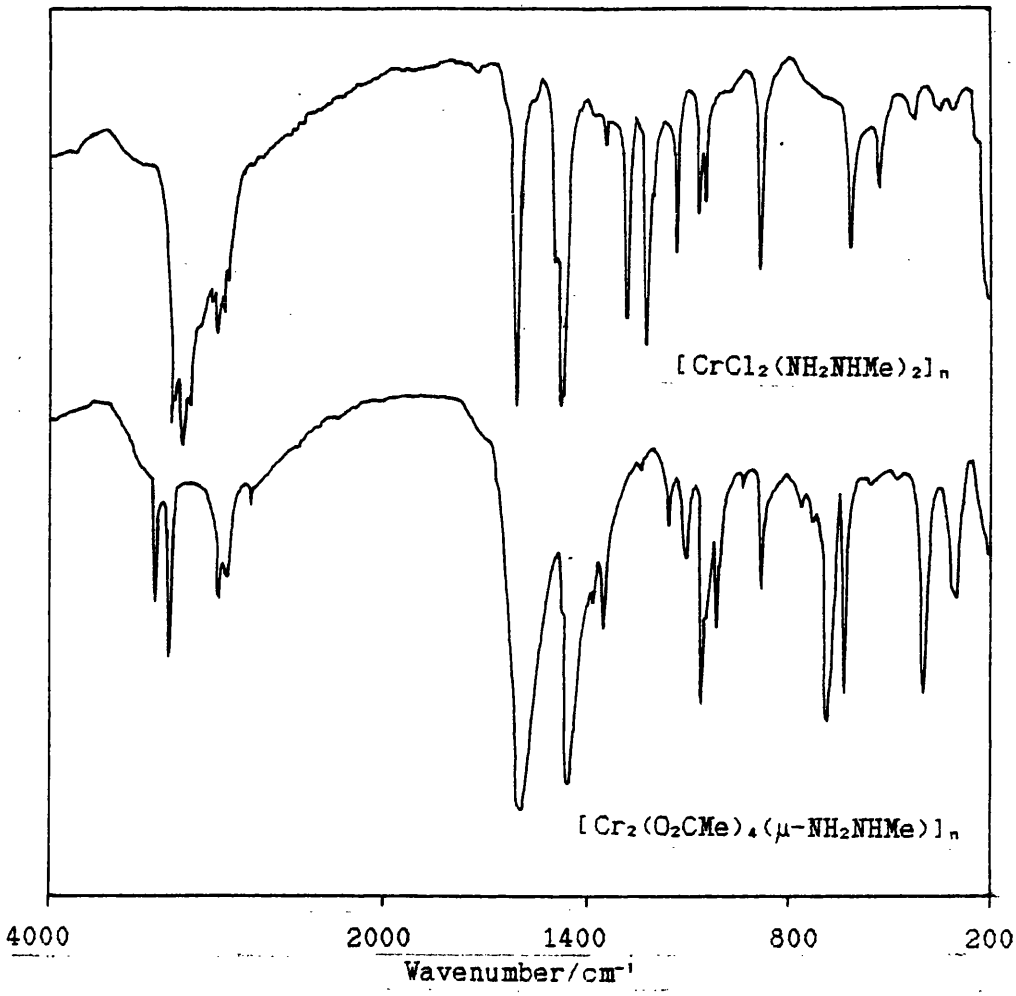

The final N-H motions to be assigned are two NH bends found at 1137 and 821 cm^{-1} in $MeNHNH_2$ itself. The complexity of the region where these bands are expected in the complex prohibits definite assignments. However, bands at 1271 and 877 cm^{-1} may be due to these motions, with increases of 135 and 56 cm^{-1} respectively on coordination. It should be stressed that many of the bands shown by coordinated $MeNHNH_2$ are likely to be of mixed character. This appears to be especially true for b(NH) and $r(NH_2)$ modes.

The $\nu(CH_3)$ absorptions are little affected by coordination. Durig *et al.* [223] had some difficulty assigning $\omega(CH_3)$ and $r(CH_3)$ modes due to the large number of fundamentals in the expected frequency region, but tentatively assigned them to bands at 1200

and 1118 cm^{-1}, respectively. A band at 1127 cm^{-1} in the spectrum of $[Cr(NH_2NHMe)_2Cl_2]_n$ is assignable to $r(CH_3)$, but no $\omega(CH_3)$ is found at ~1200 cm^{-1}. The band at 1216 cm^{-1} may be assigned to a skeletal stretching vibration.

TABLE No 5.2 Infra-red Spectrum of $[Cr(NH_2NHMe)_2Cl_2]_n$ with the Vibrational Spectrum of $MeNHNH_2$ / cm^{-1}.

$[Cr(NH_2NHMe)_2Cl_2]_n$	$MeNHNH_2$	Assignment
3222 (s)	3316	
3203 (m,sh)	3304	$\nu(NH_2)$
3166 (s)	3258	
3136 (m,sh)		
2973 (w,br)	2926	
2956 (w,br)	2938	$\nu(CH_3)$
2922 (w)	2782	
1597 (vs)	1622	$\delta(NH_2)$
1481 (m)	1469	
1464 (m)	1445	$\delta(CH_3)$
	1412	
1327 (w)	1305	$\omega(NH_2)$
1271 (s)	1137	b(NH)
1216 (s)	1104	Antisym. skeletal
	1200	stretch or $\omega(CH_3)$?
1127 (ms)	1118	$r(CH_3)$
1056 (m)	992	Sym. skeletal stretch
1039 (m)	888	$r(NH_2)$
877 (s)	821	b(NH)
610 (ms)	447	Skeletal bend
524 (m)	315	$t(NH_2)$
	257	$t(CH_3)$
426 (w)		$\nu(MN)$
359 (w)		
326 (vw,br)		
307 (vw,br)		

The skeletal stretches can be approximately localised as ν(CN) and ν(NN). In $MeNHNH_2$ these vibrations occur at 992 and 1104 cm^{-1}, but nevertheless shift appreciably on deuteration indicating some NH and CH character. They should, therefore be affected by coordination to some degree, so bands at 1216 and 1056 cm^{-1} in the spectrum of $[Cr(NH_2NHMe)_2Cl_2]_n$ are so assigned. The skeletal bending mode of $MeNHNH_2$ (447 cm^{-1}) appears to shift to 610 cm^{-1} on coordination.

The remaining torsional modes, t(NH_2) and t(CH_3), occur at 315 and 257 cm^{-1} respectively in $MeNHNH_2$. The latter is not expected to shift much on coordination but has not been identified in the spectrum of $[Cr(NH_2NHMe)_2Cl_2]_n$. However, t(NH_2) shifts ~200 cm^{-1} to 524 cm^{-1} on coordination, a feature previously observed for NH_3 on coordination to metals.

In common with $[Cr(N_2H_4)_2Cl_2]_n$, two ν(MN) vibrations appear in the spectrum of $[Cr(NH_2NHMe)_2Cl_2]_n$ at 426 and 359 cm^{-1}. Assuming both complexes adopt a common structure, ν(MCl) should occur below 230 cm^{-1} following the work of Goldstein and Unsworth [156].

The spectral data acquired suggests that $[Cr(NH_2NHMe)_2Cl_2]_n$ and $[Cr(N_2H_4)_2Cl_2]_n$ are isostructural with bridging NH_2NHR (R=H or Me) groups and terminal chlorines. However, deuteration studies seem necessary to support the tentative vibrational assignments presented in this work.

5.1.3 REACTION OF CHROMIUM(II) ACETATE WITH METHYLHYDRAZINE

The reaction of $Cr_2(O_2CMe)_4(EtOH)_2$ (prepared by the addition of anhydrous $Cr_2(O_2CMe)_4$ to anhydrous EtOH) with $MeNHNH_2$ in EtOH under N_2 resulted in the formation of the red/orange air-sensitive solid $[Cr_2(O_2CMe)_4(\mu\text{-}NH_2NHMe)]_n$ (see 5.1). This product is also formed by

the reaction of $Cr_2(O_2CMe)_4(OH_2)_2$ with $MeNHNH_2$ in EtOH, but appears to be contaminated with a hydroxide impurity, the $MeNHNH_2$ presumably deprotonating a H_2O molecule to form hydroxide anions. Use of the ethanol adduct $Cr_2(O_2CMe)_4(EtOH)_2$ appears to eliminate this undesirable reaction.

$$Cr_2(O_2CMe)_4(OH_2)_2 \xrightarrow[in\ vacuo]{\Delta} Cr_2(O_2CMe)_4 \xrightarrow[N_2]{EtOH} Cr_2(O_2CMe)_4(EtOH)_2$$
$$\xrightarrow[N_2]{MeNHNH_2/EtOH} [Cr_2(O_2CMe)_4(\mu\text{-}MeNHNH_2)]_n \qquad (5.1)$$

The magnetic susceptibility (χ_{corr} = 0.65×10^{-6} cm^3g^{-1}, μ_{eff} = 0.49 BM per Cr at 296K) indicates the retention in the product of the quadruple metal-metal bond of the ethanol adduct.

Diffuse reflectance and MeOH solution electronic spectra also support the presence of a quadruple metal-metal bonded structure for the product (see TABLE No 5.3).

TABLE No 5.3 Electronic Spectra of $[Cr_2(O_2CMe)_4(\mu\text{-}L)]_n$ (L = $MeNHNH_2$, N_2H_4) / nm.

L =	$MeNHNH_2$		N_2H_4	Assignment[b]
	Reflectance	Solution[a]	Reflectance	
	476 (m,br)	484 (m,br)	478 (s,br)	$\delta \rightarrow \pi^*$
	349 (m,sh)	346 (m,sh)	360 (s,sh)	
	331 (s)	326 (s)	333 (vs)	$np_x \rightarrow \pi^*$

[a] - MeOH solution, [b] - assignments based on [205]

The infra-red spectrum of $[Cr_2(O_2CMe)_4(\mu\text{-}MeNHNH_2)]_n$ (see TABLE No 5.4 and FIG No 5.1) reveals the presence of coordinated acetate

and methylhydrazine. The acetate absorptions have been assigned by comparison with the spectrum of $[Cr_2(O_2CMe)_4(\mu\text{-}N_2H_4)]_n$ (see SECTION

TABLE No 5.4 Infra-red Spectrum of $[Cr_2(O_2CMe)_4(\mu\text{-}MeNHNH_2)]_n$ / cm^{-1}.

Spectrum	Tentative assignment
3344 (w) 3269 (mw)	ν(NH)
2974 (w) 2925 (w)	$\nu(CH_3)$
1590 (vs, br)	$\nu(CO_2)$ + $\delta(NH_2)$
1439 (vs, br)	$\nu(CO_2)$ + $\delta(CH_3)$
1374 (s)	
1343 (m)	$\delta(CH_3)$ (acetate)
1305 (vw) 1273 (vw)	b(NH) ?
1228 (vw)	Antisym. skeletal stretch or $\omega(CH_3)$ ($MeNHNH_2$)
1149 (w)	$r(CH_3)$ ($MeNHNH_2$)
1102 (w) 1095 (w)	Sym. skeletal stretch ($MeNHNH_2$)
1048 (m) 1034 (m, sh)	$r(CH_3)$
1007 (m)	
934 (vw)	ν(CC) (acetate) ?
882 (w)	b(NH) ?
684 (vs) 628 (s)	δ(OCO) π(COO)
~559 (w, br)	$t(NH_2)$?
~475 (vw, br)	ν(MN) ?
398 (s) 310 (m) 302 (m)	ν(MO)
284 (w, sh)	

3.3), but it has not been possible to assign all the expected fundamentals of $MeNHNH_2$ by comparison with $[Cr(NH_2NHMe)_2Cl_2]_n$.

It is possible that different configurations for coordinated $MeNHNH_2$ occur in $[Cr_2(O_2CMe)_4(\mu\text{-}MeNHNH_2)]_n$ and $[Cr(NH_2NHMe)_2Cl_2]_n$. However, Durig *et al.* [223] calculated a rotational barrier of 15.6 kJ mol^{-1} between the two skew forms ('inner' and 'outer') which would appear to rule out an easy change of configuration.

The two $\nu(NH)$ vibrations, at 3344 and 3269 cm^{-1}, shift less than in $[Cr(NH_2NHMe)_2Cl_2]_n$ from their positions in $MeNHNH_2$. The $\delta(NH_2)$ vibration is obscured by the intense $\nu_a(CO_2)$ absorption at 1590 cm^{-1}, and no other NH derived absorptions can confidently be assigned although two absorptions appear in similar positions to the bands assigned to b(NH) in $[Cr(NH_2NHMe)_2Cl_2]_n$ and the broad weak band at 559 cm^{-1} could be assigned to $t(NH_2)$. By contrast, the acetate absorptions are easily assigned by comparison with the IR spectrum of $[Cr_2(O_2CMe)_4(\mu\text{-}N_2H_4)]_n$. The $\nu(CO_2)$ vibrations at 1590 and 1439 cm^{-1} give rise to a Δ value of 151 cm^{-1}, in line with the expected bridging nature of the acetate ligands. Other acetate absorptions are assigned in TABLE No 5.4.

It is concluded that reaction of $MeNHNH_2$ with $Cr_2(O_2CMe)_4$ results in the formation of the methylhydrazine-bridged polymer, $[Cr_2(O_2CMe)_4(\mu\text{-}MeNHNH_2)]_n$, directly analogous to the hydrazine derivative.

5.2 THE METHYLCARBAZATE ANION

5.2.1 BACKGROUND

The reaction of $MeNHNH_2$ with CO_2 has received only scant attention, whereas the reaction with CS_2 has been investigated more thoroughly, thermally stable methylhydrazinium(1+) 2-

methyldithiocarbazate, $[MeNH_2NH_2][S_2C(Me)NNH_2]$ being formed. Protonation of this species using dilute HCl results in decomposition rather than the expected formation of 2-methyldithiocarbazic acid, $\overset{-}{S_2}CMe\overset{+}{N}HNH_2$ [252]. Surprisingly, the corresponding diselenocarbazic acid, $\overset{-}{Se_2}CMe\overset{+}{N}HNH_2$ can be successfully produced by protonation of $[MeNH_2NH_2][Se_2CMeNNH_2]$.

The *in situ* formation of methylcarbazate anion and its reaction with nickel salts has been claimed by Srivastava and Tarli [145], but they did not attempt to isolate it from solution. So-called 'methylcarbazate' has also been reported to have a toxic effect on pineapples! [253].

5.2.2 THE REACTION OF $MeNHNH_2$ WITH CARBON DIOXIDE

The passage of CO_2 into a solution of $MeNHNH_2$ in ethanol resulted in a colourless hygroscopic precipitate which by analogy to hydrazinium(1+) carbazate was assumed to be $[MeNH_2NH_2][O_2CMeNNH_2]$ Unfortunately, this product was thermally unstable even at room temperature and no elemental analysis could be obtained.

$$2\ MeNHNH_2 + CO_2 \xrightarrow{EtOH,\ 0^\circ} [MeNH_2NH_2][O_2CMeNNH_2] \qquad (5.2)$$

Unlike carbazic acid itself, methylcarbazic acid appears not to have formed. Reaction of CO_2 with $MeNHNH_2$ in aqueous solution (following the method of preparation of $\overset{-}{O_2}CNH\overset{+}{N}H_3$ from N_2H_4) did not result in methylcarbazic acid owing to rapid hydrolysis.

Protonation and nitration studies have shown that both nitrogens in $MeNHNH_2$ can be protonated resulting in a $[MeNH_2NH_2]^+$:$[MeNHNH_3]^+$ ratio of 2.6:1 (in dil $HCl/HClO_4$ media) [254,255]. Also the reaction of the alkyl carbonates $(RO)_2CO$

(R=Me,Et) with methylhydrazine similarly yields two isomers (5.3) [256].

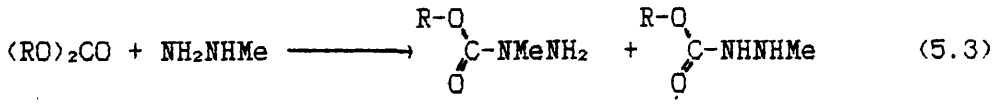

$$(RO)_2CO + NH_2NHMe \longrightarrow R\text{-}O\text{-}C(=O)\text{-}NMeNH_2 + R\text{-}O\text{-}C(=O)\text{-}NHNHMe \qquad (5.3)$$

However, reaction of CO_2 with $MeNHNH_2$ produces only one carbazate isomer, as implied by IR spectroscopy and subsequent complex formation. Electronic considerations would suggest the MeNH- nitrogen to be the most basic and hence the favoured position of CO_2 attack (structure I) (5.4).

I II

A study of the reactions of the methylcarbazate anion with first-row transition metal ions have led to claims by Srivastava that methylcarbazato-complexes can be isolated. Thus, reactions with $[Ni(OH_2)_6]Cl_2$ in EtOH were said to give $[MeNH_2NH_2][Ni(O_2CMeNNH_2)_3].2H_2O$ [145], and the cobalt(II) [147] and copper(II) [117] analogues were also reported. The neutral chromium(III) complex $[Cr(O_2CMeNNH_2)_3]$ was also reported [146].

5.2.3 REACTION OF METHYLCARBAZATE ANION WITH CHROMIUM(III)

Srivastava reported [146] that reaction of CO_2 with an ethanolic solution of chromium(III) chloride and methylhydrazine produced the violet-blue solid $Cr(O_2CMeNNH_2)_3$.

A similar reaction using $[Cr(OH_2)_4Cl_2]Cl.2H_2O$ and $MeNHNH_2$ in EtOH carried out in this work yielded a pale blue solid. Analytical and spectroscopic data suggest the product to be a

hydroxochromium(III) species containing one uncoordinated methylhydrazine or methylhydrazinium moiety per metal atom. We have therefore not been able to confirm that the procedure reported by Srivastava leads to tris(methylcarbazato)chromium(III).

However, the reaction of $[Cr(OH_2)_4Cl_2]Cl.2H_2O$ with preformed $[MeNH_2NH_2][O_2CMeNNH_2]$, (prepared by passage of CO_2 through a solution of $MeNHNH_2$ in EtOH for several hours), in EtOH at ~70°C resulted in the precipitation of the pink, microcrystalline, air and thermally stable compound $Cr(O_2CMeNNH_2)_3.H_2O$. This complex appears to be insoluble in all common solvents, except water which causes decomposition.

$$6MeNHNH_2 \xrightarrow[CO_2]{EtOH,\Delta} 3[MeNH_2NH_2][O_2CMeNNH_2] \xrightarrow[CO_2]{[Cr(OH_2)_4Cl_2]Cl/EtOH} Cr(O_2CMeNNH_2)_3.H_2O \qquad (5.5)$$

The magnetic susceptibility (χ_{corr} = 18.08×10^{-6} cm^3g^{-1}, μ_{eff} = 3.84 BM at 292K) and diffuse reflectance electronic spectrum (see TABLE No 5.5) of the complex are consistent with a t_{2g}^3 octahedral chromium(III) electronic configuration.

TABLE No 5.5 Diffuse Reflectance Electronic Spectra of Chromium(III) Carbazates / nm.

$Cr(O_2CMeNNH_2)_3.H_2O$	$Cr(O_2CNHNH_2)_3.2H_2O$	Assignment
517 (s)	523 (s)	$^4T_{2g} \leftarrow {}^4A_{2g}$
384 (ms)	395 (ms)	$^4T_{1g} \leftarrow {}^4A_{2g}$

The parameter Δ_o (19300 cm^{-1}), obtained directly from the $^4T_{2g} \leftarrow {}^4A_{2g}$ transition. is slightly greater than that calculated for

$Cr(O_2CNHNH_2)_3.2H_2O$ (19100 cm^{-1}). The B and β values of 644 cm^{-1} and 0.70 have been calculated from the spectral data of $Cr(O_2CMeNNH_2)_3.H_2O$. These can be compared to B and β values of 587 cm^{-1} and 0.64 calculated for $Cr(O_2CNHNH_2)_3.2H_2O$, which indicates a slight decrease in metal-ligand covalency on moving from carbazate to methylcarbazate.

The infra-red spectrum shows the presence of coordinated methylcarbazate groups and uncoordinated water molecules, the broad $\nu(OH_2)$ indicating some hydrogen-bonding (see TABLE No 5.6 and FIG No 5.2).

FIGURE No 5.2 Infra-red spectrum of $Cr(O_2CMeNNH_2)_3.H_2O$

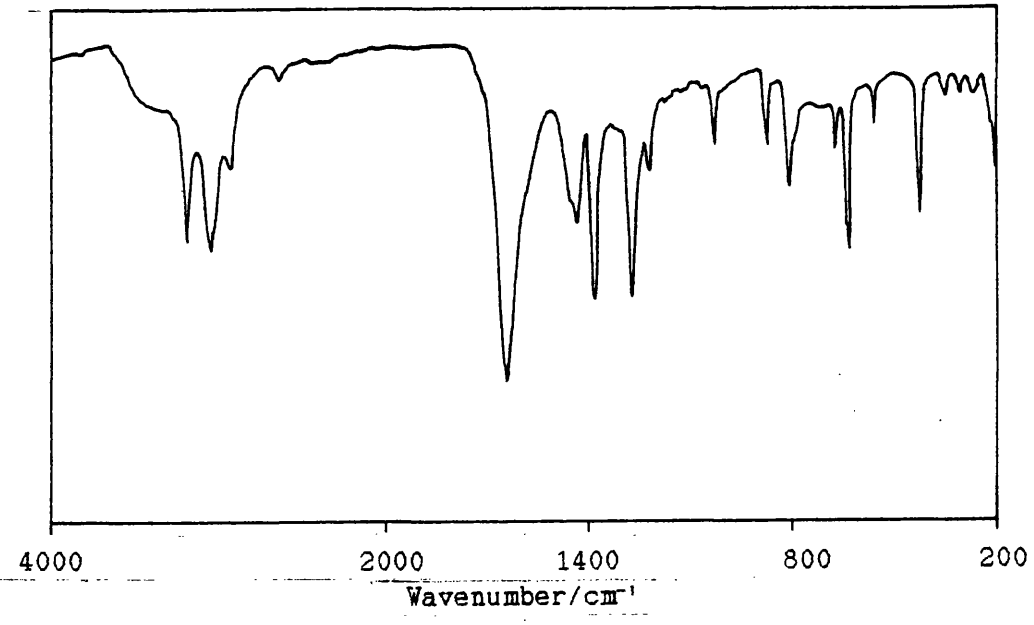

The spectrum is difficult to assign with confidence, as no IR data for the few other known methylcarbazate complexes have been reported. In a simplified treatment, the IR spectrum of the methylcarbazate anion may be approximated to the $-NH_2$ of Me_2NNH_2,

TABLE No 5.6 Infra-red Spectrum of $Cr(O_2CMeNNH_2)_3.H_2O$

Spectrum / cm^{-1}	Tentative Assignment
~3320 (w,br)	ν(OH) -uncoordinated H_2O
3182 (ms)	$\nu(NH_2)$
3041 (ms)	
2931 (mw)	$\nu(CH_3)$
1635 (vs)	$\nu_a(CO_2)$ + $\delta(NH_2)$
1453 (mw)	$\delta(CH_3)$
1432 (m,br)	$\nu_s(CO_2)$
1380 (ms)	$\delta(CH_3)$
1320 (vw)	$\omega(NH_2)$?
1266 (s)	skeletal stretch
1218 (m)	$\omega(CH_3)$
1168 (vw)	
1008 (m)	$r(NH_2)$
871 (m)	skeletal stretch
805 (ms)	δ(OCO) ?
792 (m,sh)	
666 (m)	$t(NH_2)$?
659 (mw,sh)	
635 (ms,sh)	π(COO)
630 (s)	
554 (mw)	r(COO)
415 (s)	ν(MO) + ν(MN)
348 (w)	
302 (w)	

the MeNH of $MeNHNH_2$ and a $-CO_2$ moiety, and the provisional assigments of TABLE No 5.6 take this approach.

The amino group in Me_2NNH_2 has 6 fundamental vibrations which can be described as two $\nu(NH_2)$ modes, as well as $\omega(NH_2)$, $r(NH_2)$, $\delta(NH_2)$ and $t(NH_2)$ vibrations [257]. Bands can be assigned to each of these with varying degrees of confidence. The $\nu(NH_2)$ vibrations are easily assigned to bands at 3182 and 3041 cm^{-1}, but $\delta(NH_2)$ is hidden beneath the intense $\nu_a(CO_2)$ at 1635 cm^{-1}. The weak absorption

at 1320 cm^{-1} is possibly associated with $\omega(NH_2)$, the corresponding vibration in $Cr(O_2CNHNH_2)_3.2H_2O$ being assigned to a band at 1308 cm^{-1}. The $r(NH_2)$ motion has been assigned to a medium intensity absorption at 1008 cm^{-1}.

Vibrations associated with the methyl group are barely shifted from their positions in $MeNHNH_2$ [223], but no band appears in the 1120 cm^{-1} region as expected for $r(CH_3)$.

The CO_2 vibrations (see TABLE No 5.6) appear at values typical of coordinated carboxylates. The separation between the anti-symmetric and symmetric $\nu(CO_2)$ vibrations, (203 cm^{-1}), indicates that the carboxylate part of each anion is probably unidentate (this is the only firm trend which is thought to be obtained from a consideration of Δ values [161]), as expected if the methylcarbazates are *O,N*-chelating.

The DTA and TG investigations of $Cr(O_2CMeNNH_2)_3.H_2O$ were carried out in air. Five exothermic DTA peaks (see TABLE No 5.7 and FIG No 5.3) were detected.

The first exothermic peak at 195°C relates to water loss and the onset of carbazate decomposition. However, TG does not show a specific step, only a slight shoulder on the main decomposition step. The heat change associated with the DTA peak at 195°C is the greatest of the five heat changes, and as with $Cr(O_2CNHNH_2)_2.H_2O$, the loss of water probably results in a fundamental structural change, which destroys the inherent stability displayed by the original complex. As a result the methylcarbazate rapidly decomposes. It is apparent that the water in $Cr(O_2CMeNNH_2)_3.H_2O$ is more strongly bound than that in $Cr(O_2CNHNH_2)_3.2H_2O$ as DTA of the latter complex shows that the water molecules are lost with endothermic heat changes at lower temperatures (136 and 169°C).

TABLE No 5.7 DTA of $Cr(O_2CMeNNH_2)_3.H_2O$ in Air.

Peak Positions (heat change) / °C
195 (+), 231 (+), 256 (+), 288 (+), 410 (+)

The methylcarbazate decomposition appears complex, three exothermic DTA peaks being detected. This complexity may be related to the presence of oxygen. Unfortunately, the DTA of $Cr(O_2CMeNNH_2)_3.H_2O$ could not be run in argon for comparative purposes due to the unavailability of the equipment. The final exothermic peak at 410°C appears to be related to an oxide modification resulting in the formation of Cr_2O_3.

$$Cr(O_2CMeNNH_2)_3.H_2O \xrightarrow{195^\circ} 'Cr(O_2CMeNNH_2)_3' \xrightarrow{231/256/288^\circ} 'CrO_x' \xrightarrow{410^\circ} Cr_2O_3 \qquad (3.6)$$

FIGURE No 5.3 DTA and TG of $Cr(O_2MeNNH_2)_3.H_2O$

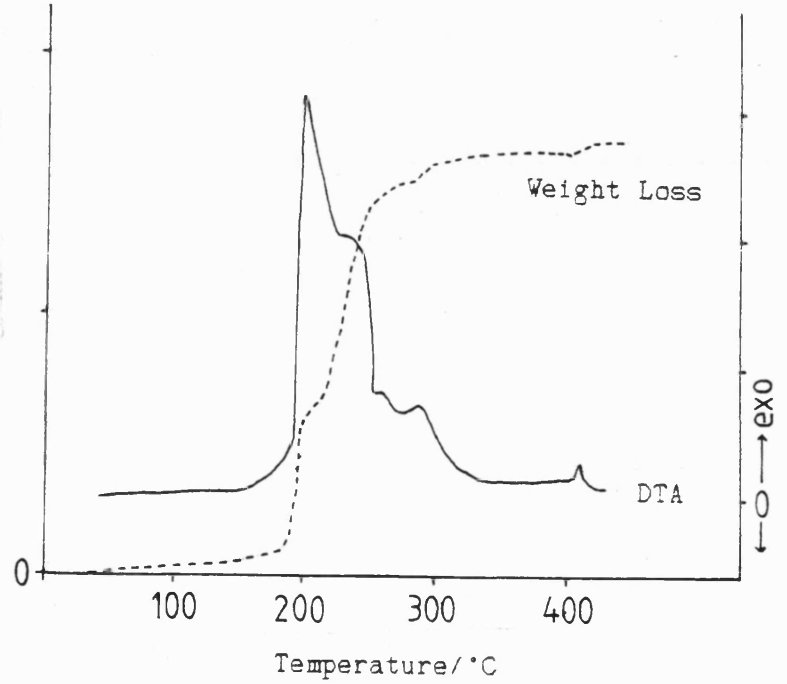

As demonstrated for $Cr(O_2CCH_2NH_2)_3.H_2O$ [227], $Cr(O_2CMeNNH_2)_3.H_2O$ is likely to be enantiomorphic. There appears to be strong hydrogen bonding involving the water molecules within the complex, and this feature plays a key role in the stability of the complex. Once the water is lost the complex is no longer stable and rapidly decomposes.

The above results are not in agreement with those of Srivastava [140], who reported the formation of anhydrous $Cr(O_2CMeNNH_2)_3$ from either the reaction of CO_2 with solutions of $MeNHNH_2$ and $[Cr(OH_2)_4Cl_2]Cl.2H_2O$ in ethanol or the addition of $[Cr(OH_2)_4Cl_2]Cl.2H_2O$ in EtOH to CO_2-saturated $MeNHNH_2$. The data presented in this work, clearly suggest that $Cr(O_2CMeNNH_2)_3.H_2O$, and not the anhydrous compound, is formed in the chromium(III)-methylcarbazate system.

5.2.4 REACTION OF THE METHYLCARBAZATE ANION WITH CHROMIUM(II)

It has been shown that the addition of a methyl substituent to hydrazine does not appear to significantly alter the coordination potential of the hydrazine with respect to chromium(II). Comparisons of $[Cr(N_2H_4)_2Cl_2]_n$ and $[Cr(NH_2NHMe)_2Cl_2]_n$ suggest similar structural features occur, although the methylhydrazine complex appears somewhat less stable to atmospheric exposure. Given the formation of an air-stable chromium(II) carbazate, $Cr(O_2CNHNH_2)_2.H_2O$, it seemed reasonable to expect that methylcarbzate would also form a stable chromium(II) species.

The reaction of $[Cr(OH_2)_6]^{2+}$ with $[MeNH_2NH_2][O_2CMeNNH_2]$, (preformed in solution), in EtOH at 0°C under N_2/CO_2 initially gave a dark blue solution. This parallels the initial stages of $Cr(O_2CNHNH_2)_2.H_2O$ formation. However, instead of the precipitation

of a chromium(II) product, on leaving at 0°C under N_2/CO_2 rapid oxidation ensued producing $Cr(O_2CMeNNH_2)_3.H_2O$ (3.7).

$$[Cr(OH_2)_6]^{2+} + [MeNH_2NH_2][O_2CMeNNH_2] \xrightarrow[CO_2,N_2]{EtOH,0^\circ} \text{'}Cr(O_2CMeNNH_2)_2\text{'} \quad \textit{non-isolable}$$

$$\xrightarrow{\text{rapid}} Cr(O_2CMeNNH_2)_3.H_2O \qquad (3.7)$$

As discussed previously (see SECTION No 3.5), $Cr(O_2CNHNH_2)_2.H_2O$ can be isolated as a stable complex as a result of its rapid precipitation from the reaction solution. In the corresponding methylcarbazate reaction that advantage is not present, the chromium(II) methylcarbazate produced remains in solution so that oxidation can occur rapidly to produce a chromium(III) species. The same oxidation can be induced for the unsubstituted carbazate system but requires the presence of a higher concentration of $[N_2H_5][O_2CNHNH_2]$.

It is possible that although chromium(II) methylcarbazate does form in solution, it does not contain in its structure a hydrogen-bonded water which earlier has been suggested to play a crucial role in stabilizing carbazate and substituted carbazate complexes. As a result a solid product is not produced and so oxidation can rapidly occur.

THE 1,1-DIMETHYLHYDRAZINE/DIMETHYLCARBAZATE SYSTEM

5.3 1,1-DIMETHYLHYDRAZINE

5.3.1 BACKGROUND

1,1-Dimethylhydrazine may be expected to show some differences in its coordination behaviour when compared to hydrazine and methylhydrazine. The substitution of two methyl groups on a nitrogen, affects the donor ability of the lone pair on that nitrogen in two opposing ways. Firstly, the basicity of the lone pair will be enhanced by electron donation from the methyl groups, but secondly, there will be an undesirable steric hindrance effect.

The reactions of first-row transition metal ions with Me_2NNH_2 result in the formation of complexes of general formula $[MX_2(Me_2NNH_2)_2]$ (M=Fe, X=Cl,Br [85]; M=Co, X=Cl,Br,I,NCS [25,40]; M=Ni, X=Cl [26]). From electronic spectral and magnetic evidence tetrahedral structures with unidentate Me_2NNH_2 ligands were proposed for the cobalt complexes. However, the iron and nickel complexes were thought to be octahedral polymers with either halide or dimethylhydrazine bridges. The compounds TiX_4 (X=Cl,Br,I) were reported to react with Me_2NNH_2 by solvolysis forming mixtures of $TiX_3(Me_2NNH)$ and $2Me_2NHNH_2X$ [91].

A crystal structure determination of $[Ru(\eta^4\text{-cod})(Me_2NNH_2)_3][PF_6]$ [49] shows the presence of unidentate Me_2NNH_2 ligands coordinated by their non-methylated nitrogen atoms, clearly the steric hindrance factor is more important than increased lone pair basicity of the dimethylated nitrogen in determining the coordination mode in this complex. However, in $[(RuCl(H)(\eta^4\text{-cod}))_2(\mu\text{-}Me_2NNH_2)]$ [48], Me_2NNH_2 acts as an unsymmetrical bridging ligand, the Ru-NMe_2 bond (2.24Å) being longer than the Ru-NH_2 bond (2.12Å).

No reactions of chromium(II) with Me_2NNH_2 have been reported previously. So an investigation of the chromium(II)-1,1-dimethylhydrazine system was undertaken.

5.3.2 REACTION OF CHROMIUM(II) CHLORIDE WITH 1,1-DIMETHYLHYDRAZINE

The reaction of $CrCl_2(MeCN)_2$ (prepared from anhydrous $CrCl_2$ and MeCN), with Me_2NNH_2 in anhydrous MeCN at room temperature under N_2 results in the formation of the blue-green air-sensitive solid $[CrCl_2(Me_2NNH_2)_2]_n$ (5.8).

$$CrCl_{2\,(s)} \xrightarrow[N_2]{MeCN} CrCl_2(MeCN)_2 + 2Me_2NNH_2 \xrightarrow[N_2]{MeCN} [CrCl_2(Me_2NNH_2)_2]_n \quad (5.8)$$

Reaction of Me_2NNH_2 with $[Cr(OH_2)_6]X_2$ (X=Cl,Br) in aqueous /ethanolic media resulted in chromium(II) hydroxide formation. The bromide analogue $[CrBr_2(Me_2NNH_2)_2]_n$ could not be prepared because of the unavailability of anhydrous $CrBr_2$.

The product has a magnetic moment (χ_{cgs} = 39.90×10^{-6} cm^{3}g^{-1}, μ_{eff} = 4.85 BM at 298K) consistent with a mononuclear high spin d^4 electronic configuration. The magnetic moment is close to 4.90 BM, the spin-only value, indicating little orbital contribution.

The diffuse reflectance electronic spectrum of $[CrCl_2(Me_2NNH_2)_2]_n$ contains a prominent band at 662 nm, assigned to superimposed $^5B_{2g}, ^5E_g \leftarrow {}^5B_{1g}$ transitions. The low energy $^5A_{1g} \leftarrow {}^5B_{1g}$ transition has not been observed in the expected position below 1200 nm, though it may be hidden by background noise. Additional shoulders observed at 477 and 460 nm may be due to chromium(III) impurity.

The electronic spectrum of $[CrCl_2(Me_2NNH_2)_2]_n$ indicates that the ligand environment of the chromium(II) is more like that of $[CrCl_2(NH_2NHPh)_2]_n$ than those of $[CrCl_2(NH_2NHR)_2]_n$ (R=H and Me) (see TABLE No 5.1). The Δ_o value (15100 cm^{-1}) is slightly greater than Δ_o of $[Cr(OH_2)_6]^{2+}$ (14000 cm^{-1}) [221] as would be expected from the ligation effect of nitrogen donors. The molecular structure of $[CrCl_2(NH_2NHPh)_2]_n$ is suspected to contain bridging chlorides and unidentate phenylhydrazines (see SECTION 4.1), whilst it is known that $[Cr(N_2H_4)_2Cl_2]_n$ contains bridging hydrazine ligands (see SECTION 3.3). Given the similarity of the electronic spectra of $[CrCl_2(NH_2NHPh)_2]_n$ and $[CrCl_2(Me_2NNH_2)_2]_n$, the latter may adopt a structure containing bridging chloride and unidentate dimethylhydrazine ligands.

The infra-red spectrum of $[CrCl_2(Me_2NNH_2)_2]_n$ has been assigned by reference to the assignment of the vibrational spectrum of uncordinated Me_2NNH_2 published by Durig and Harris [257] and the vibrational spectra of $MX_2(Me_2NNH_2)_2$ complexes (M=Zn,Cd; X=Cl,Br,I) reported by Green [258] (see TABLE No 5.8 and FIG No 5.4).

Durig and Harris assigned the vibrational spectra of Me_2NNH_2 and Me_2NND_2 by assuming C_1 symmetry and a *gauche* conformation. Independently, Anthoni, Larsen and Nielsen [259] also assigned the infra-red spectra of Me_2NNH_2, Me_2NNH_2-d_2 and Me_2NNH_2-d_8, but assumed the point group C_s was appropriate. Consequently, some assignments of the two studies differ.

The assignments of Durig and Harris have been used here, mainly because of the consistency of their assignments with those of N_2H_4 [155] and $MeNHNH_2$ [223].

NH_2 vibrations

Six fundamental vibrations are associated with the amino group in 1,1-dimethylhydrazine and can conveniently be described as two NH_2 stretching motions, a deformation or scissoring mode, wagging and rocking vibrations and a torsional oscillation.

Three $\nu(NH_2)$ absorptions are found in the IR spectrum of $[CrCl_2(Me_2NNH_2)_2]_n$ at 3233, 3208 and 3183 cm^{-1}. This is a ~100 cm^{-1} decrease from the $\nu(NH_2)$ vibrations of free Me_2NNH_2. The fact that $\nu(NH_2)$ shifts so substantially on coordination implies that the amino nitrogen is directly coordinated to the chromium. If the Me_2NNH_2 ligands are unidentate they must be bonded only through their amino nitrogen atoms as in $[RuH(cod)(NH_2NMe_2)_3]^+$ [49], rather than *via* the dimethylamino nitrogen as favoured on electronic grounds.

The $\delta(NH_2)$ mode is split in $[CrCl_2(Me_2NNH_2)_2]_n$ with components at 1588 and 1574 cm^{-1}, again a slight decrease from that found in free Me_2NNH_2 (1587 cm^{-1}). The wagging mode in free Me_2NNH_2 is found at 1319 cm^{-1}. In N_2H_4 complexes, the frequency of $\omega(NH_2)$ increases on coordination [141], so has been assigned to the 1354 cm^{-1} band in $[CrCl_2(Me_2NNH_2)_2]_n$. Durig and Harris [257] assigned $r(NH_2)$ in Me_2NNH_2 to a band at 908 cm^{-1} while Anthoni *et al.* [259] preferred a band at 945 cm^{-1}. In N_2H_4 complexes, this vibration is sensitive to coordination, increasing by ~100 cm^{-1}. In $[CrCl_2(Me_2NNH_2)_2]_n$ a band at 1020 cm^{-1} has, therefore, been assigned to $r(NH_2)$, a shift of ~110 cm^{-1} (This band could also be due to $r(CH_3)$). Green [258] found this band in $[MX_2(Me_2NNH_2)_2]_n$ (M=Zn,Cd; X=Cl,Br) to be at best very weak in the infrared, often being only Raman active. However it is intense in the spectrum of $[CrCl_2(Me_2NNH_2)_2]_n$, possibly indicating a change of structure between the two types of

complexes. A band at 280 cm^{-1} has been assigned to $t(NH_2)$ of Me_2NNH_2 [257], and this band should increase on coordination, but no suitable absorption appears in the IR specrum of $[CrCl_2(Me_2NNH_2)_2]_n$. Green [257] assigned $t(NH_2)$ in $[ZnX_2(Me_2NNH_2)_2]_n$ (X=Cl, Br, I) to medium/weak absorptions in the 560-545 cm^{-1} region. However, these complexes were thought to have monomeric tetrahedral structures and the change to octahedral symmetry for $[CrCl_2(Me_2NNH_2)_2]_n$ may alter the nature of the $t(NH_2)$ vibration.

CH_3 vibrations

Eighteen of the 30 fundamental vibrations of Me_2NNH_2 are expected to arise from motions of the two methyl groups. These comprise six CH_3 stretching vibrations. six methyl deformations, four rocking vibrations and two torsional vibrations.

If the Me_2NNH_2 ligands of $[CrCl_2(Me_2NNH_2)_2]_n$ are unidentate, being bonded via the amino nitrogens, the methyl vibrations would not be expected to show significant shifts from their free ligand positions. The assignments given in TABLE No 5.8 are based on this assumption.

Skeletal vibrations

Three skeletal stretches are expected and although mixed in character they can conveniently be described as two $\nu(CN)$ and one $\nu(NN)$ vibrations.

The three skeletal vibrations in Me_2NNH_2 are assigned to bands at 1246, 966 and 808 cm^{-1}. The predominately NN skeletal stretch should be most sensitive to coordination, while the two $\nu(CN)$ vibrations are expected to be less so. A band at 1286 cm^{-1} is assigned as the highest frequency skeletal stretch, a shift of 40

cm^{-1} on coordination. The free Me_2NNH_2 skeletal stretch at 966 cm^{-1} is found as a weak band at 991 cm^{-1} in $[CrCl_2(Me_2NNH_2)_2]_n$. This band is not found in the IR spectra of $[MX_2(Me_2NNH_2)_2]_n$ (M=Zn,Cd) [258], but is strong in the Raman spectra of these complexes, indicating a likely skeletal nature to the vibration.

The third skeletal stretch cannot confidently be assigned for $[CrCl_2(Me_2NNH_2)_2]_n$, although a band is found in the IR spectrum at 809 cm^{-1} which could correspond to the skeletal stretch of Me_2NNH_2 reported at 808 cm^{-1}. The lack of sensitivity to coordination is puzzling.

Three skeletal bending modes of Me_2NNH_2 are found at 459, 441 and 411 cm^{-1}, with $[CrCl_2(Me_2NNH_2)_2]_n$ displaying bands at 441 and 434 cm^{-1}. However, comparison with the spectra of $[Cr(N_2H_3R)_2X_2]_n$ suggests that ν(MN) stretches are also expected in this region. Without the advantage of deuteration studies or comparisons with the spectra of other $[CrX_2(Me_2NNH_2)_2]_n$ complexes, it is not possible to unambiguously assign these absorptions, but assignments as ν(CrN) stretches are favoured. A further band in this region at 302 cm^{-1} is assigned to ν(CrCl). Such assignments are in line with those suggested for $[CrCl_2(NH_2NHPh)_2]_n$, ν(MN) = 390 cm^{-1} and ν(MCl) = 323 cm^{-1}. A *trans*-MN_2X_4 unit of D_{4h} symmetry is predicted to possess one ν(MN) and one ν(MX) IR active band. As $[CrCl_2(Me_2NNH_2)_2]_n$ appears to show two ν(MN) absorptions. some distortion from D_{4h} symmetry may be indicated, although one band may be a ligand skeletal bending mode.

The spectroscopic data presented here indicate that $[CrCl_2(Me_2NNH_2)_2]_n$ is likely to be polymeric with bridging chloride and unidentate dimethylhydrazine ligands, the latter being coordinated *via* their $-NH_2$ nitrogen atoms.

TABLE No 5.9 Infra-red Spectra of $[MCl_2(Me_2NNH_2)_2]_n$ (M=Cr,Zn,Cd) and the Vibrational Spectrum of Me_2NNH_2 / cm^{-1}.

Me_2NNH_2[a]	$CrCl_2(Me_2NNH_2)_2$[b]	$ZnCl_2(Me_2NNH_2)_2$[c]	$CdCl_2(Me_2NNH_2)_2$[c]	Assignment
3338	3233 (s)	3240	3265	
3315	3208 (m,sh)	3170	3155	$\nu(NH_2)$
	3183 (mw)	3010	3091	
	3071 (ms)			
2980	2986 (w)	2990		
2061	2952 (ms)	2959	2940	
2816	2893 (mw)	2920	2905	$\nu(CH_3)$
2777	2868 (m)	2870	2860	
	2833 (m)	2814	2825	
	2784 (m)	2799	2775	
1587	1588 (s)	1597	1588	$\delta(NH_2)$
	1574 (mw,sh)			
1464	1453 (s)	1458	1454	
1449	1430 (mw)	1427	1426	$\delta(CH_3)$
1402	1402 (w)	1404	1398	
1319	1354 (w)		1340	$\omega(NH_2)$
1246	1286 (s)	1297	-	skeletal stretch
1215	1222 (mw)	1218	1215	
1144	1154 (s)	1160		$r(CH_3)$
		1148	1133	
1060	1090 (w)	1084	1089	
1032	1020 (m)	1010	1014	$r(CH_3)$ or $r(NH_2)$?
966	991 (vw)	992 R	989 R	skeletal stretch
908				$r(NH_2)$
808	809 (m)	800	802 R	skeletal stretch
		720		
295	703 (ms)	705		$t(NH_2)$?
		559	620	
	441 (m,sh)		432	$\nu(MN)$
	434 (s)	412	411	
	302 (s)	293	207 R	$\nu(MCl)$
		241		

R - Raman active only, [a] - from ref. [257], [b] - present work,

[c] - from ref. [258].

FIGURE No 5.4 Infra-red Spectra of $[CrCl_2(Me_2NNH_2)_2]_n$ and $[Cr_2(O_2CMe)_4(\mu\text{-}Me_2NNH_2)]$.

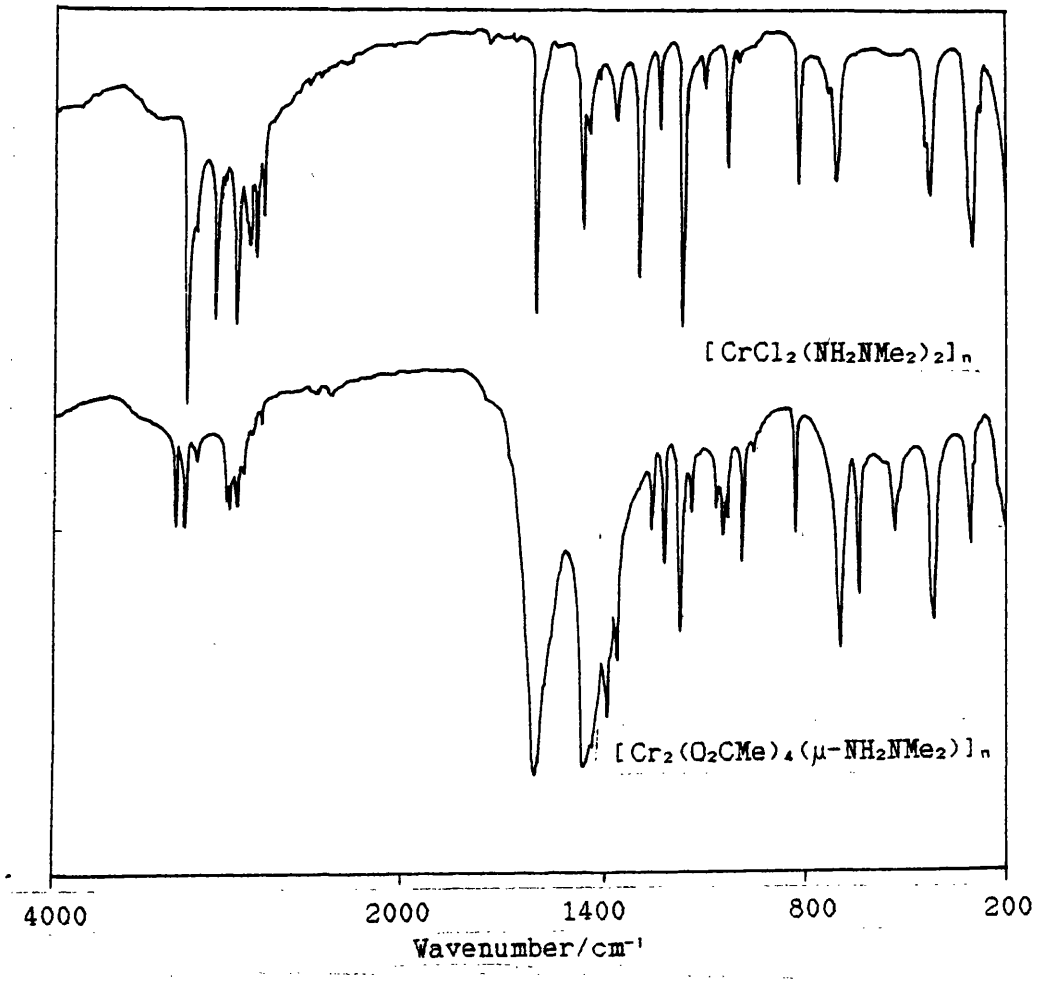

5.3.3 REACTION OF CHROMIUM(II) ACETATE WITH 1,1-DIMETHYLHYDRAZINE

The reaction of $Cr_2(O_2CMe)_4(EtOH)_2$ with Me_2NNH_2 in EtOH at room temperature under N_2 produces a red-orange. air-sensitive, solid with analysis consistent with the formulation $Cr_2(O_2CMe)_4(NH_2NMe_2)$ (see 5.9). The stoichiometry implies that Me_2NNH_2 coordinates in a bridging manner.

$$Cr_2(O_2CMe)_4(H_2O)_2 \xrightarrow[in\ vacuo]{110^\circ} Cr_2(O_2CMe)_4 \xrightarrow[N_2]{EtOH} Cr_2(O_2CMe)_4(EtOH)_2 \qquad (5.9)$$

$$Cr_2(O_2CMe)_4 \xrightarrow[N_2]{Me_2NNH_2/EtOH} Cr_2(O_2CMe)_4(NH_2NMe_2)$$

The addition of EtOH to this product appears to partially cleave chromium-nitrogen bonds to form a species containing coordinated dimethylhydrazine and ethanol as indicated by IR evidence. However, no other characterisation was carried out.

The quadruple metal-metal bond of the hydrate is retained on reaction with Me_2NNH_2 as shown by magnetic susceptibility (χ_{corr} = 1.06×10^{-6} cm^3g^{-1}, μ_{eff} = 0.59 BM per Cr at 296K) and electronic spectral measurements (see TABLE No 5.9).

TABLE No 5.9 Electronic Spectral Measurements of $Cr_2(O_2CMe)_4L_2$ species / nm.

L =	½(Me_2NNH_2)		½(N_2H_4)	H_2O	Assignment
	reflectance	solution*	reflect.	reflect.	
	479 (m,br)	491 (m,br)	478 (m,br)	486 (s,br)	$\delta \rightarrow \pi^*$
	464 (w,sh)				
	359 (s,sh)	345 (s,sh)	360 (s,sh)	347 (s,sh)	
	333 (vs)	327 (vs)	333 (vs)	326 (vs)	$np_x \rightarrow \pi^*$

* - MeOH solution.

The electronic spectrum of $[Cr_2(O_2CMe)_4(\mu\text{-}Me_2NNH_2)]$ in MeOH shows a significant shift of the $\delta \rightarrow \pi^*$ transition when compared to the solid-state reflectance spectrum, perhaps indicative of further reaction with alcohols as mentioned above. Indeed, the peak maximum of the $\delta \rightarrow \pi^*$ transition, 491 nm, for $[Cr_2(O_2CMe)_4(\mu\text{-}Me_2NNH_2)]$ in MeOH is close to that of $Cr_2(O_2CMe)_4(H_2O)_2$, 486 nm, which may indicate *O*-donors rather than *N*-donors coordinating axially to the $Cr_2(O_2CMe)_4$ unit in solution. However, the $\delta \rightarrow \pi^*$ transition has yet to be shown to be a specific indicator of axial coordination to the $Cr_2(O_2CMe)_4$ core.

The infra-red spectrum of $[Cr_2(O_2CMe)_4(\mu\text{-}Me_2NNH_2)]_n$ shows the presence of both coordinated acetate and dimethylhydrazine (see TABLE No 5.10 and FIG No 5.4). Assignments have been made by reference to the spectra of $Cr_2(O_2CMe)_4(H_2O)_2$ and other Me_2NNH_2 complexes. However, some absorptions presumably associated with bridging Me_2NNH_2 vibrations in the dinuclear complex are found at unexpected positions and consequently are difficult to assign by comparison with mononuclear complexes containing unidentate dimethylhydrazine ligands.

The $\nu(NH_2)$ absorptions (see TABLE No 5.10), show smaller coordination shifts than are found for $[CrCl_2(Me_2NNH_2)_2]_n$. Other NH-derived vibrations are difficult to assign, and it is also impossible to distinguish between the $\nu(CH_3)$ absorptions derived from the acetate groups and those of dimethylhydrazine. The carboxylate absorptions of the acetate groups are, however, easily assigned. The frequency difference between the antisymmetric and symmetric $\nu(COO)$ absorptions is 140 cm^{-1} indicative of bridging acetate groups, as expected. A band at 469 cm^{-1} has been assigned to $\nu(CrN)$ in $[Cr_2(O_2CMe)_4(\mu\text{-}N_2H_4)]_n$, so a band at 521 cm^{-1} with a shoulder at 508 cm^{-1} in the IR spectrum of $[Cr_2(O_2CMe)_4(\mu\text{-}Me_2NNH_2)]$, may be similarly assigned. The two components probably relate to the unsymmetrical nature of the Me_2NNH_2 bridge as found in $[\{RuCl(H)(\eta^4\text{-cod})\}_2(\mu\text{-}NH_2NMe_2)]$ [49].

In summary, the evidence acquired suggests that in $[Cr_2(O_2CMe)_4(\mu\text{-}Me_2NNH_2)]$, dimethylhydrazine is acting as a bridging ligand between two $Cr_2(O_2CMe)_4$ units. However, the Cr-N bonds appear relatively weak being cleaved by dissolution in methanol and ethanol.

TABLE No 5.10 Infra-red Spectrum of $[Cr_2(O_2CMe)_4(\mu\text{-}Me_2NNH_2)]$

Spectrum / cm^{-1}	Assignment
3310 (mw)	
3257 (mw)	$\nu(NH_2)$
3167 (vw)	
3005 (w)	
2980 (mw)	
2933 (mw, br)	$\nu(CH_3)$
2923 (mw, br)	
2883 (vw)	
1589 (vs)	$\nu_a(CO_2) + \delta(NH_2)$
1449 (vs)	$\nu_s(CO_2) + \delta_a(CH_3)$
1418 (s, sh)	$\delta_s(CH_3)$
1346 (ms)	$\omega(NH_2)$
1240 (mw)	skeletal stretch ?
1202 (m)	
1157 (s)	$r(CH_3)$ - Me_2NNH_2
1119 (w)	
1077 (vw)	
1050 (mw)	$r(CH_3)$ - O_2CMe
1029 (m)	
1014 (mw)	$r(NH_2)$?
975 (m)	skeletal stretch
936 (vw)	$\nu(CC)$
816 (m)	skeletal stretch
683 (s)	$\delta(OCO)$
632 (m)	$\pi(COO)$
521 (mw)	$\nu(MN)$
508 (w, sh)	
408 (s)	$\nu(MO)$
301 (m)	

5.4 REACTIONS OF Me_2NNH_2 WITH CO_2 AND CHROMIUM IONS

5.4.1 BACKGROUND

1,1-Dimethylhydrazine has long been known to form a carbazate on reaction with CO_2 [260,261], however little characterisation has

been reported. For example, it is not known whether [Me_2NHNH_2]-[$O_2CNHNMe_2$] or Me_2NNHCO_2H is the final product.

The reaction of trimethylsilyl-1,1-dimethylhydrazine, $Me_2NNHSiMe_3$ (and the analogous trimethylgermyl derivative) with CO_2 has been reported to give the trimethylsilyl ester of 3,3-dimethylcarbazate, $Me_2NNHCO_2SiMe_3$, a colourless thermally stable, solid (m.pt 76.6-77.0°C) [262,263].

The reaction of Me_2NNH_2 with CS_2 or CSe_2 was reported by Anthoni [264] to result in the formation of [Me_2NHNH_2][$X_2CNHNMe_2$] (X=S,Se). Treatment of these salts with aqueous 6N HCl resulted in the free dimethyldithio- (or diseleno-) carbazic acid, $X_2CNHNHMe_2$. A dipolar 'zwitterionic' configuration was proposed to account for the high stability observed for these compounds.

5.4.2 REACTION OF Me_2NNH_2 WITH CO_2

Only some preliminary work has been carried out on the Me_2NNH_2/CO_2 system and its interaction with chromium(II) and (III). Therefore, little characterisation of the products can be reported.

The passage of CO_2 through a solution of Me_2NNH_2 in Et_2O at 0°C for 3 hrs, resulted in a colourless, hygroscopic, thermally unstable, solid which is assumed to be [Me_2NHNH_2][$O_2CNHNMe_2$]. The product displays a complex IR spectrum (major absorptions; ν(NH) 3430, $\delta(NH_2)+\nu_a(CO_2)$ ~1620, $\nu_s(CO_2)$ 1450 cm^{-1}).

The passage of CO_2 through a methanol solution of Me_2NNH_2 in the presence of NaOH, resulted in the precipitation of a white solid (5.11), presumably sodium dimethylcarbazate.

$$Me_2NNH_2 + NaOH \xrightarrow[CO_2]{MeOH} Me_2NNHCO_2Na\ ? \qquad (5.11)$$

The IR spectrum of the solid indicates the presence of carboxylate ($\nu(CO_2)$, 1620, 1345?; $\delta(OCO)$, 810 cm^{-1}) and methyl ($\nu(CH)$, 2995,2930; $\delta(CH_3)$, 1475, 1440; $r(CH_3)$, 1075 cm^{-1}) vibrations, but no bands are assignable to NH vibrations, although $\nu(NH)$ would be expected to be broad and weak in a hydrogen-bonded structure.

Given the use of NaOH and CO_2 in the reaction, some carbonate formation may occur followed by further reaction with Me_2NNH_2.

The reaction of preformed $[Me_2NHNH_2][O_2CNHNMe_2]$ with NaOH in MeOH, results in the formation of a colourless solid, which, although showing some similarities with the solid discussed above, appears to be a different species. Similar carboxylate (1635, 1375 and 820 cm^{-1}) and methyl bands are present in the IR spectrum, but again no NH bands could be distinguished. These products remain to be characterised.

5.4.3 REACTIONS OF 1,1-DIMETHYLCARBAZATE WITH CHROMIUM(III)

Reaction of $[Me_2NHNH_2][O_2CNHNMe_2]$ with $[Cr(OH_2)_4Cl_2]Cl.2H_2O$ in EtOH produces a dark violet solution, from which a pale lilac solid precipitates on addition of excess Et_2O or MeCN. IR spectroscopy, however, suggests that the product is not a chromium(III) dimethylcarbazate, but rather a product containing dimethylhydrazinium cations. This system appears to resemble the chromium(III)-phenylcarbazate system from which no discrete product could be isolated.

Srivastava [146] reported that $Cr(O_2CNHNMe_2)_3$ could be prepared by passing CO_2 through a solution of $[Cr(OH_2)_4Cl_2]Cl.2H_2O$ and Me_2NNH_2 in EtOH. The above observations and the unreliability of other carbazate work reported by Srivastava suggests that this claim requires independent reinvestigation.

5.4.4 REACTION OF 1,1-DIMETHYLCARBAZATE WITH CHROMIUM(II)

The reaction of $[Me_2NHNH_2][O_2CNHNMe_2]$ with $[Cr(OH_2)_6]Cl_2$ in EtOH at 0°C under N_2/CO_2 resulted in a dark blue/violet solution without formation of a solid. Once isolated by evaporation or by addition of inert solvents, the solid was extremely air-sensitive exhibiting pyrophoric behaviour. IR spectroscopy indicates that the chromium(II) product was contaminated with Me_2NHNH_2Cl.

The reaction of supposed 'Me_2NNHCO_2Na' with $[Cr(OH_2)_6]Cl_2$ in MeOH at 0°C under N_2/CO_2 results in the precipitation of a purple solid, which was not isolated.

The coordination displayed by $Me_2NNHCO_2^-$ towards chromium(II) may be similiar to that shown by $PhNHNHCO_2^-$ in $Cr_2(O_2CNHNHPh)_4(MeOH)_2$ i.e *O,O*-bridging carboxylate type coordination. On the basis of electronic spectral evidence the complex $Cr(Me_2NNHCS_2)_3$ was considered to display *S,S*-coordination rather than *S,N*-coordination [226]. Therefore, it is likely that $Me_2NNHCO_2^-$ will show *O,O*-coordination towards metal ions.

5.5 EXPERIMENTAL

$MeNHNH_2$ was purified before use by distillation from KOH under N_2, at atmospheric pressure. The middle fraction (B.Pt 87-88°C) was collected.

5.5.1 REACTIONS OF CHROMIUM(II) AND (III) WITH $MeNHNH_2$

a) Preparation of $[CrCl_2(MeNHNH_2)_2]_n$

To a suspension of $CrCl_2$ (0.59 g, 4.79 mmol) in anhydrous MeCN (25 cm^3) under N_2 was added a solution of $MeNHNH_2$ (0.53 cm^3, 10.01 mmol) in anhydrous MeCN (20 cm^3). The light blue product formed rapidly, was filtered off under N_2, washed with MeCN, Et_2O and dried under a stream of N_2.

$C_2H_{12}Cl_2CrN_4$. Requires: C, 11.17; H, 5.63; N, 26.05. Found: C, 10.89; H, 5.21; N, 25.53 %.

b) Preparation of $[Cr_2(O_2CMe)_4(\mu\text{-}MeNHNH_2)]_n$

The complex $Cr_2(O_2CMe)_4(H_2O)_2$ was prepared as in 3.10.3d., 1.27 g, (3.37 mmol) being dehydrated *in vacuo* at 110°C for several hours. The resulting brown $Cr_2(O_2CMe)_4$ was added to anhydrous EtOH (25 cm^3) under N_2. This suspension was stirred at room temperature for 120 mins, before a solution of $MeNHNH_2$ (0.54 cm^3, 10.20 mmol) in anhydrous EtOH (15 cm^3) was added under N_2. The resulting reaction mixture was stirred for 60 mins, before the red-orange product was filtered off under N_2, washed with Et_2O and dried under a stream of N_2.

$C_9H_{18}Cr_2N_2O_8$. Requires: C, 27.88; H, 4.70; N, 7.25. Found: C, 28.34; H, 5.21; N, 6.76 %.

c) Reaction of $[Cr(OH_2)_4Cl_2]^+$ with $MeNHNH_2$

To a heated solution of $MeNHNH_2$ (1.24g, 27 mmol) in EtOH (50 cm^3) was added a solution of $[Cr(OH_2)_4Cl_2]Cl.2H_2O$ (0.80 g, 3 mmol) in EtOH (20 cm^3). The light blue-grey product precipitated almost immediately. The solid was filtered off in air, washed with EtOH and Et_2O and dried *in vacuo*.

Found; C, 6.43; H, 5.21; Cl, 10.80; Cr, 28.09; N, 13.82 %.

This corresponds to an elemental ratio of $CH_{9.6}Cl_{0.6}CrN_{1.8}$.

5.5.2 REACTIONS OF $MeNHNH_2$ WITH CO_2 AND CHROMIUM

a) Preparation of $[MeNH_2NH_2][O_2CMeNNH_2]$

Carbon dioxide was passed through a solution of $MeNHNH_2$ (2.30 g, 50 mmol) in EtOH (50 cm^3) for 180 mins. After this time the colourless product had precipitated, was filtered off under N_2 and dried *in vacuo*. The product was very hygroscopic, decomposing on contact with H_2O.

b) Preparation of $Cr(O_2CMeNNH_2)_3.H_2O$

A solution of $[MeNH_2NH_2][O_2CMeNNH_2]$ (25 mmol) was prepared by the passage of CO_2 through a solution of $MeNHNH_2$ (2.30 g, 50 mmol) in EtOH (90 cm^3) at 60°C for 120 mins. To this solution was added a solution of $[Cr(OH_2)_4Cl_2]Cl.2H_2O$ (1.33 g, 5.0 mmol) in EtOH (40 cm^3). The resulting pink, microcrystalline product was filtered off under N_2, washed with MeOH and Et_2O and dried *in vacuo*. The product was found to be soluble in DMSO, sparingly soluble in DMF, but decomposes on contact with H_2O.

$C_6H_{12}CrN_6O_7$. Requires: C, 21.37; H, 5.08; N, 24.92; Cr, 15.42.

Found: C, 20.97; H, 4.65: N, 24.32: Cr, 15.26 %.

c) Reaction of $[MeNH_2NH_2][O_2CMeNNH_2]$ with Chromium(II)

To a solution of $[MeNH_2NH_2][O_2CMeNNH_2]$ (12.5 mmol) in MeOH (30 cm^3) (formed as in 5.5.2b) under N_2/CO_2 at -10°C, was added a solution of $[Cr(OH_2)_6]Cl_2$ (1 mmol) in MeOH (formed by reaction of conc aqueous HCl (0.17 cm^3, 2 mmol) with electrolytic chromium metal (0.50 g) in deoxygenated MeOH (15 ml) under N_2). Initially a purple solution formed without solid formation, but on standing $Cr(O_2CMeNNH_2)_3.H_2O$ gradually precipitated.

5.5.3 REACTIONS OF CHROMIUM(II) WITH Me_2NNH_2

Me_2NNH_2 was purified before use by distillation from KOH under N_2, at atmospheric pressure. the middle fraction (B.Pt 62-63.5°C) being collected.

a) Preparation of $[CrCl_2(Me_2NNH_2)_2]_n$

To a suspension of $CrCl_2$ (0.71 g, 5.74 mmol) in anhydrous MeCN (25 cm^3) under N_2, was added a solution of Me_2NNH_2 (0.92 cm^3, 12.03 mmol) in anhydrous MeCN (20 cm^3). On addition, a blue solution formed from which the pale blue/green product rapidly precipitated. The product was filtered off under N_2, washed with MeCN and Et_2O and dried under a stream of N_2.

$C_4H_{16}CrN_4Cl_2$. Required: C, 19.76; H, 6.63; N, 23.05. Found: C, 19.48; H, 6.85; N, 22.73 %.

b) Preparation of $[Cr_2(O_2CMe)_4(\mu\text{-}Me_2NNH_2)]_n$

The complex $Cr_2(O_2CMe)_4(H_2O)_2$ (1.30 g, 3.45 mmol) was dehydrated as in 5.5.1b. To a suspension of $Cr_2(O_2CMe)_4$ in anhydrous EtOH (25 cm^3) under N_2 at room temperature was added

a solution of Me_2NNH_2 (0.84 cm^3, 10.99 mmol) in anhydrous EtOH (10 cm^3). The product was filtered off under N_2, washed with Et_2O and dried under a stream of N_2.

$C_{10}H_{20}Cr_2N_2O_8$. Required: C, 30.01; H, 5.04: N, 7.00. Found: C, 29.96; H, 6.58; N, 5.33 %.

5.5.4 REACTIONS OF Me_2NNH_2 WITH CO_2 AND CHROMIUM

a) Preparation of $[Me_2NHNH_2][O_2CNHNMe_2]$

The passage of CO_2 through a solution of Me_2NNH_2 (2.50 cm^3, 32.7 mmol) in Et_2O (50 cm^3) at 0°C for 145 minutes, precipitated the white product, which was filtered off and dried under a stream of N_2. The solid was found to be hygroscopic and thermally unstable.

b) Reaction of Me_2NNH_2 with CO_2 in the presence of NaOH

i) Carbon dioxide was passed through a stirred solution of Me_2NNH_2 (5.00 cm^3, 65.4 mmol) and NaOH (2.62 g, 65.4 mmol) in EtOH (40 cm^3). After 180 minutes a white solid had precipitated. This was filtered off, washed with Et_2O and dried *in vacuo*.

ii) To a solution of $[Me_2NHNH_2][O_2CNHNMe_2]$ (16.4 mmol) in MeOH (40 cm^3) (prepared as in 5.5.4a), was added a solution of NaOH (1.36 g, 34 mmol) in MeOH (40 cm^3). After stirring for 30 minutes, a white solid had precipitated, which was filtered off, washed with MeOH and Et_2O and dried *in vacuo*. IR spectroscopy showed the products from i) and ii) to be different.

c) Reaction of $Me_2NNHCO_2^-$ with Chromium(II)

Carbon dioxide was passed through a solution of Me_2NNH_2 (0.70 cm^3, 9.16 mmol) in MeOH (25 cm^3) at 0°C for 100 minutes under N_2. To this solution was added a solution of chromium(II) in MeOH (prepared by reaction of conc. aq. HCl (0.43 cm^3, 5 mmol) with electrolytic Cr (0.25 g) in deoxygenated MeOH (15 cm^3) under N_2). A dark violet solution was formed but no precipitation of a solid.

d) Reaction of $Me_2NNHCO_2^-$ with Chromium(III)

Carbon dioxide was passed through a solution of Me_2NNH_2 (8.60 cm^3, 112.5 mmol) in EtOH (40 cm^3) for 120 minutes. To this solution was added a solution of $[Cr(OH_2)_4Cl_2]Cl.2H_2O$ (5.00 g, 18.75 mmol) in EtOH (20 cm^3). A dark purple solution was formed but no solid precipitated even on cooling to -16°C. The addition of excess MeCN caused precipitation of all solution products.

CHAPTER No 6

INVESTIGATION OF THE EFFECT OF DISSOLVED CHROMIUM ON THE RATE OF HOMOGENEOUS CATALYTIC DECOMPOSITION OF HYDRAZINE

INVESTIGATION OF THE EFFECT OF DISSOLVED CHROMIUM ON THE RATE OF HOMOGENEOUS CATALYTIC DECOMPOSITION OF HYDRAZINE

6.1 INTRODUCTION

During long-term storage anhydrous hydrazine undergoes slow decomposition to produce mainly nitrogen and ammonia. The decomposition ($3N_2H_4 \rightarrow N_2 + 4NH_3$) is subject to both heterogeneous catalysis at containment vessel surfaces and homogeneous catalysis within the bulk liquid (see SECTION 1.2) [265].

The majority of investigations into hydrazine decomposition have concentrated on vapour-phase studies at low partial pressures, studies under these conditions being experimentally convenient. However, such studies do not reflect actual operating pressures of hydrazine decomposition reactors.

Liquid-phase N_2H_4 decomposition is more difficult to study as most container surfaces contribute to some degree to the overall rate of gas evolution.

Glass (borosilicate and quartz) vessels have been shown to exhibit the lowest N_2H_4 decomposition rates. Ten year storage tests determined the N_2H_4 decomposition rate to be 0.015 % yr^{-1} (~0.10 cm^3 N_2 $kg^{-1}day^{-1}$) in the absence of metal surfaces and catalytic contaminants. In the presence of the most inert metallic specimens, specifically Ti-6Al-4V alloy, the rate of decomposition increased to 0.15 % yr^{-1} (~1.03 cm^3 N_2 $kg^{-1}day^{-1}$) [266]. Much higher N_2H_4 decomposition rates have been observed in the presence of stainless steel. It was found that various stainless steels gave rates of gas evolution per unit area from 6.8×10^{-3} (S527) to ~130×10^{-3} cm^3 N_2 cm^{-2} day^{-1} (S526) (c.f. Ti-6Al-4V, 0.7×10^{-3} cm^3 N_2 $cm^{-2}day^{-1}$) [267]. It was also observed that exposure of stainless steels to the atmosphere whilst wet with N_2H_4 caused marked increases in the rate of

decomposition on subsequent immersion in hydrazine with rates as high as ~1 cm^3 N_2 $cm^{-2}day^{-1}$. This was thought to be due to absorption of CO_2 and the formation of carbazic acid. It is known that carbazic acid has a detrimental effect on the decomposition of N_2H_4 in the presence of steel, (see below) [13].

The effect of contaminants on decomposition rates of hydrazine has been extensively studied by several groups.

The effect of acid (as $N_2H_5NO_3$) on N_2H_4 decomposition at 426-474K was studied by Rubtsov and Mabelis [268], who found the rate of decomposition was dependent on the concentration of both N_2H_4 and $N_2H_5^+$. The balancing nitrate anion had no effect on the decomposition rate.

The effect of acid on N_2H_4 decomposition has also been studied by Ross *et al.* [269] who showed that addition of either $\overset{-}{O}_2CNH\overset{+}{N}H_3$ or NH_4Cl to N_2H_4 in glass apparatus, gave large increases in N_2H_4 decomposition rates. This was attributed to the formation of $N_2H_5^+$ which subsequently initiated decomposition.

The importance of dissolved CO_2, which in N_2H_4 is in the form $[N_2H_5][O_2CNHNH_2]$, in promoting liquid-phase decomposition of hydrazine, especially following exposure of the contaminated propellant to stainless steel, was demonstrated in an extensive study by Axworthy *et al.* working at Rocketdyne [9]. It was found that all acidic impurities increased N_2H_4 decomposition and, like $\overset{-}{O}_2CNH\overset{+}{N}H_3$, were especially effective in the presence of stainless steel. However, since the kinetic experiments were conducted at comparatively high temperatures (128-171°C) the findings of the Rocketdyne group may not be applicable to normal storage temperatures. More recent work [12,13] has revealed that at moderate temperatures (40°C) very low levels of CO_2 in N_2H_4 (< 250

ppm) can cause significant stainless steel corrosion and lead to an increase in the concentration of trace metal ions in N_2H_4. This process has been shown to be accompanied by a corresponding increase in the rate of homogeneous decomposition of N_2H_4 [270].

It has been suggested [13,15] that the increase in N_2H_4 decomposition rates of CO_2-doped N_2H_4 in the presence of stainless steel, is due to metal ion induced homogeneous catalysis, the metal ions being leached from the stainless steel surface by the corrosive effect of hydrazinium carbazate.

To date only the work of Bellerby [15,16] has been concerned with the possible involvement of specific metal ions in this homogeneous catalysis. These results will now be discussed in detail, and will provide the basis for the work presented here.

In an early study [15], Bellerby investigated both iron and chromium carbazate complexes, these being the most likely species given the presence of hydrazine and carbon dioxide. However, these complexes were found to have no effect on the decomposition rate of hydrazine. Conversely, in a more recent study [16], both chromium and manganese were shown to affect the N_2H_4 decomposition rate.

Chromium, in the form of $Cr(O_2CNHNH_2)_3.2H_2O$ dissolved in N_2H_4, was found to have a slightly negative effect on hydrazine decomposition rates (up to 0.002M, the limit of reported addition), as measured in glassware at 43°C. However, the addition of an acid (2-naphthol) to the chromium-doped solution produced an almost three-fold increase in N_2H_4 decomposition rate. The rate was further increased by a second acid addition.

Previous studies [15] have shown that a linear relationship exists between hydrazinium ion ($N_2H_5^+$) concentration and the homogeneous decomposition rate of anhydrous hydrazine in contact

with stainless steel. Consideration of this result led to the proposal that a catalytic cycle for the homogeneous decomposition of hydrazine may involve a metal ion and an acidic species acting in tandem.

Manganese, in the form of $MnCl_2.4H_2O$ in N_2H_4, was also found to suppress the N_2H_4 decomposition rate (up to 0.0035M, the limit of addition), according to the relationship: rate α $[Mn]^{-1/2}$.

Further studies involved the addition of the acid NH_4Cl, which had previously been shown [15] to have no significant effect on the homogeneous decomposition rate of N_2H_4, to a sample of N_2H_4 containing both manganese (0.0034M) and chromium (0.002M) in the forms described above. The decomposition rates of the blank, chromium and mixed chromium + manganese solutions were all found to be similar, but addition of the acid NH_4Cl resulted in a three-fold increase in rate, as measured in titanium vessels at 50°C. Further additions of this acid gave sufficient data for the relationship rate α $[H^+]^{1/2}$ to be proposed.

It was concluded that a significant increase in the rate of homogeneous decomposition of hydrazine at 50°C is observed on the addition of an acid to samples of hydrazine containing manganese and chromium.

The aim of the kinetic investigation presented in this work was to confirm and extend the results reported by Bellerby. His results were obtained only at one temperature (43°C), therefore in this work results have been obtained for a range of temperatures in an attempt to determine activation energy parameters.

6.2 EXPERIMENTAL

Decomposition rate measurements on hydrazine were carried out using a closed vessel of internal volume 1313 cm^3, fabricated from titanium, equipped with a ball-jointed entry port and fitted with a strain-gauge pressure transducer, (conversion factor: mV → mmHg = 15.080) (see FIG No 6.1),. The vessel was housed in a thermostatically controlled hot-air oven (Townson & Mercer, maximium power output = 1.8 kW). Temperature was monitored with a Thandor digital thermometer fitted with a Type K (Ni-Cr alloy) thermocouple.

Hydrazine used in the decomposition rate studies was supplied by Royal Ordnance, Westcott and stated to conform to the US Monopropellant Grade specification [11]. The complex $Cr(O_2CNHNH_2)_3.2H_2O$ was prepared as described in SECTION 3.10.7a and a weighed amount dissolved in N_2H_4 under N_2 to give a 0.100M solution. A solution of $[N_2H_5][O_2CNHNH_2]$ in N_2H_4 was prepared by dissolving $(NH_4)_2CO_3$ (0.79 g, 10 mmol) in N_2H_4 (100 cm^3) under N_2 to form a 0.100M solution [134].

Decomposition rates were calculated from gas pressure increases using a computer program originally written at PERME, Westcott, but now modified to run on a BBC B microcomputer (see Appendix No 3).

In order to quantitatively relate the rates of pressure rise in ullages of closed systems to rates of N_2H_4 decomposition, the solubilities of the produced nitrogen and ammonia in hydrazine must be considered (see SECTION 1.2 for solubility expressions for N_2 and NH_3).

In addition, the fraction of the gas, (predominately N_2), produced by decomposition that is released to the ullage is a

FIGURE No 6.1 Diagram of Titanium Vessel

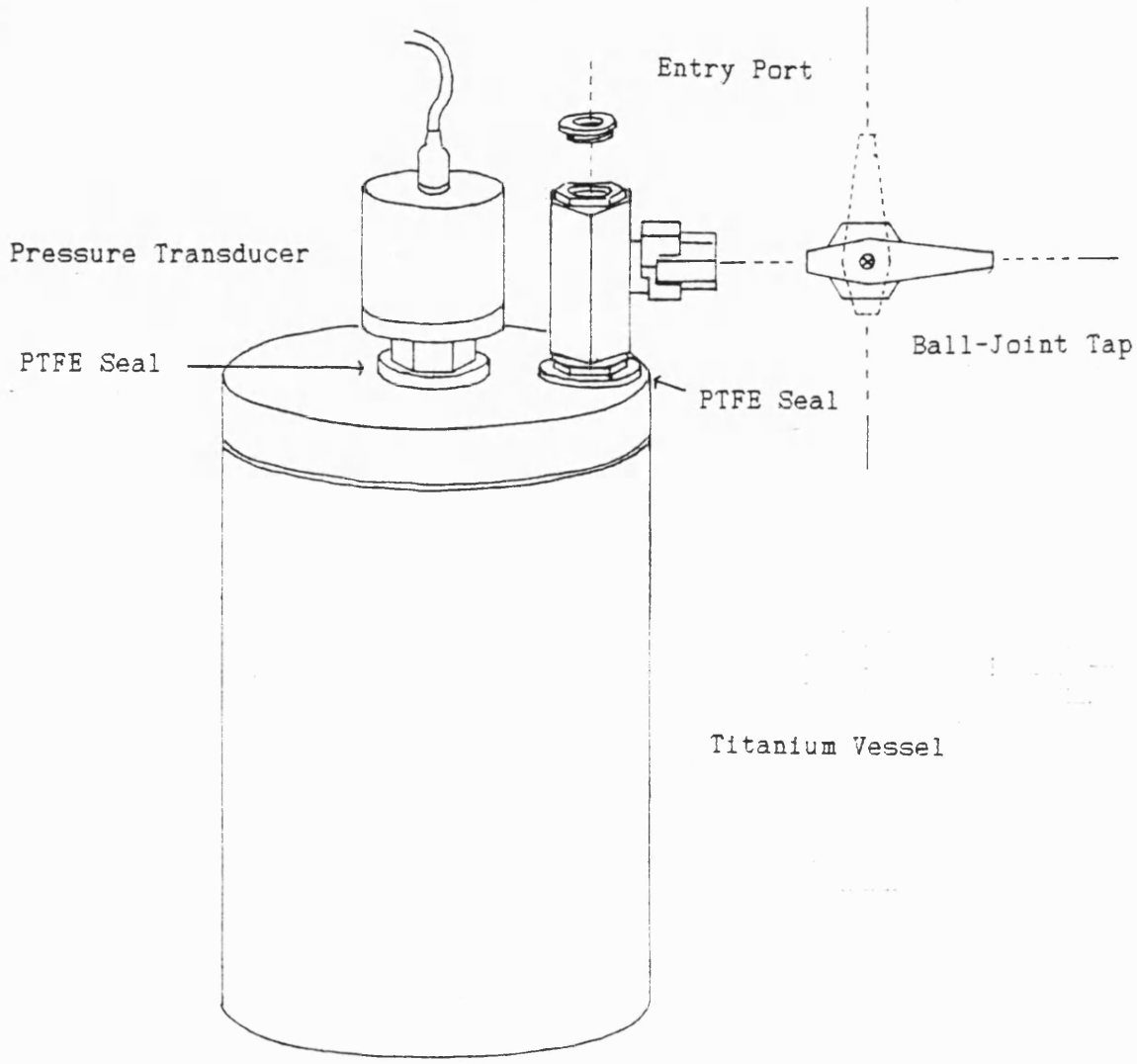

function of the relative sizes of the ullage and liquid phases, as well as a function of the variation in the solubility of the gas with temperature.

The fraction of the produced gas which is released to the ullage has been determined by an empirical equation (6.1) [267].

$$\text{Fraction of gas in ullage} = \frac{V_U}{V_U + \frac{2.564KV_HDT}{(1-K)}} \qquad (6.1)$$

V_H = volume of N_2H_4 ≡ % N_2H_4
V_U = volume of ullage ≡ % ullage
D = density in g cm^{-3}
T = temperature in K
K = mole fraction of dissolved gas in N_2H_4 in equilibrium with a partial pressure of 1 atmosphere of the gas.

The calculation of decomposition rates from rates of pressure rise can be achieved in the following manner [267];

It is assumed that the rate of pressure rise in atmospheres per unit time, dp/dt at a given temperature T (K), and the volume of the ullage V_U (cm^3) at that temperature are known. Also the total volume of the system is known. The rate of pressure is first converted to a rate of gas generation in standard cubic centimetres (scc) per unit time (6.2);

$$\text{Rate of gas generation} = V_U \times \frac{dp}{dt} \times \frac{273}{T} \text{ scc unit time}^{-1} \qquad (6.2)$$

It is next assumed that the decomposition proceeds according to (6.3);

$$3\ N_2H_4 \longrightarrow 4\ NH_3 + N_2 \qquad (6.3)$$

It is assumed that *b* (scc) of N_2 is being generated per unit time. By use of the expression (6.1) above, the fraction of this N_2 that

is released to the ullage, (for the % ullage of the system at temperature T), can be estimated (f_{N2}).

Similarly the volume of NH_3 generated per unit time is $4b$, and the fraction released to the ullage, f_{NH3}, is therefore (6.4);

$$4b\, f_{NH3} + b\, f_{N2} = \frac{273V_U}{T} \times \frac{dp}{dt} \qquad (6.4)$$

from which the value of b can be calculated. This can be converted to weight of N_2H_4 decomposed per unit time knowing that 96 g (N_2H_4) yields 22400 scc (N_2).

The volume of hydrazine contained in the vessel was kept constant at 1087.24 cm^3 throughout the series of kinetic runs, thus maintaining an ullage of approximately 17 % (at 20°C) for the total assembly including the pressure transducer. Contaminant samples were introduced by injection into the vessel via the entry port in air. Pressure readings were not taken for at least 2 days after addition to allow for initial high gas evolution resulting from the reaction: $N_2H_4 + O_2 \rightarrow N_2 + 2H_2O$. At the end of each run, the vessel was allowed to cool to room temperature before the accumulated gas build-up was vented and the vessel resealed for a subsequent run.

For each run, the following infomation was recorded; DAY; TIME (in fractions of hours); PRESSURE (in mV) and TEMPERATURE (in °C). As a result of the method of thermostating the oven, the temperature was found to vary by ~±0.3°C. In each case the lowest temperature achieved during the cyclical operation of the thermostat was recorded.

Using the approach given above the rate of pressure increase is related to total gas evolution and hence to the decomposition rate. The computer routine performs a Linear Squares Analysis on the data pairs (PRESSURE:TIME) to give a Best Fit Line, based on the assumption that a first order rate equation applies (i.e. linear increase of lnP versus TIME).

The program also calculates the standard error (σ) of the data set, and from this, 90 and 95 % confidence limits for the N_2H_4 decomposition rates. This is achieved by the multiplication of σ by the normal distribution values for 90 % (0.95) and 95 % (0.9975) [271].

6.3 RESULTS

It was hoped to confirm and extend the work already reported on the effect of adding chromium and/or manganese species together with acid on the rate of homogeneous decomposition of hydrazine [16]. However, because of difficulties in obtaining a suitable thermostatically controlled oven and overcoming sealant failures on the titanium vessel, data collection did not start until January 1986. The results presented here, therefore, represent constant data collection over an eight month period.

Just three chromium additions and one acid addition could be completed during this limited period. Further acid additions and subsequent manganese additions will clearly be required in the future in order to extend the results presented here.

The N_2H_4 used already contained 2×10^{-9} mol Cr from previous experiments. It was originally thought that this would have little overall effect on experiments involving further chromium additions.

Chromium, in the form of $Cr(O_2CNHNH_2)_3.2H_2O$ in N_2H_4 (0.100M), was added as successive 5, 10 and 10 µl aliquots (Hamilton syringe) and the subsequent decomposition rates determined at ~50, 60, 70 and 80°C. Then acid, in the form of a 10 µl aliquot (1×10^{-9} mol) of $(NH_4)_2CO_3$ in N_2H_4 (0.100M), was added to the chromium-doped N_2H_4.

The individual data points are listed in Appendix No 4. The Best-Fit Equation constants and resulting decomposition rates obtained from computer analysis for each addition at each of the four temperatures are listed in TABLE No 6.1. FIG's No 6.2-6.6 show the PRESSURE:TIME data pairs plotted, with the calculated Best-Fit Lines for each temperature set.

The internal consistency of the rates arising from each addition data set can be checked graphically by plotting ln(RATE) versus 1/TEMP and assessing the linearity of the resulting plot. From this an activation energy can be calculated from the Arrhenius expression, $\ln(RATE) = E_{act}/RT + constant$. Activation energies have been calculated from a further Least Squares Analysis of the plot (see APPENDIX No 3). FIG No's 6.7-6.11 show the plots of ln(RATE) versus 1/TEMP.

i) Blank

From FIG No 6.7, it can be seen that the 50.63° rate does not lie on the line drawn through the other three points. Least Squares Analysis of the three consistent points gives an Activation Energy of 39.88 ± 0.67 kJ mol^{-1} compared to 61.6 ± 11.6 kJ mol^{-1} calculated from all four points. An estimated decomposition rate of 1.3286 cm^3 N_2 $kg^{-1}day^{-1}$ at 50.63° can also be calculated from this new analysis.

TABLE No 6.1 Calculated N_2H_4 Decomposition Rates

Equation of Best-Fit Line:

PRESSURE = TIME(×Pressure rise) + (Intercept)

a) 'Blank Decomposition Rates' - initially doped with 2×10^{-9} mol Cr

Temperature / °C	Rate of Pressure Increase (± σ)	± 90/95 % c/limits	Intercept (± σ)	Rate/cm³N₂ kg⁻¹day⁻¹	± 90/95 % c/limit
50.63	0.1853 ±0.0065	±0.0105 ±0.0181	15.47 ±0.07	0.6467	±0.0365 ±0.0630
61.59	0.6683 ±0.0098	±0.0160 ±0.0276	23.74 ±0.11	2.1387	±0.0513 ±0.0885
70.18	1.0373 ±0.0354	±0.0354 ±0.0611	28.06 ±0.22	3.0959	±0.1058 ±0.1824
80.43	1.6761 ±0.0365	±0.0365 ±0.0629	41.82 ±0.25	4.5911	±0.0999 ±0.1723

b) Decomposition Rates after first Chromium Add'n - 5×10^{-10} mol Cr

Temperature / °C	Rate of Pressure Increase (± σ)	± 90/95 % c/limits	Intercept (± σ)	Rate/cm³N₂ kg⁻¹day⁻¹	± 90/95 % c/limit
49.85	0.1538 ±0.0029	±0.0048 ±0.0083	14.63 ±0.05	0.5397	±0.0169 ±0.0291
59.83	0.2335 ±0.0037	±0.0060 ±0.0103	21.60 ±0.04	0.7579	±0.0194 ±0.0334
70.82	0.5330 ±0.0053	±0.0086 ±0.0148	29.83 ±0.07	1.5953	±0.0257 ±0.0442
79.51	1.2363 ±0.0112	±0.0183 ±0.0316	39.86 ±0.08	3.4131	±0.0506 ±0.0871

c) Decomposition Rates after second Chromium Add'n - 1×10^{-9} mol Cr

Temperature / °C	Rate of Pressure Increase (± r)	± 90/95 % c/limits	Intercept (± r)	Rate/cm³N_2 $kg^{-1}day^{-1}$	± 90/95 % c/limit
50.99	0.1313 ±0.0083	±0.0135 ±0.0232	15.56 ±0.08	0.4567	±0.0468 ±0.0807
61.22	0.2370 ±0.0128	±0.0208 ±0.0359	18.77 ±0.10	0.7605	±0.0669 ±0.1153
71.13	0.7477 ±0.0337	±0.0550 ±0.0948	27.20 ±0.24	2.2142	±0.1628 ±0.2806
80.96	1.1638 ±0.0287	±0.0469 ±0.0808	39.77 ±0.16	3.1735	±0.1278 ±0.2263

d) Decomposition Rates after third Chromium Add'n - 1×10^{-9} mol Cr

Temperature / °C	Rate of Pressure Increase (± r)	± 90/95 % c/limits	Intercept (± r)	Rate/cm³N_2 $kg^{-1}day^{-1}$	± 90/95 % c/limit
50.80	0.1210 ±0.0115	±0.0187 ±0.0323	14.77 ±0.06	0.4217	±0.0652 ±0.1125
60.40	0.3122 ±0.0133	±0.0217 ±0.0374	16.97 ±0.08	1.0085	±0.0701 ±0.1207
70.51	0.6488 ±0.0295	±0.0482 ±0.0830	25.36 ±0.17	1.9312	±0.1433 ±0.2471
80.24	1.1569 ±0.0175	±0.0286 ±0.0493	37.27 ±0.10	3.1742	±0.0784 ±0.1351

e) Decomposition Rates after Addition of Acid (1×10^{-9} mol) to Solution (d).

Temperature / °C	Rate of Pressure Increase (± σ)	± 90/95 % c/limits	Intercept (± σ)	Rate/cm^3N_2 $kg^{-1}day^{-1}$	± 90/95 % c/limit
52.33	0.1355 ±0.0129	±0.0210 ±0.0361	15.16 ±0.07	0.4666	±0.0722 ±0.1244
61.36	0.2879 ±0.0131	±0.0214 ±0.0369	22.81 ±0.07	0.9231	±0.0686 ±0.1183
71.31	0.5802 ±0.0162	±0.0265 ±0.0456	28.04 ±0.04	1.7154	±0.0783 ±0.1349
81.43	1.2300 ±0.0155	±0.0253 ±0.0436	35.44 ±0.10	3.3406	±0.0687 ±0.1184

FIGURE No 6.2 Plot of PRESSURE(mV):TIME(day) data pairs for 'Blank'

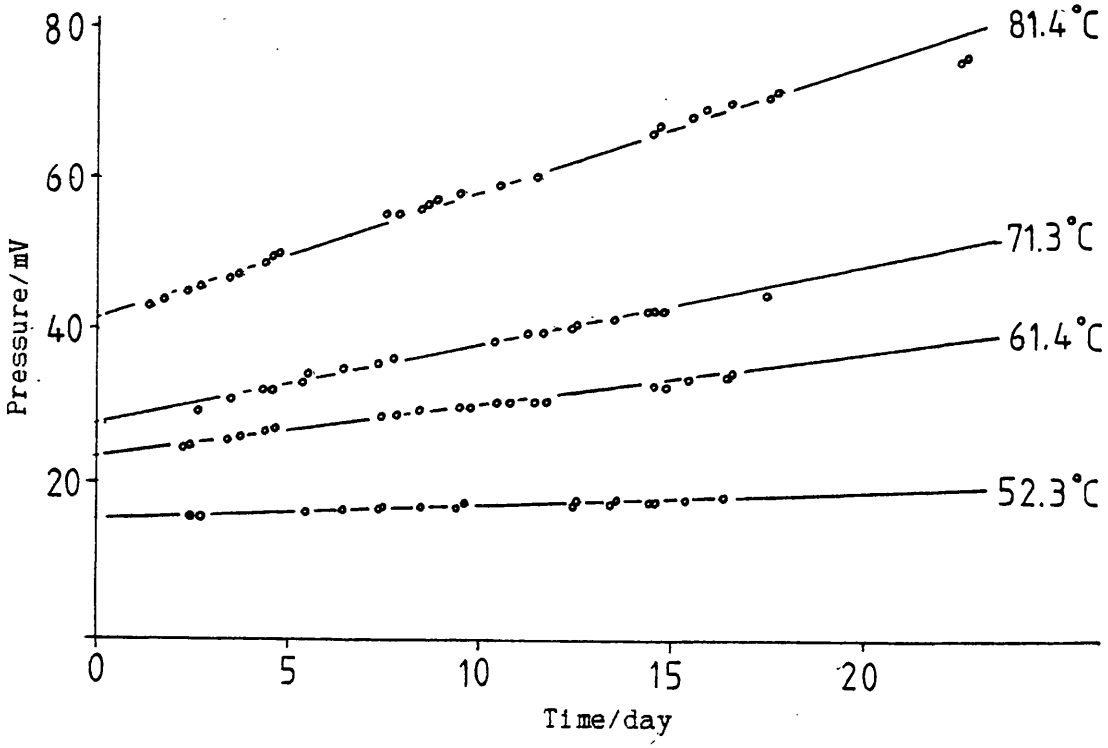

FIGURE No 6.3 Plot of PRESSURE(mV):TIME(day) data pairs for first Chromium Add'n

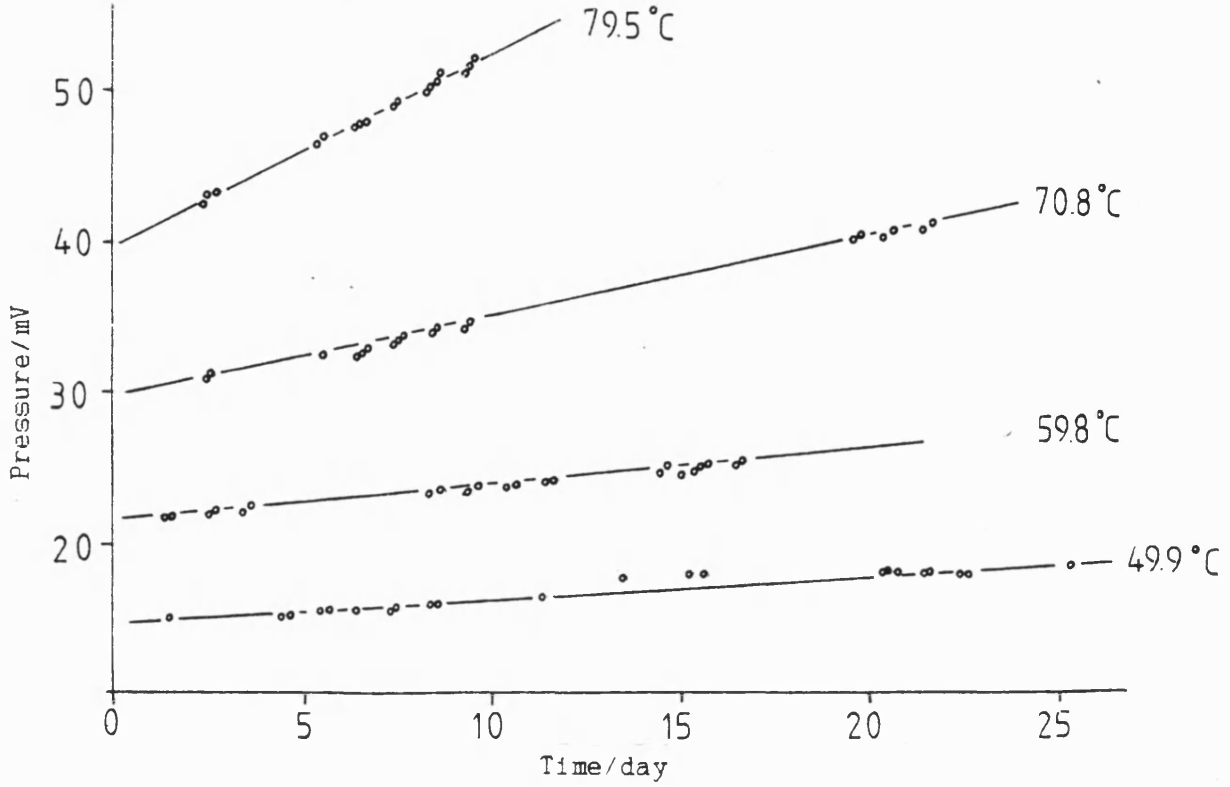

FIGURE No 6.4 Plot of PRESSURE(mV):TIME(day) data pairs for second Chromium Add'n

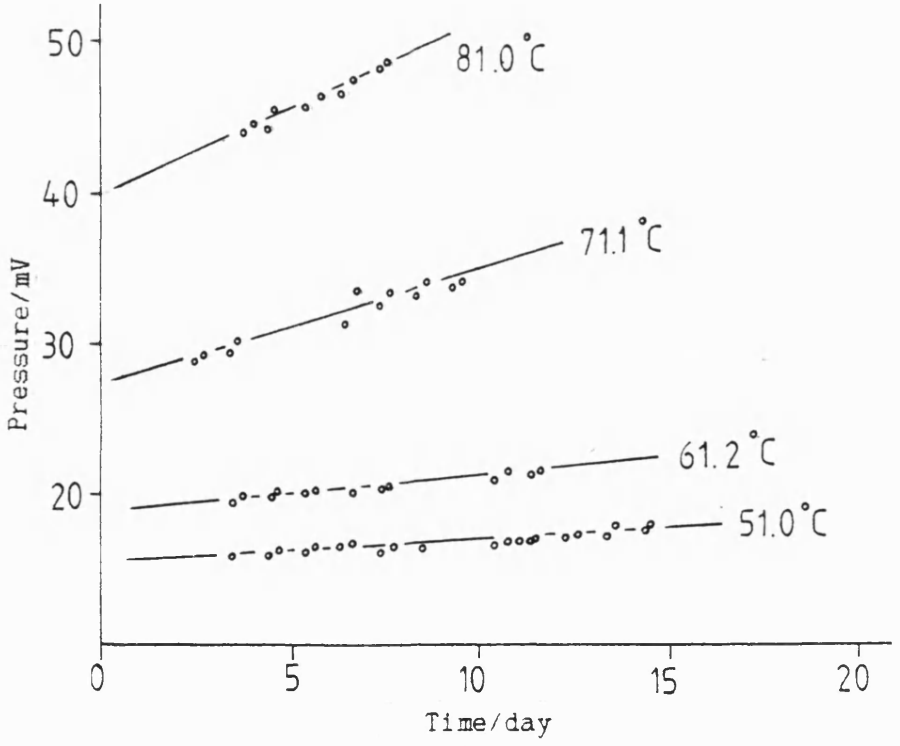

FIGURE No 6.5 Plot of PRESSURE(mV):TIME(day) data pairs for third Chromium Add'n

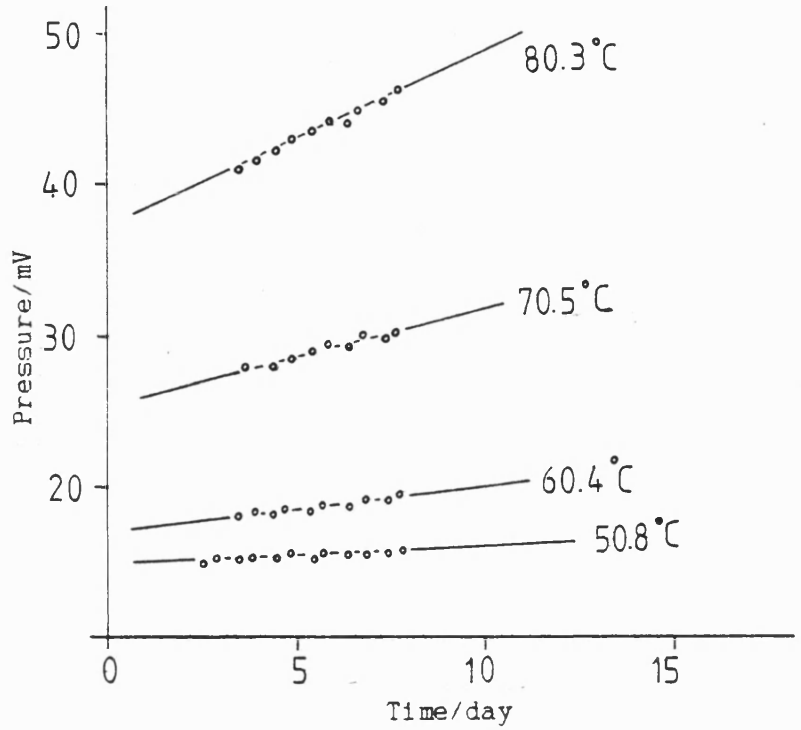

FIGURE No 6.6 Plot of PRESSURE(mV):TIME(day) data pairs for Acid Add'n

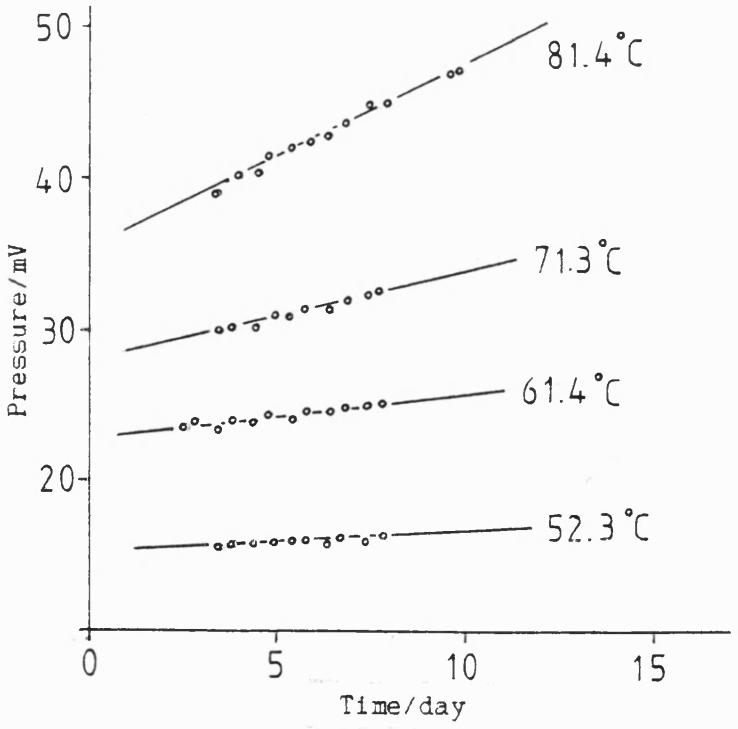

FIGURE No 6.7 Plot of ln(RATE) versus 1/TEMP for 'Blank'

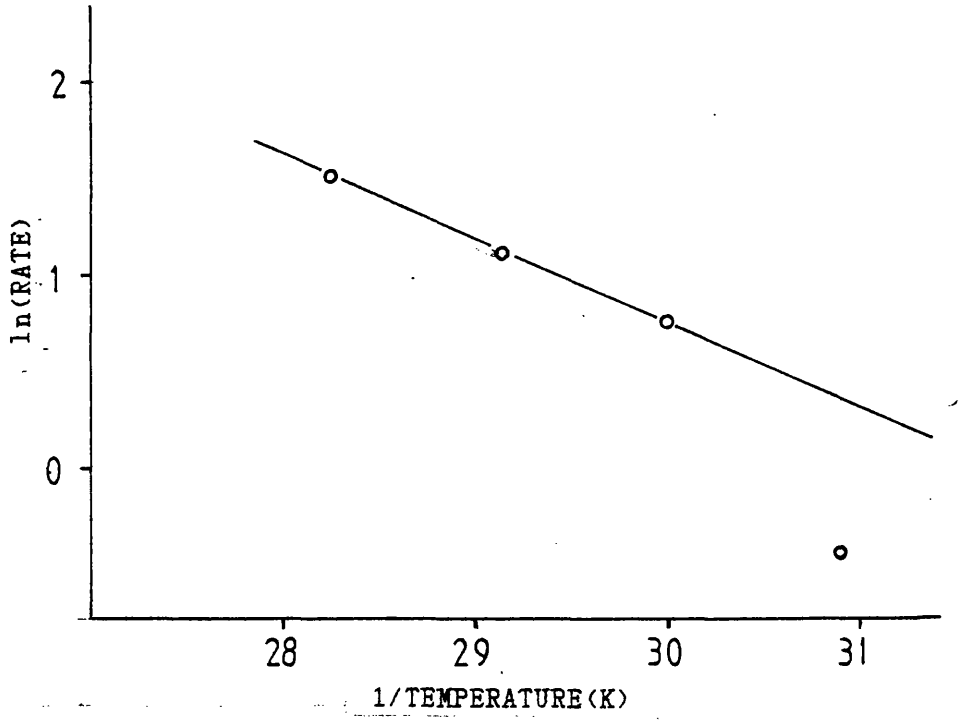

FIGURE No 6.8 Plot of ln(RATE) versus 1/TEMP for the First Chromium Add'n

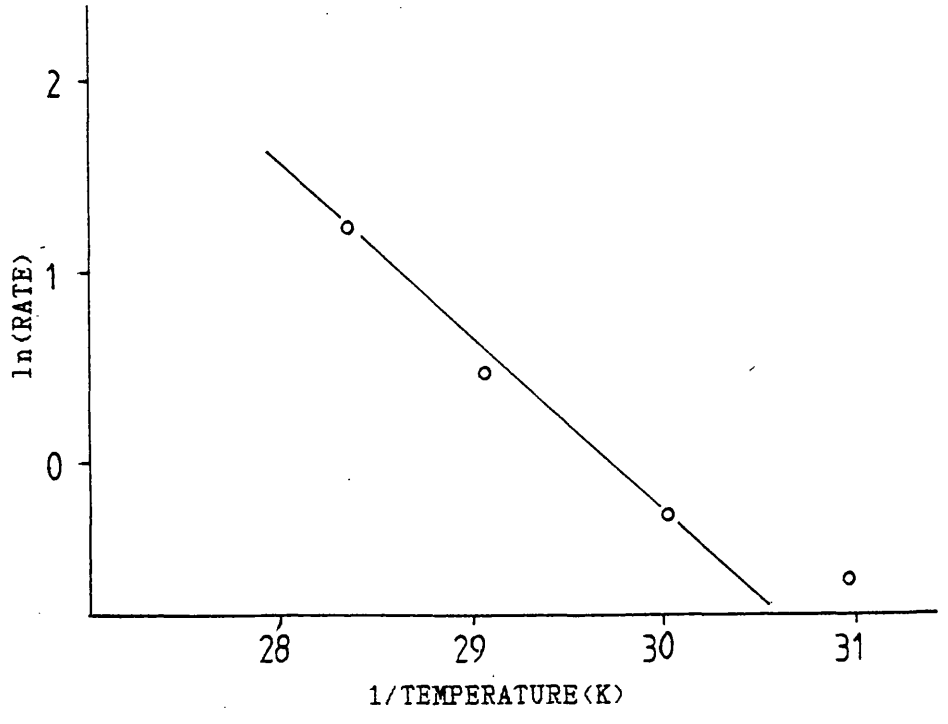

FIGURE No 6.9 Plot of ln(RATE) versus 1/TEMP for the Second Chromium Add'n

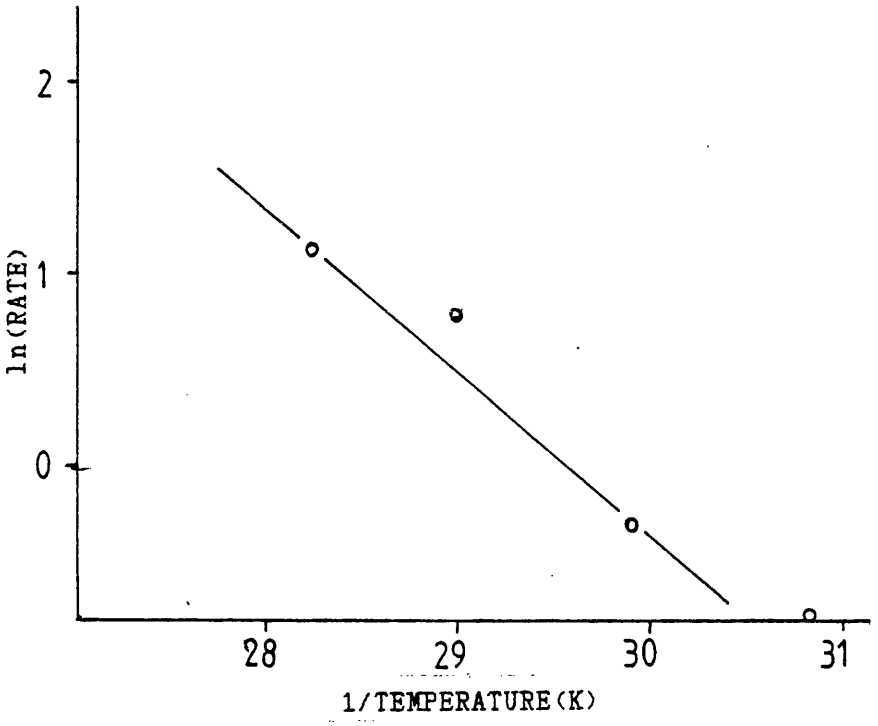

FIGURE No 6.10 Plot of ln(RATE) versus 1/TEMP for the Third Chromium Add'n

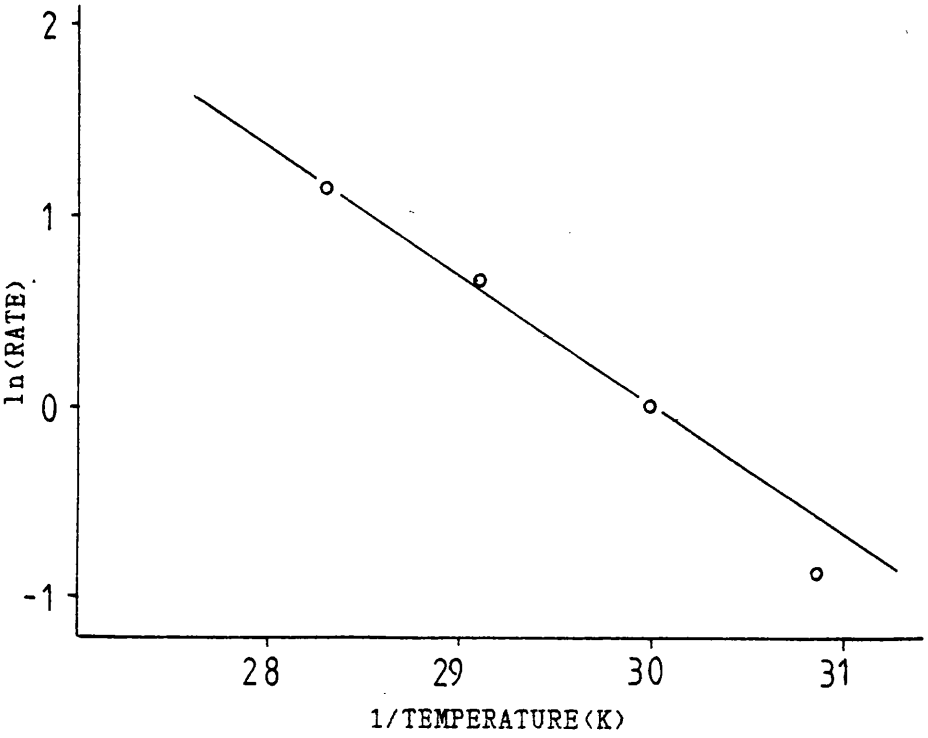

FIGURE No 6.11 Plot of ln(RATE) versus 1/TEMP for the Acid Add'n

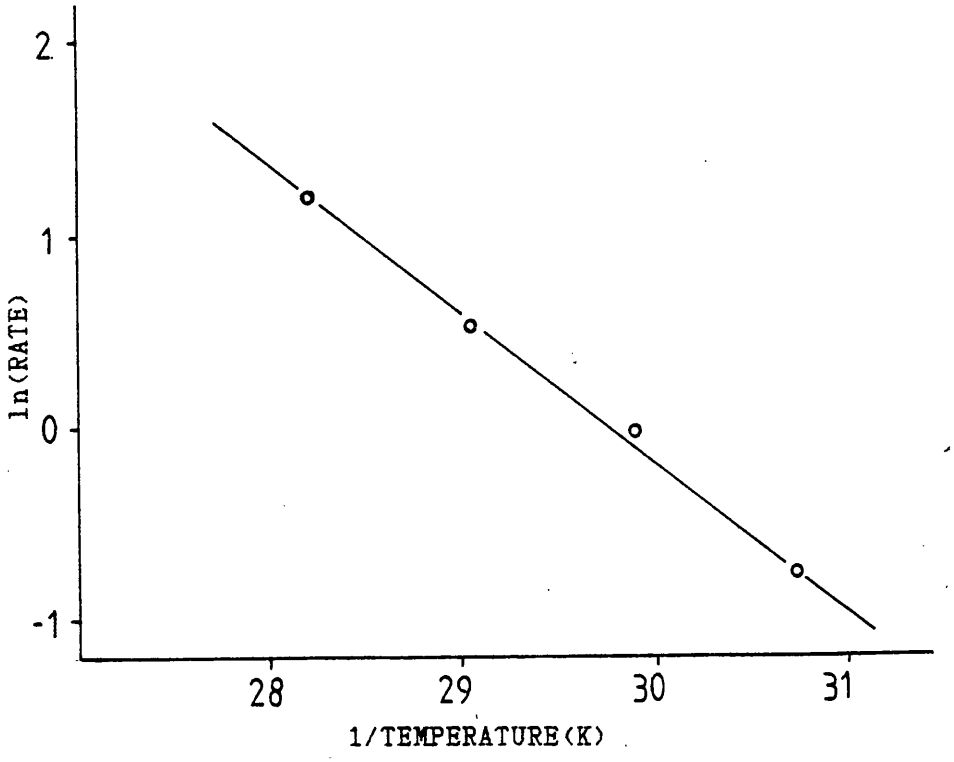

ii) First Addition of Chromium

Again a consideration of the plotted decomposition (see FIG No 6.8) shows that the rate determined at lowest temperature (49.85°) is out of line with the rates obtained at the three higher temperatures. The activation energy obtained using all four data pairs is 59.74 ± 8.15 kJ mol^{-1} whereas use of the data obtained at the three higher temperatures gives a refined Activation Energy of 74.60 ± 2.36 kJ mol^{-1}. The estimated decomposition rate at 49.85°C from this new analysis is 0.3240 cm^3 N_2 $kg^{-1}day^{-1}$ compared with the observed rate of 0.5397 cm^3 N_2 $kg^{-1}day^{-1}$.

iii) Second Addition of Chromium

The plotted data show a large scatter (see FIG No 6.9). The decomposition rate at 71.13° appears abnormally high when compared to those determined at 80.96 and 61.22°. Again the rate measured at

the lowest temperature (50.99°) appears unreliable, although with only four data pairs, no firm conclusions can be drawn. No Least Squares Analysis was attempted in view of the limited data set.

iv) Third Addition of Chromium

Consideration of the plotted rates (see FIG No 6.10) again shows that obtained at the lowest temperature (50.80°) is less than expected when compared to the rates at the three higher temperatures. Least Squares Analysis of these rate points gives a refined E_{act} of 56.72 ± 2.78 kJ mol^{-1}. Extrapolation then gives an estimated rate at 50.80° from this analysis of 0.5616 cm^3 N_2 kg^{-1} day^{-1}, (found = 0.4217).

v) Subsequent Addition of Acid

The four decomposition rates (see FIG No 6.11) appear reasonably self-consistent. An activation energy of 64.37 ± 1.14 kJ mol^{-1} can be calculated using all four rate determinations.

TABLE No 6.2 Calculation of Activation Energies from Decomposition Rates / kJ mol^{-1}

Addition	E_{act} from all 4 data pairs	Refined E_{act} (see text)
BLANK	61.61 ±11.61	39.88 ±0.67
FIRST CHROMIUM ADD'N	59.74 ±8.15	74.60 ±2.36
SECOND CHROMIUM ADD'N	65.83 ±8.74	-
THIRD CHROMIUM ADD'N	64.99 ±4.77	56.72 ±2.78
ACID ADD'N	64.37 ±1.14	-

There appears to be little correlation between calculated activation energies and increasing chromium content (see FIG No 6.12). As observed for the individual decomposition rates, the activation energies are higher after the chromium additions than for the blank, but a simple relationship with increasing chromium content has not been observed.

FIGURE No 6.12 Plot of ln(RATE) versus Chromium Concentration.

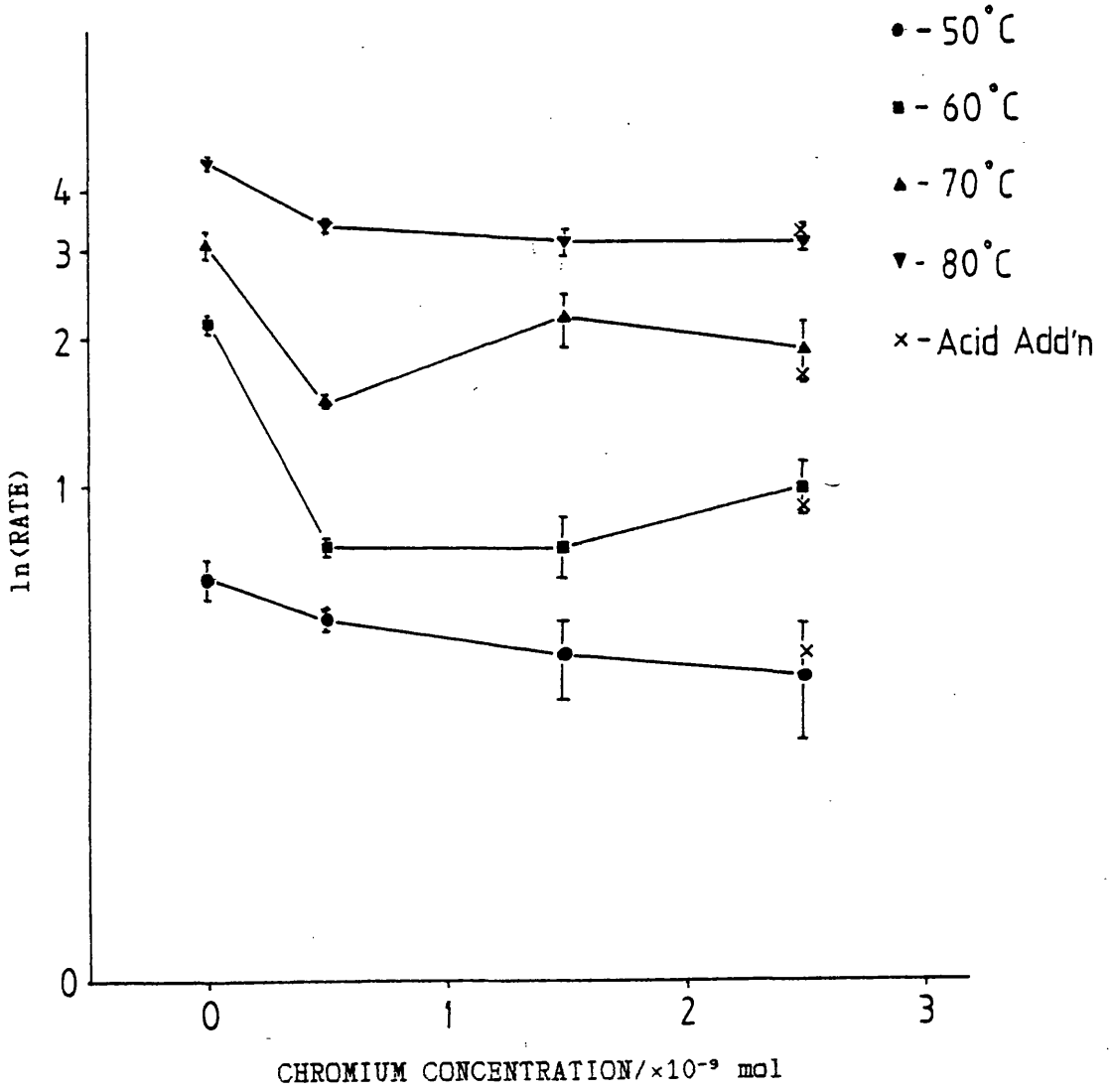

6.4 DISCUSSION

The addition of 5 µl of 0.1M Cr solution (5×10^{-10} mol) caused a large drop in the N_2H_4 decomposition rate. Analysis of the decomposition rates indicate that the rate at ~50° is not in line with the rates determined at the other temperatures. However, the overall decrease in decompsition rate appears genuine. Further additions of chromium (up to 2.5×10^{-9} mol) did not decrease the decomposition rate as markedly, but a regular slight inhibition in decomposition rate is discernable. FIG No 6.12 shows a plot of ln(RATE) against chromium content which illustrates the above trend. Each rate is plotted with its 95 % confidence limits. The rates determined after the second chromium addition appear from the Least Squares Analysis to be the most unreliable of the complete data set. This would explain the lack of correlation between the rates determined after the second and third chromium additions i.e. a decrease in the rate at ~70° is observed after the third addition, but conversely an increase in the rate at ~60° occurs after the third addition.

Bellerby observed an increase in decomposition rate after the addition of an acid [16]. However, in this work it has been found that addition of acid (1×10^{-9} mol) failed to cause such an increase in decomposition rate. In fact, all rates determined after acid addition fall within the 95 % confidence limits (in some cases 90 %) of the rates determined after the third chromium addition. Therefore acid does not seem to affect the N_2H_4 decomposition rate under the experimental conditions employed in this work.

So despite the anticipation of obtaining results which would confirm those of Bellerby, a number of differences have emerged. some of which may relate to changes in experimental conditions.

The decomposition rates reported by Bellerby [16] for chromium-doped hydrazine (43°C; ~0.22 - 0.18 cm^3 N_2 $kg^{-1}day^{-1}$) are lower than those found in this work (~50°C; 0.65 - 0.42 cm^3 N_2 kg^{-1} day^{-1}). This may be a consequence of using a titanium container in this study whereas an all-glass apparatus was used by Bellerby. As noted previously, (see SECTION 6.1), titanium induces a higher hydrazine decomposition rate than does glass [266].

Also the concentration of added chromium differs in the two studies. In Bellerby's work, Cr concentrations of up to 2 mmol were used whereas in the present study much lower concentrations of up to 2.5×10^{-9} mol Cr were used. Given the higher 'blank' decomposition rate determined in this study, smaller additional amounts of chromium may not have such a noticeable effect on the N_2H_4 decomposition rate.

In order to complete a reasonable series of results in the time available it was necessary to limit the data collection for each run to 7 days. Allowing a two day delay before results could be collected (see earlier) effective data collection was limited to only 5 days. This may introduce errors that a longer time period might eliminate.

The failure of the addition of the acid to the chromium-doped N_2H_4 to cause an increase in decomposition rate is surprising, as numerous studies have noted the detrimental effect of protons on N_2H_4 decomposition rates [15,268,269]. The low concentration of added acid may partially explain the absence of a significant effect (H^+:Cr ratio = 1:4.5), although Bellerby observed a three-fold increase in decomposition rate with H^+:Cr ratio = 1:1.33. However the overall concentrations of both chromium and acid were higher than those used in this present study.

In view of the variation in experimental conditions employed in this work and that of Bellerby [16], it is concluded that comparisons between the two sets of data are of limited value.

The failure to observe a simple relationship between N_2H_4 decomposition rates and increasing chromium concentrations may be related to a number of factors. For example, a time period of approximately six months elapsed between the initial chromium doping of the N_2H_4 and the introduction of the first chromium addition in the present study. The hydrazine supplied by PERME, Westcott used in this study conformed to the US monopropellant specification [11] at the time of analysis. However, no subsequent analyses have been carried out at Bath. Also, time allowed only a few chromium additions and this may limit the conclusions that can be drawn. Additionally, the design of the apparatus did not allow each chromium or acid aliquot to be loaded under an inert atmosphere, thus increasing the possibility of contamination by CO_2, H_2O or other impurities. However, introduction of CO_2 in particular would be expected to enhance rather than inhibit the decomposition rates.

6.5 CONCLUSION

The results presented in this work have given this laboratory an introduction to kinetic investigations of hydrazine decomposition by the measurement of pressure increases within closed systems. It is hoped that this study will be extended in the manner outlined in SECTION 6.3.

Very few definite conclusions can be made at this stage. It appears that chromium alone does have some retarding effect on the decomposition of hydrazine, but no clear reaction kinetics can be

discerned. As discussed above, few useful comparisons can be made with the earlier work of Bellerby [16], but both studies seem broadly in agreement. However, the effect of acid on the hydrazine decomposition rate remains to be further explored.

It is suggested that strictly purified hydrazine be used in future investigations of the effects of contaminants on hydrazine decomposition. The use of purified hydrazine rather than 'propellant' grade hydrazine, would eliminate possible effects from permitted concentrations of contaminants and allow the effect of a single deliberately added contaminant to be studied.

APPENDIX No 1

PHYSICAL METHODS AND INSTRUMENTATION

a) CONDUCTIVITY

Conductivity measurements were determined at 25°C under N_2 using a Wayne-Kerr autobalance bridge and a dip-type cell with platinium electrodes (for N_2H_4 measurements) and platinium black electrodes (for MeOH measurements). Cell constants of 174.1 and 41775 respectively were determined by measurement of the conductance of standard aqueous 0.1000M KCl solution.

b) ELECTRONIC SPECTRA

i) Reflectance spectra of liquid paraffin mulls of powdered solids held between quartz plates were obtained using a Perkin-Elmer 330 spectrophotometer equipped with an integrating sphere assembly.

ii) Solution absorption spectra were obtained using a Cecil Instruments CE 595 spectrophotometer with 1 cm pathlength silica cells.

c) ELECTRON SPIN RESONANCE SPECTRA

Spectra of solids and solutions were obtained using a Varian E-3 EPR spectrometer at room temperature with an operating frequency of ~9.55 GHz. Spectra were calibrated using diphenylpicrylhydrazyl ($g = 2.0037 \pm 0.002$).

d) DIFFERENTIAL THERMAL ANALYSIS/THERMOGRAVIMETRY

DTA/TG runs were performed on powdered solids heated in air or argon using a Stanton Redcroft STA 780 Differential Thermal

Analyser at RMCS Shrivenham. Samples were referenced using alumina and heated at 10°C/min, to 600°C.

e) INFRA-RED SPECTRA

Infra-red spectra were obtained on a Perkin-Elmer 599B spectrometer using liquid paraffin or hexachlorobutadiene mulls between NaCl (4000-700 cm^{-1}) or CsI (700-200 cm^{-1}) plates. Calibration of spectra was achieved by reference to the 2850.7 and 1028.0 cm^{-1} absorptions of polystyrene.

f) RAMAN SPECTRA

Raman spectra of powdered solids held in capillary tubes were obtained using a Spex 1401 spectrometer and a Lexel 85 argon ion laser. A cooled photomultiplier and photon counting detection were employed. Spectra were calibrated by reference to the 965, 924 and 896 cm^{-1} bands of $KReO_4$.

g) MAGNETIC SUSCEPTIBILITY MEASUREMENTS

i) **Gouy Method**: Measurements were made using a Newport Instruments electromagnet and a Stanton Instruments MC3 balance at a current of 8A. Samples were held in 4 or 6 mm o.d. glass tubes and calibrated using $[Ni(en)_3](S_2O_3)$ (χ_{cgs} = 11.03×10^{-6} cm^3g^{-1}).

ii) **Evans Method** [211A]: Measurements were made on a Hitachi Perkin Elmer R-24B ^1H nuclear magnetic resonance spectrometer at an operating frequency of 60 MHz at 23°C. The methyl resonance of MeCN (2.0 ppm) was used as the paramagnetic shift indicator. The reference $MeCN/N_2H_4$ was held in a sealed capillary (1.5 mm o.d.) which was suspended freely in the

sample solution. The frequency separation, $\Delta\nu$, was determined by measurement of the peak differences and related to the susceptibility of the species, χ, by the expression;

$$\chi = \frac{3\Delta\nu}{2\pi\nu c} + \chi_o$$

where χ_o is the mass susceptibility for the pure solvent (-0.62×10^{-6} cm^3g^{-1} for N_2H_4), ν is the operating frequency (60×10^{-6} Hz) and c is the concentration of the species in g cm^{-3}.

h) MASS SPECTRA

Mass spectra were recorded on a VG 70 70E spectrometer equipped with a DS 2025 data system using direct insertion probes and an ionising energy of 70eV. Fast Atom Bombardment spectra were obtained on samples dispersed in glycerol matrices using xenon as the fast atom beam.

i) ^{13}C NUCLEAR MAGNETIC RESONANCE SPECTRA

^{13}C nmr spectra were measured on a Jeol GX 270 MHz FT spectrometer using tetramethylsilane (TMS) as an external reference. Samples were dissolved under nitrogen and held in 4 mm o.d. silica tubes. Gold Label (99.5 %) MeOH-d_4 was used as received without purification.

j) X-RAY PHOTOELECTRON SPECTRA

X-Ray photoelectron spectra were recorded on the Vacuum Generators spectrometer at Bristol Polytechnic. Samples were loaded into the instrument as powders dusted on to double-sided adhesive tape. The Al $K_{\alpha1,2}$ line (1486.6 eV) was used as

the X-ray excitation source. Surface charging effects were eliminated by use of an electron "floodgun" which bathes the sample surface in a flux of very low energy electrons (0.35 mA, 0.5 V). Wide survey scans (0-1000 eV binding energies) and detailed high resolution scans (571-596 eV for Cr 2p, 36.75-99.25 for Cr 3s and 256-319.25 eV for C 1s) were carried out.

k) ANALYSIS

Carbon, hydrogen and nitrogen analyses were determined by microanalytical techniques using the University of Bath's microanalytical service.

Chromium was determined either by a) oxidation to $Cr_2O_7^{2-}$ using $KBrO_3$ and subsequent determination of reduced I_2 by $S_2O_3^{2-}$ [272] or b) direct ignition of the sample to Cr_2O_3 by thermal decomposition at 500°C in air.

Chloride was determined gravimetrically as AgCl [273]. Insoluble samples were decomposed by dil. HNO_3 before analysis.

PREPARATION AND HANDLING OF AIR-SENSITIVE COMPOUNDS

Air- and moisture-sensitive compounds were prepared in flame-dried glassware under a dry dinitrogen atmosphere. Compounds so prepared were filtered and washed with deoxygenated solvents in a filter-stick similar to that described by Holah [274]. Compounds were normally dried by washing with deoxygenated diethylether and subsequent evaporation under a stream of N_2.

Handling of air-sensitive compounds for subsequent physical measurement (e.g. Magnetic susceptibility measurements, IR

mull preparation etc.) involved transfer within filter-stick apparatus for further manipulation within glove box or dry bag systems.

APPENDIX No 2

SOLVENTS, REAGENTS AND STARTING MATERIALS

SOLVENTS

All Standard Laboratory Reagent grade solvents were dried over molecular sieves and thoroughly purged with dry nitrogen gas before use. In addition several solvents required further treatment as outlined below;

i) **Methanol and Ethanol**: Dehydration of CH_3OH or CH_3CH_2OH was achieved by refluxing under N_2 over Mg turnings with an initial addition of I_2 to promote alkoxide formation.

ii) **Acetonitrile**: CH_3CN was refluxed under N_2 over P_2O_5 for several hours before being distilled under N_2 and stored over molecular sieves until use.

iii) **Tetrahydrofuran**: $\overline{CH_2CH_2CH_2CH_2O}$ was distilled from sodium-lead alloy under N_2 with benzophenone as dehydration indicator. The solvent was stored over fresh Na-Pb alloy under N_2 until further use.

REAGENTS

Unless otherwise stated Analar and Standard Laboratory Reagents were used as recieved without further purification.

Anhydrous hydrazine, N_2H_4 was supplied by R.O. Westcott, analysis having shown that it conformed to the U.S. Monopropellant Specification [11]. The N_2H_4 was used as received except for conductiometric measurements when further purification was performed (see SECTION 3.10.4a).

$N_2H_4.H_2O$-d_6 (98 %) was obtained from Merck, Sharp & Dohme and used as recieved.

Methyl- and 1,1-dimethyl-hydrazine were purified by distillation under N_2 from KOH. Methyl- and phenylhydrazines were obtained from commerical sources, while 1,1-dimethyl-hydrazine was a gift from R.O. Westcott.

STARTING MATERIALS

Starting materials for particular reactions are described in the appropiate experimental sections.

TOXICITY OF HYDRAZINES

Hydrazines are known to be hazardous. TABLE A2.1 shows the LC_{50} (lethal concentration at which 50% of the test animals survive) and the hazard index (quotient of vapour pressure at ambient temperature and the threshold limit value) of N_2H_4, $MeNHNH_2$ and Me_2NNH_2.

TABLE A2.1 Hazard Indices of Hydrazine and Methylhydrazines

Compound	Vapour Pressure 25°C (mmHg)	LC_{50} (4 hrs) (ppm)	Hazard Index (mmHg/ppm)
Hydrazine	14.4	570	0.03
Methylhydrazine	49.6	74	0.67
1,1-Dimethylhydrazine	156.8	252	0.62

Hydrazine itself has the least vapour toxicity of all hydrazine fuels. In particular two types of exposure are important, vapour inhalation and liquid splashing. The first type of exposure would cause predominantly respiratory and systemic effects (e.g. nose and throat irritation, tracheitis, bronchitis, dizziness, nausea, anorexia etc), whereas in the latter case, skin effects and

eye effects must be considered in addition to respiratory and systemic effects.

In the routine use of these compounds, special care should be taken to avoid both vapour and liquid exposure, by using fume extraction systems at all times.

APPENDIX No 3 LISTINGS OF 'BASIC' COMPUTER PROGRAMS USED IN THE CALCULATION OF HYDRAZINE DECOMPCOSITION RATES AND ACTIVATION PARAMETERS

a) Program to calculate Hydrazine Decomposition Rates from DAY, TIME, PRESSURE and TEMPERATURE measurements.

```
10INPUT "Transducer Conversion from mV to mmHg ";CONFAC
20INPUT "Volume of the vessel ";VOLUME
30INPUT "Weight of hydrazine in the vessel ";WEIGHT
40INPUT "Number of pairs of data points ";N
50REM Setting up of array to accept data points
60DIM DAY(N)
70DIM TIM(N)
80DIM PMV(N)
90DIM TEMP(N)
95 DIM PMMHG(N)
100REM Reading of data into array
110FOR I=1 TO N
120READ DAY(I)
125 REM Read in TIME data in fractions of 24 hour clock
130 READ TIM(I)
140 READ PMV(I)
150 READ TEMP(I)
160NEXT
170REM Calculate the maximum and minimum values of the pressure
180PMIN=1000.0
190PMAX=0.0
200FOR I=1 TO N
210 DAY(I)=DAY(I)+TIM(I)/24
220PMMHG(I)=PMV(I)*CONFAC
230IF PMV(I)<PMIN THEN PMIN=PMV(I)
240IF PMV(I)>PMAX THEN PMAX=PMV(I)
250NEXT
260REM Calculate the average temperature over the run
270TAV=0.0
280FOR I=1 TO N
290TAV=TAV+TEMP(I)
300NEXT
310TAV=TAV/N
320REM Calculate Dp/Dt by simple least squares regression
330SY=0.0
340SX=0.0
350SXY=0.0
360SX2=0.0
370SY2=0.0
380SD2=0.0
390FOR I=1 TO N
400SX=SX+DAY(I)
410SY=SY+PMV(I)
420SXY=SXY+(DAY(I)*PMV(I))
430SX2=SX2+(DAY(I)*DAY(I))
440SY2=SY2+(PMV(I)*PMV(I))
450NEXT
460TP=(N*SXY-SX*SY)
470 DEL=(N*SX2)-(SX*SX)
480DPDT=TP/DEL
490DTDP=TP/((N*SY2)-(SY*SY))
500R=SQR(DPDT*DTDP)
510RINTER=((SY*SX2)-(SX*SXY))/DEL
520REM Calculate the rate of decomposition in Scc/day
530TAVK=TAV+273
540DENSITY=1.23078-6.2668E-4*TAVK-4.5284E-7*TAVK*TAVK
550VU=VOLUME-(WEIGHT/DENSITY)
560PERCENT=100.0*(VU/VOLUME)
570FACTOR=CONFAC*VU*273.0/(760.0*TAVK)
580RATE=DPDT*FACTOR
590REM Modification allowing for the different solubilities of NH3 & N2
600 RKN2=EXP(-1185.93/TAVK-7.84)
610 RKNH3=EXP(2615.08/TAVK-11.32)
615 QUO=(VU+(2.56*RKN2*WEIGHT*TAVK)/(1.0-RKN2))
620FKN2=VU/QUO
625QUP=(VU+(2.56*RKNH3*WEIGHT*TAVK)/(1.0-RKNH3))
630FKNH3=VU/QUP
640FAC2=(4.0*FKNH3)+FKN2
650RATE=RATE/FAC2
652 @%=&20209
654 PRINT
655 PRINT TAB(5);"Day";TAB(13);"Temp";TAB(22);"PmV";TAB(30);"PmmHg"
656 PRINT
660FOR I=1 TO N
670PRINT DAY(I),TEMP(I),PMV(I),PMMHG(I)
680NEXT
690 PRINT
```

```
700PRINT "Average Temperature =";TAV; " degrees Centigrade"
710PRINT
712 @%=&20409
720PRINT "Rate= ";RATE; " scc/day"
730REM Calculate the Standard Errors of the Slope and the Intercept
740NU=N-2
750FOR I=1 TO N
760SD2=SD2+(DPDT*DAY(I)+RINTER-PMV(I))^2
770NEXT I
780RMSQE=SD2/NU
790SESLOPE=SQR(N*RMSQE/DEL)
800SEINTER=SQR(SX2*RMSQE/DEL)
810PRINT
820PRINT "Standard Error of Slope =";SESLOPE
830PRINT
840PRINT "Standard Error of the Intercept =";SEINTER
850 PRINT
860 PRINT "Equation of Best Fit =";DPDT;"+";SESLOPE;" + ";RINTER;"+";SEINTER
```

b) Program to calculate Activation Energies from Hydrazine Decomposition Rates and Temperature Measurements.

```
 10 REM Program to calculate the Activation Energy from decomposition rates
 20 REM using a least squares analysis
 30 INPUT "Number of Data Points = ";N
 40 DIM TEMP(N)
 50 DIM RECIPT(N)
 60 DIM RATE(N)
 70 DIM RLN(N)
 80 GASCON1=1.9872E-03
 90 GASCON2=8.3143E-03
100 XMIN=300.0
110 XMAX=0.0
120 YMIN=+1E38
130 YMAX=-1E38
140 FOR I = 1 TO N
150   READ RATE(I)
160   READ TEMP(I)
170   TEMPK=TEMP(I)+273.15
180   RECIPT(I)=1/TEMPK
190   RLN(I)=LN(RATE(I))
200   IF RECIPT(I) < XMIN THEN XMIN=RECIPT(I)
210   IF RECIPT(I) > XMAX THEN XMAX=RECIPT(I)
220   IF RLN(I) < YMIN THEN YMIN=RLN(I)
230   IF RLN(I) > YMAX THEN YMAX=RLN(I)
240   NEXT
250 XY=0.0
260 Y=0.0
270 X=0.0
280 X2=0.0
290 XX=0.0
300 FOR I=1 TO N
310   XY=XY+(RECIPT(I)*RLN(I))
320   Y=Y+RLN(I)
330   X=X+RECIPT(I)
340   X2=X2+(RECIPT(I)^2)
350    NEXT
360  XX=X*X
370 M1=(N*X2)-XX
380 M=((N*XY)-(X*Y))/M1
390 B=((X*XY)-(X2*Y))/(XX-(N*X2))
400 QUO=0.0
410 FOR I=1 TO N
420   QUO=QUO+(RLN(I)-(RECIPT(I)*M)-B)^2
430   NEXT
440 SIGMA=QUO/(N-2)
450 ALPHAM=SQR((N*SIGMA)/(N*X2-XX))
460 ALPHAB=SQR((SIGMA*X2)/(N*X2-XX))
470  @%=&2040F
480 PRINT "Slope of line = ";M
490 PRINT
500 PRINT "LN R = ( ";M;"+";ALPHAM;" ) 1/T + ( ";B;" + ";ALPHAB;" )  "
510 PRINT
520 ACT1=-GASCON1*M
530 ACT2=-GASCON2*M
540 SDA1=GASCON1*ALPHAM
550 SDA2=GASCON2*ALPHAM
560  PRINT "Temperature/C       Decomposition Rate/scc/day        Ln Decomp Rate
"
570  FOR I=1 TO N
580    PRINT TEMP(I),RECIPT(I),    RATE(I),      RLN(I)
590    NEXT
600  @%=131594
610  PRINT
620 PRINT "RATE= ( ";ACT1;"+";SDA1;" ) 1/T + ( ";B;" + ";ALPHAB;" ) Kcal/mol"
630 PRINT
640 PRINT "RATE= ( ";ACT2;"+";SDA2;" ) 1/T + ( ";B;" + ";ALPHAB;" ) KJ/mol"
650  @%=10
```

APPENDIX No 4 DAY, TIME, PRESSURE AND TEMPERATURE DATA OF THE HYDRAZINE DECOMPOSITION EXPERIMENTS DISCUSSED IN CHAPTER No 6

HYDRAZINE BLANK; 50'C

Day	Time (hr)	Mv	Temp (C)
2	10.7	15.96	50.7
2	16.93	15.98	50.5
5	9.9	16.45	50.7
6	9.92	16.6	50.6
6	11.57	16.87	50.8
7	9.52	16.64	50.6
7	9.93	16.7	50.7
7	10.7	16.82	50.8
8	10.8	17.22	50.8
9	9.6	17.09	50.7
9	10.37	17.2	50.5
12	9.68	17.59	50.6
12	10.77	17.78	50.7
12	11.97	18	50.7
13	9.82	17.87	50.6
13	10.87	18.08	50.7
13	11.75	18.16	50.7
14	0.43	18.01	50.5
14	11.83	18.06	50.4
15	9.8	18.32	50.6
15	10.83	18.3	50.4
16	10.12	18.5	50.5

HYDRAZINE BLANK; 60'C

Day	Time (hr)	Mv	Temp (C)
2	10.78	24.83	61.5
2	16.03	25.27	61.4
3	9.83	26.07	61.6
3	17.85	26.17	61.4
4	9.27	26.9	61.6
4	17.33	27.08	61.6
7	10.5	28.93	61.6
7	18.93	29.07	61.4
8	9.88	29.7	61.6
9	9.37	30.1	61.6
9	14.25	30.29	61.5
10	9.42	30.87	61.6
10	18.63	30.96	61.4
11	9.55	31.27	61.4
11	10.37	31.37	61.4
11	17.13	31.52	61.4
14	10.4	33.51	61.8
14	20.22	33.29	61.6
15	9.78	33.95	61.8
16	9.27	34.55	61.9
16	9.43	34.62	61.9
16	10	34.84	61.9

HYDRAZINE BLANK; 70'C

Day	Time (hr)	Mv	Temp (C)
2	15.18	29.76	69.9
3	10.28	31.16	70.4
3	11.23	31.49	70.5
4	10.7	32.44	70.4
4	13.75	32.56	70.2
5	9.33	33.57	70.6
5	10.57	33.92	70.5
5	12	34.56	70.5
6	9.93	35.34	70.2
7	9.92	36.08	70.2
7	18.75	36.79	70.4
10	9.53	39.11	70.2
11	9.38	39.74	69.9
11	17.97	40.1	69.9
12	9.92	41.12	70
12	13.5	41.6	70.1
13	9.53	41.92	70
13	11.22	42.03	70
14	9.88	42.86	70
14	11.08	43.05	70
14	17.95	43.3	70.1
17	10.33	45.35	69.9

HYDRAZINE BLANK; 80'C

Day	Time (hr)	Mv	Temp (C)
1	9.28	43.44	80.2
1	10.12	43.68	80.3
1	16.2	44.2	80.2
1	19.53	44.37	80.3
2	10.17	45.32	80.4
2	11.22	45.3	80.3
2	15.47	45.73	80.2
3	10.22	47.22	80.4
3	11.42	47.5	80.5
3	17.25	47.63	80.4
3	18.22	47.81	80.3
4	10	49.14	80.4
4	11.45	49.24	80.4
4	13.63	49.5	80.5
4	17.82	49.85	80.4
7	11.2	55.12	80.5
7	18.27	55.21	80.4
8	10.13	56.15	80.4
8	11.23	56.23	80.4
8	14.48	56.58	80.5
8	16.42	56.73	80.5
8	18.48	57.01	80.5
9	10	58.27	80.5
9	11	58.51	80.5
10	10.12	59.06	80.5
11	9.58	60.51	80.6
14	9.55	66.06	80.6
14	10.25	66.31	80.6
14	12.15	66.55	80.5
14	13.65	66.78	80.6
14	15.82	66.6	80.4
15	9.67	68.52	80.4
15	10.75	68.46	80.4
15	12.23	68.68	80.5
15	16.85	68.84	80.3
15	18.03	69.34	80.5
16	8.85	70.15	80.5
17	9.9	71.13	80.3
17	13.4	71.76	80.4
22	10.23	76.25	80.5
22	12.57	76.76	80.7

CHROMIUM ADD'N I: 50'C

Day	Time (hr)	Mv	Temp (C)
1	9.57	14.89	49.9
1	10.55	14.96	49.9
4	9.28	15.2	49.9
4	14.57	15.36	49.9
5	9.68	15.45	49.9
5	13.93	15.53	50
6	9.37	15.58	49.9
7	10.23	15.62	49.8
7	11.57	15.72	49.8
8	9.68	15.91	49.9
8	10.67	15.95	49.9
11	9.15	16.29	49.9
11	10.15	16.62	50.1
13	9.97	16.79	50
15	11.2	16.81	49.7
15	15.38	16.88	49.8
15	18.65	16.9	49.8
20	9.35	18.02	49.9
20	11.37	17.96	49.8
20	14.85	17.74	49.8
20	16.67	17.79	49.7
21	9.83	18.09	49.8
21	10.42	18	49.7
21	11.67	17.93	49.8
22	9.42	17.95	49.8
22	12.38	18.01	49.8
22	14.45	18.09	49.8
22	15.43	18.11	49.8
25	9.82	18.44	49.8

CHROMIUM ADD'N I: 60'C

Day	Time (hr)	Mv	Temp (C)
1	9.72	21.97	59.9
1	10.95	21.93	59.9
2	9.78	22.08	59.9
2	10.48	22.09	59.9
2	15.62	22.2	59.9
3	9.12	22.33	59.8
3	10.12	22.45	60
3	13.28	22.58	60
3	16.02	22.63	60
8	9.28	23.6	60
8	10.55	23.51	59.8
8	12.22	23.56	59.8
8	15.02	23.59	59.8
9	9.75	23.62	59.8
9	10.93	23.65	59.8
9	15.73	23.85	59.8
9	17.93	23.86	59.8
10	9.58	23.91	59.8
10	11.03	24.93	59.8
10	12.57	24.1	59.9
10	14	24.13	59.8
10	15.2	24.17	59.8
11	9.4	24.17	59.8
11	10.2	24.22	59.8
11	11.33	24.3	59.9
11	14.53	24.42	59.8
11	16.97	24.4	59.8
14	11.13	24.88	59.7
14	15.95	25.17	59.9
14	22.67	24.8	59.6
15	9.5	24.95	59.7
15	13.2	25.23	59.7
15	14.83	25.31	59.8
15	15.67	25.37	59.8
16	9.37	25.43	59.7
16	10.28	25.49	59.8
16	11.43	25.55	59.9
16	14.3	25.62	59.8

CHROMIUM ADD'N I: 70'C

Day	Time (hr)	Mv	Temp (C)
2	9.72	31.07	69.9
2	11.02	31.21	69.8
2	12.28	31.23	69.8
2	13.2	31.25	69.8
5	10.42	32.84	69.8
5	11.68	32.97	69.9
5	12.42	33.03	69.9
5	14.62	32.42	69.9
5	16.45	32.5	70
6	10.27	32.61	69.7
6	10.85	32.86	69.8
6	11.87	32.95	69.7
6	14.28	33	69.7
6	17.02	33.06	69.9
7	9.2	33.21	69.7
7	10.23	33.42	69.7
7	11.52	33.51	69.6
7	12.67	33.56	69.7
7	15.2	33.66	69.7
8	9.75	34.03	69.8
8	19.77	34.1	69.8
8	11.83	34.16	69.7
8	12.78	34.21	69.7
9	9.5	34.38	69.7
9	11.07	34.7	71
19	11.58	39.97	69.8
19	12.4	40	69.8
19	14.38	40	69.9
19	17.48	40.38	69.9
20	9.12	40.41	69.7
20	10.62	40.52	69.7
20	15.08	40.61	69.8
20	16.57	40.71	69.8
21	9.03	41.08	69.8
21	10.55	41.22	69.9
21	11.68	41.23	69.8

CHROMIUM ADD'N I: 80'C

Day	Time (hr)	Mv	Temp (C)
2	9.73	42.63	79.3
2	10.58	42.8	79.4
2	11.55	42.94	79.4
2	12.65	43.1	79.3
2	13.53	43.19	79.4
2	15.82	43.37	79.5
5	10.03	46.43	79.4
5	11.2	46.57	79.5
5	12.07	46.65	79.7
5	14.22	46.84	79.4
6	9.62	47.58	79.4
6	11.33	47.74	79.4
6	13.28	48.02	79.6
6	15.65	48.15	79.5
7	9.22	49.04	79.6
7	10.2	48.88	79.4
7	11.33	49.05	79.7
7	12.38	49.15	79.5
7	13.57	49.24	79.8
7	15.43	49.37	79.5
8	9.87	49.97	79.5
8	11.5	50.17	79.4
8	15.3	50.65	79.7
8	16.47	50.78	79.7
8	18.38	50.9	79.5
9	9.45	51.29	79.5
9	10.37	51.52	79.6
9	12.03	51.71	79.7
9	14.05	51.95	79.6

CHROMIUM ADD'N II; 50'C

Day	Time (hr)	Mv	Temp (C)
3	9.35	16.09	51
3	10.47	16.21	51.1
4	9.32	16.08	50.9
4	10.55	16.11	50.8
4	12	16.18	50.9
4	13.33	16.25	51
4	15.02	16.27	51
5	9.77	16.27	50.8
5	11.28	16.39	50.9
5	13.7	16.45	51
6	9.23	16.4	51
6	10.18	16.53	51
6	11.27	16.61	51.1
6	13.18	16.67	51.1
7	9.48	16.22	50.8
7	10.97	16.32	50.9
7	13.2	16.45	50.9
7	14.62	16.56	50.9
7	17.73	16.64	51
8	13.2	16.52	50.8
10	9.08	16.63	50.8
10	10.73	16.7	50.8
10	14.17	16.75	50.8
10	15.35	16.79	51.8
10	16.57	16.8	50.9
11	9.7	16.83	50.8
11	11.03	16.87	50.8
11	13.07	16.91	50.9
11	14.38	16.99	50.9
12	9.25	17	50.8
12	10.33	17.08	50.9
12	15.48	17.14	51.1
12	17.33	17.22	51.1
13	9.67	17.14	51
13	10.53	17.29	51
13	11.42	17.4	51.1
13	12.93	17.62	51.3
13	14.55	17.71	51.3
13	15.87	17.75	51.3
14	9.63	17.56	51
14	10.63	17.71	51.1
14	11.9	17.84	51.2

CHROMIUM ADD'N II; 70'C

Day	Time (hr)	Mv	Temp (C)
2	11	28.82	71
2	12.67	29.06	71
2	14.12	29.23	71.1
3	9.97	29.42	70.9
3	13.78	29.78	71
3	15.92	30.04	71.1
6	10.08	31.54	70.9
6	11.45	31.68	71
6	13.23	32.1	71.2
6	14.53	32.32	71.2
6	16.32	33.41	71.1
7	9.63	32.48	71.1
7	10.72	32.97	71.2
7	12.32	32.97	71.1
7	14.47	33.23	71.4
7	16.32	33.41	71.3
8	8.92	33.16	71.1
8	10.18	33.59	71.2
8	12.08	33.49	71.2
8	13.55	33.73	71.2
8	15.6	33.93	71.4
9	9.03	33.76	71.1
9	10.5	33.93	71.2
9	12.77	33.99	71.1

CHROMIUM ADD'N II; 60'C

Day	Time (hr)	Mv	Temp (C)
3	10.45	19.54	61.3
3	11.47	19.74	61.3
3	13.87	18.86	61.4
3	15.32	19.87	61.4
4	10.42	19.87	61.2
4	13.18	19.77	61.3
4	15.85	20.06	61.2
4	17.97	20.14	61.3
5	9.12	19.86	61.1
5	19.13	20	61.3
5	11.27	20.16	61.2
5	12.42	20.26	61.2
5	14.05	20.25	61.2
5	15.48	20.33	61.3
6	9.47	20.22	61.2
7	9.1	20.42	61
7	10.27	20.52	61.2
7	11.57	20.47	61.2
10	9.67	21.13	61.2
10	10.53	21.21	61.2
10	11.98	21.29	61.2
10	14.2	21.32	61.2
10	15.8	21.38	61.3
10	18.98	21.41	61.2
11	9.3	21.3	61.1
11	10.63	21.44	61.2
11	11.67	21.54	61.2
11	12.77	21.57	61.2

CHROMIUM ADD'N II; 80'C

Day	Time (hr)	Mv	Temp (C)
3	9.67	43.5	80.9
3	10.7	43.62	80.9
3	11.88	43.78	81
3	13.37	44.04	80.9
3	14.93	44.21	81
3	16.72	44.37	81.1
4	9.35	44.49	80.7
4	11.08	44.89	80.9
4	12.5	45.14	80.9
4	14.48	45.47	81
5	9.6	45.86	80.9
5	10.82	46.04	81
5	13.75	46.25	81
5	15.28	46.37	80.9
5	17.87	46.41	81
6	9.47	46.85	80.9
6	10.25	47.02	80.9
6	11.65	47.25	80.9
6	12.63	47.39	81
6	14.28	47.59	81.1
6	15.68	47.74	81
6	17.3	47.87	81.1
7	9.25	48.16	81
7	10.55	48.34	81
7	11.78	48.55	81
7	13.98	48.8	81

CHROMIUM ADD'N III; 50'C

Day	Time (hr)	Mv	Temp (C)
2	11.02	14.9	50.8
2	12.02	14.98	50.9
2	13	15.05	50.9
2	14.02	15.11	50.9
2	15	15.16	51
2	16.48	15.2	50.9
2	17.5	15.19	50.9
2	18.93	15.19	50.9
3	9.97	15.13	50.8
3	11.93	15.23	50.8
3	12.98	15.3	50.9
3	15	15.35	50.8
3	16.83	15.35	50.9
3	18.08	15.37	50.9
4	9.27	15.25	50.8
4	10.52	15.28	50.8
4	13.5	15.36	50.9
4	16.95	15.5	50.9
4	19.75	15.45	50.9
5	9.97	15.05	50.6
5	10.05	15.13	50.7
5	11.35	15.2	50.7
5	12.45	15.26	50.7
5	13.7	15.31	50.8
5	15.95	15.33	50.8
5	17.5	15.39	50.7
6	8.77	15.41	50.7
6	9.97	15.45	50.7
6	10.78	15.51	50.8
6	11.67	15.6	50.8
6	14	15.7	50.9
6	15.3	15.74	50.9
6	16.93	15.74	50.9
6	19.37	15.68	50.7
6	20.13	15.64	50.8
7	9.78	15.61	50.7
7	10.83	15.72	50.7
7	12.13	15.77	50.7
7	13.47	15.75	50.7
7	14.73	15.82	50.8
7	16.32	15.74	50.7
7	19.02	15.73	50.7

CHROMIUM ADD'N III; 60'C

Day	Time (hr)	Mv	Temp (C)
3	9.93	18	60.3
3	11.08	18.1	60.3
3	12.07	18.15	60.3
3	13.62	18.25	60.4
3	15.68	18.24	60.4
3	16.55	18.2	60.4
3	17.78	18.21	60.3
3	19.43	18.19	60.3
3	21.22	18.13	60.4
4	9.35	18.09	60.3
4	10.32	18.18	60.2
4	11.23	18.26	60.2
4	12.75	18.44	60.4
4	13.9	18.47	60.3
4	15.65	18.58	60.4
4	18.5	18.59	60.3
4	19.58	18.52	60.3
4	20.5	18.5	60.2
4	21.07	18.34	60.1
5	9.13	18.44	60.3
5	10.23	18.51	60.3
5	11.2	18.57	60.5
5	12.47	18.64	60.5
5	14.97	18.65	60.4
5	15.85	18.71	60.5
5	17.07	18.79	60.5
5	18	18.82	60.6
5	19.22	18.79	60.5
5	21.07	18.72	60.3
6	9.93	18.69	60.3
6	11.68	18.82	60.4
6	13.15	19	60.6
6	15.35	19.04	60.5
6	16.17	19.09	60.6
6	18.23	19.13	60.6
6	19.53	19.1	60.4
6	20.47	19.07	60.5
7	9.38	19.19	60.5
7	11	19.35	60.5
7	13.75	19.47	60.7
7	14.57	19.5	60.6
7	15.77	19.51	60.5
7	16.68	19.48	60.5

CHROMIUM ADD'N III; 70'C

Day	Time (hr)	Mv	Temp (C)
3	14.33	27.87	70.4
3	15.78	27.88	70.1
4	8.5	27.86	70.2
4	9.7	27.85	70.3
4	10.87	27.95	70.2
4	12.78	28.16	70.5
4	13.77	28.23	70.2
4	15.5	28.39	70.5
4	17.93	28.44	70.3
4	18.73	28.46	70.4
4	19.78	28.47	70.3
4	20.6	28.47	70.3
5	9.92	28.87	70.5
5	12.28	29.11	70.7
5	13.07	29.17	70.9
5	14.05	29.24	70.8
5	17.83	29.4	70.7
5	19.13	29.35	70.6
5	20.07	29.34	70.7
6	9.5	29.36	70.5
6	10.62	29.41	70.5
6	11.63	29.54	70.6
6	13	29.66	70.6
6	14.5	29.73	70.6
6	16.28	29.83	70.7
6	17.82	29.87	70.7
6	21	29.77	70.5
7	8.78	29.74	70.4
7	10.72	30.06	70.7
7	12.6	30.17	70.7
7	14.38	30.3	70.7

CHROMIUM ADD'N III; 80'C

Day	Time (hr)	Mv	Temp (C)
3	10.13	41.05	80.1
3	11.07	41.17	80.1
3	12.2	41.32	80.1
3	13.17	41.38	80.2
3	14.87	41.47	80.1
3	16.37	41.54	80.1
3	17.95	41.6	80.2
3	19.47	41.62	80.3
3	21.78	41.63	80.1
4	9.25	42.25	80.1
4	10.52	42.41	80.3
4	12.4	42.63	80.3
4	13.82	42.72	80.4
4	16.05	42.78	80.3
4	17.6	42.81	80.2
4	19.85	42.82	80.2
4	21.15	42.87	80.2
5	9	43.35	80
5	10.63	43.63	80.2
5	11.82	43.81	80.4
5	14.08	44.01	80.5
5	15.92	44.1	80.5
5	18.42	44.14	80.3
5	20.63	44.14	80.3
5	21.88	44.11	80.2
6	9.33	44.36	80.1
6	10.77	44.57	80.3
6	11.82	44.72	80.4
6	14.47	44.96	80.3
6	15.38	44.98	80.2
7	8.83	45.52	80.2
7	10.03	45.69	80.2
7	13.18	46.07	80.4
7	15.58	46.17	80.4
7	17.62	46.28	80.2

ACID ADD'N; 50'C

Day	Time (hr)	Mv	Temp (C)
3	9.55	15.51	52.2
3	10.8	15.57	52.2
3	12.88	15.59	52.3
3	14.73	15.63	52.3
3	16	15.67	52.3
3	18.55	15.64	52.3
3	20	15.67	52.3
4	9.8	15.68	52.3
4	11	15.77	52.3
4	12.25	15.81	52.3
4	13.48	15.87	52.4
4	15.07	15.88	52.3
4	17.1	15.88	52.4
4	20.97	15.83	52.3
5	9.73	15.79	52.4
5	10.87	15.86	52.3
5	13.95	16.05	52.4
5	15.95	16.07	52.4
5	17.02	16.03	52.3
5	18	15.99	52.3
6	9.8	15.71	52.2
6	12.2	15.96	52.3
6	13.58	16.07	52.4
6	14.68	16.12	52.4
6	16.23	16.13	52.4
6	17.67	16.12	52.3
7	9.92	15.87	52.2
7	10.8	16.04	52.3
7	12.4	16.18	52.4
7	14.12	16.25	52.4
7	16.6	16.3	52.4
7	17.42	16.28	52.4
7	18.92	16.23	52.4

ACID ADD'N; 60'C

Day	Time (hr)	Mv	Temp (C)
2	12.13	23.61	61.3
2	14.85	23.7	61.4
2	17.97	23.78	61.4
2	19.1	23.73	61.4
3	9.95	23.5	61.2
3	11.15	23.6	61.2
3	12.47	23.68	61.3
3	13.53	23.73	61.3
3	16.38	23.87	61.3
3	17.8	23.91	61.4
3	19.37	23.93	61.4
4	9.27	24.03	61.3
4	10.52	24.1	61.3
4	11.57	24.15	61.4
4	13.18	24.27	61.4
4	15.82	24.36	61.4
4	17.08	24.4	61.5
5	9.45	24.11	61.3
5	10.77	24.21	61.3
5	11.93	24.28	61.3
5	12.87	24.33	61.4
5	14.12	24.39	61.3
5	15.97	24.46	61.4
5	17.47	24.48	61.4
5	18.83	24.49	61.4
5	20.53	24.4	61.3
5	22.3	24.36	61.3
6	9.78	24.47	61.3
6	10.72	24.55	61.3
6	13.22	24.77	61.4
6	14.52	24.79	61.5
6	15.77	24.85	61.5
6	17.25	24.87	61.5
6	18.85	24.83	61.4
7	9.75	24.82	61.3
7	11.13	24.97	61.4
7	12.68	25.02	61.4
7	14.08	25.05	61.4
7	16	25.11	61.4
7	18.02	25.1	61.4

ACID ADD'N; 70'C

Day	Time (hr)	Mv	Temp (C)
3	9.3	29.93	71.2
3	10.82	30.09	71.2
3	12.93	30.2	71.3
3	14.3	30.27	71.3
3	15.78	30.34	71.3
3	17.2	30.39	71.3
3	18.42	30.36	71.3
3	20	30.32	71.2
4	9.45	30.27	71.2
4	10.5	30.36	71.1
4	12.18	30.54	71.3
4	13.28	30.6	71.3
4	15.42	30.74	71.3
4	16.87	30.79	71.4
4	18.85	30.85	71.3
4	19.55	30.82	71.3
4	21.33	30.81	71.3
5	8.93	31	71.2
5	11.13	31.17	71.3
5	12.23	31.27	71.3
5	13.42	31.3	71.4
5	16.08	31.45	71.4
5	17.5	31.48	71.4
6	9.62	31.4	71.2
6	10.75	31.6	71.3
6	12.05	31.78	71.3
6	13.87	31.98	71.4
6	15.32	32	71.4
6	17.48	32.04	71.4
6	18.82	31.94	71.3
6	20.88	31.9	71.3
7	9.37	32.3	71.4
7	10.55	32.49	71.4
7	11.87	32.56	71.5
7	13.17	32.51	71.3
7	14.73	32.52	71.4
7	17.28	32.53	71.4

ACID ADD'N; 80'C

Day	Time (hr)	Mv	Temp (C)
3	9.53	39.38	81.4
3	11.08	39.83	81.5
3	12.62	39.83	81.5
3	13.57	39.79	81.3
3	16.98	39.92	81.4
3	18.72	40.05	81.4
3	20.33	40.19	81.4
3	21.35	40.3	81.4
4	9.5	40.47	81.3
4	10.57	40.59	81.3
4	12.43	40.88	81.4
4	13.57	41.02	81.4
4	14.65	41.12	81.4
4	16.85	41.3	81.5
4	19.15	41.41	81.5
5	9.77	42.28	81.5
5	10.98	42.27	81.5
5	12.92	42.86	81.4
5	14.18	42.4	81.4
5	15.75	42.27	81.4
5	16.83	42.51	81.4
5	19	42.52	81.4
5	20.88	42.56	81.3
6	9.08	42.98	81.3
6	10.27	43.24	81.3
6	11.62	43.41	81.4
6	12.95	43.48	81.5
6	14.2	43.58	81.5
6	16.62	43.76	81.5
6	18.5	43.83	81.5
7	10.47	44.97	81.6
7	11.85	45.07	81.6
7	14.35	44.91	81.5
7	15.4	44.9	81.5
7	16.88	44.97	81.4
7	20.97	44.98	81.4
9	13.53	47.07	81.5
9	14.87	47.18	81.5
9	16.4	47.27	81.5
9	17.87	47.33	81.5
9	19.93	47.33	81.4

REFERENCES

[1] T.Curtius, *J.Prakt.Chem.*, **39**, 107 (1889).

[2] E.Schmitt. *Hydrazine and Its Derviatives; Preparation, Properties and Applications*, John Wiley & Sons (1984). This work is the most definitive text of all aspects of hydrazine chemistry published to date.

[3] H.Ulich, H.Peisher and L.F.Audreith, *Chem. Ber.*, **68B**, 1677 (1935).

[4] Y.Morino, T.Ijima and Y.Murata, *Bull.Chem.Soc.Jpn.*, **33**, 46 (1960).

[5] A.Yamaguschi, I.Ichishima, T.Shimanouchi and S-I.Mizushima, *J.Chem.Phys.*, **31**, 843 (1959).
A.H.Cowley, D.J.Mitchell, M-H.Whangbo and S.Wolfe, *J.Am.Chem.Soc.*, **101**, 5224 (1979).

[6] R.Stollé and K.Hofmann, *Ber.dtsch.chem.Ges.*, **37**, 4523 (1904)

[7] D.F.Johnson, Aerojet Engineering Corp, Research Tech. Memo No 62, ATI 87316 (13.4.1950).

[8] Launch of Explorer 1 (31.1.58) was the first use of UDMH as space-borne rocket propellant. The first use of hydrazine as a rocket propellant was the launch of Gemini 1 (29.7.64) on a Titan II rocket. Hydrazine was used in a 50:50 mix with UDMH (Aerozine 50).

[9] A.E.Axworthy, J.M.Sullivan, S.Cohz and E.Wela, AFRPL-TR-69-146, (July 1969).

[10] E.L.Harris, Wright Air Dev. Center (WADC), TR-58-157 (Feb 1958).

[11] Military Specification, Propellant Hydrazine MIL-P-26536C. Amendment 2, U.S.DoD (Feb 1982).

[12] R.L.Green, J.P.Stebbins, A.W.Smith and K.E.Pullen, Boeing Aerospace Company, Report D180-14839-2 (Dec 1973).

[13] L.R.Toth, W.A.Cannon, C.D.Coulbert and H.R.Long, JPL Technical Memorandum 33-799 (Aug 1976).

[14] J.M.Bellerby, PERME Memorandum 226 (Aug 1983)

[15] J.M.Bellerby, *J.Hazard.Mater.*, **7**, 187 (1983).

[16] J.M.Bellerby, *J.Hazard.Mater.*, **13**, 57 (1986).

[17] F.Bottomley, *Q.Rev.Chem.Soc.*, **1970**, 617. The first review of hydrazine coordination chemistry.

[18] J.R.Dilworth, *Coord.Chem.Revs.*, **21**, 29 (1976). Complementary review to [17], concentrating on the coordination chemistry of substituted hydrazines.

[19] T.Curtius and F.Schrader, *J.Prakt.Chem.*, **50**, 311 (1894).

[20] K.A.Hofmann and E.C.Marburg, *Ber.dtsch.chem.Ges.*, **60**, 2019 (1897).

[21] H.Franzen and O.von Meyer, *Z.Anorg.Allgem.Chem.*, **60**, 247 (1908).
H.Franzen and H.L.Lucking, *ibid.*, **70**, 145 (1911).

[22] A.Braibanti, F.Dallavalle, M.A.Pellinghelli and E.Laporati, *Inorg.Chem.*, **7**, 1430 (1968).

[23] L.Sacconi and A.Sabatini, *J.Inorg.Nucl.Chem.*, **25**, 1389 (1963).

[24] A.Ferrari, A.Braibanti and G.Bigliardi, *Acta.Cryst.*, **16**, 498 (1963).

[25] D.Nicholls, M.Rowley and R.Swindells, *J.Chem.Soc.(A).*, **1966**, 950.

[25A] K.H.Linke, F.Bürholz and P.Hädiche, *Z.Anorg.Allgem.Chem.*, **356**, 113 (1968).

[26] D.Nicholls and R.Swindells, *J.Inorg.Nucl.Chem.*, **30**, 2211 (1968).

[27] A.Ferrari, A.Braibanti, G.Bigliardi and A.M.Lanfredi, *Z.Krist.*, **122**, 259 (1965).

[28] I.A.Latham, G.J.Leigh, G.Hüttner and I.Jibril, *J.Chem.Soc., Dalton.Trans*, **1986**, 385.

[29] J.A.McCleverty, A.E.Rae, I.Wolochowicz, N.A.Bailey and J.M.A.Smith, *J.Chem.Soc., Dalton.Trans.*, **1983**, 71.

[30] K.Gebreyes, J.Zubieta, T.A.George, L.M.Koczon and R.C.Tisdale, *Inorg.Chem.*, **25**, 405 (1986).

[31] D.L.Hughes, I.A.Latham and G.J.Leigh, *J.Chem.Soc., Dalton. Trans.*, **1986**, 393.

[32] D.Sellmann, E.Böhlen, M.Waeber, G.Hüttner and L.Zsolnai, *Angew.Chem., Int.Ed.Engl.*, **24**, 981 (1985).

[33] L.Blum, I.D.Williams and R.R.Schrock, *J.Am.Chem.Soc.*, **106**, 8316 (1984).

[34] J.R.Dilworth, S.A.Harrison, D.R.M.Walton and E.Schwedu, *Inorg.Chem.*, **24**, 2594 (1985).

[35] T-C.Hsieh, K.Gebreyes and J.Zubieta, *J.Chem.Soc., Chem. Commun.*, **1984**, 1172.

[36] I.A.Latham, G.J.Leigh, G.Hüttner and I.Jibril, *J.Chem.Soc., Dalton.Trans.*, **1986**, 377.

[37] D.Bright and J.A.Ibers, *Inorg.Chem.*, **8**, 703 (1969).

[38] R.J.Doedens and J.A.Ibers, *Inorg.Chem.*, **6**, 204 (1967).

[39] E.N.Maslen, C.L.Raston, B.W.Shelton and A.H.White, *Aust.J.Chem.*, **28**, 739 (1975).

[40] A.Anagnostopoulos and D.Nicholls, *J.Inorg.Nucl.Chem.*, **38**, 1615 (1976).

[41] C.H.Stapfer and R.W.D'Andrea, *Inorg.Chem.*, **10**, 1224 (1971).

[41A] M.Sieprawski, J.Said and R.Cohen-Adad, *J.Chim.Phys.Phys-Chim.Biol.*, **70**, 1417 (1973).

[42] A.Ferrari, A.Braibanti and A.M.Lanfredi, *Ann.Chim.(Italy)*., **48**, 1238 (1958).

[43] A.Ferrari, A.Braibanti, G.Bigliardi and A.M.Lanfredi, *Acta.Cryst.*, **18**, 367 (1965).

[44] A.Ferrari, A.Braibanti, G.Bigliardi and A.M.Lanfredi, *Acta.Cryst.*, **19**, 548 (1965).

[45] A.Ferrari, A.Braibanti, G.Bigliardi and F.Dallevalle, *Z.Krist.*, **119**, 284 (1963).

[46] D.T.Cromer, A.C.Larson and R.B.Roof, *Acta.Cryst.*, **20**, 279 (1966).

[47] D.Sellmann, P.V.Kreutzer, G.Hüttner and A.Frank, *Z.Naturforsh.,B;Anorg.Chem.Org.Chem.*, **33B**, 1341 (1978).

[48] T.V.Ashworth, M.J.Nolte and E.Singleton, *J.Chem.Soc., Dalton.Trans.*, **1978**, 1040.

[49] T.V.Ashworth, M.J.Nolte, R.H.Reimann and E.Singleton, *J.Chem.Soc., Dalton.Trans.*, **1978**, 1043.

[50] S.D.Ittel and J.A.Ibers, *Inorg.Chem.*, **14**, 636 (1975).

[51] N.A.Bailey, P.D.Frisch, J.A.McCleverty, N.W.Walker and J.Williams, *J.Chem.Soc., Chem.Commun.*, **1975**, 350.

[52] R.Tsuchiya, M.Yonemura, A.Uehara and E.Kyuno, *Bull.Chem.Soc.Jpn.*, **47**, 660 (1974).

[53] B.Banerjee, P.K.Biswas and N.Ray Chaudhuri, *Bull.Chem.Soc.Jpn.*, **56**, 2509 (1983).

[54] E.A.Nikonenko, E.I.Krylov and V.A.Sharov, *Zh.Neorg.Khim.*, **14**, 669 (1969).

[55] B.Banerjee, P.K.Biswas and N.Ray Chaudhuri, *Thermochim.Acta.*, **68**, 261 (1983).

[56] B.Banerjee, P.K.Biswas and N.Ray Chaudhuri, *Thermochim.Acta.*, **76**, 47 (1984).

[57] B.Banerjee and N.Ray Chaudhuri, *Thermochim.Acta.*, **71**, 93 (1983).

[58] B.Banerjee, A.Ghosh and N.Ray Chaudhuri, *Thermochim.Acta.*, **71**, 2173 (1983).

[59] T.B.Shkodina, E.I.Krylov and V.A.Sharov, *Zh.Neorg.Khim.*, **17**, 353 (1972).

[60] T.B.Shkodina, E.I.Krylov and V.A.Sharov, *Zh.Neorg.Khim.*, **17**, 1823 (1972).

[61] E.A.Nikonenko, E.I.Krylov and V.A.Sharov, *Zh.Neorg.Khim.*, **18**, 1569 (1973).

[62] D.Gajapathy and K.C.Patil, *Mater.Chem.Phys.*, **9**, 423 (1983).

[63] K.C.Patil, D.Gajapathy and V.R.Pai Verneker, *J.Mater.Sci.Lett.*, **2**, 272 (1983).

[64] T.V.Ashworth, E.Singleton and J.J.Hough, *J.Chem.Soc., Dalton.Trans.*, **1977**, 1809.

[65] H.E.Oosthuizen, E.Singleton, J.S.Field and G.C.Van Niekerk, *J.Organomet.Chem.*, **279**, 433 (1985).

[66] W.Rigby, J.A.McCleverty and P.M.Maitlis, *J.Chem.Soc., Dalton. Trans.*, **1979**, 382.

[67] R.J.Maurel, J.C.Menezo and J.Barrault, *J.Chim.Phys.Phys. -Chim.Biol.*, **70**, 1221 (1973).

[68] F.Bottomley and J.R.Crawford, *J.Am.Chem.Soc.*, **94**, 9092 (1972).

[69] F.Bottomley, S.G.Clarkson and S-B.Tong, *J.Chem.Soc., Dalton. Trans.*, **1974**, 2344.

[70] D.B.Musaev, M.N.Guseinov, N.G.Klyuchnikov and R.Ya.Aliev, *Zh.Neorg.Khim.*, **31**, 1127 (1986).

[71] R.Ya.Aliev, *Zh.Obshch.Khim.*, **46**, 9 (1976).

[72] R.Ya.Aliev, *Zh.Neorg.Khim.*, **21**, 2563 (1976).

[73] V.T.Athavale and C.S.Padmanaba Iyer, *J.Inorg.Nucl.Chem.*, **29**, 1003 (1967).

[74] D.Sellmann, A.Brandl and R.Endell, *J.Organomet.Chem.*, **111**, 303 (1976).

[75] D.Sellmann, A.Brandl and R.Endell, *J.Organomet.Chem.*, **97**, 229 (1975).

[76] D.Sellmann, A.Brandl and R.Endell, *Z.Naturforsch., B:Anorg. Chem., Org.Chem.*, **33B**, 542 (1978).

[77] D.Sellmann, *J.Organomet.Chem.*, **44**, C46 (1972).
D.Sellmann, R.Gerlach and K.Jödden, *J.Organomet.Chem.*, **178**, 433 (1979).

[78] D.Sellmann and E.Kleinschmidt, *Z.Naturforsch.,B:Anorg.Chem., Org.Chem.*, **32B**, 795 (1977).

[79] J.T.Moelwyn-Hughes, A.W.B.Garner and A.S.Howard, *J.Chem.Soc.(A).*, **1971**, 2361. *ibid*, **1971**, 2370.

[80] D.Petredis, A.Burke and A.L.Balch, *J.Am.Chem.Soc.*, **92**, 428, (1970).

[81] I.D.Brown and J.D.Dunitz, *Acta.Cryst.*, **13**, 28 (1960).

[82] M.W.Bishop, J.Chatt and J.R.Dilworth, *J.Organomet.Chem.*, **73**, C59 (1974).

[83] A.A.Diamantis, J.Chatt, G.J.Leigh and G.A.Heath, *J.Organomet.Chem.*, **84**, C11 (1975).

[84] D.Carrillo, P.Gouzerh and Y.Jeannin, *Nouv.J.Chim.*, **9**, 749 (1985).

[85] A.Anagnostopoulos, D.Nicholls and J.Reed, *Inorg.Chim.Acta.*, **32**, L17 (1979).

[86] W.K.Glass and J.O.McBreen, *J.Inorg.Nucl.Chem.*, **36**, 747 (1974).

[87] M.S.Novakovskii, V.A.Starodub and E.V.Golovinova, *Zh.Neorg. Khim.*, **19**, 3288 (1974).

[88] L.Mau Queng and M.S.Novakovskii, *Zh.Neorg.Khim.*, **13**, 2403 (1968).
M.S.Novakovskii, L.K.Bessarabenko, V.K.Yushko and V.A.Starodub, *Zh.Neorg.Khim.*, **17**, 2107 (1972).
M.S.Novakovskii and V.A.Starodub, *Zh.Neorg.Khim.*, **18**, 1128 (1973).
M.S.Novakovskii and L.K.Bessarabenko, *Zh.Obshch.Khim.*, **44**, 764 (1974).

[89] M.S.Novakovskii and V.A.Starodub, *Zh.Obshch.Khim.*, **43**, 1426 (1973).

[90] S.M.F.Rahman, J.Ahmad and M.M.Azharul Haq, *J.Inorg.Nucl.Chem.*, **33**, 4351 (1971).

[91] D.Nicholls and R.Swindells, *J.Chem.Soc.*, **1964**, 4204.

[92] F.Fitcher and B.Becker, *Ber.dtsch.chem.Ges.*, **44**, 3481 (1911).

[93] A.Callegari, *Gazz.Chim.Ital.*, **36**, 63 (1906).

[94] E.Ebler and E.Schott, *J.Prakt.Chem.*, **79**, 72 (1909).

[95] P.V.Gogorishvili, M.V.Karkarashvili and L.D.Tsitsishvili, *Zh.Neorg,Khim.*, 1, 1731 (1956).

[96] P.V.Gogorishvili, M.V.Karkarashvili and L.D.Tsitsishvili, *'Trudy.Inst-Khim.im.P.G.Melikishvili'.Akad.Nauk.Gruzin. S.S.R.*, 12, 121 (1956).

[97] P.V.Gogorishvili, M.V.Karkarashvili and L.D.Tsitsishvili, *Zh.Neorg.Khim.*, 1, 2753 (1956).

[98] P.V.Gogorishvili and M.G.Tsitsishvili, *Soobshcheriya. Akad.Nauk.Gruzin.S.S.R.*, 23, 281 (1959).

[99] P.V.Gogorishvili and T.M.Khonelidze, *Zh.Neorg.Khim.*, 6, 1291 (1961).

[100] H.Funk, A.Eichoff and G.Giesder, *Omagiu.Raluca.Ripan.,Edit. Acad.Rep.Soc.Romania.*, 247 (1966).

[101] A.Braibanti, G.Bigliardi, A.M.Lanfredi and A.Tiripicchio, *Nature (London)*, 211, 1174 (1966).

[102] K.C.Patil, R.Soundarajan and E.P.Goldberg, *Synth.React.Inorg.Metal-Org.Chem.*, 13, 29 (1983).

[103] R.K.Agarwal, V.Kapur, P.Kumar and A.K.Srivastava, *Oriental. J.Chem.*, 1, 85 (1985).

[104] L.Golic, J.Slivnik, M.Levstek and A.Rihar, *Monatsh.Chem.*, 99, 289 (1968).

[105] K.Broderson, *Z.Anorg.Allgem.Chem.*, 290, 24 (1957).

[106] A.Braibanti, G.Bigliardi and R.Canali-Padovani, *Ateneo. Parmense.Sez II.*, 1, 75 (1965).

[107] A.Braibanti, A.M.Manotti Lanfredi and A.Tiripicchio, *Z.Krist.*, 124, 335 (1967).

[108] P.Ravindranathan and K.C.Patil, *Proc.Indian.Acad.Sci. (Chem.Sci).*, 95, 345 (1985).

[109] K.C.Patil, R.Soundarajan and V.R.Pai Verneker, *Proc.Indian. Acad.Sci.,Sect A.*, 88A, 211 (1979).

[110] A.Braibanti, A.Tiripicchio, F.Dallevalle and E.Leporati, *Ric.Sci.*, 36, 1153 (1966).

[110A] A.Braibanti, F.Dallevalle and A.Tiripicchio, *Ric.Sci.*, 36, 1156 (1966).

[111] A.Braibanti, A.Tiripicchio, A.M.Manotti Lanfredi and F.Dallevalle, *Ric.Sci.*, 36, 1210 (1966).

[112] F.Bigoli, A.Braibanti, A.Tiripicchio and M.Tiripicchio-Camellini, *Acta.Cryst.*, 27, 2453 (1965).

[113] I.C.Furber, PERME Memorandum 147, Nov 1980.

[114] A.Braibanti, G.Bigliardi and R.Canali Padovani, *Gazz.Chim. Ital.*, **95**, 877 (1965).

[115] A.Braibanti, A.M.Manotti Lanfredi, M.A.Pellinghelli and A.Tiripicchio, *Acta.Cryst.*, **B27**, 2448 (1971).

[116] A.Braibanti, A.M.Manotti Lanfredi, A.Tiripicchio and F.Bigoli, *Acta.Cryst.*, **B25**, 100 (1969).

[117] A.K.Srivastava, *Transition.Met.Chem.(Weinheim.Ger.).*, **5**, 161 (1980).

[118] R.C.Comben, University of Bath, Final Year Report No 318 1985.

[119] J.Mácek, J.Slivnik and A.Rahten, *Vestn.Slov.Kem.Drus.*, **24**, 55 (1977).

[120] J.Slivnik and A.Rihar, *Monatsh.Chem.*, **103**, 1572 (1972).

[121] B.Barlic, L.Golic and F.Lazarini, *Cryst.Struct.Comm.*, 3, 407 (1974).

[122] J.Macek, A.Rahten and J.Slivnik, *Vestn.Slov.Kem.Drus.*, **29**, 249 (1982).

[123] P.V.Gogorishvili and M.V.Karkaraishvili, *Zh.Neorg.Khim.*, 10, 2664 (1965).

[124] J.Slivnik, A.Rahten and B.Sedej, *Vestn.Slov.Kem.Drus.*, **26**, 461 (1979).

[125] J.Macek, A.Rahten and J.Slivnik, *Proc.Eur.Symp.Therm.Anal.*, **1976**, 161.

[126] A.Braibanti, A.Tiripicchio, A.M.Manotti Lanfredi and F.Bigoli, *Z.Krist.*, **126**, 307 (1968).

[127] A.Braibanti, G.Bigliardi and A.M.Manotti Lanfredi, *Ateneo.Parmense.Sez.II.*, 1, 81 (1965).

[128] A.Braibanti, A.M.Manotti Lanfredi, M.A.Pellinghelli and A.Tiripicchio, *Acta.Cryst.*, **B27**, 2261 (1971).

[129] A.Ferrari, A.Braibanti, G.Bigliardi and A.M.Lanfredi, *Z.Krist.*, **122**. 259 (1965).

[130] A.Braibanti, A.M.Manotti Lanfredi, A.Tiripicchio and F.Bigoli, *Acta.Cryst.*, **B26**, 806 (1970).

[131] E.N.Maslen, C.L.Rasten, B.W.Skelton and A.H.White, *Aust.J. Chem.*, **28**, 739 (1975).

[132] A.Braibanti, A.Tiripicchio, A.M.Manotti Lanfredi and M.Camellini, *Acta.Cryst.*, **23**, 248 (1967).

[133] J.Slivnik, A.Rihar and B.Sedej, *Monatsh.Chem.*, 98, 200 (1967).

[134] K.C.Patil, J.S.Budkuley and V.R.Pai Verneker, *J.Inorg.Nucl. Chem.*, **41**, 953 (1979).

[135] P.V.Gogoroshvili, M.V.Karkarashvili and N.Ya.Kiknadze, USSR Patent 355,955.

[136] P.V.Gogoroshvili and M.G.Tskitishvili, *Tr.Inst.Khim.,Akad. Nauk.Gruz.S.S.R.*, **19**, 3 (1964).

[137] D.Hanzel and F.Sevsek, *J.Solid.State.Chem.*, **28**, 385 (1979).

[138] D.Hanzel, D.Hanzel and F.Sevsek, *Fizika.(Zagreb).*, **12**, 239 (1980).

[139] P.V.Gogoroshvili, M.E.Chkoniya, D.A.Akhobadze and T.V.Chkoniya, *Tr.Gruz.Politekh.Inst.*, **1969**, 7.

[140] M.K.Guseinova, M.A.Porai-Koshits, P.V.Gogoroshvili and A.S.Antsyshkina, *Dok.Akad.Nauk.SSSR.*, **169**, 577 (1966).

[141] D.N.Sathyanarayana and D.Nicholls, *Spectrochim.Acta.*, **34A**, 263 (1978).

[142] E.Fischer, *Ann.*, **190**, 123 (1878).

[143] A.Stern, *J.Prakt.Chem.*, **60**, 235 (1899).

[144] P.Bartz and H.P.Fritz, *Z.Naturforsch.*, **276**, 1131 (1972).

[145] A.K.Srivastava and F.Tarli, *J.Inorg.Nucl.Chem.*, **39**, 1793 (1977).

[146] A.K.Srivastava, *Croat.Chem.Acta.*, **52**, 293 (1979).

[147] A.K.Srivastava, A.L.Varshney and D.R.Singh, *Acta.Cienc. Indica.,[Ser].Phys.*, **9**, 62 (1983).

[148] P.Ray and P.V.Sarkar, *J.Chem.Soc.*, **117**, 321 (1920).

[149] P.Glavic, A.Bole and J.Slivnik, *J.Inorg.Nucl.Chem.*, **35**, 3979 (1973).

[150] F.J.Arnaiz Garcia, *An.Quim.*, 73, 1121 (1977).

[151] R.Y.Aliev, A.D.Kuliev and N.G.Klyuchnikov, *Zh.Neorg.Khim.*, 17, 3282 (1972).

[152] T.M.Zhdanovskikh, E.I.Krylov, V.A.Sharov and N.G.Fedotovskikh, *Zh.Neorg,Khim.*, **18**, 1234 (1973).

[153] K.C.Patil, C.Nesamani and V.R.Pai Verneker, *Synth.React. Inorg.Met-Org.Chem.*, **12**, 383 (1982).

[154] R.D.Dowsing, J.F.Gibson, M.Goodgame and P.J.Hayward, *J.Chem.Soc.(A).*, **1970**, 1153.

[155] J.Durig, S.F.Bush and E.E.Mercer, *J.Chem.Phys.*, **44**, 4238 (1966).

[156] M.Goldstein and W.D.Unsworth, *Spectrochim.Acta.*, **28A**, 1297 (1972).

[157] M.Goldstein and W.D.Unsworth, *Inorg.Chim.Acta.*, **4**, 342 (1970).

[158] R.A.Bailey, S.L.Kozak, T.W.Michelson and W.N.Miles, *Coord. Chem.Revs.*, **6**, 407 (1971).

[159] R.G.Pearson, *J.Chem.Ed.*, **45**, 581, 643 (1968).

[160] K.Nakamoto, *Infrared and Raman Spectra of Inorganic and Coordination Compounds*, 3rd Ed, John Wiley & Sons (1978).

[161] G.B.Deacon and R.J.Phillips, *Coord.Chem.Revs.*, **33**, 227 (1980).
G.B.Deacon, F.Huber and R.J.Phillips, *Inorg.Chim.Acta.*, **104**, 41 (1985).

[162] T.C.Downie, W.Harrison, E.S.Raper and M.A.Hepworth, *Acta.Cryst.*, **B27**, 706 (1971).

[163] M.A.Hitchman and G.L.Rowbottom, *Coord.Chem.Revs.*, **42**, 55 (1982).

[163A] J.E.Bennett, J.F.Gibson, D.J.E.Ingram, T.M.Houghton, G.A.Kerkut and K.A.Munday, *Proc.Roy.Soc.*, **A262**, 395 (1961).

[164] R.D.Dowsing, J.F.Gibson, M.Goodgame and P.J.Hayward, *J.Chem.Soc.(A).*, **1969**, 187.

[165] R.D.Dowsing and J.F.Gibson, *J.Chem.Phys.*, **50**, 294 (1969).

[166] R.D.Dowsing, J.F.Gibson, D.M.L.Goodgame, M.Goodgame and P.J.Hayward, *Nature (London)*, **219**, 1037 (1968).

[167] R.B.Birdy and M.Goodgame, *Inorg.Chim.Acta.*, **50**, 183 (1981).

[168] D.Taupin, *J.Appl.Crystallogr.*, **1**, 178 (1968).

[169] L.M.Barrow, *Physical Chemistry*, 4th Ed., 508 , McGraw-Hill (1979).

[170] F.A.Cotton and G.Wilkinson, Advanced Inorganic Chemistry, 4th Ed, John Wiley & Sons (1980).

[171] S.Vermura, A.Spencer and G.Wilkinson, *J.Chem.Soc.,Dalton. Trans.*, **1973**, 2565.

[172] B.A.Goodman and J.B.Raynor, *Adv.Inorg.Chem.Radiochem.*, 13, 135 (1970).

[173] A.R.E.Baikie, M.B.Hursthouse, L.New, P.Thornton and R.G.White, *J.Chem.Soc.,Chem.Commun.*, **1980**, 684.

[174] A.R.E.Baikie, M.B.Hursthouse, D.B.New and P.Thornton, *J.Chem.Soc.,Chem.Commun.*, **1978**, 62.

[175] J.Chatt, C.D.Falk, G.J.Leigh and R.J.Pashe. *J.Chem.Soc.(A).*, **1969**, 2288.

[176] F.Bottomley, *Can.J.Chem.*, **48**, 351 (1970).

[177] P.C.H.Mitchell and R.S.Scarle, *Nature (London)*, **240**, 417 (1972).

[178] J.R.Gilmore and J.M.Mellor, *J.Chem.Soc.(C).*, **1971**, 2355.

[179] E.Staal and C.Fourholt, *Dansk.Tids.Farm.*, **25**, 1 (1951).

[180] M.Caplow, *J.Am.Chem.Soc.*, **90**, 6795 (1968).

[181] J.E.Vanhalst and E.Brinckman, Ger.Offen 1,956,713 (C1.G03c).

[182] L.F.Larkworthy and J.M.Tabatabai, *Inorg.Chim.Acta.*, 21, 265 (1977).

[183] C.A.McAuliffe, J.V.Quagliano and L.M.Vallarino, *Inorg.Chem.*, **5**, 1997 (1966).
B.W.Fitzsimmons, A.Hume, L.F.Larkworthy, M.H.Turnball and A.Yavari, *Inorg.Chim.Acta.*, **106**, 109 (1985).

[184] E.Nachbaur and G.Lieseder, *Monatsh.Chem.*, **102**, 1718 (1971).

[185] U.Anthoni, D.M.Dahl, Ch.Larsen and P.H.Nielsen, *Acta.Chem.Scand.*, **23**, 1061 (1969).

[186] M.Tsuboi, T.Onishu, I.Nakagawa, T.Shimanouchi and S-I.Mizushima, *Spectrochim.Acta.*, **12**, 253 (1958).

[187] E.Spinner, *J.Chem.Soc.*, **1964**, 4217.

[188] K.Itoh and H.J.Bernstein, *Can.J.Chem.*, **34**, 170 (1958).

[189] V.Schettino and R.E.Salomen, *Spectrochim.Acta.*, **30A**, 1445 (1974).

[190] S.Milicéur and J.Mácek, *Spectrochim.Acta.*, **41A**, 651 (1985).

[191] W.Traube and W.Passarge, *Ber.dtsch.chem.Ges.*, **46**, 1505 (1913)

[192] F.Hein and G.Bähr, *Z.Anorg.Allgem.Chem.*, **252**, 55 (1943).

[193] S.M.F.Rehman and A.Malik, *Z.Anorg.Allgem.Chem.*, **323**, 83 (1963).

[194] A.Earnshaw, L.F.Larkworthy and K.S.Patil, *Z.Anorg.Allgem.Chem.*, **334**, 163 (1964).

[195] G.B.Kauffman and N.Sugisaka, *Z.Anorg.Allgem.Chem.*, **344**, 92 (1966).

[196] R.Ya.Aliev, *Zh.Obshch.Khim.*, **42**, 2370 (1972).

[197] P.Glavic, J.Slivnik and A.Bole, *Vestn.Slov.Kem.Drus.*, **29**, 227 (1982).

[198] D.W.Hand and C.K.Prout, *J.Chem.Soc.(A).*, **1966**, 168.

[199] C.K.Prout and H.M.Powell, *J.Chem.Soc.*, **1961**, 4177.

[200] H.Lux and G.Illman, *Chem.Ber.*, **91**, 2143 (1958).
H.Lux, L.Eberle and D.Sarre, *ibid*, **97**, 503 (1964).

[201] J.P.Fackler and D.G.Holah, *Inorg.Chem.*, **4**, 954 (1965).

[202] L.F.Larkworthy, A.J.Roberts, B.J.Tucker and A.Yavari, *J.Chem.Soc.,Dalton.Trans.*, **1980**, 262.

[203] F.A.Cotton and T.R.Felthouse, *Inorg.Chem.*, **19**, 328 (1980).

[204] L.F.Larkworthy and J.M.Tabatabai, *Inorg.Nucl.Chem.,Letters.*, **16**, 427 (1980).

[205] S.F.Rice, R.B.Wilson and E.I.Solomen, *Inorg.Chem.*, **19**, 427 (1980).

[206] M.G.Lyapilina, E.I.Krylov and V.A.Sharov, *Zh.Neorg.Khim.*, **20**, 392 (1975).

[207] M.G.Lyapilina, E.I.Krylov and V.A.Sharov, *Zh.Neorg.Khim.*, **20**, 816 (1975).

[208] V.A.Sharov, N.V.Povarova, V.A.Perelyaev and E.I.Krylov, *Koord.Khim.*, **5**, 537 (1979).

[209] V.A.Sharov, N.V.Povarova and E.I.Krylov, *Zh.Neorg.Khim.*, **25**, 2153 (1980).

[210] K.C.Patil, K.C.Nesameri and V.R.Pai Verneker, *Chem.Ind.(London).*, **24**, 901 (1979).

[211] A.J.Ratcliffe, Industrial Training Report, PERME Westcott, 1983.

[211A] D.F.Evans, *J.Chem.Soc.*, **1959**, 2003.

[212] C.F.Wells and M.A.Salam, *J.Chem.Soc.(A).*, **1968**, 1568.

[213] W.Schmidt, J.H.Swinehart and H.Taube, *Inorg.Chem.*, **7**, 1984 (1968).

[214] S.L.Brahn, A.Bakae and S.H.Espenson, *Inorg.Chem.*, **25**, 535 (1986).

[215] A.B.P.Lever, *J.Chem.Ed.*, **45**, 711 (1968).

[216] N.N.Greenwood and A.Earnshaw, *Chemistry of the Elements*, Pergamon Press (1984), p 1197.

[217] J.T.Veal, D.Y.Jeter, J.C.Hempel, R.P.Eckberg, W.E.Hatfield and D.J.Hodgson, *Inorg.Chem.*, **12**, 2928 (1973).

[218] H.Lux, L.Eberle and D.Sarre, *Chem.Ber.*, **97**, 503 (1964).

[219] S.Herzog and W.Kalies, *Z.Anorg.Allgem.Chem.*, **351**, 237 (1967).

[220] L.F.Larkworthy and J.M.Tabatabai, *Inorg.Chim.Acta.*, **21**, 265 (1977).

[221] A.Earnshaw, L.F.Larkworthy, K.C.Patil and G.Beech, *J.Chem. Soc.(A).*, **1969**, 1334.

[222] L.F.Larkworthy and K.A.R.Salib, *Trans.Met.Chem.*, **11**, 121 (1986).

[223] J.R.Durig, W.C.Harris and D.W.Wertz, *J.Chem.Phys.*, **50**, 1449 (1969).

[224] K.Starke, *J.Inorg.Nucl.Chem.*, **11**, 77 (1959).

[225] M.Arbon, A.Bino, S.Cohen and T.R.Felthouse, *Inorg.Chem.*, **23**, 3450 (1984).

[226] R.A.Haines and W.J.Louch, *Inorg.Chim.Acta.*, **71**, 1 (1983).

[227] R.F.Bryan, P.T.Greene, P.F.Stokely and E.W.Wilson, *Inorg.Chem.*, **10**, 1468 (1971).

[228] C.E.Skinner and M.M.Jones, *Inorg.Nucl.Chem.Lett.*, **3**, 185 (1967).

[229] L.J.Vieland and R.P.Seward, *J.Chem.Phys.*, **59**, 466 (1955).

[230] E.Fischer, *Ann*, **190**, 67 (1878).

[231] G.Martina, *L'Orosi.*, **37**, (1892).

[232] J.Ville and J.Moitessier, *Compt.rend.*, **124**, 1242 (1897). J.Moitessier, *ibid*, **124**, 1306, 1529 (1897).

[233] J.C.Evans, *Spectrochim.Acta.*, **16**, 428 (1960).

[234] A.T.Hutton and D.A.Thornton, *Spectrochim.Acta.*, **34A**, 645 (1978).

[235] E.Milla, G.Giustina and R.Margaria, *Boll.soc.ital. biol.sper.*, **29**, 805 (1953).

[236] A.W.Frances, *J.Phys.Chem.*, **58**, 1099 (1954).

[237] J.S.Morrow, P.Keim and F.R.N.Gurd, *J.Biol.Chem.*, **249**, 7484 (1974).

[238] W.J.Geary, *Coord.Chem.Revs.*, **7**, 81 (1971).

[239] M.Linhard and M.Weigard, *Z.Anorg.Allgem.Chem.*, **264**, 321 (1951).

[240] M.A.Bernard, M.M.Borel, A.Grandin and A.Leclaire, *Rev.Chim. Mater.*, **16**, 477 (1979).

[241] F.Calderazzo, D.B.Dell'Amico, R.Netti and M.Pasquali, *Inorg.Chem.*, **17**, 471 (1978).

[242] M.H.Chisholm and W.W.Reichert, *Inorg.Chem.*, **17**, 767 (1978).

[243] D.B.Dell'Amico, F.Calderazzo, B.Giovannitti and G.Pelizzi, *J.Chem.Soc.,Dalton.Trans.*, **1984**, 647.
F.Calderazzo, D.B.Dell'Amico and G.Pelizzi, *Gazz.Chim.Ital.*, **115**, 145 (1985).

[244] T.W.Coffindaffer, I.P.Rothwell and J.C.Huffman, *Inorg.Chem.*, **23**, 1433 (1984).

[245] M.H.Chisholm, F.A.Cotton and M.W.Extine, *Inorg.Chem.*, **17**, 2000 (1978).
M.H.Chisholm, L-S.Tan and J.C.Huffman, *J.Am.Chem.Soc.*, **104**, 4879 (1982).

[246] M.H.Chisholm, F.A.Cotton, M.W.Extine and D.C.Rideout, *Inorg. Chem.*, **17**, 3536 (1978).

[247] D.Petredis, A.Burke and A.L.Balch, *J.Am.Chem.Soc.*, **92**, 428 (1978).

[248] A.K.Srivastava, A.L.Varshney and P.C.Pais, *J.Inorg.Nucl. Chem.*, **42**, 47 (1980).

[249] D.B.Brown, K.A.Donner, J.W.Hall, S.R.Wilson, R.B.Wilson, D.J.Hodgson and W.E.Hatfield, *Inorg.Chem.*, **18**, 2635 (1979).

[250] J.P.Collman and E.T.Kittleman, *Inorg.Synth.*, **8**, 150 (1966).

[251] D.Nicholls and R.Swindells, *J.Inorg.Nucl.Chem.*, **31**, 3313 (1969).

[252] U.Anthoni, B.Dahl, Ch.Larsen and P.H.Nielsen, *Acta.Chem.Scand.*, **24**, 959 (1970).

[253] D.P.Gowing and R.W.Leeper, *Botan.Gazz.*, **123**, 134 (1961).

[254] F.E.Condon, R.T.Reeve, D.G.Shapiro, D.C.Thakkar and T.Briks Goldstein, *J.Chem.Soc.,Perkin.Trans.2*, **1974**, 1112.

[255] J.R.Perrott, G.Stedman and N.Uysal, *J.Chem.Soc.,Perkin. Trans.2*, **1977**, 274.

[256] G.Zinner and U.Gebhardt, *Arch.Parmaz.*, **304**, 706 (1971).

[257] J.R.Durig and W.C.Harris, *J.Chem.Phys.*, **51**, 4457 (1969).

[258] S.K.Green, University of Bath, Final Year Report. No 350 (1986).

[259] U.Anthoni, Ch.Larsen and P.H.Nielsen, *Acta.Chem.Scand.*, **22**, 1025 (1968).

[260] W.G.Strunk, *Chem.Eng.Progr.*, **54**, 45 (1958).
C.W.Raleigh and P.F.Derr, *Corrosion*, **16**, 115 (1961).

[261] J.A.Herickes, G.H.Damon and M.G.Zabetakis, Determining the Safety Characteristics of Unsymmetrical Dimethylhydrazine. Report of Investigations, 5635, US Dept. of the Interior, Bureau of Mines, 1960.

[262] L.K.Peterson and K.I.Thé, *Can.J.Chem.*, **50**, 562 (1972).

[263] V.D.Sheludyakov, E.S.Rodionov, A.D.Kirilin and V.F.Mironov, *Zh.Obshch.Khim.*, **46**, 2265 (1976).

[264] U.Anthoni, *Acta.Chem.Scand.*, **20**, 2742 (1966).

[265] J.M.Bellerby and C.R.Bennet, Homogeneous and heterogeneous contributions to the liquid phase decomposition of N_2H_4 in glass, stainless steel and titanium vessels, PERME Technical Report 267, April 1984.

[266] C.Moran and R.Bjorklund, Propellant/Material Compatibility Program and Results, Ten-Year Milestone, JPL Publ. 82-62 (Jul 82), also JPL Publ. 83-87 (Apr 83) and AIAA Paper 83-1382

[267] C.R.Bennet, D.R.B.Saw and D.Sutton, *J.Hazard.Mater.*, **4**, 23 (1980).

[268] Y.I.Rubtsov and G.B.Marelis, *Zh.Fiz.Khim.*, **43**, 1675 (1969).

[269] D.S.Ross, D.G.Henry and N.A.Kirshen, Study of the Basic Kinetics of Decomposition of MMH and MHF and their Effects on Their Stability, SRI-7982-FR, AFRPL-TR-71-114 (Sept 74).

[270] W.Berry, I.M.Gibbon, R.Dolinf and D.R.B.Saw, A Study of Material Compatibility with Hydrazine, Part II, ESRO CR-85, Aug 72.

[271] D.M.Hirst, Mathematics For Chemists, The Macmillan Press, London (1976).

[272] I.M.Kolthoff and E.B.Sandell, *Ing.Eng.Chem.(Anal).*, **2**, 140 (1930).

[273] A.J.Vogel, Quantitative Inorganic Analysis, 3rd Ed, p 460 (1961) Longman Group, London.

[274] D.G.Holah, *J.Chem.Ed.*, **42**, 561 (1965).